Carter, R.M., McCave, I.N., Richter, C., Carter, L., et al., 1999
Proceedings of the Ocean Drilling Program, Initial Reports Volume 181

6. Site 1122: Turbidites with a Contourite Foundation[1]

Shipboard Scientific Party[2]

BACKGROUND AND OBJECTIVES

General Description

Site 1122 is located 275 km south of the Chatham Islands, midway between the Chatham and Bounty Islands, and 830 km east of Dunedin, eastern South Island (Fig. F1). The site was drilled in a water depth of 4432 m on the left (north) bank levee of the abyssal Bounty Fan. The fan is located in the most seaward axial deep of the Bounty Trough, a Cretaceous rift basin formed during the separation of New Zealand and Antarctica across the newly forming mid-Pacific Rise (Carter and Carter, 1993, 1996; Davey, 1993). The Bounty Channel feeds sediment along the axis of the trough and onto the adjacent 95-Ma oceanic crust of the Southwest Pacific abyssal plain.

Site 1122 is located on New Zealand Oceanographic Institute (now NIWA) single-channel seismic and 3.5-kHz line 88-2023 (Figs. F2A, F2B, F3). The three main units that compose the Bounty Fan at this crossing (seismic Units C–A; Table T1) all show strong angular onlap onto the folded surface of pre-Unit C sediments. In ascending order, and at the drill site (Fig. F2B), these units consist of 150 ms of irregularly and lightly reflective sediment (Unit C, capped by a strong reflector, R-7), 110 ms of thin-bedded and regularly reflective sediment passing up into strongly reflective sediment (Unit B, capped by reflector R-5), and upper Unit A which is 470 ms thick and comprises a field of spectacular sediment waves. The waves initiate as small features just above reflector R5, (the Unit B/A boundary), and grow in both wavelength (up to 6 km apparent) and height (up to 17 m) as they rise through the sediment pile to the seabed, where they were apparently still active in the recent past (Carter et al., 1990). The sediment waves are best developed, and

F1. Locality map for Site 1122, p. 38.

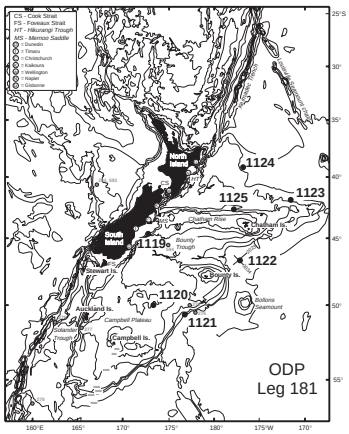

F2. Portion of seismic lines, p. 39.

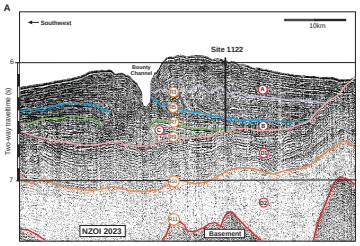

F3. Portion of 3.5-kH line, p. 41.

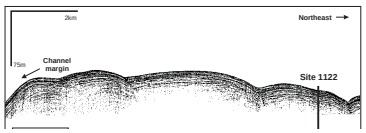

[1]Examples of how to reference the whole or part of this volume.
[2]Shipboard Scientific Party addresses.

were drilled, beneath the 315-m-high north bank levee of the Bounty Channel. Similar waves, though of smaller amplitude, occur underneath the 90-m lower crest of the south bank of the Bounty Channel. Sediment waves have been described from a number of Northern Hemisphere deep-sea environments, including submarine fans where they are most prominent on channel right banks (Damuth, 1979; Normark et al., 1980; Brew, 1995). Fan levees are inferred to have been built by overspilling turbidity currents, whose top surfaces are deflected right or left, according to the effect of Coriolis force on fluids in motion in the Northern and Southern Hemispheres, respectively (Menard, 1955; Komar, 1969). As a turbidity current overtops its levee, it may develop a series of antidune surges that cause the formation and growth of sediment waves across the levee crest (Normark et al., 1980).

The sediment waves form the upper unit (A) of the fourfold seismic stratigraphy we describe (Table T1). A zone of harder acoustic reflection extends down from the floor of the present-day channel obliquely to the left (south), where it has its initiation at or a little above reflector R9 (Fig. F2A). This zone marks the movement through time of the axis of the paleo-Bounty Channel. Seismic Units C–A compose the core of the Bounty Fan, and all appear to have been deposited as part of the north bank levee of the Bounty Fan's main sediment feeder, the Bounty Channel. The fan sediments rest on a regional unconformity (Y), here equivalent to reflector R9, below which the sediments of Unit D are gently folded and eroded. The lateral equivalents of Unit D are exposed in the inner and outer sills of the Bounty Trough, where dredged samples have provided Miocene microfossils, suggesting that the deformation and unconformity formation were of middle late Miocene age. The lower part of Unit A has been dated previously as late Pliocene (Mangapanian), on the basis of a microfauna cored from the lower north wall of the channel (Carter et al., 1994).

T1. Summary of seismic unit depth and reflectors, p. 83.

Site Objectives

Site 1122 was drilled to establish the history of deposition of the Bounty Fan, and the degree to which fan-growth has been affected by the fact that the current fan is building out into the path of the Southwest Pacific Deep Western Boundary Current (DWBC). For instance, a breach in the left bank levee of the fan, at depths of ~4650 m, may have been caused by DWBC erosion or may be a turbidity current avulsion point maintained by the boundary flow. The current may also be causing sediment unmixing and sand mobility across the middle and lower fan (Carter and Carter, 1996). The sediment waves under the left bank levee are the subject of an earlier study by Carter et al. (1990), who described core and 3.5-kHz profile evidence for the presence of alternating cycles of glacial turbidite deposition and interglacial biopelagic ooze accumulation. Carter and Carter (1992) therefore interpreted the pattern of regular reflectors on deep seismic profile NZ01 2023 as evidence for a similar glacial/interglacial pattern of lithologic change with depth, and, by comparison with the global isotope stage record, predicted an isotope Stage 100 (~2.4 Ma) age for reflector R7 of this study (Table T1). The Site 1122 cores were expected to yield a test of this prediction. Finally, because of the location of the site just south of the Subtropical Convergence (STC), information from Site 1122 should help test for the stability of position of the STC between glacial and interglacial times (Fenner et al., 1992; Nelson et al., 1993; Weaver et al., 1998).

OPERATIONS

Hole 1122A

The 341-nmi voyage to Site 1122 (proposed site SWPAC-8A) was accomplished at an average speed of 9.6 kt. The vessel proceeded directly to the Global Positioning System coordinates of the location. The positioning beacon was dropped at 2254 hr on 5 September. The hydrophones and thrusters were extended and the vessel settled on location. The advanced hydraulic piston core/extended core barrel (APC/XCB) bottom-hole assembly (BHA) was assembled using a 9-⅞-in PDC bit. Hole 1122A was spudded with the APC at 1210 hr on 6 September. The recovery indicated that the water depth was 4435.00 meters below sea level (mbsl). Piston coring advanced to refusal at 75.8 mbsf, and Cores 1H through 8H were taken (Table **T2,** also in **ASCII format**). The hole was deepened with the XCB to 123.9 mbsf, which was considered the objective for the initial hole of the site. APC cores were oriented starting with Core 181-1122A-3H. The bit cleared the seafloor at 0415 hr on 7 September, ending operations at Hole 1122A.

T2. Site 1122 expanded coring summary, **p. 84.**

Hole 1122B

The vessel was offset 20 m to the west and the second hole of the site was spudded with the APC at 0615 hr on 7 September. To obtain a stratigraphic overlap for interhole correlation, the bit was positioned 5 m higher than at Hole 1122A. However, the recovered core barrel was full, which required another attempt to obtain a mudline core.

Hole 1122C

The bit was raised at the same location by an additional 5 m, and Hole 1122C was spudded with the APC at 0740 hr. The mudline core indicated that the water depth was 4431.80 mbsl. The APC was advanced by recovery to 103.7 mbsf and Cores 1H through 13H were obtained (Table **T2**). The last three cores (11H, 12H, and 13H) did not achieve a full stroke.

Coring was switched to the XCB and advanced without incident to 204.3 mbsf with good to poor recovery (Table **T2**). Very rapid XCB coring continued with recovery ranging from 1% to 97% from 204.3 to 627.4 mbsf. After making a drill pipe connection following the retrieval of Core 68X (617.8 to 627.4 mbsf), the drill string became stuck and could not be rotated with up to 700 A of top drive current. The driller worked the pipe for over an hour with overpulls as large as 200 kilopounds (kips), while maintaining a circulation rate of 1000 gal/min at 2200 psi pressure before the drill string came free. It was considered imprudent to attempt to deepen the hole past this depth, and preparations for logging were started.

Logging Operations at Hole 1122C

In preparation for logging, the hole was swept with 60 barrels of high-viscosity mud. The bit was pulled back in the hole to 520 mbsf and the hole was displaced with 175 barrels of sepiolite mud. The bit was then pulled back and positioned at 83 mbsf. At 0700 hr on 11 September, the logging equipment was rigged up and the first tool suite

(triple combination: DIT/HLDS/APS/HNGS) was deployed in the drill pipe. The tool string was unable to pass the bit more than 12 m and after repeated attempts by the logging winch operator, it was decided to recover the logging tool in rapidly deteriorating weather conditions. After the logging tool was disassembled, operations at the site were terminated because of heavy seas and high winds. The combined sea state was exceeding 10 m and wind gusts were recorded as high as 55 kt.

When overpulls as large as 200 kips were unable to free the drill string, the top drive was picked up. For 2 hr, the stuck drill pipe was worked with 200 kips of overpull while maintaining a circulating rate of 1000 gal/min. At 1530 hr on 11 September, the pipe was free and the drill string was recovered. The bit cleared the seafloor at 1625 hr. By 0800 hr the drilling equipment was secured for the voyage to the next site and the beacon was recalled and recovered. At 0800 hr on 12 September, the vessel was under way on a northeasterly course to Site 1123.

LITHOSTRATIGRAPHY

Introduction

Bounty Fan is the terminus for a sediment-transport system that begins in the rapidly rising Southern Alps of New Zealand. During glacial periods of low sea level, large quantities of terrigenous sediment were delivered by rivers to an emergent continental shelf. These rivers continued across the shelf to discharge their loads at the paleoshoreline which, in major lowstands such as those that occurred during isotope Stage 2, was near to the shelf edge. There, sediment was captured by a suite of submarine canyons as well as being deposited on the upper continental slope. Mobilization of the sediment periodically generated turbidity currents that swept down canyons and into the Bounty Channel system (Carter and Carter, 1987, 1993). These currents traveled 900 km along the channel to eventually disgorge onto Bounty Fan at the mouth of Bounty Trough. En route, the overspilling turbidity currents deposited an extensive levee complex, characterized by a higher left bank (facing downchannel) that formed in response to deflection by the Southern Hemispheric Coriolis force. Instability within the overspilling currents ultimately was responsible for the formation of an extensive field of sediment waves (Carter et al., 1990).

In sharp contrast to this glacial regime of active transport and deposition, interglacial periods were previously thought to have been times of relative quiescence in Bounty Trough, judging by piston cores described by Griggs et al. (1983), Neil (1991), and Carter and Carter (1988). Under the Holocene highstand of sea level, the cores suggest that terrigenous sediment was diverted from the trough head, thereby allowing the deposition of mainly calcareous pelagite. The exception is near the head of Bounty Trough, where small turbidites accumulated in the upper reach of the channel system.

The abyssal Bounty Fan has developed across the path of the DWBC near the zone where the modern Antarctic Circumpolar Current (ACC) turns east from the margin of Campbell Plateau. Acoustical facies derived from 3.5-kHz profiles suggest that the outer Bounty Fan has been eroded by the abyssal currents (Carter and Carter, 1996). Ostensibly, the dominant flow was the DWBC, but there is an argument that this flow may have been reinforced by the ACC in glacial times when the Subantarctic Front, marking the northern limit of the ACC, proba-

bly migrated northward (Nelson et al., 1993). Such a change would presumably have been a response to a northward expansion of subantarctic waters and equatorward migration of strong winds (e.g., Nelson et al., 1993).

Site 1122 was positioned on the crest of a prominent left bank levee containing a 350-m thick sequence of Pleistocene sediment waves, resting on an additional 240 m of normally layered sediment interpreted as extending back to the Miocene (Carter et al., 1994). Coring at Site 1122 obtained a detailed record of Quaternary climatically controlled turbidite sedimentation on the levee, underlain by Pliocene and Miocene contourite drift deposits recording earlier DWBC flow across most of Bounty Trough.

Description of Lithostratigraphic Units

Unit I

Unit I consists predominantly of a thick sequence of turbidites, which is subdivided into four subunits (Fig. F4). The upper three subunits are distinguished mainly by the thickness and grain size of the turbidites. The lowest subunit, Subunit ID, shows the transition from a turbidity current–dominant to bottom current–influenced depositional environment in its lower half. Unit I extends from 0 to 386.9 mbsf.

F4. Summary log for Site 1122, p. 42.

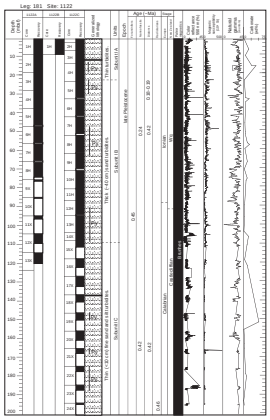

Subunit IA

Interval: Sections 181-1122A-1H-1 through 2H-5; Sections 181-1122B-1H-CC; Sections 181-1122C-1H through 4H-6
Depth: 0–16.6 mbsf (Hole 1122A); 0–9.5 mbsf (Hole 1122B); 0–22.7 mbsf (Hole 1122C)
Age: Holocene to late Pleistocene

The upper 20 cm of Subunit IA is composed of light brownish gray (2.5Y 6/2) silty clay, which may represent Holocene sediments. Because of an offset between Holes 1122A and 1122C, the Holocene sediments and the upper ~8 m are absent from Hole 1122A (see "Operations," p. 3). Underneath, Subunit IA is composed of greenish gray (5GY 6/1) silty clay with intercalations of gray (5Y 5/1) very fine sand turbidites. These turbidites are generally <15 cm thick (Table T3), sharp based and normally graded, fining upward into greenish gray (5GY 5/1) silty clay (Fig. F5).

T3. Turbidite thicknesses, p. 97.

F5. Sequence of turbidites in Subunit IA, p. 46.

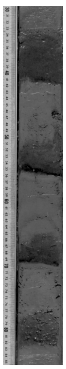

At 4.2 mbsf, an interval appears where the bases of the turbidites are pyritized. A similar pyritization zone occurs between 15 and 18 mbsf. These zones of pyritization are typical features throughout the upper three subunits of Unit I.

A tephra layer occurs at 11.93 mbsf, which probably is the Kawakawa Tephra, dated at 22,590 radiocarbon years (26,000 calibrated years; I.N. McCave, pers. comm., 1998). The base of Subunit IA is probably close to the isotope Stage 3/Stage 4 boundary at 59 ka.

Subunit IB

Interval: Sections 181-1122A-2H-5 through 11X-1; Sections 181-1122C-4H-6 through 15X-1
Depth: 16.6–95.0 mbsf (Hole 1122A); 22.71–109.35 mbsf (Hole 1122C)
Age: late Pleistocene

Subunit IB is composed of greenish gray (5G 4/1) silty clay that is interbedded with dark greenish gray and greenish gray (5BG 4/1, 5G 5/1) sand and fine sand turbidites. The thickness of the turbidites is greater than in Subunit IA, varying from 10 to 100 cm (Fig. F6). This subunit also contains three intervals with significant pyrite in the basal sands of the turbidites (23.5–28 mbsf, 47.2–62 mbsf, and 91.7–109.5 mbsf). Subunit IB is moderately bioturbated throughout; only the top of the Section 181-1122C-14X (103.7–104.2 mbsf) represents heavy bioturbation and may reflect an interglacial stage. The lower boundary of Subunit IB is marked by a color change at 109.35 mbsf from greenish gray (5GY 5/1) to grayish green (5BG 5/1). The base of this subunit is estimated to be close to the isotope Stage 8/9 boundary at 285 ka.

F6. Sand turbidite in Subunit IB, p. 47.

Subunit IC

Interval: Sections 181-1122A-11X-1 through 13X-CC; Sections 181-1122C-15X-1 through 31X-1
Depth: 95.0–123.9 mbsf (Hole 1122A); 109.35–261.7 mbsf (Hole 1122C)
Age: middle to late Pleistocene

Subunit IC is composed of sequences of dark greenish gray (5GY 4/1) silt and very fine sand turbidites with intercalations of grayish green (5GB 5/1) and greenish gray (5GY 5/1) silty clay. The thickness of the turbiditic layers is <20 cm. It is probable that the apparent decrease in turbidite thickness, compared to Subunit IB, is an artifact of the change from APC to XCB drilling. Low recovery rates (averaging ~40%) indicate the likelihood of washout of the thicker sand beds. Three intervals of higher pyrite content are present in Subunit IC (at 146.5–150.43 mbsf, 157.2–166.4 mbsf, and 242.9–245 mbsf). Below 245 mbsf, zones of pyritization are not observed. On average, bioturbation is moderate throughout the entire subunit. In Core 181-1122C-20X there occurs a heavily bioturbated, light greenish gray and light gray (5BG 6/1, 2.5Y 8/1) nannofossil-rich, silty clay. A tephra layer occurs in Section 181-1122C-18X-1 at 138.24 mbsf.

Subunit ID

Interval: Sections 181-1122C-31X-1 through 44X-1
Depth: 261.7–386.9 mbsf (Hole 1122C)
Age: early to middle Pleistocene

Subunit ID includes greenish gray and gray (5GY 5/1, 5Y 5/1) silty clay interbedded with dark greenish gray (5GY 4/1) very fine sand and silt turbidites of <10-cm thickness. The top of Subunit ID, Core 181-1122C-31X (261.7–271.36 mbsf), marks the first appearance of turbidites with eroded upper contacts and planar lamination. A lighter colored interval with color change from light gray to olive-yellow (5Y 7/1 to 5Y 6/6) coincides with heavier bioturbation. In Section 181-1122C-34X-2, another gradational color change to olive (5Y 5/3) is observed, which is followed by an interval of higher bioturbation in Core 181-1122C-35X (300–308.01 mbsf). There are two tephra layers in Subunit ID, in Section 181-1122C-37X-1 (320.3 mbsf) and in 37X-6 (327.92 mbsf) (Fig. F7).

Subunit ID shows a gradational transition upward from a current-influenced depositional environment to a more turbidite-dominated facies. The higher intensity of bioturbation in the hemipelagic sediment separating turbidite units may indicate a slower rate of deposition or a lower frequency of turbidity currents compared to Subunits IA–IC.

F7. Tephra layer in Subunit ID, p. 48.

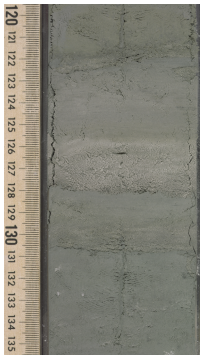

Unit II

Unit II represents bioturbated, pelagic/hemipelagic sediments interspersed with current-laminated deposits. This unit extends from 386.9 to 550.4 mbsf and is divided into the three Subunits IIA, IIB, and IIC, according to compositional changes.

Subunit IIA

Interval: Sections 181-1122C-44X-1 through 52X-6
Depth: 386.9–472.3 mbsf (Hole 1122C)
Age: Pleistocene to late Pliocene

Poor core recovery in Core 181-1122C-43X suggests that a suitable upper boundary for Subunit IIA lies at the top of Core 44X. The improved core recovery downhole, starting at Core 44X, produced sediments quite distinct from Unit I. The mottled, greenish gray (5G 5/1 to 5GY 5/1) olive-gray (5Y 5/2) or light greenish gray (5BG 7/1) pelagic/hemipelagic silty clay beds are commonly bioturbated with *Zoophycos, Planolites, Terebellina, Chondrites, Anconichnus,* and *Gyrolithes*. Pyritization is very sporadic being typically limited to pyritized *Zoophycos* traces. Interbedded with the silty clay is dark gray (N 4) or dark greenish gray (5GY 4/1) fine sand and silt beds that commonly exhibit scoured basal contacts and conspicuous planar and cross laminations. Such structures suggest a stronger, episodic benthic flow regime, in contrast to that of the decelerating turbidity currents. Laminae are accentuated by concentrations of foraminifers and carbonate debris. Sporadic ripples were observed in the thicker beds (>10 cm) (Figs. **F8, F9**). Top and bottom contacts of the fine sand and silt beds are generally sharp, with few gradational boundaries. These sand and silt beds are tentatively interpreted as contourite deposits (see **"Interpretation and Discussion,"** p. 9). Interspersed among the contourites are sporadic fine sand beds with sharp basal contacts and normal grading, which suggests a turbidity current origin. These beds may have been deposited during periods of weak contour-current activity.

Pinkish gray (5YR 6/2) tephra occurs in Sections 181-1122C-44X-2 (388.96–388.99 mbsf), 50X-5 (450.82–450.86 mbsf), and 51X-1 (454.48–454.52 mbsf). Drilling disturbance increases toward the base of Subunit IIA with moderate to heavy biscuiting starting in Core 181-1122C-47X.

F8. Contourite with planar and cross laminae, Subunit IIA, **p. 49.**

F9. Planar and cross laminae, Subunit IIA, **p. 50.**

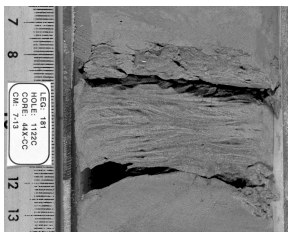

Subunit IIB

Interval: Sections 181-1122C-52X-6 through 55X-2
Depth: 472.3–494.5 mbsf (Hole 1122C)
Age: early Pliocene

Subunit IIB is heralded by a sudden downcore increase in detrital chlorite. The contact between Subunits IIA and IIB is marked by the occurrence of a pale olive (5Y 6/3) silty clay. Dark greenish gray (5GY 4/1 to 5G 4/1) to greenish gray (5G 5/1 to 5GY 6/1) pelagic/hemipelagic silty clay beds are interspersed with light brownish gray (2.5Y 6/2) to gray (5Y 6/1), nannofossil-rich layers. Bioturbation is common throughout the silty clay beds and includes an ichnofauna of *Zoophycos, Chondrites, Planolites, Terebellina, Thalassinoides,* and *Teichichnus*. The interbedded dark greenish gray (5G 4/1) to greenish gray (5GY 5/1) fine sand and silt beds contain sharp, typically scoured basal contacts, sharp upper contacts, and planar laminations; gradational boundaries are not common.

We suggest that the sand and silt beds are contourites (see "Interpretation and Discussion," p. 9) Intense disturbance has caused brecciation in Core 181-1122C-53X, and moderate biscuiting is observed in Core 54X.

Subunit IIC

Interval: Sections 181-1122C-55X-2 through 60X-CC
Depth: 494.5–550.4 mbsf (Hole 1122C)
Age: middle Miocene

The top of Subunit IIC occurs in Core 181-1122C-55X at a distinct color change from the normal greenish gray (5G 4/1) silty clay of Subunit IIB. The color changes gradationally to a yellowish brown to light reddish brown (10YR 6/4) in Section 181-1122C-55X-2, to (10YR 6/3) in Section 55X-3, to a 20-cm white (10YR 8/1) bed to pale yellow (5Y 7/3) in Section 55X-4, and finally to pale olive (5Y 6/3) in Section 55X-5. The suggested location of the boundary between Subunit IIB and Subunit IIC is placed at the beginning of the gradational color change in Section 181-1122C-55X-2 (494.5 mbsf). The extensive bioturbation in Section 55X-2 by *Thalassinoides* suggests the possibility of a firmground or discontinuity in deposition. The interval of distinct color variability (494.5–499.15 mbsf) is rich in nannofossils and foraminifers and coincides with the unconformity separating the early Pliocene and the middle Miocene.

The dominant lithology of Subunit IIC is dark greenish gray (5GY 4/1 to 5G 4/1) to greenish gray (5G 5/1 to 5GY 6/1) pelagic/hemipelagic silty clay beds that are interspersed with white (5Y 8/1) nannofossil ooze layers. Detrital chlorite is observed in smear slides (see the "Core Descriptions" contents list). Bioturbation is common throughout the silty clay beds and includes an ichnofauna of *Zoophycos, Chondrites,* and *Planolites*. The *Thalassinoides* at the upper boundary of the subunit are interpreted to be ichnofaunal (Pliocene?) reworking of the Miocene-age sediments. The interbedded dark greenish gray (5G 4/1) to greenish gray (5GY 5/1) fine sand and silt beds contain sharp, typically scoured basal contacts, sharp upper contacts, and planar laminations; gradational boundaries are not common. We suggest that the sand and silt beds are contourites (see "Interpretation and Discussion," p. 9). Moderate biscuiting is observed throughout Subunit IIC.

Unit III

Unit III represents bioturbated, pelagic/hemipelagic sediments interspersed with laminated current deposits common to drift deposits. Toward the bottom of the hole, two probable debris-flow deposits have been identified. This unit extends from 550.4 to 617.85 mbsf and is divided into Subunits IIIA and IIIB, according to a change in lithification and the appearance of debris-flow deposits. Recovery was poor, averaging <25%.

Subunit IIIA

Interval: Sections 181-1122C-61X-1 through 64X-1
Depth: 550.4–580.62 mbsf (Hole 1122C)
Age: middle Miocene

Because of the poor recovery in Core 181-1122C-60X the upper contact of Subunit IIIA is located at the top of Core 181-1122C-61X. The green

(5G 5/1, Munsell plant color chart) to greenish gray (5G 5/1, Munsell soil color chart) clayey silt to silty clay, composing these pelagic/hemipelagic sediments, tend to be coarser grained than those of Unit II. Sediments are commonly bioturbated with observed traces of *Zoophycos, Chondrites, Planolites, Terebellina,* and *Gyrolithes.* Interbedded throughout are distinctive fine sand and silt beds of a greenish hue (5G 5/1, Munsell plant color chart) and greenish gray (5G 5/1-5G 6/1) to dark greenish gray (5G 4/1) as well as interspersed white (10Y 8/1) or gray (10YR 5/1) to dark gray (10YR 4/1) nannofossil-bearing foraminifer sand (Fig. **F10**). Sand and silt beds have pronounced planar laminae. Top and bottom contacts of the sand and silt beds are sharp with normal grading only sporadically in sand beds. The sand and silt interbeds are interpreted as contourite deposits with intermittent, unreworked turbidites (see **"Interpretation and Discussion,"** p. 9).

F10. White foraminifer sand with bioturbated top, Subunit IIIA, **p. 51.**

Subunit IIIB

Interval: Sections 181-1122C-64X-CC through 68X-CC
Depth: 580.62–617.8 mbsf (Hole 1122C)
Age: early Miocene

The upper contact of Subunit IIIB is located in Section 181-1122C-64X-CC at the top of a poorly sorted, greenish gray (5G 5/1) fine sand that is reverse graded to gravelly coarse sand. This bed has greenish gray (5GY 6/1) intraclasts of silty clay up to 1.2 cm long, and the beds also contain abundant wood fragments that are typically <1 cm. These features suggest the deposits were emplaced as debris flows. Another debris-flow deposit with similar composition is observed in Section 181-1122C-67X-1, 608.8 mbsf (Fig. **F11**). Between the two debris flows is a series of heavily bioturbated, interbedded greenish gray (5GY 5/1) to dark greenish gray (5GY 4/1) fine sand–bearing siltstones and light greenish gray (5BG 7/1) foraminifer-bearing nannofossil chalks, which appear to be the lithified equivalents of Subunit IIIA. The siltstone beds in Core 181-1122C-65X contain abundant wood fragments. Observed trace fossils in the chalk and siltstone beds include *Chondrites* and *Planolites*. Interspersed among the siltstone and chalk beds are greenish gray (5GY 5/1) laminated, fine sand beds. The fine sand beds have sharp top and bottom contacts and are usually not graded. Drilling disturbance is pronounced throughout the subunit, with moderate to heavy biscuiting and very poor recovery (averaging <20%).

F11. Reverse-graded debris-flow deposit, Subunit IIIB, **p. 52.**

Interpretation and Discussion

The overall pattern of deposition at Site 1122 exhibits the interplay between the DWBC, possibly reinforced by the ACC, and the inflowing turbidity currents carrying their high sediment load from the Bounty Channel.

Unit III contains pelagic/hemipelagic sediments interbedded with contourites and a few turbidites. The debris-flow deposits in Subunit IIIB indicate a closer source than the South Island. Unit II continues to be affected strongly by boundary currents, with most of the sand and silt beds containing fine planar laminae and cross laminae, which imply steady flow conditions. The presence of chlorite-bearing sediments in Subunit IIB suggests either (1) a source off the Campbell Plateau that has been eroded by the DWBC and redeposited as contourites at Site 1122, or (2) a South Island source in the Bounty Trough catch-

ment. Isolated turbidites do occur throughout Units II and III, but are a minor component of the coarser grained deposits.

Unit I shows the stronger influence and greater sediment load brought by the Bounty Channel. Subunit ID contains mainly thin turbidites that have been eroded and slightly reworked, with typically sharp top contacts. Subunits IC to IA contain sequences of turbidites that represent the emplacement of the prograding channel/levee complex of the Bounty Fan.

Units II and III have distinctive nongraded, laminated fine sand and silt beds indicating the presence of a persistent but variable current. This flow caused basal scouring, yet allowed alternating deposition of cross-laminae and planar laminae. It is likely that sporadic influxes from the Bounty Channel interacted with the DWBC, which was (1) reinforced at times by benthic storms such as those recorded at the High Energy Benthic Boundary Layer Experiment (HEBBLE) site off Nova Scotia (Hollister and McCave, 1984), (2) affected by glacial/interglacial cyclicity, or (3) periodically reinforced by the ACC.

The reverse-graded, coarse-grained sediments containing clay intraclasts and wood fragments are interpreted as debris-flow deposits. Several lines of evidence suggest the debris flows carried sediment from proximal sources into deep water: (1) the deposits are interbedded with pelagic sediments, (2) the composition is different from the distal turbidites of the Bounty Fan, and (3) the benthic foraminiferal fauna is shallow water (see **"Biostratigraphy,"** p. 13). The most likely sources of the debris flows are the flanks of the Chatham Rise and the Campbell Plateau. Several of the fine sands and white foraminifer sands appear to be turbidites, which may also represent shallower material originally deposited on Chatham Rise or Campbell Plateau.

The observed changes in the depositional environments also document the changes in the character of DWBC and its effect on the area. The DWBC was a dominant factor in the depositional history of Units II and III. The chlorite-bearing sands and muds within an abyssal flow sequence may reflect erosion upstream by the combined DWBC/ACC. These sediments may represent the unroofing of chlorite-bearing sediments at the base of the Campbell Plateau (see **"Lithostratigraphy,"** p. 3, in the "Site 1121" chapter). The presence of reworked Eocene diatoms also suggests erosion of earlier deposits (see **"Biostratigraphy,"** p. 13).

The ACC can be argued to have reinforced the DWBC at least during the time of deposition (and erosion) in Subunit IIC where the foraminifers in the silty clay located in Section 181-1122C-55X-4 comprise almost entirely well-sorted, cold-water Antarctic taxa.

Subunits IA–IC consist of a 262-m-thick Pleistocene turbidite sequence in which the sediment was delivered to the shelf and slope by river input during glacial sea-level lowstands and deposited by turbidity flows that may coincide with eustacy, seismicity, or other triggering mechanisms. The base of Unit I approximates seismic reflector R2a, which is the contact between large-amplitude sediment waves above and a planar bedded sediment wedge below. It appears that the turbidite-dominant Unit I marked the main period of levee growth by the Bounty Channel.

One of the major concerns in separating out the lithostratigraphic units and subunits is the generally poor core recovery. This is particularly related to the observed changes in thickness and grain size of the turbidite intervals throughout Unit I (Fig. **F12**). Four variables control fan sediments, namely the degree of glacial sea-level lowstands, seismic-

F12. Thickness of turbidites and sand, fine sand, and silt layers, **p. 53.**

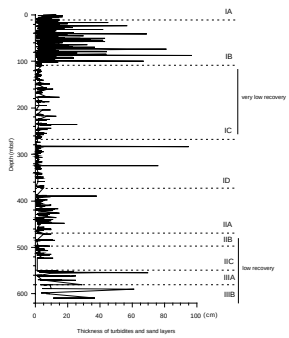

ity affecting the slope, sediment supply, and the influence of the passing DWBC. However, any evaluation of these variables must be made with due consideration of the drilling operations. Of significance is the apparent change in both turbidite thickness and coarsest grain size from Subunit IB to Subunit IC. With the beginning of XCB coring at Core 181-1122C-14X, the amount of recovered core dropped significantly (<50% recovery). It is likely that the use of XCB coring washes out the less cohesive and thicker sand layers, causing only the fine-grained, thinner sands and muds to be recovered in the core. Because of the lack of supporting data such as downhole logs, it is imprudent to interpret the lithology of the missing intervals. When defining the units and subunits, changes that were apparent in lithology, deposition, or composition were considered primarily; core recovery was a necessary secondary consideration, as the definition of the units could not be based entirely on what was observed. For example, it is uncertain if a lithologic change exists between Subunit IB to IC, or whether the change rather represents an artifact of the drilling method.

The transition from a current-influenced (Unit II) to a more turbiditic-influenced environment (upper part of Subunit ID) is marked by an abrupt increase in coarser sand and silt beds. There, the very fine sand and silt turbidite intervals are relatively thin (<10 cm) and sometimes are truncated and reworked. These coarser beds probably represent an early stage of the Bounty Fan with a less distal sedimentation of the terrigenous material. The overlying Subunit IC contains slightly thicker silt and very fine sand turbidites (~10 to 20 cm thick). An erosional influence from the DWBC is not apparent because the turbidites are normally graded. Compared to the overlying turbidites of Subunit IB, Subunit IC beds are relatively thin and could indicate a slow progradation of the fan. Subunit IB has thick (<100 cm) sandy turbidites, implying more rapid fan progradation. Subunit IA is composed of thinner, fine-grained turbidites and could represent either a marked restriction in sediment supply through the Bounty Channel or that the height of the levees allowed only the fine fraction of the turbidity currents to overspill. Another possibility is that the alternation in turbidite thickness is tied to deposition on a migrating sediment wave field. The migration of these antidunes would cause the deposition of thicker turbidites on the upcurrent side and thinner turbidites on the lee side of an antidune. As the sediment waves migrated relative to the location of the drill site, a periodic pattern of thicker and thinner turbidites might be expected.

Pyritized bases of the turbidites appear in distinct intervals of several decimeters to several meters thickness throughout Unit I (Fig. **F13**). These intervals probably depend on the content or concentration of organic matter being deposited and its degradation under reducing conditions. There appears to be a connection at ~260 mbsf between the last interval of pyritized bases and the elevated methane content (see **"Inorganic Geochemistry,"** p. 27), which would confirm a higher organic content in Unit I. Total organic carbon, however, does not show a clear trend of higher values, but the reason for this could be the low-resolution sampling.

Pyritized zones develop best in the bases of sand turbidites but also occur in the very fine sand and silt turbidites. This leads to the possibility that organic detritus carried within the turbidity currents is percolating through the sand bed and is reduced at the contact with the underlying fine-grained deposit. This slows down the interstitial-water circulation. However, the mechanism is not supported by the occur-

F13. Turbidites with pyritized bases in basal Subunit IA, **p. 54.**

rence of pyritized bases in fine-grained turbidites. Therefore, a more likely explanation is the rapid burial of organic-rich surface sediment (silty clay hemipelagic sediment below turbidites), thereby causing a sudden change from oxidizing to reducing conditions during degradation of organic matter. Still another explanation for the pyrite zones is that the higher permeability of the basal turbidite sands promotes the concentration of reducing pore waters expelled from the muds below. Only in distinct intervals is the supply of organic matter higher; this may be correlated with glacial periods in which productivity and organic carbon content of hemipelagic sediments is higher (Lean and McCave, 1998).

Trace Fossils

In Unit III, the observed trace fossils in the lithified pelagic sediments of Subunit IIIB and the unlithified pelagic sediments of Subunit IIIA include *Zoophycos, Planolites, Chondrites, Terebellina,* and *Gyrolithes*. The low diversity and the high abundance imply a *Zoophycos* ichnofacies, which indicates a fairly low depositional rate in a slightly oxygen-poor, deep-water environment (Pemberton and MacEachern, 1995).

Subunit IIC contains an ichnofauna abundant with *Zoophycos, Planolites,* and *Chondrites,* continuing the *Zoophycos* ichnofacies from Unit III. The top of the subunit in Core 181-1122C-55X is likely to be directly related to the unconformity separating early Pliocene age sediment in Core 181-1122C-54X from the middle Miocene age sediments in Core 181-1122C-56X. The unconformity is marked by the start of a gradational color change in Section 181-1122C-55X-2. The presence of *Thalassinoides* at the top of Subunit IIC is interpreted as later (possibly Pliocene) burrowing into the Miocene sediment.

Subunit IIB possesses a more variable depositional history. The trace fossil assemblage in the subunit includes *Zoophycos, Chondrites, Planolites, Terebellina, Thalassinoides,* and *Teichichnus*. The presence of *Thalassinoides* and *Teichichnus* suggests a transition from *Zoophycos* ichnofacies to a *Cruziana* ichnofacies, signifying a more energetic and oxygenated environment (Fig. **F14**). The carbonate sediments of Core 181-1122C-55X mark the first (last downcore) occurrence of *Thalassinoides*.

In Subunit IIA, the presence of *Chondrites, Terebellina, Anconichnus,* and deep-spiraling *Zoophycos* in relatively high abundance, but low diversity, again implies a *Zoophycos* ichnofacies. Nannofossil-bearing sediments increase in this unit and may represent glacial-interglacial periods of higher carbonate levels relative to terrigenous input into the ocean.

Unit I contains few identifiable trace fossils; those observed traces are generally robust burrows of opportunistic colonization (primarily *Skolithos,* with singular occurrences of *Thalassinoides* in Core 181-1122C-16X and *Gyrolithes* in Core 181-1122C-17X). The lack of identifiable trace fossils in the hemipelagic silty clays suggests the depositional rates were high, thereby preventing a well-developed ichnofabric from being established. Starting at 280 mbsf and occurring more consistently from 300 mbsf to 389.9 mbsf is an ichnofauna limited to *Chondrites,* which suggests a lower depositional rate accompanied by a restriction in oxygen (Pemberton et al., 1992) (Fig. **F15**).

F14. *Teichichnus, Zoophycos,* and *Planolites* in Unit IIB, **p. 55.**

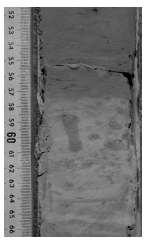

F15. *Chondrites* in Subunit ID, **p. 56.**

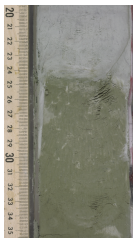

BIOSTRATIGRAPHY

Introduction and Summary

The stratigraphic sequence recovered at Site 1122 consists of Miocene through Pleistocene strata, consisting of lower and middle Miocene sediments (~130 m), overlain by a thin and stratigraphically highly condensed and incomplete upper Miocene and Pliocene section (<50 m) and a 450-m-thick Pleistocene section. The uppermost few meters at the site include the Holocene. Calcareous and siliceous microfossils are present throughout the whole section. The preservation of microfossils is good or very good in the upper part of the sequence but deteriorates downward.

The main paleontological results are summarized in Figure **F16.** The sequence of biohorizons indicates an apparently continuous section at the top, ranging from the upper Quaternary to the upper Pliocene. Calcareous nannofossil data indicate a slight unconformity at ~454 mbsf, which separates the Pleistocene–upper Pliocene sediments from a short lower Pliocene interval. A more pronounced hiatus is detected at ~490 mbsf. Below this unconformity, the sediments are middle Miocene in age, ranging from ~10.9 Ma (based on the last occurrence [LO] of *Coccolithus miopelagicus,* which is still present in the section) down to 16.7 Ma (last common occurrence [LCO] of *Globorotalia zealandica*).

In the Pliocene–Pleistocene interval, the planktonic foraminiferal assemblages are characteristic of an oceanic environment, and benthic assemblages are a mixture of deep-water and redeposited shelf forms. The upper part of the Miocene sequence is characterized by almost barren sediment or by rare deep-water benthic species, while the lowermost part of the section has a normal oceanic plankton fauna and mixed mid-shelf and deep-water benthic assemblages.

In the late Pleistocene interval, diatoms are represented by a mixture of autochthonous pelagic species and neritic-nearshore species (probably derived from the inner part of the Bounty Trough). The early Pleistocene and Pliocene sediments are rich in reworked older Pliocene and Miocene Antarctic/subantarctic species as well as some Paleogene diatom valves. The Miocene sediments yield again higher numbers of autochthonous Antarctic and subantarctic species, whereas in the lowermost part of the section only reworked Paleogene diatoms (Eocene and Oligocene in age) occur.

F16. Biostratigraphic summary chart, **p. 57.**

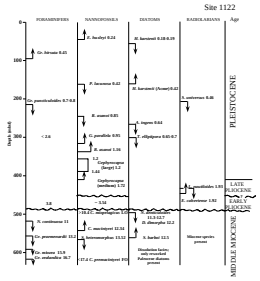

Age

The micropaleontological biostratigraphy of Site 1122 is mostly based on the onboard study of core-catcher samples. Hole 1122A samples were used for the uppermost part of the section and Hole 1122C samples for the lower part. Additional samples were taken from within selected cores to address specific age and paleoenvironmental questions. The absolute ages assigned to biostratigraphic datums follow the references listed in Tables **T2,** p. 59, **T3,** p. 60, **T4,** p. 63, and **T5,** p. 64, all in the "Explanatory Notes" chapter).

Calcareous Nannofossils

Nannofossils obtained from Cores 181-1122A-1H to 13X (0–119.97 mbsf) and from core catchers of Cores 181-1122C-15X to 68X (111.28–617.80 mbsf) were analyzed. There is an 8.6-m overlap between the two

holes in our analysis. Additional samples were selected and investigated strategically to increase biostratigraphic resolution. The occurrence of taxa are presented in Table T4. Because of the paucity of major marker species, especially during the Miocene, we did not attempt to correlate the sequence with Martini's (1971) standard zonation.

T4. Identification and abundance of nannofossils, p. 116.

Calcareous nannofossils are common and well preserved in the upper part of the sequence (0–400 mbsf), except for several short turbidite intervals where only a few nannofossils were found. The preservation of nannofossils deteriorates downward from Core 181-1122C-46X (400–617.8 mbsf) at the same time as the concentration of nannofossils in sediments increases. Reworked nannofossils occur frequently throughout the sequence. The common presence of reworked species makes it hard to use last occurrence datum levels, as, for instance, with *Helicosphaera sellii* and *Cyclicargolithus floridanus*.

Thirteen nannofossil biohorizons were recognized and used for dating the drilled sequence. The upper 420 m represents apparently a continuous sequence of Pleistocene–late Pliocene age, if small diastems were negligible. The absence of marker species as well as the frequent occurrence of reworked nannofossils makes it difficult to date the lower part of the sequence (420–617.8 mbsf). Nevertheless, two hiatuses were detected at ~454 mbsf and 490 mbsf. A short early Pliocene interval (~3.5 Ma in age) is sandwiched between these two hiatuses (Fig. F16). Beneath the lower hiatus, a middle Miocene sequence (between 11 to 17.4 Ma as constrained by nannofossils) was recovered.

Samples 181-1122A-1H-CC to 7H-CC contain abundant, moderately preserved nannofossils characterized by the presence of *Emiliania huxleyi*. This interval is correlated with Zone NN21 (Martini, 1971), with its bottom estimated at 0.24 Ma (Naish et al., 1998). Because of the dilution effect of terrigenous influx caused by turbidites, it was difficult to assess the dominance of *E. huxleyi,* and, therefore, the acme zone of this species was not recognized within Zone NN21. The base of NN20, the LO of *Pseudoemiliania lacunosa,* estimated at 0.42 Ma (Sato and Kameo, 1996; Naish et al., 1998), was recognized at Sample 181-1122C-22X-CC.

From Samples 181-1122C-22X-CC to 44X (176.9–391.5 mbsf), the sequence contains assemblages diagnostic of the early to late Pleistocene (e.g., Matsuoka and Okada, 1989; Takayama, 1993; Sato and Kameo, 1996). Sato and Kameo's (1996) recent revision of the estimated ages of Pleistocene nannofossil datum levels was adopted for dating this core section. The LO of *Helicosphaera sellii* was assessed to be at Sample 181-1122C-44X-3, 13 cm, which is inconsistent with other biohorizons, and, therefore, was not included in the age-depth model.

A biostratigraphic break occurs between Samples 181-1122C-50X-CC and 51X-2, 58 cm. Below this break, well-preserved *Sphenolithus neoabies* and *Dictyococcites antarcticus* occur commonly and persistently. The occurrence of *Sphenolithus neoabies* (mean LO estimated to be slightly younger than 3.54 Ma; Spencer-Cervato et al., 1994) and *Pseudoemiliania lacunosa* (FO at 3.54 Ma; Spencer-Cervato et al., 1994) in Sample 181-1122C-51X-2, 58 cm, to 51X-CC (452.2–463.6 mbsf) suggests a correlation of this interval to the NN15 Zone of the late early Pliocene. The break itself might represent a small hiatus separating the late Pliocene from early Pliocene. Sample 181-1122C-52X-CC yields a few *Helicosphaera sellii,* whose first appearance was reported to be at the basal boundary of Zone NN12 (de Kaenel and Villa, 1996), indicating an age younger than 5.5 Ma (Berggren et al., 1995).

Samples taken from Core 181-1122C-54X are almost barren of nannofossils and, therefore, no age assessment can be made for this core.

Below this barren interval, Sample 181-1122C-55X-CC yields assemblages characteristic of middle Miocene age. We surmise that a major hiatus separating the lower Pliocene from the middle Miocene occurs between Samples 181-1122C-55X-CC (499.7 mbsf) and 53X-CC (477.8 mbsf), at around 490 mbsf. The samples immediately below the unconformity are characterized by the occurrence of a moderately preserved assemblage containing *Calcidiscus premacintyrei, Coccolithus miopelagicus,* and medium-sized *Reticulofenestra* spp. Although these species occur also in samples above this unconformity as a result of reworking, they occur in large quantities with better preservation below this level. The top of the sequence below the unconformity is estimated to be older than 10.9 Ma, based upon the appearance of *Coccolithus miopelagicus* (Gartner, 1992).

The middle Miocene section (499.7–617.8 mbsf) contains a few badly preserved *Discoaster* spp. The general paucity of major marker species hampers our effort to correlate the sequence with Martini's (1971) zonation. Nevertheless, several constraints can be given: (1) the bottom of the deepest core contains *Calcidiscus premacintyrei,* which indicates an age younger than 17.4 Ma (Gartner, 1992); (2) Sample 181-1122C-60X-CC (541.1 mbsf) marks the FO of *Calcidiscus macintyrei,* which indicates a middle Miocene age of 12.34 Ma (Raffi and Flores, 1995); and (3) the LO of *Sphenolithus heteromorphus* (dated 13.52 Ma, Raffi and Flores, 1995) in Sample 181-1122C-62X-CC (563.3 mbsf) gives another constraint to bracket the interval into the middle Miocene. In summary, nannofossil assemblages suggest that the lower quarter of the core (499.7–617.8 mbsf) was deposited between 17.4 and 10.9 Ma.

Foraminifers

The uppermost part of Site 1122 is late Pleistocene to Holocene in age (0–0.45 Ma), based on the sporadic presence of *Globorotalia hirsuta* (Samples 181-1122B-1H-CC, 181-1122A-7H-CC, and 181-1122A-11X-CC). Many high spiro-conical globorotaliids, with features similar to those in *Globorotalia hirsuta* and *G. praehirsuta,* occur in Samples 181-1122C-30X-CC and 31X-CC, but they are here considered to be precursors of true *G. hirsuta* populations and are not indicators of a similar late Pleistocene age (Tables **T5, T6**).

Globorotalia inflata is the dominant unkeeled globorotaliid from the top of the section down to Sample 181-1122C-34X-CC, where it is replaced in dominance by *Globorotalia puncticuloides*. In other parts of the region, this datum has been estimated to be ~0.9 Ma (Hornibrook and Jenkins, 1994). At Site 1122, this datum lies ~10 m above the Brunhes/Matuyama boundary (0.78 Ma), indicating that the previously estimated level may be a little too old. As in other stratigraphic sections in this region (e.g., DSDP Site 594 and Site 1119), *Globorotalia truncatulinoides* is sporadic and small when it first appears close to the FCO of *Globorotalia inflata* (in Sample 181-1122C-26X-2, 7–8 cm, well above the Brunhes/Matuyama boundary). Similarly, the age of the FO *G. truncatulinoides,* previously estimated for this region at ~0.9 Ma, is possibly also a little early.

Assemblages with unkeeled globorotaliids dominated by *G. puncticuloides* (3.6–0.7 Ma) and with common *Globorotalia crassula* (2.6–0 Ma) extend down to Sample 181-1122C-31X-CC and indicate a late Pliocene to early Pleistocene age for this section. Unaccompanied *G. puncticuloides* extends down to Sample 181-1122C-51X-CC and indicates that

T5. Identification and abundance of planktonic foraminifers, **p. 120.**

T6. Identification and abundance of benthic foraminifers, **p. 121.**

this interval is no older than ~3.6 Ma (middle Pliocene). Sample 181-1122C-53X-CC contains the LO *Globorotalia puncticulata* (3.7 Ma).

No planktonic foraminifers or age-specific benthic forms are present in Samples from 181-1122C-54X-CC to 57X-CC, nor from 1122C-59X-CC to 61X-CC, with the exception of a 7-cm whitish marl interval in otherwise brown-green clay at 181-1122C-55X-4, 22–24 cm. The assemblage in the latter sample is a fine silt fraction (~60 µm) foraminifer ooze, exclusively composed of cold water–mass taxa, including *Globigerina quinqueloba* and *Neogloboquadrina pachyderma* (FO ~11.3 Ma). The assemblage is undoubtedly winnowed, either from current erosion or suspension separation in a gravity flow. A small assemblage in Sample 181-1122C-58X-CC contains several *Globorotalia miotumida* (FO 13.2 Ma), numerous *Neogloboquadrina continuosa* (LO ~11 Ma), and *Paragloborotalia mayeri* (LO 10.8 Ma), indicating a late middle Miocene age (11–13.2 Ma, late Lillburnian–Waiauan Stages).

Sample 181-1122C-62X-CC heralds a return of planktonic foraminifers and contains *Globorotalia praemenardii* (LO ~13.2 Ma), *G. conica* (LO ~13 Ma), and one *Orbulina suturalis* (FO 15.1 Ma). These indicate a middle Miocene age (15–13.2 Ma, Lillburnian Stage). The evolutionary transition from *Globorotalia miozea* to *G. praemenardii* occurs in Sample 181-1122C-63X-CC, indicating an early middle Miocene age (~15.8 Ma, Clifdenian Stage). The lower 40 m of the hole extends back across the early to middle Miocene boundary, with the lowest Sample (181-1122C-68X-CC) containing numerous five-chambered *Globorotalia miozea* (FO 16.7 Ma), one *Globigerinoides bisphericus* (FO 17 Ma), and the first good specimens of *Globorotalia zealandica* (LCO 16.7 Ma), indicating a late early Miocene age (~16.7 Ma, mid- to late Altonian Stage) for the bottom of Hole 1122C.

Diatoms

Diatoms are present nearly throughout the whole recovered sequence except for the lowermost 34 m, which is characterized by silica diagenesis that led to dissolution of diatoms and formation of authigenic zeolites. In the cores above, preservation of diatoms varies (Table **T7**).

The upper Pleistocene sequence of turbidites is dominated by autochthonous, planktonic diatoms of the Bounty Trough surface waters, whereas the early Pleistocene turbidite and Pliocene contourite deposits below are dominated by reworked older diatoms from the Pliocene, Miocene, and Paleogene.

In the upper Pleistocene turbiditic sequence, down to the Brunhes/Matuyama boundary (i.e., 0–300 mbsf), autochthonous, planktonic diatoms provide three datums: the well-dated late Pleistocene shifts in abundance of *Hemidiscus karstenii* and *Actinocyclus ingens* and also the last occurrence of *Thalassiosira elliptipora* (Figs. **F16, F17;** Tables **T7, T8;** and Table **T4,** p. 63, in the "Explanatory Notes" chapter).

For the deposits below, a comparison with the biostratigraphic results from calcareous nannofossils, foraminifers, and the paleomagnetic reversal record showed that in the interval from Sample 181-1122B-52X-CC to 62X-CC (470 to 570 mbsf), the occurrences of *Denticulopsis dimorpha* (10.1–10.7 to 12.2 Ma) and *Simonseniella barboi* (1.2–1.8 to 12.5 Ma) fit with the middle Miocene age determined by these other methods. Here the planktonic foraminifers are also better preserved and more diverse, which suggests that this is a period of higher sedimentation rates, resulting in the preservation of at least the more robust

T7. Identification and abundance of diatoms, **p. 123.**

F17. Age-depth curve for Hole 1122C, **p. 58.**

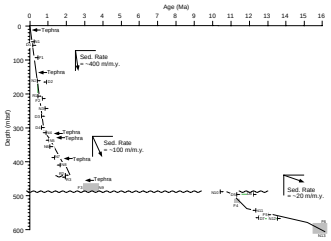

T8. Age of events in Ma, **p. 127.**

autochthonous planktonic diatoms. In the contourite sediments above and below (300–470 mbsf and 570 mbsf to core base), age-diagnostic, autochthonous diatoms cannot be found and dissolution-resistant reworked diatoms from Eocene and Oligocene strata are present (see discussion under paleoenvironment).

Radiolarians

The radiolarian biostratigraphy at Site 1122 is based on the examination of 81 core-catcher samples (Table T9). Throughout the turbidite and contourite units, radiolarians are sporadic and occur very rarely. However, radiolarian faunas in twenty samples are moderately well-preserved and provide useful age and paleoenvironmental information. Most samples between 0 and 402 mbsf yield common to abundant *Antarctissa denticulata, Antarctissa strelkovi, Lithelius nautiloides,* and *Saccospyris antarctica,* which represent subantarctic waters. The lower sandy units (>452 mbsf) are almost barren, except for Samples 181-1122B-62X-CC and 63X-CC.

The uppermost interval between Samples 181-1122C-1H-CC and 17X-CC (0–133 mbsf) is of late Pleistocene age (younger than 0.46 Ma), based on the LO of *Stylatractus universus* (0.46 Ma) in Sample 181-1121C-18X-CC (140.5 mbsf). This datum is well known and well established worldwide; however, in this section, *Stylatractus universus* occurs only sporadically. Rare, reworked forms of middle to upper Miocene species like *Cyrtocapsella japonica,* C. *tetrapera, Stichocorys peregrina,* and *Eucyrtidium calvertense* were observed in the upper part of the section.

Samples 181-1122C-48X-CC and 49X-CC yield common *Eucyrtidium calvertense* (LO 1.92 Ma) and 49X-CC also contains *Lithelius nautiloides* (FO 1.93 Ma). Therefore, the interval between 181-1122C-18X-CC and 48X-CC (140.5–432.4 mbsf) is dated as latest Pliocene to late Pleistocene (0.46–1.9 Ma). The FO datum of *Lithelius nautiloides* is apparently too high, resulting from reworking, because samples below 444 mbsf were barren or contained only rare radiolarians. Samples 181-1122C-62X-CC and 63X-CC yield common radiolarians including *Calocycletta* sp., *Lychnocanoma* sp., and *Cyrtocapsella tetrapera* of Miocene age.

T9. Identification and abundance of radiolarians, p. 128.

Paleoenvironment

Foraminifers

In the upper Pliocene–Quaternary section (Cores 181-1122A-1H to 181-1122C-53X; 0–478 mbsf), lithostratigraphic Subunits IA through IC consist of turbidite beds of graded, very fine sand to silt ("coarse beds"), deposited on the Bounty Channel levee by periodic turbidity currents, which are interbedded with thin beds of hemipelagic to pelagic mud ("fine beds") deposited from suspension during the intervening periods (Fig. F18).

Samples from the "fine beds" (e.g., Samples 181-1122A-3H-CC, 181-1122C-25X-CC, and 181-1122C-26X-2, 7–8 cm) have planktonic forms composing ~80%–98% of the foraminifers. The benthic foraminiferal assemblage (Table T6) is dominated by typical upper abyssal calcareous assemblages containing varying mixtures of fairly small *Trifarina angulosa, Epistominella exigua, Melonis barleeanum, Cassidulina carinata, Cibicides pachyderma, Oridorsalis umbonatus, Pyrgo murrhina, Quinqueloculina venusta,* and *Globocassidulina subglobosa*. The fine beds also contain a

F18. Summary of changing foraminiferal faunas, p. 59.

Litho-stratigraphic Unit			Planktonic Fauna	Benthic Fauna		
UNIT I	A to D	Turbidite-dominated	Normal, well-preserved, oceanic fauna	Deep-water assemblage with addition of small shelf and bathyal forms		Pliocene-Pleistocene
				Only deep-water assemblage		
UNIT II	A	Contourite-dominated	Large, thick-walled, oceanic fauna, few or no small forms	Only deep-water assemblage	Dissolution	
	B		Barren or rapidly buried fauna of small forms (winnowings) - minor reworked Oligocene	Barren or only deep-water assemblage		Miocene
UNIT III	A	Debris flows and coarse sediments	Variable oceanic fauna	Only deep-water assemblage		
	B		Normal oceanic fauna	Dominantly mid-shelf fauna (large and small) with minor deep-water assemblage		

few, small, shallow-water, benthic forms derived from "inner and mid-"shelf depths (e.g., *Elphidium advenum* and *E. charlottense*).

Samples from the "coarse beds" (e.g., Samples 181-1122A-7H-CC, 9X-CC, and 12X-CC) have planktonic forms comprising 75%–90% of the foraminifers. The benthic foraminiferal assemblage is dominated by small (mostly <0.2 mm) *Elphidium advenum, E. charlottense, Uvigerina dirupta, Miliolinella subrotundata, Nonionellina flemingi, Notorotalia,* and *Pileolina* spp. apparently displaced in with the turbiditic sand from "shelf" depths, and mixed with other deeper water bathyal or abyssal forms (e.g., *Trifarina angulosa, Melonis* spp., *Pullenia bulloides,* large *Globocassidulina* spp., and *Nuttallides umbonifera*) that may have either been picked up en route or have lived in the turbiditic sediment after it was deposited on the levee. The benthic foraminifers in these turbidites thus exhibit a mixed origin from inner shelf depths (e.g., *Pileolina* spp. and *Zeaflorilus parri*) through to abyssal.

The Quaternary planktonic foraminiferal assemblages in lithostratigraphic Unit I are dominated by a mix of small *Neogloboquadrina pachyderma, Globigerina quinqueloba,* larger *Globigerina bulloides, Globorotalia inflata,* and lower in the interval by *Globorotalia puncticuloides* and *G. crassula*. Some samples have a cooler water aspect with a greater dominance of small *N. pachyderma* and *G. quinqueloba* (e.g., Samples 181-1122C-26X-CC and 34X-CC); others have a slightly warmer aspect with the addition of a moderate number of large *Orbulina universa, Globorotalia crassula,* and *G. hirsuta,* and a greater percentage of large *Globorotalia inflata* or *G. puncticuloides* (e.g., Samples 181-1122A-7H-CC, 181-1122C-16X-CC, and 181-1122C-20X-CC).

In the lower part (lithostratigraphic Subunit IIA) of the Pliocene–Quaternary section (from Samples 181-1122C-47X-CC to 53X-CC), most of the planktonic assemblages are sparse and mainly composed of bigger, thicker-walled specimens with only a few, small, thin-walled forms present. It would seem that the planktonic assemblage is being affected by dissolution, with only the thicker-walled specimens and a few rapidly buried thinner-walled ones not being dissolved. The assemblages suggest that the Carbonate Compensation Depth (CCD) was possibly at a slightly higher level during this period than it was later in the Quaternary. Alternatively, corrosive cold-water flow may have been active.

The Miocene section (Cores 181-1122C-54X to 68X, 488 to 618 mbsf) contained foraminiferal assemblages that are predominantly partly recrystallized and poorly to moderately preserved. In the upper half of the interval (lithostratigraphic Subunit IIB), many of the fine sands are barren of foraminifers (e.g., Samples 181-1122C-54X-CC, 56X-CC, 59X-CC, and 61X-CC).

A light mud (Sample 181-1122C-55X-4, 22–24 cm) from this largely barren interval contains a rich assemblage of extremely small planktonic and benthic foraminifers, the result of winnowing from currents or suspension separation in a gravity flow. Its low-diversity planktonic assemblage with *Neogloboquadrina pachyderma* and *Globigerina quinqueloba* indicates cool water above. This sample also contains evidence (two minute specimens of *Chiloguembelina*) of reworking from Oligocene oceanic strata. A similar assemblage of dominantly small planktonic forms occurs in Sample 181-1122C-55X-CC, together with a sparse assemblage of deep-water benthic foraminifers, which is dominated by large *Nodosaria longiscata* and frequent *Oridorsalis umbonatus*.

Sample 181-1122C-55X-CC contains no planktonic foraminifers and a sparse deep-water benthic assemblage (e.g., *Bolivinopsis, Cibicidoides*

pachyderma, Eggerella bradyi, Globocassidulina subglobosa, Laticarinina pauperata, Melonis pompilioides, and *Oridorsalis umbonatus*). We conclude that the site was below the CCD and that all planktonic foraminifers dissolved before they settled on the bottom, whereas the benthic forms were preserved by rapid burial.

Foraminiferal assemblages are present throughout the lower half (lithostratigraphic Unit III) of this Miocene interval and contain rich, planktonic assemblages with a wide range of sizes. Temperate overhead water is indicated by the abundance of forms from the *Globorotalia miozea* and *Globorotalia zealandica* lineages. The almost total absence of orbulines argues against any subtropical influence.

Entirely deep-water benthic assemblages are present in Samples 181-1122C-62X-CC and 63X-CC (lithostratigraphic Subunit IIIA), but below this in Subunit IIIB there is a substantial component of "mid-shelf" (~50–100 m depth) benthic foraminifers. These benthic forms appear to be of similar age as the deep-water assemblage to which they have been added, although a late Oligocene or early Miocene age cannot be entirely ruled out. The unusual aspect of these allochthonous shallow-water benthic assemblages is the large size of many specimens (>0.25 mm) and their abundance (composing up to 90% of the benthic assemblage in Samples 181-1122C-66X-CC and 67X-CC). Although abrasion and breakage is evident in some specimens, others still have crisply preserved ornament and show little rounding. This suggests downslope transport by mass-flow mechanisms and no long-distance transport by strong bottom currents. The shallow-water assemblage is dominated by varying mixtures of *Notorotalia spinosa* and *Nonionella novozealandica,* a well-known New Zealand, lower Miocene association from middle shelf depths (~50–100 m). Other shallow-water components include *Anomalinoides fasciatus, A. macraglabra, Cibicides perforatus, C. notocenicus, Discorotalia tenuissima, Elphidium advenum, Kolesnikovella australis, Melonis maorica,* and *Siphonina australis.*

Thus the lower half (lithostratigraphic Subunit IIIB) of the Miocene interval has an allochthonous, planktonic-dominated assemblage that accumulated at similar abyssal depths as today and a large component of mostly benthic foraminifers derived from middle shelf depths.

Diatoms and Silica Diagenesis

In the upper Pleistocene section, the diatom assemblages are a mix of subantarctic and cosmopolitan, planktonic species with an additional input of local neritic and shallow-water species from the Bounty Trough head. The diatom valves are well preserved because of the high sedimentation rates of fine-grained, clastic terrigenous material. The sediment facies is mainly turbidites interbedded with thin hemipelagic sediments. The characteristic occurrence of diatom assemblages within these turbidites is that no diatoms are found in the quartz sand at the turbidite bases, whereas higher in the clayey part of the turbidite, autochthonous, planktonic diatoms occur together with species typical for more nearshore areas and with benthic diatoms, which must be derived from shallow, coastal areas. With the transition to nonturbidite sediments, these dislocated shallower water diatoms decrease in abundance.

The provenance of the diatoms is different in the underlying early Pleistocene turbiditic sequence and the Miocene–Pliocene contourite sediments (below 300 mbsf; Fig. F19), the latter being shaped by Antarctic Bottom Water (AABW). The average sedimentation rates deter-

F19. Provenance of diatoms in the Neogene, p. 60.

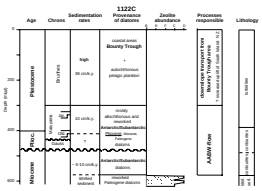

mined for these sediments are considerably lower than for the upper Pleistocene turbidite sequence above: approximately one-quarter lower for the lower Pleistocene turbiditic sequence and one-eighth to one-quarter lower for the contourite deposits. Here, only the relatively dissolution-resistant diatom valves are preserved. In these sediments, subantarctic/Antarctic diatoms of Pliocene and Miocene age are found as well as reworked Eocene–Oligocene species. Except for the middle Miocene section mentioned above, where the ages derived from diatoms agree with those derived from the calcareous microfossils, a large part of the assemblage has to be considered allochthonous or reworked, brought in by AABW.

The changing sedimentation rates and the changing provenance of the diatoms indicate that the dominating influence of the AABW, which is characteristic through most of the Neogene sediments at this site, is overcome by turbidite sedimentation during the late Pleistocene. This change in sedimentation rate and provenance of diatoms may reflect an increased late Pleistocene uplift of South Island New Zealand, which has been reported to reach 6 mm/yr for the Marlborough ranges (e.g., van Dissen and Yeats, 1991).

Radiolarians

Upper Pliocene to Pleistocene radiolarian faunas obtained from the section (Cores 181-1122A-1H to 181-1122C-49X) are characterized by the consistent occurrences of abundant *Antarctissa denticulata, Antarctissa strelkovi, Cycladophora davisiana davisiana, Lithelius nautiloides,* and *Saccospyris antarctica*. These species are representative of Antarctic/subantarctic affinity. In addition, there is common to abundant occurrence of *Cycladophora davisiana davisiana* in Samples 181-1122A-1H-CC, 181-1122A-6H-CC, 181-1122B-1H-CC, 181-1122C-14X-CC, and 181-1122C-35X-CC. It is well known that the relative abundance curve of *Cycladophora davisiana* corresponds well with oxygen isotope curve (Morley and Hays, 1979).

PALEOMAGNETISM

Core archive-halves from Holes 1122A and 1122C were measured on the shipboard pass-through cryogenic magnetometer. Declination, inclination, and intensity of natural remanent magnetization (NRM) and 20-mT alternating field (AF) demagnetization steps were measured at 5-cm intervals. The first few cores of each hole were also measured at a 10-mT demagnetization step; this step added little extra information and, because of time constraints, only the 20-mT step was continued. In situ tensor tool data were collected for Cores 181-1122A-3H through 8H and 181-1122C-3H through 13H. Tensor tool data were good for APC cores from Hole 1122C, but a problem with the shipboard pass-through cryogenic magnetometer prevented the use of declination for polarity determination in the APC cores. Therefore, only inclination could be used to determine magnetic polarity of Holes 1122A and 1122C. At least two discrete oriented samples were collected from the working half of each core interval for progressive AF and thermal demagnetization and rock magnetic studies. Whole-core magnetic susceptibility was measured on all cores using a Bartington susceptibility loop on the automated multisensor track (MST). For the purposes of this initial report, only Hole 1122C is discussed in detail below.

Magnetic susceptibility and intensity of magnetic remanence define several zones of magnetic behavior in Hole 1122C (Fig. F20). The upper 110 mbsf have high susceptibility ($0.5^{-1} \times 10^{-3}$ SI) and high intensity of magnetic remanence. NRM values averaged 0.1–0.2 A/m and dropped only slightly to 0.05–0.1 A/m after 20 mT of AF demagnetization. Between 110 and 260 mbsf, average susceptibility values dropped to 2×10^{-4} SI, but average remanence values remained high for both NRM and 20-mT levels. Beneath 260 mbsf, susceptibility and remanence values were both low (2×10^{-4} SI and 10^{-4} A/m, respectively), except for the interval between 320 and 360 mbsf in the vicinity of two tephra horizons, where susceptibility and NRM values increased to 5×10^{-4} SI and 8×10^{-2} A/m respectively. These zones defined by magnetic susceptibility and intensity of remanence are roughly equivalent to lithologic changes in the core (see "Lithostratigraphy," p. 4).

Paleomagnetic Behavior and Rock Magnetism

NRM measurements displayed consistent, steeply positive (downcore) inclinations ranging between +70° and +80°, consistent with a drill-string overprint induced during coring. The single 20-mT AF demagnetization step proved very effective in removing the overprint and elucidating a polarity reversal stratigraphy (Fig. F21). Intensity of magnetization was strong enough that discrete samples could be subjected to stepwise AF demagnetization up to 80 mT in the shipboard pass-through cryogenic magnetometer (Fig. F22). The drilling-induced overprint was only observed in reversed polarity samples (e.g., Fig. F22A, F22B, F22G, F22H, F22I), and it only accounted for a very small percentage of the NRM intensity. Further stepwise AF demagnetization demonstrated that all samples had reached a stable primary remanence direction by 20 mT of demagnetization (Fig. F22). Several samples from Hole 1122C demonstrate radial remagnetization from demagnetization attempts with AF fields above 50 mT (e.g., Fig. F22B, F22C). Figure F23 shows acquired isothermal remanence magnetizations (IRM) to saturation (SIRM) and backfield SIRM. Most of the samples subjected to SIRM are magnetically "soft" and were saturated by an applied field of 300 mT. However, samples from 450–580 mbsf did not saturate fully until applied fields were above 700 mT (Fig. F23C). Despite this difference in SIRM, coercivity of remanence (B_{cr}) was between 25 and 75 mT in all cases. Samples from between 300 and 400 mbsf are particularly uniform in rock magnetic character, with an SIRM of 300 mT and B_{cr} of 25 mT. AF and thermal demagnetization of the SIRM demonstrates two types of behavior caused by variations in magnetic mineralogy and magnetic grain-size. Samples from the upper 200 mbsf of Hole 1122C have very low unblocking temperatures (350°–400°C) and "soft" but distributed coercivity spectra (Fig. F24A, F24B). Beneath 200 mbsf, unblocking temperatures are mostly higher (~600°C) (Fig. F24C, F24E, F24F).

The "soft" SIRM, low B_{cr}, distributed unblocking temperatures up to ~600°C, and distributed coercivity spectra demonstrate that magnetite of distributed grain size is the main carrier of remanence in samples from beneath 200 mbsf in Hole 1122C. In each case a secondary component of magnetization is clear, from a variable but small loss of intensity between 320° and 360°C in the unblocking temperature spectra (Fig. F24C, F24E, F24F). This may be a result of the presence of sulfide minerals, which, in turn, may also explain the slight "hardness" of SIRM acquisition in some cases (Fig. F23). Above 200 mbsf, however,

F20. Magnetic susceptibility and NRM intensity from Hole 1122C, p. 61.

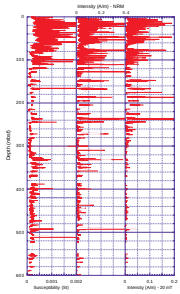

F21. Whole-core inclination and polarity interpretation of Hole 1122C, p. 62.

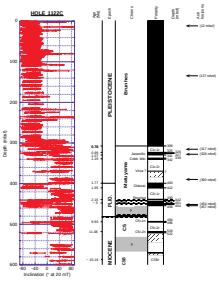

F22. Vector component diagrams of AF demagnetization behavior, p. 63.

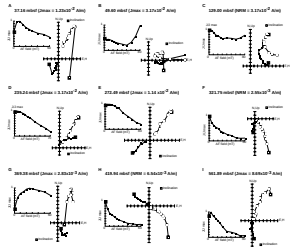

F23. Isothermal remanent magnetization, p. 64.

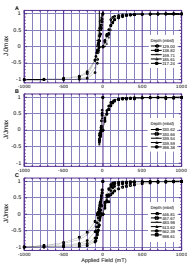

F24. Plots of normalized intensity of magnetization, p. 65.

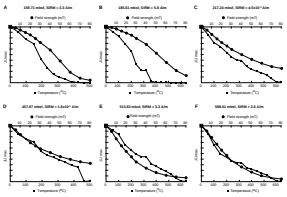

the carrier of magnetic remanence is more difficult to isolate. The low unblocking temperatures rule out magnetite as a magnetic carrier and suggest that a sulfide mineral might be the sole carrier of remanence. However, the IRM acquisition curve is saturated at low applied fields (Fig. F23A), and B_{cr} values are between 50 and 75 mT.

Magnetostratigraphy

After 20 mT of demagnetization, the inclination record from Hole 1122C is well defined and allows a clear pattern of magnetic polarity to be established (Fig. F21). Two zones of characteristic polarity behavior are identified: above 309 mbsf, polarity is normal except for short excursions that do not have fully reversed inclinations. Beneath 309 mbsf, polarity alternates between normal and reversed intervals but is dominantly reversed. In the XCB cores (beneath 110 mbsf), polarity interpretation is complicated by the low recovery. It was not possible to determine a characteristic polarity pattern beneath 520 mbsf. Despite poor recovery, most of the polarity transitions occur in recovered intervals rather than in "core breaks." Furthermore, polarity transitions occur within intervals of continuous sedimentation rather than at stratigraphic breaks identified in the core (see "Lithostratigraphy," p. 4). Several key biostratigraphic datum events (see "Biostratigraphy," p. 13) define a unique correlation between the magnetic polarity record of Hole 1122C and the Geomagnetic Polarity Time Scale (GPTS) (Berggren et al., 1995; Cande and Kent, 1995) (Fig. F25).

The uppermost 309 mbsf of Hole 1122C is of normal polarity and the last occurrences (LO) of *Globorotalia puncticulinoides* (F2, 0.7–0.8 Ma), *Actinocyclus ingens* (D3, 0.64 Ma), and *Thalassiosira elliptipora* (0.65–0.7 Ma) at 213, 265, and 300 mbsf, respectively, suggest that this interval is entirely within the Brunhes normal chron (C1n). Several short excursions are recognized above 309 mbsf (Fig. F21). These may correlate with intervals of depressed NRM and 20-mT intensity (Fig. F20). Further paleomagnetic and dating work may define them well enough to correlate with polarity excursions known from high-resolution terrestrial records (e.g., Worm, 1997) and high-resolution marine intensity records from the equatorial regions (e.g., Meynadier et al., 1995).

Between 309 and 487 mbsf, nannofossils provide the key datums for correlation (Fig. F25). The FO of *Gephyrocapsa parallela* (0.95 Ma, N4) and *Reticulofenestra asanoi* (1.06 Ma, N5) confine the mainly reversed polarity with short normal polarity intervals, between 309 and 350 mbsf to the upper part of the Matuyama Chron (C1r). The normal polarity intervals between 325 and 331 mbsf are correlated with the Jaramillo Subchron (C1r.1n) and the lower normal polarity event (339–342 mbsf) is correlated with the Cobb Mountain Event. Between 342 and 442 mbsf the normal-reversed-normal-reversed (N-R-N-R) polarity pattern is correlated with the lower part of the Matuyama Chron. The occurrence of *Gephyrocapsa* (large) (N6–N7, 1.1–1.36 Ma) between 356 and 388 mbsf and the FO of *Gephyrocapsa* (medium) (N8, 1.66 Ma) at 410 mbsf confines the uppermost reversed polarity interval of the N-R-N-R pattern to Subchron C1r.2r. A short excursion at ~370 mbsf may correlate with the Vrica or younger Olduvai Subchron (Baksi, 1995). Two radiolarian datums (LO *Lithelius nautiloides,* 1.93 Ma and FO *Eucyrtidium calvertense,* 1.92 Ma) confine the remaining N-R-N pattern to Subchrons C2r.1n (Reunion Subchron), C2r.1r, and Chron C2n (Olduvai Chron), respectively.

F25. Age model and correlation of Hole 1122C magnetic polarity zonation, p. 66.

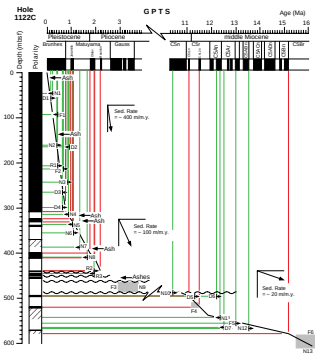

Foraminifer (F3) and nannofossil (N9) faunas beneath 461 mbsf suggest that a disconformity at this level separates the underlying lower Gauss Chron–age strata from the overlying Matuyama Chron–age strata. At 487 mbsf, all microfauna and microflora identify a major stratigraphic disconformity with underlying strata of middle Miocene age (see **"Biostratigraphy,"** p. 13). Magnetic polarity stratigraphy in this interval (442–487 mbsf) suggests an even more complex situation, with additional stratigraphic discontinuities, as the Gauss Chron (C2An) is of mostly normal polarity, yet in Hole 1122C the magnetic polarity at this level is mostly reversed. Beneath the disconformity at 487 mbsf, foraminifers (*Neogloboquadrina continuosa, N. pachyderma,* and LO of *Gr. praemenardii,* F5), nannofossils (LO *Coccolithus miopelagicus,* N10, FO *Calcidiscus macintyrei,* N11, and LO *Sphenolithus heteromorphus,* N12), and diatoms (LO of *Denticulopsis dimorpha,* D6, and FO *Simonseniella barboi,* D7) all suggest that the interval between 487 and ~575 mbsf ranges in age between 10 and 12.5 Ma. A characteristic magnetic polarity reversal pattern of two short normal events within an interval of reversed polarity allows better definition of age as Chron C5r is the only distinct interval of reversed polarity in this section of the GPTS. Chron C5r contains two short normal polarity subchrons (C5r.1n and C52.2r) that are correlated with the two short normal polarity intervals at 494–496 mbsf and 519–522 mbsf, respectively. Foraminifers (co-occurrence *of Gr. zealandica* and *Gr. miozea,* F6) and the LO of the nannofossil *C. premacintyrei* (N13) suggest that the base of Hole 1122C is older again (~16–17 Ma). The basal 20 m of the hole is of reversed polarity and may correlate with Chron C5Br. However, poor recovery makes this correlation uncertain.

From the age model presented in Figures **F21** and **F25,** average sedimentation rates are on the order of 400 m/m.y. for Subunits IA, IB, and IC (see **"Lithostratigraphy,"** p. 4) and 100 m/m.y. for Subunits ID and IIA. Average sedimentation rates could not be determined accurately for the lowermost part of Hole 1122C (lithostratigraphic Subunits IIB, IIIA, and IIIB) although they are likely to be an order of magnitude lower (~20 m/m.y.; Fig. **F25**). Tephras were identified at seven horizons in Hole 1122C (Figs. **F21, F25;** see **"Lithostratigraphy,"** p. 4). Dating of these will provide important additional information to help refine the magnetobiostratigraphic age model presented here. The tephra at 12 mbsf has already been identified as the Kawakawa Tephra (Carter et al., 1995). Using the average sedimentation rates from above and the stratigraphic position of the remaining tephra horizons, the following correlations with tephras reported from onland studies in New Zealand are possible: the tephra at 137 mbsf may correlate with the Rangitawa Tephra (Pillans et al., 1996); and the tephras at 317, 328, and 390 mbsf with the Kaukatea, Potaka, and Pakihikura Tephras, respectively (Pillans et al., 1994). Dating of the two tephras at 454 and 457 mbsf will provide important constraints on this interval of Hole 1122C, as the age is, as yet, poorly constrained.

Environmental Magnetism

Differences in susceptibility and intensity of magnetic remanence (NRM and 20 mT), combined with magnetic mineralogical variations (identified by IRM, SIRM, and AF and thermal demagnetization behavior), demonstrate changes in the magnetic character at depth in Hole 1122C from changes in sedimentologic processes and sources. It is clear that in Unit I the susceptibility record is driven primarily by the sandier

interbeds of the turbidite sequence, whereas the intensity of magnetic remanence is held by similar minerals of similar grain size in both the sandy and muddy interbeds. Such a record suggests a preferential loss of the coarser sediments in the XCB coring process as compared with APC coring where both coarse- and fine-grained interbeds are recovered. A change in intensity of remanence (at 20 mT of demagnetization) is noted beneath ~260 mbsf. This is coincident with the boundary between lithostratigraphic Subunits IC and ID. Thermal demagnetization experiments show that this is most likely because of a change in magnetic mineralogy. An increase in fine-grained magnetite beneath 260 mbsf suggests a possible change in sediment source. Variations in intensity of magnetic remanence in the upper 100 mbsf of Hole 1122C (Fig. F20) suggests fluctuations in sedimentation rates not recognized in the lithostratigraphic record and/or variations in intensity of the geomagnetic field at time of deposition.

COMPOSITE DEPTHS

A composite section for Site 1122, constructed using data from Holes 1122A, 1122B, and 1122C, yielded overlapping records for the upper ~83 meters composite depth (mcd). At least one gap in continuity exists in this composite record at ~73 mcd. Three high-resolution data sets proved useful for correlation at this site: magnetic susceptibility (MS) and gamma-ray attenuation porosity evaluator (GRAPE), both measured on whole cores on the MST, and spectral reflectance at 550 nm (the center wavelength of the range measured), measured on split cores. The wavelength of variation in natural gamma-ray intensity (NGR) is too broad to be useful for hole-to-hole correlation at this site. Magnetic susceptibility proved the most reliable measurement for correlation, whereas GRAPE and reflectance records primarily provided confirmation of ties. Exceptions are (1) ties from Cores 181-1122C-3H to 181-1122A-2H and from 181-1122C-4H and 181-1122A-3H, both based on GRAPE density records, and (2) the correlation between Cores 181-1122B-1H and 181-1122C-1H, based on reflectance variability. The final composite section is illustrated in Figure F26.

Hole-to-hole correlation at the top of the sedimentary sequence, including determination of the mudline, presented a particular challenge at Site 1122. Core 181-1122C-1H is undoubtedly a mudline core, whereas Core 181-1122B-1H virtually filled the core liner. A thick sand recovered in Core 181-1122C-1H is represented by high MS and GRAPE density values. This sand was apparently washed out or disturbed in Hole 1122B, an inference based on anomalously low GRAPE density values near the equivalent depth of the sand layer in Core 181-1122B-1H. Excluding this sand layer, magnetic susceptibility and GRAPE density data do not vary enough to allow correlation. However, if one assumes that the top of Core 181-1122B-1H corresponds to the mudline recovered at the top of Core 181-1122C-1H, reflectance records agree well between Cores 181-1122B-1H and 181-1122C-1H. Based on reflectance data, we placed the top of Core 181-1122B-1H at the mudline. An alternative relationship, though less probable, is that the data from Core 181-1122C-1H represent an interval of strata recovered at some ill-defined level above the top of Core 181-1122B-1H. To calculate depths for this alternative relationship, 2.41 m has to be added to all mcd depths in Tables T10 and T11 (both also in ASCII format) except those depths for Core 181-1122C-1H. The relationship advocated here, with

F26. Composite sections, p. 68.

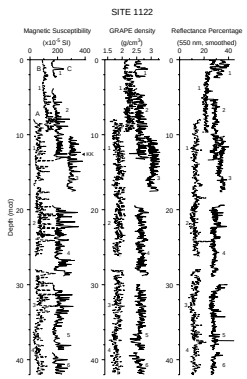

T10. Composite depth section, p. 131.

T11. Splice tie points, p. 138.

the mudline in both Cores 181-1122B-1H and 181-1122C-1H, places the Kawakawa Tephra at ~12.6 mcd in the splice in Core 181-1122A-H1 (Fig. F26).

Two coring irregularities occurred at Site 1122. First, Core 181-1122A-1H was shot when the end of the APC piston had already penetrated the topmost sediment by ~8 m, rather than close to the mudline. This large depth offset of Core 181-1122A-1H is based on convincing correlations via MS, GRAPE, and color reflectance. Additionally, the Kawakawa Tephra (Fig. F26) is found in both Holes 1122A and 1122C at levels agreeing with the composite section correlation (Fig. F26). Second, the top of Core 181-1122C-3H represents an interval that overlaps with the base of Core 181-1122C-2H, including a repeat recovery of the Kawakawa Tephra. The recoring of this interval may be related to advancing the drill string based on core recovery following retrieval of Core 181-1122C-2H.

Two correlations in the composite depth section are based on only small overlaps (1) between Cores 181-1122C-3H and 181-1122A-2H, and (2) between Cores 181-1122C-4H and 181-1122A-3H (Fig. F26). These correlations, based on GRAPE density records, are the least certain overlaps in the composite section. A definite gap exists between Cores 181-1122A-8H and 181-1122C-9H. In this case, we assigned the top of Core 181-1122A-8H a composite depth equal to the base of Core 181-1122C-9H.

Downhole core offsets relative to mbsf depths do not follow a model of 10% stretch between the mbsf and mcd depth scales in the composite section. Instead the offset is ~6–8 m for the extent of Hole 1122A and 2–6 m in Hole 1122C below Core 181-1122C-3H (Fig. F27), with offsets following a slight negative slope below ~20 mbsf. Table T10 contains the offsets between the mbsf and mcd scales resulting from composite section construction.

The spliced record, based primarily on MS and GRAPE data (Fig. F28), extends to 83 mcd. Wherever possible, splice tie points (Table T11) were picked at well-defined maxima or minima where the overlap in data from Holes 1122B and 1122C are correlated. Typically, parameter values differed by less than 10% at tie levels. In all cases, ties were selected so that the spliced record was as free from noise (high-frequency variability) as possible.

F27. Downhole depth offsets, p. 70.

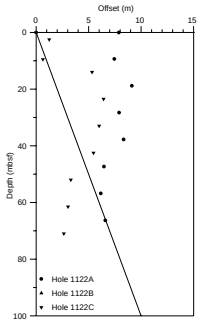

F28. Spliced record, p. 71.

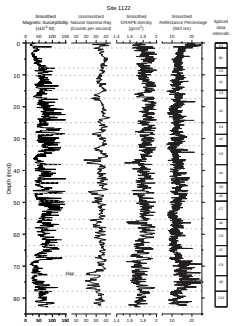

AGE MODELS AND SEDIMENTATION RATES

Biostratigraphic levels with age significance at Site 1122 were derived from LO, FO, acme, LCO, and FCO events, using diatoms, radiolarians, nannofossils, and foraminifers. The 29 levels are shown in Table T8. To show the principal trends, the assembled age-depth data are plotted together with magnetic polarity datums in Figure F17. FO events may have been estimated to be too shallow, based on limited sampling. The position of arrows in Figure F17 reflects the possibility that further work may extend these datums downhole. Last occurrence events may be too deep, again as a result of the limited sampling interval. The position of arrows in Figure F17 reflects the possibility that further work may extend these datums uphole. The solid line in Figure F17 shows the preferred age depth model using magnetic polarity constrained by the biostratigraphic datums (see "Paleomagnetism," p. 20). Given the fact that the sequence is dominated by turbidites down to ~400 mbsf, the scatter of event data is surprisingly low. Hence, average sedimenta-

tion rates may be expressed with relatively long linear segments. This observation suggests that any reworking of microfossil marker events was relatively instantaneous. An ~5-m.y. hiatus at 490 mbsf separates middle Miocene strata below from early Pliocene strata above. Below the hiatus, middle Miocene (compacted) sedimentation rates of lithostratigraphic Unit III and Subunit IIB were low, varying between 50 and 5 m/m.y. The late Miocene pelagic mud and laminated sand (contourite deposit), classified as the lower part of Unit IIA, has a much lower sedimentation rate of 2 m/m.y. Early Pliocene net sedimentation is also of low rate but poorly constrained. The sedimentation rate accelerated to ~100 m/m.y. from the latest Pliocene to early Pleistocene and became very fast (400 m/m.y.) in the middle and late Pleistocene when most of the Bounty Fan levee was deposited at this site.

Sediment decompaction and accumulation rates were assessed using 124 porosity measurements from Hole 1122C (see **"Physical Properties,"** p. 32). These were analyzed for trends, using the programs DEPOR and BURSUB (Stam et al., 1987; Gradstein et al., 1989). Coarser grained lithostratigraphic Subunits IA, IB, IIIA, and IIIB were decompacted to a greater extent, relative to the middle, finer grained Subunits IC, ID, IIA, and IIB. Next, compacted and restored rates of sedimentation were derived, with the age intervals slightly smoothed; these are shown in Table **T12.** In lithostratigraphic Unit III, decompaction resulted in an 80% increase of rates, from 50 to 80 m/m.y. Decompaction had negligible effect on sedimentation rates of younger strata. This is in accord with the measured porosities in the basal siltstones, showing accumulation rate values ~60% lower than stratigraphically higher units. It must be remembered that this decomposition was performed on data from the preferentially preserved fine material; the coarse (and less compactible) sand turbidites were washed away during drilling or were not subjected to compression testing. The results in Table **T12** are thus biased toward high values.

T12. Compacted and restored rates of sedimentation, **p. 139.**

Backtracking and Paleoceanography

The character of basement on multichannel seismic lines across Site 1122 and gravity and magnetic survey data (Davey, 1993; Carter et al., 1994) demonstrate that the distal part of the Bounty Trough is situated on oceanic crust in over 4 km of water. The abyssal ocean floor of the Bounty Fan is part of the most distal southwest Pacific Ocean, which started opening before marine magnetic Anomaly 32 (late Campanian) (Stock and Molnar, 1987). Anomaly 32 is mapped adjacent to Campbell Plateau, Bounty Trough, and Chatham Rise. The Bounty Fan Site 1122 itself is situated in the geomagnetic quiet zone, with an estimated age of ocean basement around 85 Ma (Lawver and Gahagan, 1994).

According to recent interpretations (Carter et al., 1994), the Bounty Trough is a failed and sediment-starved rift, at right angles to the Southwest Pacific Ocean spreading basin. The Bounty Trough lies between the continental blocks of Campbell Plateau to the south and Chatham Rise to the north. Drilling on the southern block has recovered a sequence of middle to upper Cretaceous coal measures and shallow marine terrigenous clastics, unconformably overlying metamorphic basement. Similar and coeval strata are inferred for the northern block (Raine et al., 1993). The Cretaceous sediments may be interpreted as synrift strata, formed during regional subsidence on a passive margin, adjacent to the rifted and opening Southwest Pacific Ocean.

The thermal history of the distal Southwest Pacific oceanic crust constrains the subsidence history and sediment accommodation space at Site 1122. Figure F29 sketches the backtrack history, based on a ridge crest age at the location of Site 1122 at 85 Ma, which is slightly older than Anomaly 32, and on the observed present-day water depth at the site of nearly 4500 m. Initial ocean sediments at the site are postulated to be Late Cretaceous through Paleocene siliceous pelagic clays (see "Lithostratigraphy," p. 3, in the "Site 1121" chapter). The presence of rare, reworked Oligocene nannofossils, diatoms, and planktonic foraminifers in middle Miocene strata at Site 1122 indicate that deep marine Oligocene strata also formed in the vicinity of the site. Regional sedimentation rate curves, considered representative for the Chatham Rise and part of the Campbell Plateau, show sustained sedimentation through the Late Cretaceous, reduced Paleocene–Eocene sedimentation, and a hiatus in the Oligocene through the early Miocene (fig. 3.2 in Wood et al., 1989). Hence, Oligocene fossils may have been transported from the New Zealand paleo-shelf.

From the seismic profile across Site 1122, the pre-middle Miocene ocean sediments are ~1 km thick. Figure F29 also shows the >130-m-thick middle Miocene marine silt and nannofossil ooze resting unconformably on older strata and the >490 m of uppermost Pliocene–Pleistocene fine sands and nannofossil ooze unconformably overlying the middle Miocene sediments. The rapid, late-stage sedimentation, beginning in the Miocene and steadily increasing thereafter, reflects the uplift of the Southern Alps in New Zealand. This shed an enormous volume of terrigenous material on the nascent shelf, slope, and rise to the east (Wood et al., 1989).

The combined evidence supports an oceanic history at the site that traces to ~85 Ma, pre-Anomaly 32 time. The abundance of shallow marine microfossils observed at some levels in the Pleistocene turbidites and middle Miocene drifts (see "Biostratigraphy," p. 13) may be explained by geologic reworking, as part of the slow and inexorable fill of Bounty Trough, estimated to have taken at least 200 m.y. at the present rate of sedimentation (Carter et al., 1994).

F29. Sketch of oceanic subsidence history of Site 1122, Bounty Fan, p. 72.

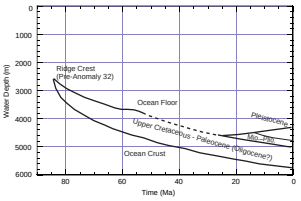

INORGANIC GEOCHEMISTRY

Interstitial Water

We collected interstitial water from 30 samples at Site 1122: 10 from Hole 1122A at depths ranging from 5.90 to 117.20 mbsf, and 20 from Hole 1122C at depths ranging from 67.40 to 591.80 mbsf (Table T13, also in ASCII format). One interstitial-water sample was taken from each core in the upper 100 mbsf. From 100 mbsf to the bottom of the hole, every third core was sampled. Samples from Holes 1122A and 1122C are plotted together in Figure F30. Stratigraphic correlation based on high-resolution data of magnetic susceptibility, GRAPE density, and spectral reflectance demonstrate that ~8 m of the upper part of Hole 1122A are missing (see "Composite Depths," p. 24). Comparison between the interstitial-water concentrations of the first sample of Hole 1122A and normal seawater values supports this conclusion. In general, the concentrations of the uppermost samples are close to the seawater composition because of the dominant water exchange at the seawater-sediment interface. The uppermost sample of Hole 1122A (5.90 mbsf) shows a large offset from the seawater values, suggesting that it origi-

T13. Summary of interstitial-water geochemistry, p. 140.

F30. Depth profiles of interstitial-water constituents at Site 1122, p. 73.

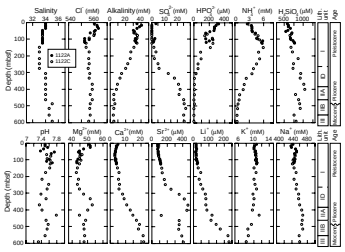

nated from a depth greater than 5.90 mbsf (see "Composite Depths," p. 24).

Salinity, Chloride, pH, and Sodium

Salinities of the interstitial-water samples show a decreasing trend from 5.95 to 272.70 mbsf, and then remain virtually constant down to 460.30 mbsf (Fig. F30). The salinity decrease results from the removal of sulfate by bacterial reduction. The local maximum (35.0) was found at 487.40 mbsf. The salinity increase in the lower part of Hole 1122C reflects the enrichment of major ion concentrations including calcium, magnesium, and sodium, as described below.

The chloride (Cl^-) concentration shows a small increase from 560 mM at 5.90 mbsf to the maximum (563 mM) at 34.20 mbsf (Fig. F30), then decreases to 554 mM at 147.90 mbsf and remains between 555 and 559 mM to the bottom of the hole. The chloride decrease seems to parallel the behavior of salinity, which has also been observed at Site 1119 (see "Inorganic Geochemistry," p. 21, in the "Site 1119" chapter). However, the reduction of chloride may not be caused by the freshwater input, but is probably the result of charge balance control accompanied by complete sulfate utilization.

Interstitial water pH values show a highly variable pattern, ranging from 7.32 to 7.79 (Fig. F30). The highest pH (7.79) occurs at 431.40 mbsf, which coincides with the concentration anomalies of magnesium, strontium, potassium, and silica.

Concentrations of sodium (Na^+) follow a similar trend to the chloride concentrations and vary from 438 to 468 mM (Fig. F30).

Alkalinity, Sulfate, Ammonium, and Phosphate

Alkalinity, sulfate, phosphate, and ammonium concentrations are strongly controlled by the availability of organic matter for bacterial degradation. The alkalinity of interstitial water decreases with depth down to 431.40 mbsf and remains almost constant toward the bottom of the hole (Fig. F30). The small variation at ~100 mbsf is caused by the depth offset between Hole 1122A and Hole 1122C (see "Composite Depths," p. 24). The alkalinity maximum at 15.20 mbsf represents the interval of the most intense sulfate reduction. The increase in alkalinity is the result of the production of bicarbonate during bacterial degradation of organic matter, primarily by sulfate reduction. The almost constant alkalinity between 45.10 and 147.90 mbsf coincides with complete sulfate reduction and the onset of methanogenesis. The linear decrease in alkalinity down to 431.40 mbsf presumably is caused by carbonate recrystallization and/or silicate reconstitution processes, which use the bicarbonate ion from interstitial water (Gieskes, 1974).

The sulfate (SO_4^{2-}) concentration decreases from 3.3 mM at 5.90 mbsf to 0 mM between 15.20 and 122.00 mbsf, followed by an increase to ~26.5 mM at 514.80 mbsf (Fig. F30). Below this depth, sulfate remains almost constant. The sulfate profile is governed by several factors, of which the most important are the abundance (and/or availability) of organic matter and the sedimentation rate. Bacterially controlled sulfate reduction processes have completely depleted sulfate in the pore waters down to ~150 mbsf, resembling nearshore settings with high organic carbon contents and higher bulk accumulation rates such as the Gulf of California (Gieskes et al., 1982) or the Peruvian margin (Suess, von Huene, et al., 1988). The complete utilization of sulfate in

the interstitial waters is consistent with the high methane level, as sulfate reduction precedes methane formation during diagenesis of organic matter (see "Organic Geochemistry," p. 30). High sulfate levels probably represent the original sulfate concentration that has not been used by bacteria, possibly because of the lack of enough metabolizable organic matter below lithostratigraphic Unit I (see "Lithostratigraphy," p. 4). In addition, the comparably low sedimentation rate (see "Age Models and Sedimentation Rates," p. 25) may have allowed significant amounts of sulfate to diffuse downward and replenish the sulfate reservoir used by bacteria.

Ammonium (NH_4^+) concentrations remain almost constant down to 53.20 mbsf, then increase to a maximum of 5.90 mM at 147.90 mbsf (Fig. F30). Below 53.20 mbsf, ammonium values steadily decrease down to 431.40 mbsf and then remain constant to the bottom. An increase of the ammonium concentration reflects the intensive bacterial degradation of organic matter, whereas a decrease indicates the results of ion exchange reactions on the surfaces of clay minerals and/or the subsequent incorporation into interlayers of diagenetically formed clay minerals (Gieskes, 1981).

The phosphate (HPO_4^{2-}) concentrations decrease with depth down to 305.90 mbsf (Fig. F30). Below 305.90 mbsf, the concentrations are relatively constant, but decrease slowly with depth. This trend indicates rather strong first-order removal, suggesting a diagenetic uptake of dissolved phosphate, most likely into sedimentary mineral phases.

Calcium, Magnesium, and Strontium

Calcium (Ca^{2+}) concentrations initially decrease from a subsurface value of 4.9 to 3.5 mM at ~100 mbsf, because of carbonate precipitation resulting from the buildup of alkalinity during sulfate reduction (Fig. F30). The absence of SO_4^{2-}, high alkalinity, and high Mg^{2+}/Ca^{2+} ratios may provide a favorable geochemical environment for dolomite formation (Baker and Kastner, 1981). Between ~300 and ~500 mbsf, Ca^{2+} concentrations increase strongly up to 18.9 mM.

The profile of magnesium (Mg^{2+}) shows high concentrations in the upper 25 mbsf of Hole 1122A (Fig. F30). High Mg^{2+} values have been observed almost ubiquitously in anoxic environments and are thought to result from the desorption of Mg^{2+} from solid phases in rapidly accumulating sediments (Gieskes et al., 1982). From ~25 mbsf, Mg^{2+} decreases with depth down to 272.70 mbsf, which indicates precipitation of dolomite. Between 300 and 450 mbsf, a distinct Mg^{2+} anomaly occurs. Concentration variations of these elements may be influenced by diagenetic controls within this lithologic unit or diffusive transport by fluid movement within this interval.

Dissolved strontium (Sr^{2+}) concentrations increase slightly from 75 µM at 5.90 mbsf to 173 µM at 243.70 mbsf and then increase rapidly to a maximum of 466 µM at 370.40 mbsf (Fig. F30). The Sr^{2+} values remain relatively constant throughout the lower part of Hole 1122C. Increasing strontium concentrations in interstitial waters may originate either from the recrystallization of biogenic carbonate (the associated strontium concentration decrease in the recrystallizing carbonate may be more than one order of magnitude) or the alteration of tephras. The maximum Sr^{2+} concentrations occur at the same level as the Mg^{2+} maximum, which indicates an additional input of these two elements into this interval. The change of the Sr^{2+} gradient at ~460 mbsf coincides

with the lithologic boundary between Subunit IIA and IIB (see "Lithostratigraphy," p. 4).

Dissolved Silica, Potassium, and Lithium

Dissolved silica (H_4SiO_4) concentrations increase gradually from 575 µM at 5.90 mbsf to 803 µM at 591.80 mbsf (Fig. F30). The dissolved silica increases indicate progressive diatom dissolution. However, the relatively large scatter of the silica data may reflect the fairly heterogeneous sediment composition.

Potassium (K^+) concentrations decrease from 10.6 mM at the subsurface to 6.5 mM at the bottom of the core (Fig. F30). This indicates large-scale removal of K^+ into clay minerals that are forming within the sediments.

The dissolved lithium (Li^+) concentrations increase slightly from 18 µM at 5.90 mbsf to 87 µM at 399.50 mbsf and increase steeply to a maximum of 231 µM at the bottom of the hole (Fig. F30). Because the Li^+ concentration is related to the biogenic silica content (Gieskes, 1981), the general increase indicates release of Li^+ during diatom dissolution and silica transformation. The abrupt increase in Li^+ concentration in the lower part of the hole, which corresponds to the boundary between Subunits IIA and IIB (see "Lithostratigraphy," p. 4), reflects an additional source of Li^+ into the pore fluids, because the dissolved silica concentrations decrease in this interval.

Summary of Interstitial Water Results

The primary controlling factor on the interstitial-water chemistry at Site 1122 is sulfate reduction and methanogenesis, which governs alkalinity, phosphate, and ammonium concentration. In contrast to the complete utilization of sulfate in the upper part of the core, the increased sulfate levels in the middle of the section represent the original sulfate concentrations during sediment deposition, possibly preserved because of a lack of sufficient metabolizable organic matter and low sedimentation rates. Other important chemical profiles are magnesium and calcium concentrations, from which we may deduce the lateral transport of magnesium-rich fluid during the dissolution of carbonate. The general chemical zonations of interstitial waters at Site 1122 correspond to those of lithostratigraphic units and paleontological age divisions. In particular, note the sharp reduction of methane at 260 mbsf, which coincides with the base of the highly pyritized turbidites of the mud-wave sequence.

ORGANIC GEOCHEMISTRY

Volatile Hydrocarbons

As part of the shipboard safety and pollution-prevention monitoring program, hydrocarbon gases were analyzed for each core of Hole 1122A and each core below 60 mbsf of Hole 1122C by the headspace technique. Gas pockets were not encountered. The headspace methane concentrations increase rapidly below the seafloor (Fig. F31). In contrast to Site 1119 (see "Organic Geochemistry," p. 24, in the "Site 1119" chapter), there is no well-defined concentration maximum in the section, but headspace methane concentrations of the sediments between 15

F31. Headspace methane concentrations in sediments from Holes 1122A and 1122C, p. 74.

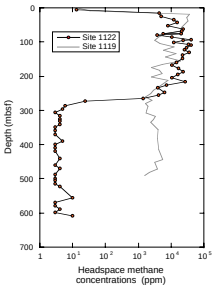

and 265 mbsf are much higher than in the uppermost sample and in the sediments below. The variation in this section (1,000–42,000 ppm) may reflect different sediment properties and/or different amounts of metabolizable organic matter in the methane-releasing sediments and, thus, changes in the sedimentary composition. The elevated methane concentrations are corroborated by low sulfate concentrations (see "Inorganic Geochemistry," p. 27). Below 265 mbsf, methane concentrations decrease suddenly by two orders of magnitude and are uniformly low down to the bottom of the hole. This distinct change matches the transition from lithostratigraphic Subunit IC to Subunit IB at 262 mbsf (see "Lithostratigraphy," p. 4), and may be a result of changes in the amount or type of organic matter. However, clear corresponding evidence of these changes cannot be found in the elemental composition (see "Carbonate and Organic Carbon," p. 31).

Carbonate and Organic Carbon

The abundance of total, inorganic, and organic carbon and of calcium carbonate in sediments from Holes 1122A and 1122B is summarized in Table T14 (also in ASCII format). Random sampling of all lithologies was performed for carbonate analysis, and one sample per core was analyzed for organic carbon.

Carbonate contents are highly variable throughout the section and lie in the range from 0.1 to 76.5 wt% (Fig. F32). There is no clear correlation with depth, age, or lithology. Because of the obvious variation in the sedimentary composition, particularly the intercalated turbidites in the hemipelagic sediments, this may be an artifact of random sampling. Nevertheless, in the upper part of the section between 0 and 140 mbsf, with exception of the section from 60 to 80 mbsf (lithostratigraphic Subunits IA and IB) and between 300 and 420 mbsf, carbonate contents are lower on average than in the rest of the section.

Sediments at Site 1122 average 0.24 wt% organic carbon (Fig. F33), which is lower than the average for deep-sea sediments of 0.3% compiled by McIver (1975) from data of DSDP Legs 1 through 33. There is no clear correlation with depth, age, or lithology, though in the deeper part of the hole concentrations seem to decrease with increasing depth. Despite the high sedimentation rate, low organic carbon concentrations are probably a consequence of organic-matter degradation caused by the long exposure to an oxic water column.

Organic Matter Source Characterization

Atomic organic carbon/nitrogen values were calculated for Site 1122 samples using TOC and total nitrogen concentrations to help identify the origin of the organic matter. The ratios vary from 0.2 to 25.9 with an average of 4.2 (Table T14). These low ratios are not accurate indicators of organic matter source. They may be an artifact of the low organic carbon content, combined with the tendency of clay minerals to adsorb ammonium ions generated during degradation of organic matter (Müller, 1977). This interpretation is supported by unrealistically low atomic $[C/N]_a$ ratios below 4.0 for organic carbon–poor samples (<0.2 wt%).

Rock-Eval analyses were not made because of low organic carbon contents (see "Organic Geochemistry," p. 22, in the "Explanatory Notes" chapter).

T14. Organic chemistry data, p. 141.

F32. Carbonate contents in sediments from Holes 1122A and 1122C, p. 75.

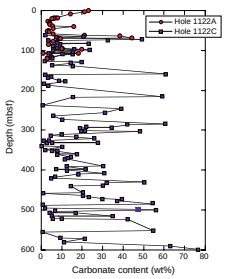

F33. Organic carbon contents in sediments from Holes 1122A and 1122C, p. 76.

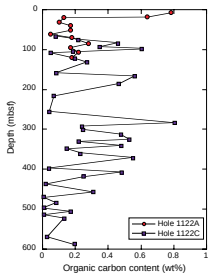

PHYSICAL PROPERTIES

Index Properties

Index properties measurements were made at a resolution of one sample every two sections in the cores from Holes 1122A and 1122C. Index properties were determined by a gravimetric method (see "Physical Properties," p. 24, in the "Explanatory Notes" chapter). Values of measured index properties (void ratio, porosity, water content, bulk density, and grain density) are presented in Table T15 (also in ASCII format). The properties measured from Holes 1122A and 1122C show cyclic variations downcore resulting from compositional variations typical of turbidite sequences (Figs. F34, F35). In the upper 500 mbsf, there is no apparent change in trend for any of the variables measured. Below 500 mbsf, the index properties show gradual downhole changes in trend, presumably from the effects of increased overburden.

Multisensor Track Measurements

The shipboard physical properties program at Site 1122 included nondestructive measurements of bulk density, magnetic susceptibility, and natural gamma-ray activity on whole sections of all cores using the MST (Figs. F36, F37). Magnetic susceptibility was measured at 4-cm intervals and at high sensitivity (4-s measurement time) in all Site 1122 holes. High-amplitude fluctuations of magnetic susceptibility in Hole 1122A and in the upper part (<110 mbsf) of Hole 1122C are associated with turbidite sequences. The presence of low magnetic susceptibility values with little variation below 110 mbsf in Hole 1122C is probably a result of low recovery of sands by XCB coring. Thus, there is a tendency for recovered core material to be clay rich. Natural gamma radiation was measured with a 15-s count every 14 cm in Holes 1122A and 1122C. Natural gamma radiation ranges from 15 to 42 counts/s. Variations occurring downcore reflect changes in mineral composition between sandy and clayey layers in the turbidite sequence. High values of natural gamma radiation give an indication of the relative abundance of clay. Low natural gamma radiation values shown in Hole 1122A are correlated with low magnetic susceptibility, indicating a possible increase in sand content. Gamma-ray attenuation porosity evaluator bulk density measurements were made at 4-cm intervals at all Site 1122 holes. The GRAPE density data exhibit fluctuations that tend to vary in direction, thickness, and intensity with those observed in the natural gamma radiation record; these fluctuations seem to correspond to variations in the occurrence of sandy and clay-rich sediment layers. A comparison of GRAPE density with the wet-bulk density determined from discrete samples shows a general agreement except in the uppermost part of the hole (Fig. F38).

Shear Strength

Measurements of shear strength, using a mechanical vane, were made on split cores from Holes 1122A and 1122C (Fig. F39). Samples were generally taken in fine-grained sediments at a resolution of one per section. No samples were taken from XCB cores. The shear strength measurements show relatively low values, except for peaks just above 35 and 65 mbsf in Hole 1122A and 42, 69, and 92 mbsf in Hole 1122C. These peaks indicate clay-rich intervals (see "Lithostratigraphy," p. 4).

T15. List of index properties measurements, p. 144.

F34. Index properties measurements from cores from Hole 1122A, p. 77.

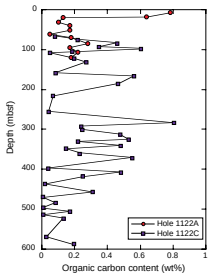

F35. Index properties measured from cores from Hole 1122C, p. 78.

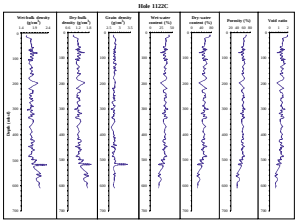

F36. MST track measurements from Hole 1122A, p. 79.

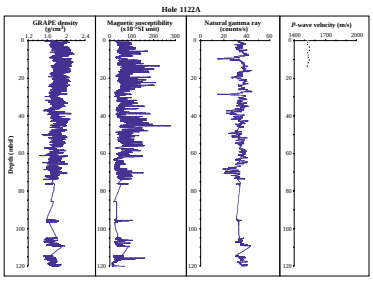

F37. MST measurements from Hole 1122C, p. 80.

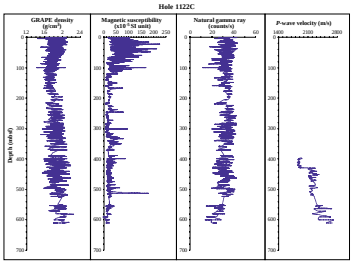

Shear strength values range from 5 to 60 kPa (maximum value of 57.15 kPa at 65 mbsf in Hole 1122A and 60.525 kPa at 91 mbsf in Hole 1122C). Low values may be associated with the presence of sand-rich intervals (see "Lithostratigraphy," p. 4). An indication of the consolidation characteristics of the sediments was made by using the classical relationship between shear strength and sedimentary overburden pressure (see "Physical Properties," p. 22, in the "Site 1121" chapter). The consolidation data from Site 1122 are similar in character to those from Site 1119 where cyclic variations also occur. Underconsolidation exists downhole as a result of rapid, increasingly sandy deposition. It is likely that the sediment is still undelrconsolidated, that is, still in the process of expelling pore water. The fact that water content and porosity remain relatively constant throughout the section supports this hypothesis.

F38. Density measurements in Hole 122C, p. 81.

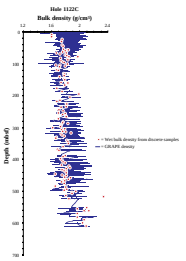

F39. Distribution of shear strength in cores, p. 82.

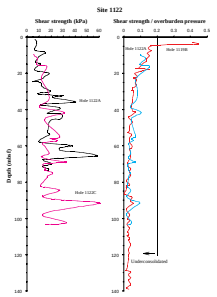

Compressional-Wave Velocity

Compressional-wave (*P*-wave) velocity was measured parallel to the core axis on split cores from Site 1122. Because the sediment cracked when the transducers of the Digital Sound Velocimeter were inserted into the sandy turbidite sediment, the measurements were only taken in the upper 20 mbsf of Hole 1122A. Values range from 1527 m/s to 1547 m/s. Below 390 mbsf in Hole 1122C, sediments were more tightly compacted, and the Hamilton frame velocimeter was used to measure sound propagation perpendicular to the sediment. A sharp increase in *P*-wave velocity from 1800 to 2000 m/s occurred around 429 mbsf between Sections 181-1122C-48X-2 and 48X-3, indicating a distinct lithologic horizon.

DOWNHOLE MEASUREMENTS

Logging Operations

Logging was attempted in Hole 1122C but was unsuccessful because of adverse weather and poor hole conditions. We planned to run one pass of the triple combination, two passes of the FMS-sonic, and then a single pass of the GHMT (for abbreviations and explanation of the tool strings see "Downhole Measurements," p. 29, in the "Explanatory Notes" chapter). Logging operations began at 0700 hr on 11 September 1998 and were terminated at 1330 hr on the same day.

After coring the hole to 627.4 mbsf, the BHA was raised to 83.12 mbsf, in preparation for logging. Raising the BHA was, however, problematic, and resulted in substantial infilling at the base of the hole (see "Operations," p. 3). The heave on the ship (>6 m) was too great to allow use of the wireline heave compensator (WHC). Because of this, it was decided not to open the calipers on the FMS and lithodensity tools, in case the excessive heave ripped them off.

The triple combination was lowered to the base of the pipe, but could not pass completely into the open hole because of an obstruction at 95 mbsf, ~12 m below the BHA. Weather at the time was poor, with 3.5-m seas, 6-m swells, and 37-kt winds. After trying unsuccessfully for 35 min to break through the obstruction, the triple combination was pulled back into the drill string. An attempt was made to pull up the BHA, but it had become stuck. At this point the triple combination was brought back up to the rig floor and disassembled.

A revised logging plan was considered, consisting of a wiper trip with the drill string to clean out the hole, followed by a single pass of a shorter tool string. The new tool string would consist of the gamma-ray, sonic, resistivity, and temperature tools. If this pass had been successful, a run of the GHMT would have followed. However, by this time weather conditions had deteriorated with the swells increasing to a maximum of 10 m and the winds to 45 kt. The forecast was for deteriorating weather. These conditions constituted a danger to the drill string and a risk to the tools. Therefore, it was decided to abandon logging operations at Hole 1122C. It took a further 2 hr to free the BHA from the hole.

REFERENCES

Baker, P.A., and Kastner, M., 1981. Constraints on the formation of sedimentary dolomite. *Science,* 213:215–216.

Baksi, A.K., 1995. Fine tuning the radiometrically derived geomagnetic polarity time scale (GPTS) for 0–10 Ma. *Geophys. Res. Lett.,* 22:457–460.

Berggren, W.A., Kent, D.V., Swisher, C.C., III, and Aubry, M.-P., 1995. A revised Cenozoic geochronology and chronostratigraphy. *In* Berggren, W.A., Kent, D.V., Aubry, M.-P., and Hardenbol, J. (Eds.), *Geochronology, Time Scales and Global Stratigraphic Correlation*. Spec. Publ.—Soc. Econ. Paleontol. Mineral. (Soc. Sediment. Geol.), 54:129–212.

Brew, D.S., 1995. Mud waves at Deep Sea Drilling Project Site 603, US Atlantic lower continental rise. *Geo-Mar. Lett.,*15:92–98.

Cande, S.C., and Kent, D.V., 1995. Revised calibration of the geomagnetic polarity timescale for the Late Cretaceous and Cenozoic. *J. Geophys. Res.,* 100:6093–6095.

Carter, L., and Carter, R.M., 1988. Late Quaternary development of left bank dominant levees in the Bounty Trough, New Zealand. *Mar. Geol.,* 78:185–197.

————, 1993. Sedimentary evolution of the Bounty Trough: a Cretaceous rift basin, southwestern Pacific Ocean. *In* Ballance, P.F. (Ed.), *Sedimentary Basins of the World—South Pacific:* Amsterdam (Elsevier), 51–67.

Carter, L., Carter, R.M., Nelson, C.S, Fulthorpe, C.S., and Neil, H.L., 1990. Evolution of Pliocene to Recent abyssal sediment waves on Bounty Channel levees, New Zealand. *Mar. Geol.,* 95:97–109.

Carter, L., Nelson, C.S., Neil, H.L., and Froggatt, P.C., 1995. Correlation, dispersal, and preservation of the Kawakawa Tephra and other late Quaternary tephra layers in the Southwest Pacific Ocean. *N. Z. J. Geol. Geophys.,* 38:29–46.

Carter, R.M., and Carter, L., 1987. The Bounty Channel system: a 55-million-year-old sediment conduit to the deep sea, Southwest Pacific Ocean. *Geo-Mar. Lett.,* 7:183–190.

————, 1992. Seismic imaging of Pleistocene deep-sea cyclothems: implications for sequence stratigraphy. *Terra Nova,* 4:682–692.

————, 1996. The abyssal Bounty Fan and lower Bounty Channel: evolution of a rifted-margin sedimentary system. *Mar. Geol.,* 130:182–202.

Carter, R.M., Carter, L., and Davy, B., 1994. Seismic stratigraphy of the Bounty Trough, Southwest Pacific Ocean. *Mar. Pet. Geol.,* 11:79–93.

Damuth, J.E., 1979. Migrating sediment waves created by turbidity currents in the northern South China Basin. *Geology,* 7:520–523.

Davey, B.W., 1993. The Bounty Trough: basement structure influences on sedimentary basin evolution. *In* Ballance, P.F. (Ed.), *Sedimentary Basins of the World—South Pacific:* Amsterdam (Elsevier), 69–92.

de Kaenel, E., and Villa, G., 1996. Oligocene–Miocene calcareous nannofossils biostratigraphy and paleoecology from the Iberia Abyssal Plain. *In* Whitmarsh, R.B., Sawyer, D.S., Klaus, A., and Masson, D.G. (Eds.), *Proc. ODP, Sci. Results,* 149: College Station, TX (Ocean Drilling Program), 79–145.

Fenner, J., Carter, L., and Stewart, R., 1992. Late Quaternary paleoclimatic and paleoceanographic change over northern Chatham Rise, New Zealand. *Mar. Geol.,* 108:383–404.

Gartner, S., 1992. Miocene nannofossil chronology in the North Atlantic, DSDP Site 608. *Mar. Micropaleontol.,* 18:307–331.

Gieskes, J.M., 1974. Interstitial water studies, Leg 25. *In* Simpson, E.S.W., Schlich, R., et al., *Init. Repts. DSDP,* 25: Washington (U.S. Govt. Printing Office), 361–394.

————, 1981. Deep-sea drilling interstitial water studies: implications for chemical alteration of the oceanic crust, layers I and II. *In* Warme, J.E., Douglas, R.G., and Winterer, E.L. (Eds.), *The Deep Sea Drilling Project: A Decade of Progress*. Spec. Publ.—Soc. Econ. Paleontol. Mineral., 32:149–167.

Gieskes, J.M., Elderfield, H., Lawrence, J.R., Johnson, J., Meyers, B., and Campbell, A., 1982. Geochemistry of interstitial waters and sediments, Leg 64, Gulf of California. *In* Curray, J.R., Moore, D.G., et al., *Init. Repts. DSDP,* 64 (Pt. 2): Washington (U.S. Govt. Printing Office), 675–694.

Gradstein, F.M., Fearon, J.M., and Huang, Z., 1989. BURSUB and DEPOR version 3.50—two FORTRAN 77 programs for porosity and subsidence analysis. *Open-File Rep.—Geol. Surv. Can.,* 1283:1–10.

Griggs, G.B., Carter, L., and Kennett, J.P., and Carter, R.M., 1983. Late Quaternary marine stratigraphy southeast of New Zealand. *Bull. Geol. Soc. Am.,* 94:791–797.

Hollister, C.D., and McCave, I.N., 1984. Sedimentation under deep-sea storms. *Nature,* 309:220–225.

Hornibrook, N. de B., and Jenkins, D.G., 1994. DSDP 594, Chatham Rise, New Zealand—Late Neogene planktonic foraminiferal biostratigraphy revisited. *J. Micropalaeontol.,* 13:93–101.

Komar, P.D., 1969. The channelized flow of turbidity currents with application to Monterey deep-sea fan channel. *J. Geophys. Res.,* 74:4544–4558.

Lawver, L.A., and Gahagan, L.M., 1994. Constraints on timing of extension in the Ross Sea region. *Terra Antarct.,* 1:545–552.

Lean, C.M.B., and McCave, I.N., 1998. Glacial to interglacial mineral magnetic and palaeoceanographic changes at Chatham Rise, SW Pacific Ocean. *Earth Planet. Sci. Lett.,* 163:247–260.

Martini, E., 1971. Standard Tertiary and Quaternary calcareous nannoplankton zonation. *In* Farinacci, A. (Ed.), *Proc. 2nd Int. Conf. Planktonic Microfossils Roma:* Rome (Ed. Tecnosci.), 2:739–785.

Matsuoka, H., and Okada, H., 1989. Quantitative analysis of Quaternary nannoplankton in the subtropical northwestern Pacific Ocean. *Mar. Micropaleontol.,* 14:97–118.

McIver, R.D., 1975. Hydrocarbon occurrences from JOIDES Deep Sea Drilling Project. *Proc. Ninth Petrol. Congr.,* 269–280.

Menard, H.W., 1955. Deep-sea channels, topography and sedimentation. *AAPG Bull.,* 39:236–255.

Meynadier, L., Valet, J.-P., and Shackleton, N.J., 1995. Relative geomagnetic intensity during the last 4 m.y. from the equatorial Pacific. *In* Pisias, N.G., Mayer, L.A., Janecek, T.R., Palmer-Julson, A., and van Andel, T.H. (Eds.), *Proc. ODP, Sci. Results,* 138: College Station, TX (Ocean Drilling Program), 779–795.

Morley, J.J., and Hays, J.D., 1979. *Cycladophora davisiana:* a stratigraphic tool for Pleistocene North Atlantic and interhemispheric correlation. *Earth Planet. Sci. Lett.,* 44:383–389.

Müller, P.J., 1977. C/N ratios in Pacific deep sea sediments: effect of inorganic ammonium and organic nitrogen compounds sorbed by clays. *Geochim. Cosmochim. Acta,* 41:765–776.

Naish, T.R., Abott, S.T., Alloway, B.V., Beu, A.G., Carter, R.M., Edwards, A.R., Journeaux, T.D., Kamp, P.J.J., Pillans, B.J., Saul, G., and Woolfe, K.J., 1998. Astronomical calibration of a southern hemisphere Plio-Pleistocene reference section, Wanganui Basin, New Zealand. *Quat. Sci. Rev.,* 17:695–710.

Neil, H.L., 1991. Late Quaternary stratigraphy, sedimentology and evolution of the Bounty Fan system, Bounty Trough, Southwest Pacific [M.Sc. thesis]. Univ. of Waikato, New Zealand.

Nelson, C.S., Cooke, P.J., Hendy, C.H., and Cuthbertson, A.M., 1993. Oceanographic and climatic changes over the past 160,000 years at Deep Sea Drilling Project Site 594 off southeastern New Zealand, Southwest Pacific Ocean. *Paleoceanography,* 8:435–458.

Normark, W.R., Hess, G.R., Stow, D.A.V., and Bowen, A.J., 1980. Sediment waves on the Monterey fan levee: a preliminary physical interpretation. *Mar. Geol.,* 37:1–18.

Pemberton, S.G., and MacEachern, J.A., 1995. The sequence stratigraphic significance of trace fossils: examples from the Cretaceous Foreland Basin of Alberta, Canada.

In Van Wagoner, J.C., and Bertram, G.T. (Eds.), *Sequence Stratigraphy of Foreland Basin Deposits*. AAPG Mem., 64:429–475.

Pemberton, S.G., van Wagoner, J.C., and Wach, G.D., 1992. Ichnofacies of a wave-dominated shoreline. *In* Pemberton, S.G. (Ed.), *Applications of Ichnology to Petroleum Exploration: A Core Workshop*. SEPM Core Workshop, 17:339–382.

Pillans, B.J., Kohn, B.P., Berger, G., Froggatt, P., Duller, G., Alloway, B.V., and Hesse, P., 1996. Multi-method dating comparison for mid-Pleistocene Rangitawa Tephra, New Zealand. *Quat. Sci. Rev.,* 15:641–653.

Pillans, B.J., Roberts, A.P., Wilson, G.S., Abbott, S.T., and Alloway, B.V., 1994. Magnetostratigraphic, lithostratigraphic and tephrostratigraphic constraints on lower and middle Pleistocene sea-level changes, Wanganui Basin, New Zealand. *Earth Planet. Sci. Lett.,* 121:81–98.

Raffi, I., and Flores, J.-A., 1995. Pleistocene through Miocene calcareous nannofossils from eastern equatorial Pacific Ocean. *In* Pisias, N.G., Mayer, L.A., Janecek, T.R., Palmer-Julson, A., and van Andel, T.H. (Eds.), *Proc. ODP, Sci. Results,* 138: College Station, TX (Ocean Drilling Program), 233–286.

Raine, J.I., Strong, C.P., and Wilson, G.J., 1993. Biostratigraphic revision of petroleum exploration wells, Great South Basin, New Zealand. *Inst. Geol. Nucl. Sci., Sci. Rep.,* 93/32.

Sato, T., and Kameo, K., 1996. Pliocene to Quaternary calcareous nannofossil biostratigraphy of the Arctic Ocean, with reference to late Pliocene glaciation. *In* Thiede, J., Myhre, A.M., Firth, J.V., Johnson, G.L., and Ruddiman, W.F. (Eds.), *Proc. ODP, Sci. Results,* 151: College Station, TX (Ocean Drilling Program), 39–59.

Spencer-Cervato, C., Thierstein, H.R., Lazarus, D.B., and Beckmann, J.-P., 1994. How synchronous are Neogene marine plankton events? *Paleoceanography,* 9:739–763.

Stam, B., Gradstein, F.M., Lloyd, P., and Gillis, D., 1987. Algorithms for porosity and subsidence history. *Computers and Geosci.,* 13:317–349.

Stock, J. and Molnar, P., 1987. Revised history of early Tertiary plate motion in the south-west Pacific. *Nature,* 325:495–499.

Suess, E., von Huene, R., et al., 1988. *Proc. ODP, Init. Repts.,* 112: College Station, TX (Ocean Drilling Program).

Takayama, T., 1993. Notes on Neogene calcareous nannofossil biostratigraphy of the Ontong Java Plateau and size variations of *Reticulofenestra* coccoliths. *In* Berger, W.H., Kroenke, L.W., Mayer, L.A., et al., *Proc. ODP, Sci. Results,* 130: College Station, TX (Ocean Drilling Program), 179–229.

Van Dissen, R., and Yeats, R.S., 1991. Hope Fault, Jordan Thrust, and uplift of the Seward Kaikoura Range, New Zealand. *Geology,* 19:393–396.

Weaver, P.P.E., Carter, L., and Neil, H., 1998. Response of surface watermasses and circulation to late Quaternary climate change, east of New Zealand. *Paleoceanography,* 13:70–83.

Wood, R.A., Andrews, P.B., Herzer, R.H., et al., 1989. Cretaceous and Cenozoic geology of the Chatham Rise region, South Island, New Zealand. *N. Z. Geol. Basin Stud.,* 3.

Worm, H.-U., 1997. A link between geomagnetic reversals and events and glaciations. *Earth Planet. Sci. Lett.*, 147:55–67.

Figure F1. Locality map for Site 1122, showing location of seismic lines 2023 and 3034 of Figure F2A, p. 39, and F2B, p. 40.

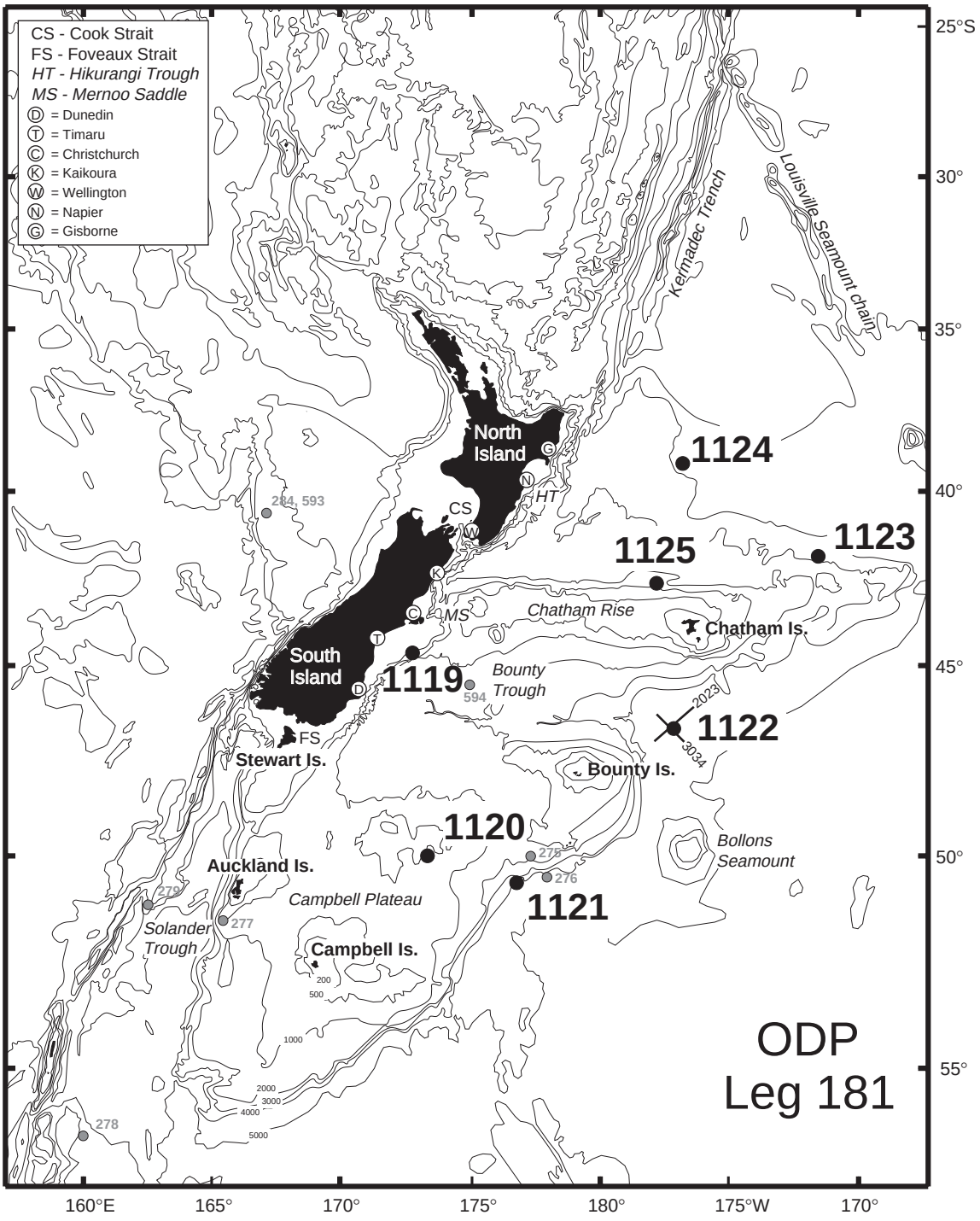

Figure F2. A. Portion of seismic line NZ01 2023 through Site 1122 (0530–1200 hr, 6 December 1998). (Continued on next page.)

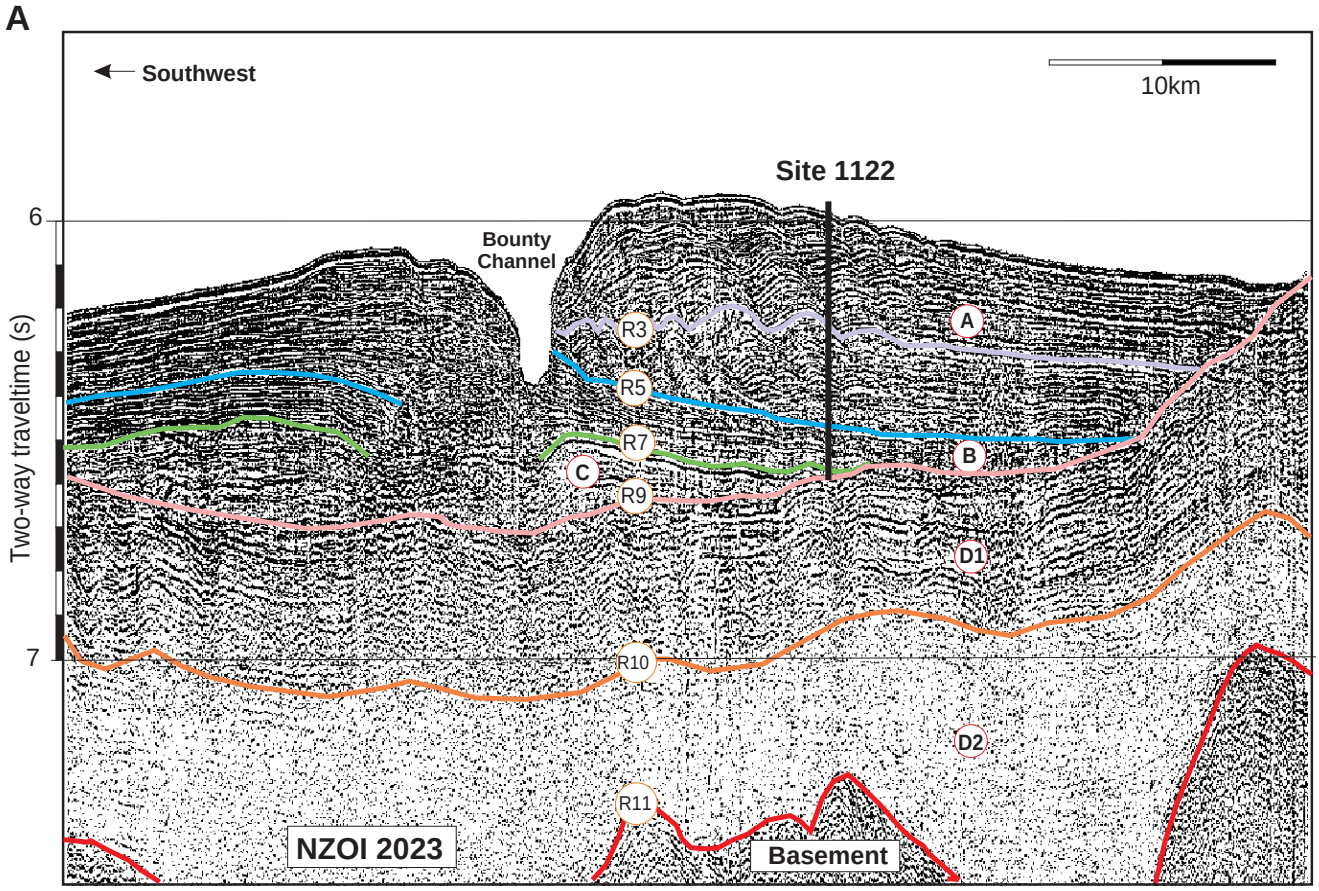

Figure F2 (continued). B. Detail of processed portion of line NIWA 3034-12 through Site 1122 (0020–0200 hr, 17 February 1997).

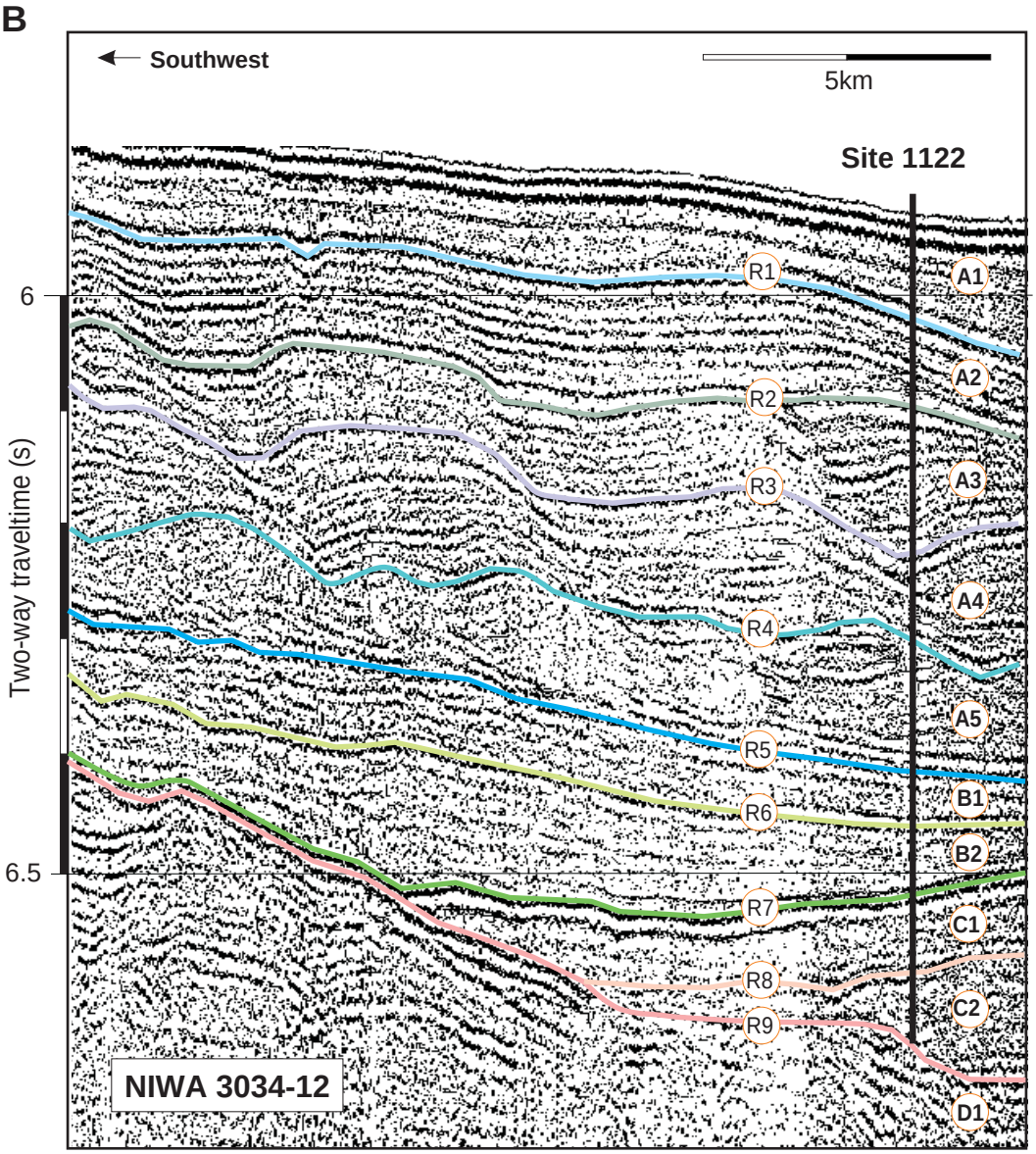

Figure F3. Portion of 3.5-kHz line NZ01 2023 through Site 1122 (0830–0940 hr, 6 December 1998).

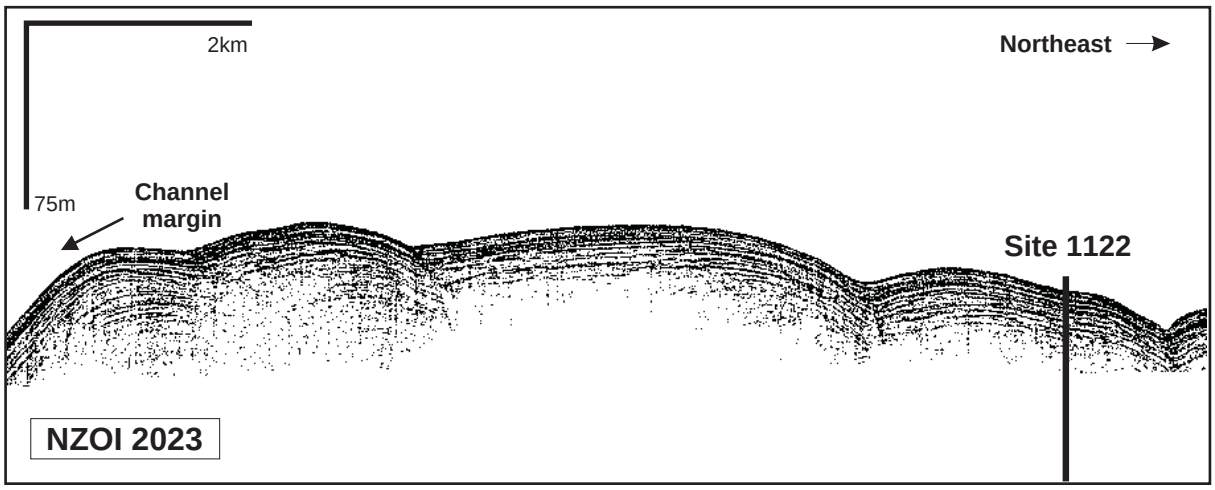

Figure F4. Summary log for Site 1122. (Continued on next three pages.)

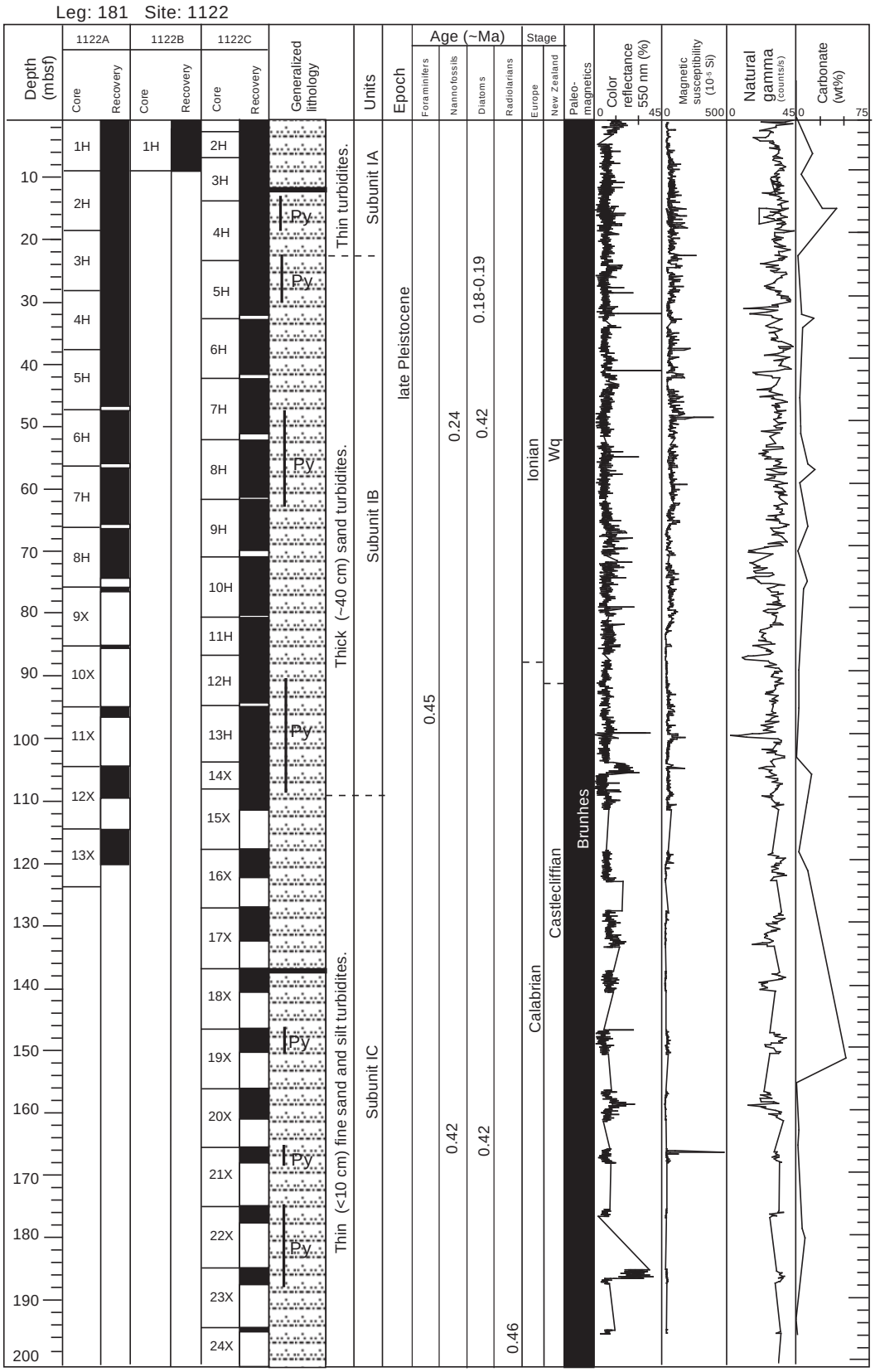

Figure F4 (continued).

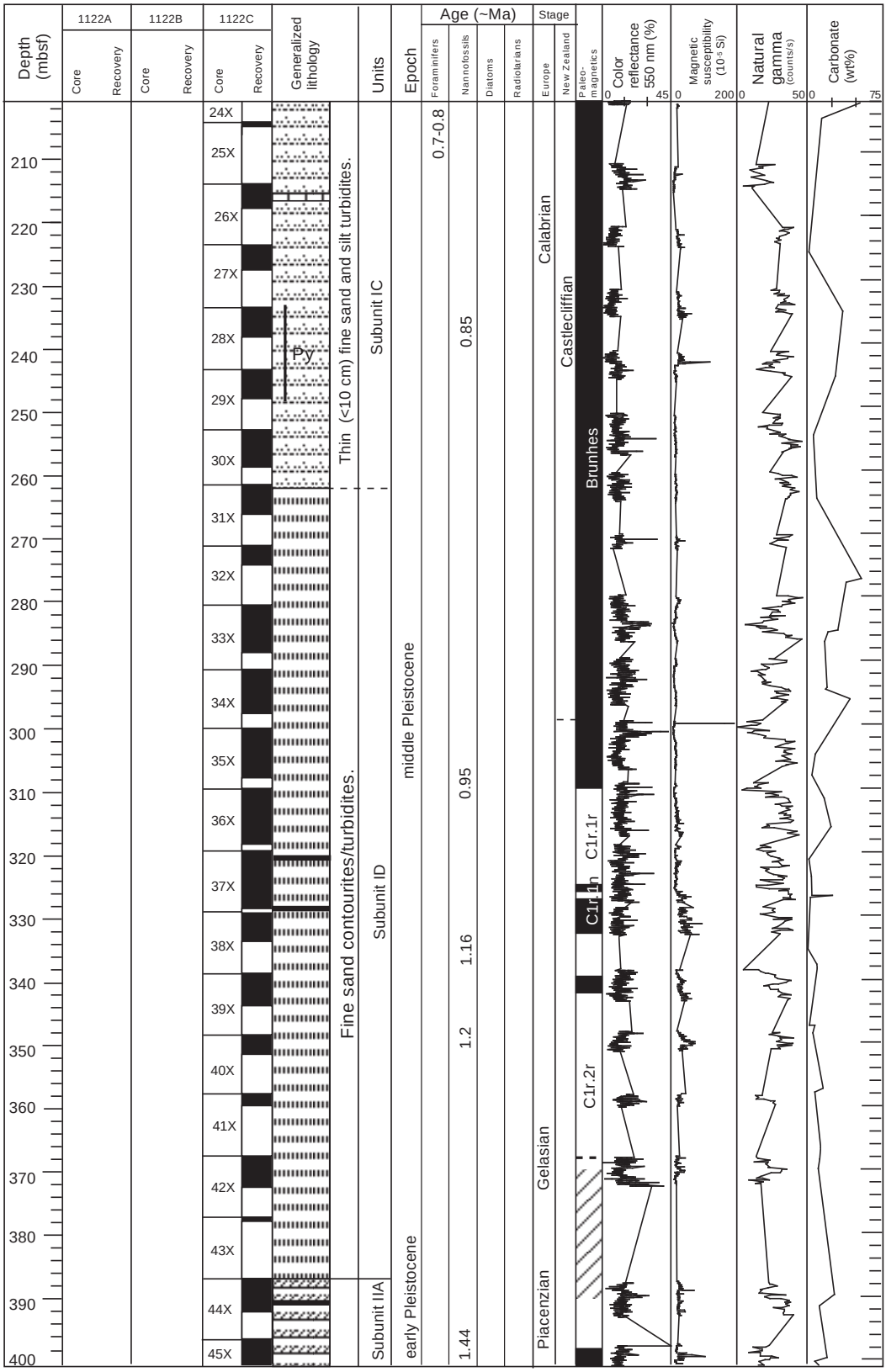

Figure F4 (continued).

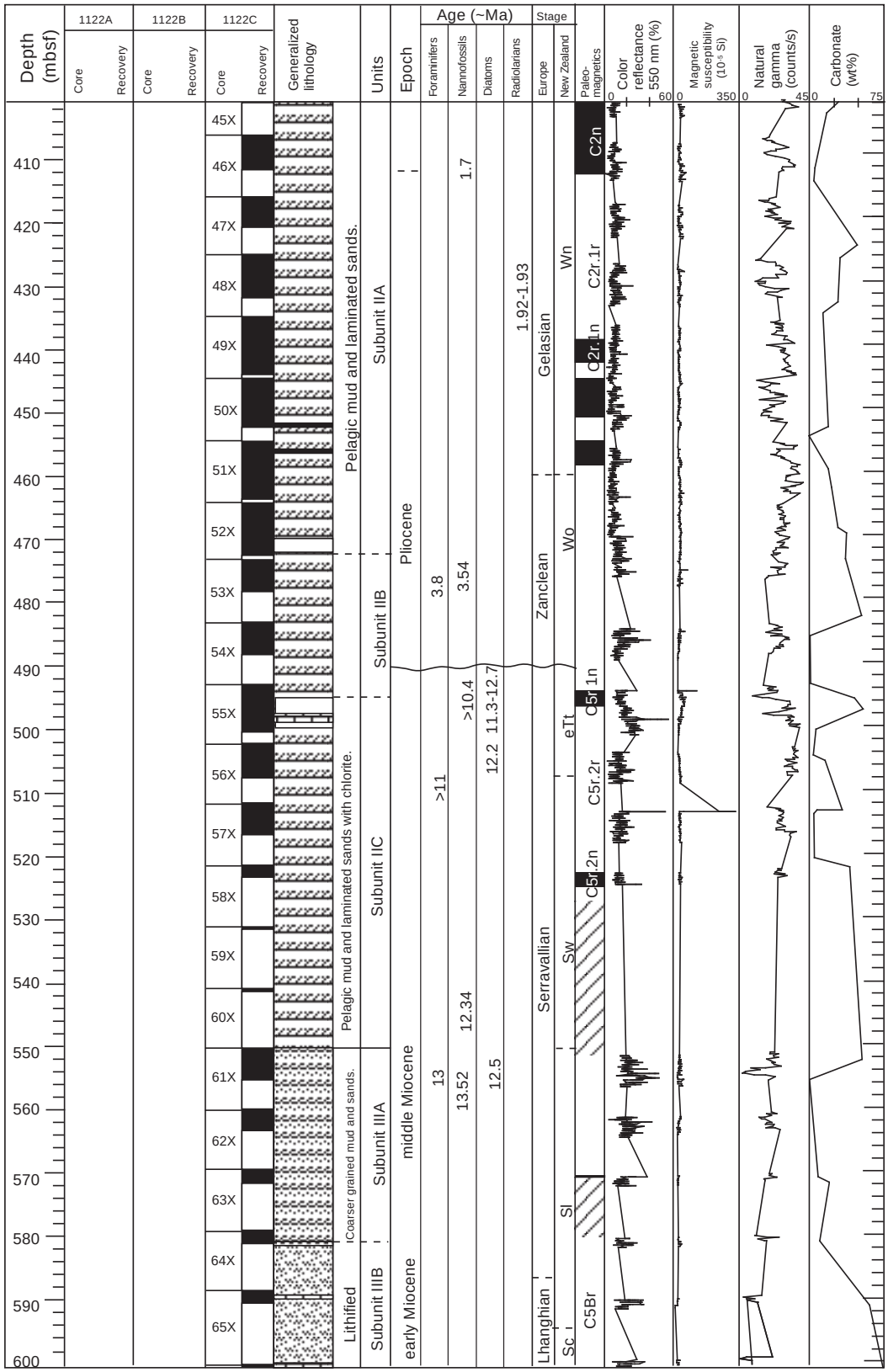

Figure F4 (continued).

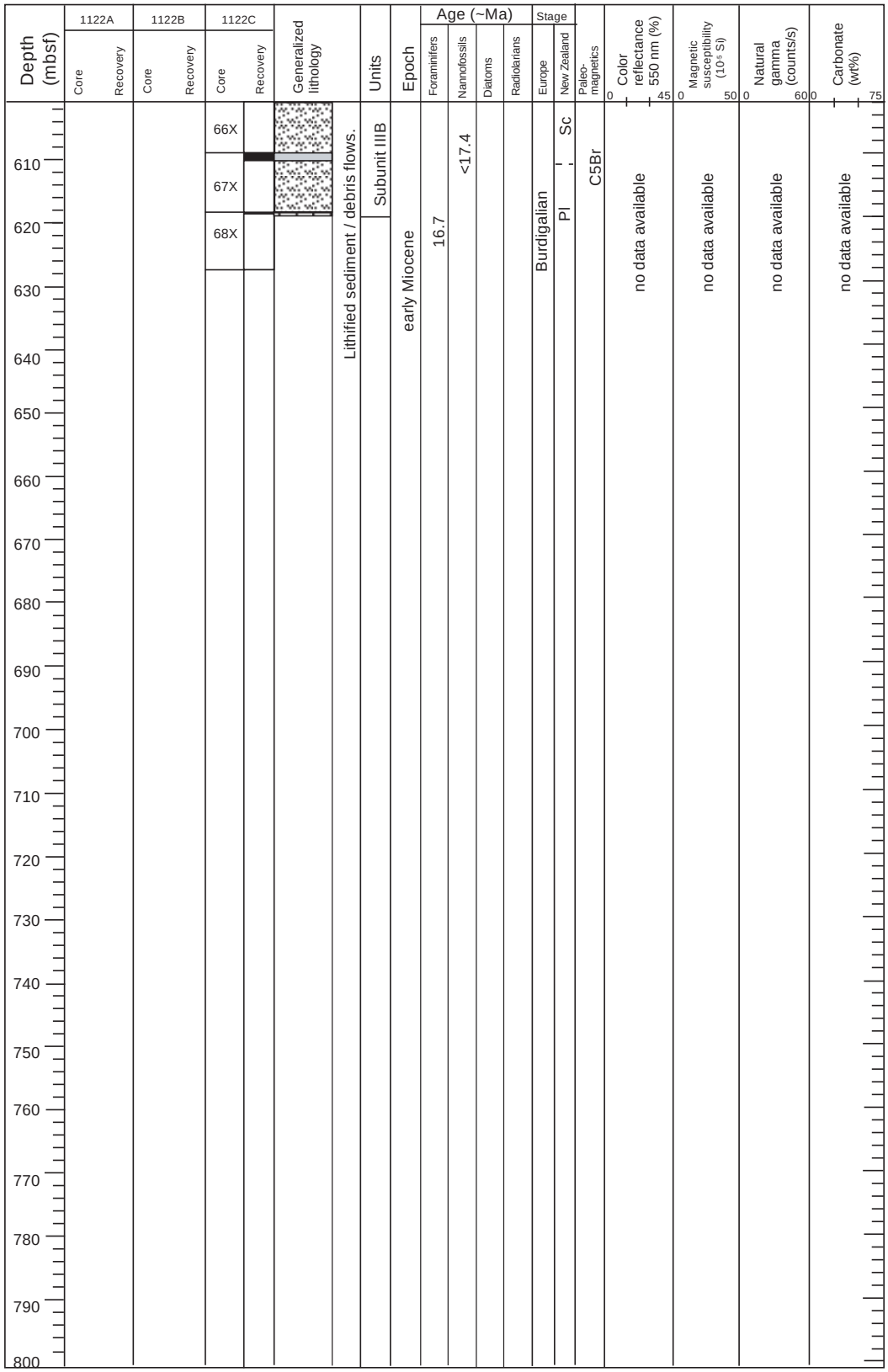

Figure F5. Sequence of turbidites in Subunit IA (interval 181-1122A-2H-5, 30–85 cm; 15.60–16.15 mbsf).

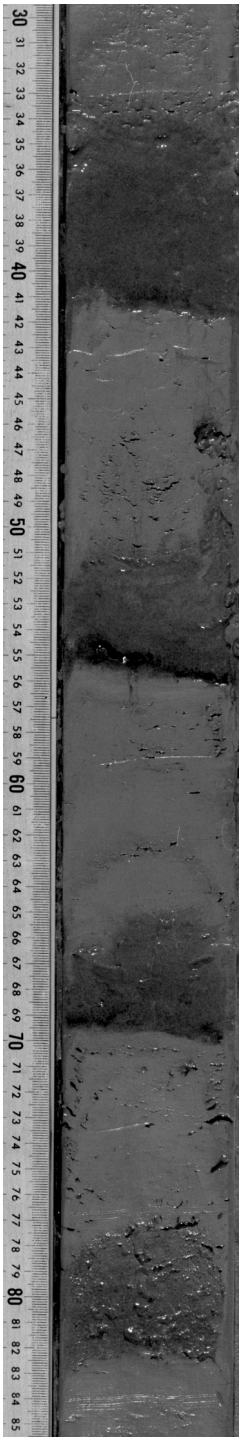

Figure F6. Sand turbidite in Subunit IB (interval 181-1122A-2H-6, 50–80 cm; 17.30–17.60 mbsf).

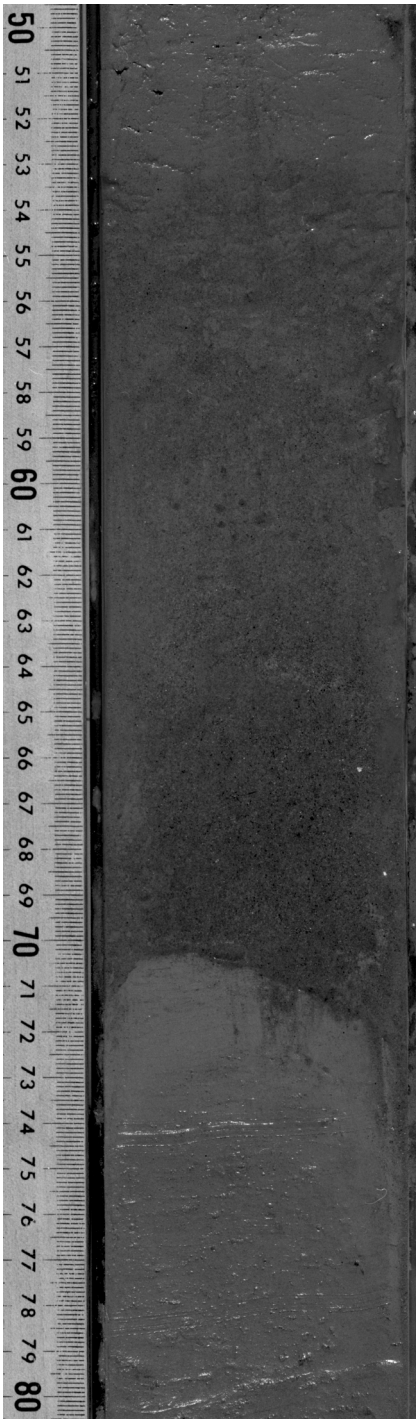

Figure F7. Tephra layer (327.92 mbsf) in Subunit ID (interval 181-1122C-37X-6, 120–135 cm; 328.00–328.15 mbsf).

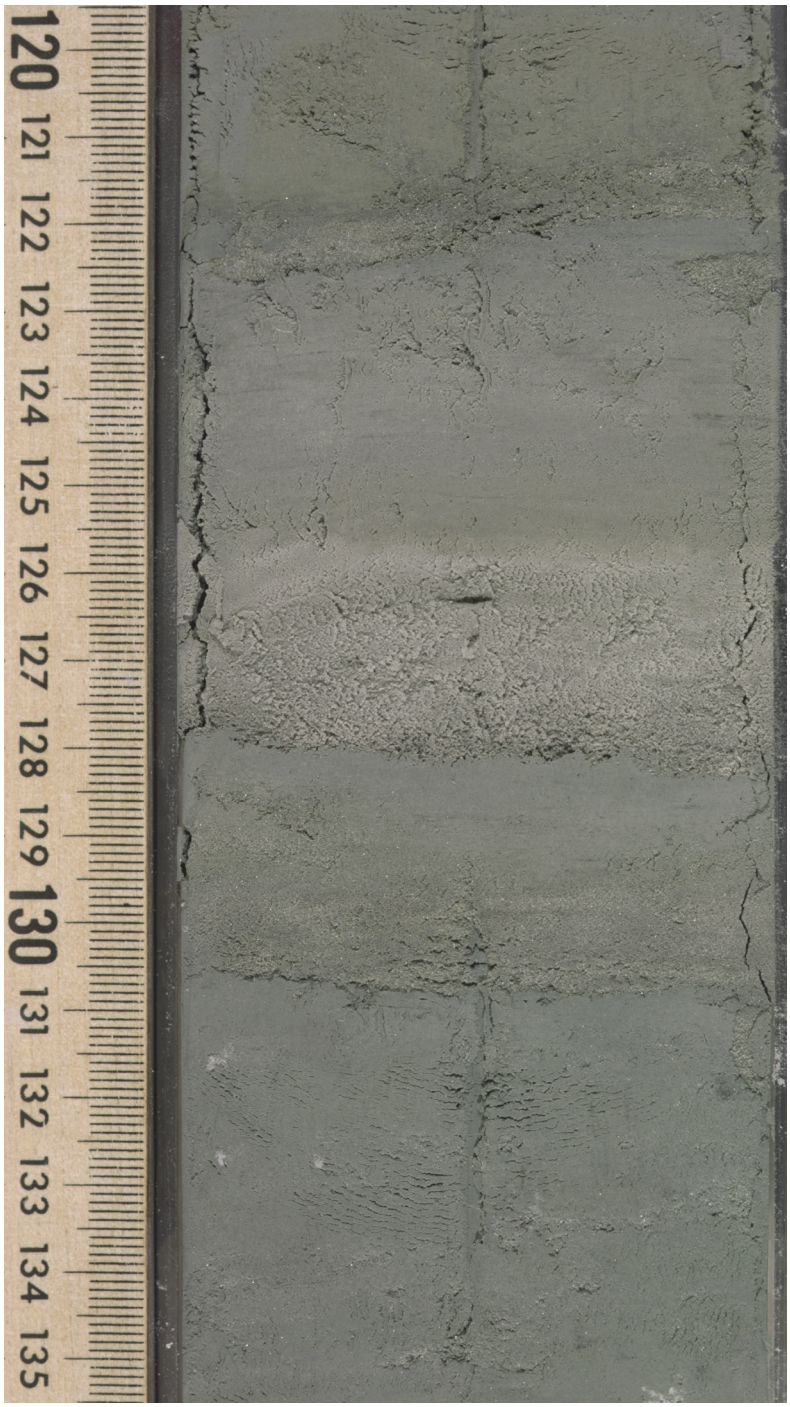

Figure F8. Contourite with planar and cross laminae in the top of Subunit IIA (interval 181-1122C-44X-2, 50–85 cm; 388.90–389.25 mbsf).

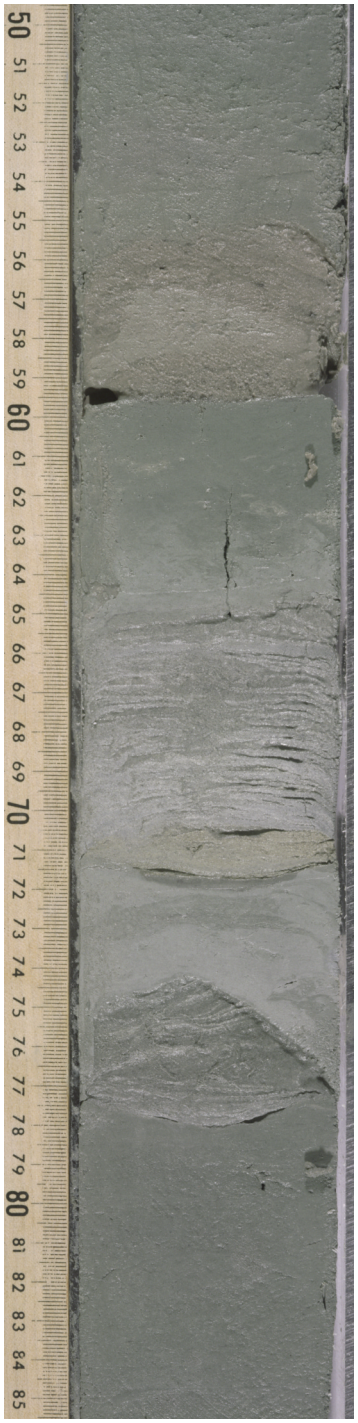

Figure F9. Planar and cross laminae in the top of Subunit IIA (interval 181-1122C-44X-CC, 7–13 cm; 392.40–392.46 mbsf).

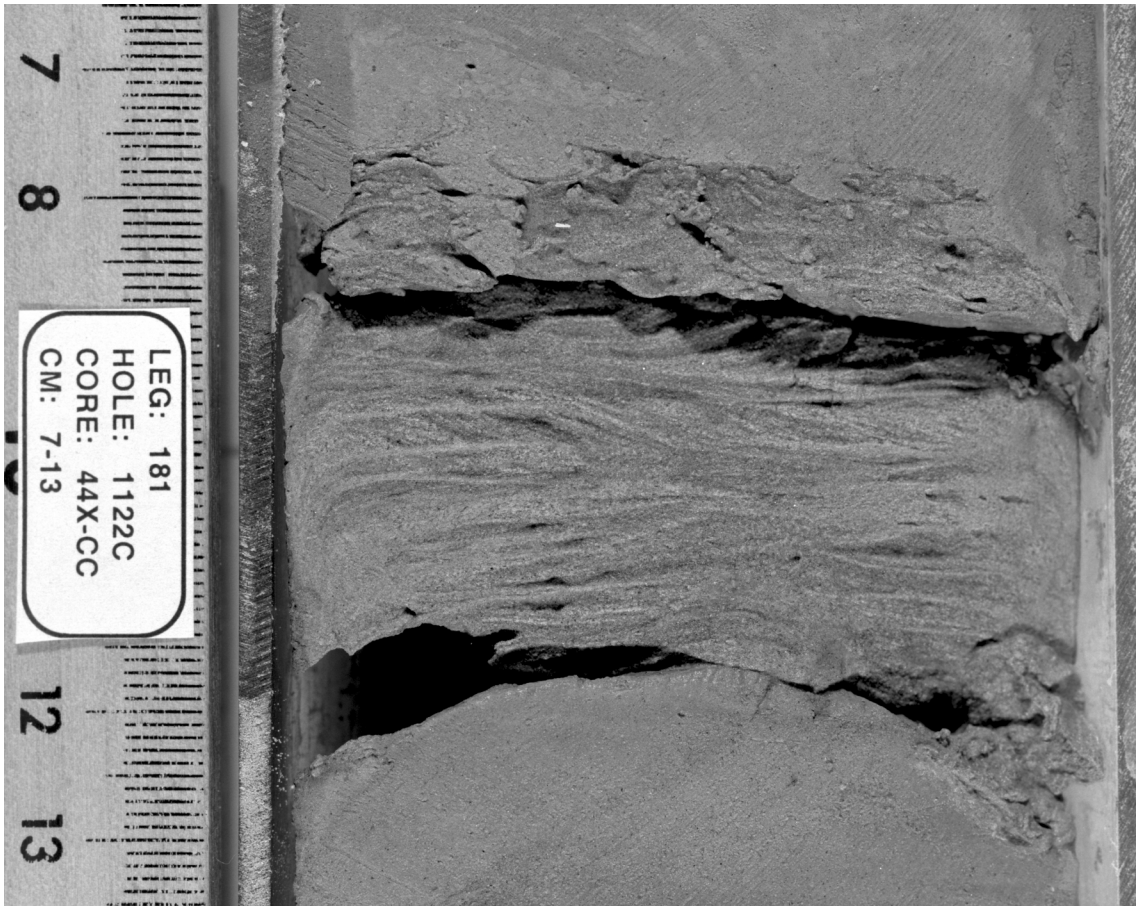

Figure F10. White foraminifer sand with bioturbated top (*Teichichnus*) and planar and cross laminae in the top of Subunit IIIA (interval 181-1122C-61X-3, 20–50 cm; 553.60–553.90 mbsf).

Figure F11. Reverse-graded debris-flow deposit in Subunit IIIB (interval 181-1122C-67X-1, 55–85 cm; 608.75–609.05 mbsf).

Figure F12. Thickness of turbidites and sand, fine sand, and silt layers in Hole 1122C.

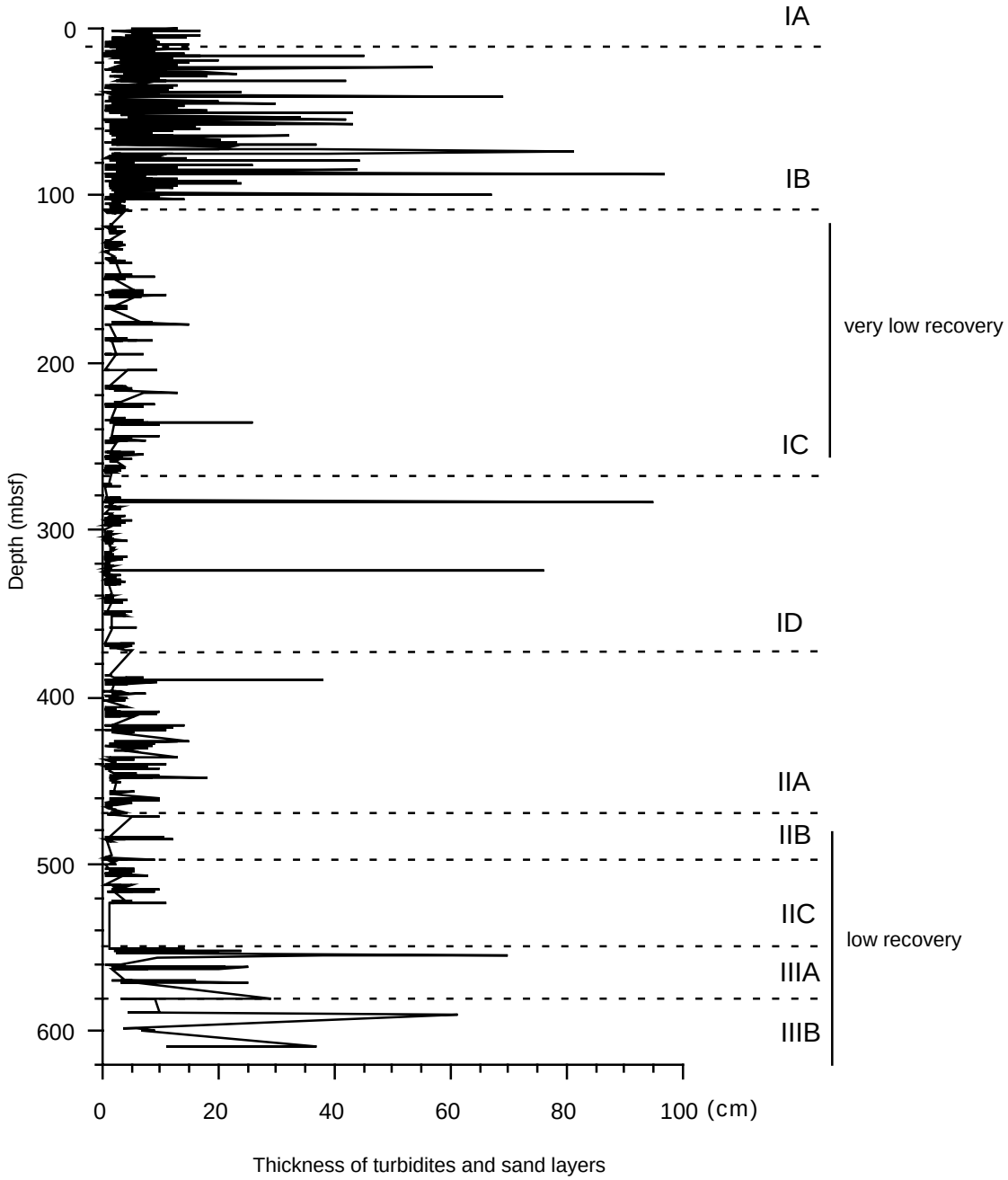

Figure F13. Turbidites with pyritized bases in basal Subunit IA (interval 181-1122A-3H-3, 57–90 cm; 22.37–22.70 mbsf).

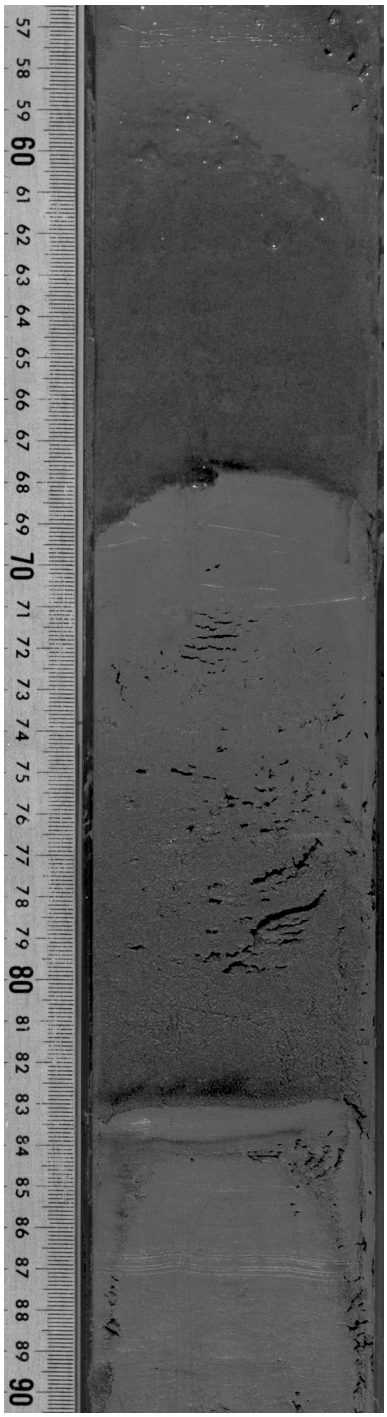

Figure F14. *Teichichnus, Zoophycos,* and *Planolites* in Subunit IIB (interval 181-1122C-53X-2, 52–66 cm; 475.42–475.56 mbsf).

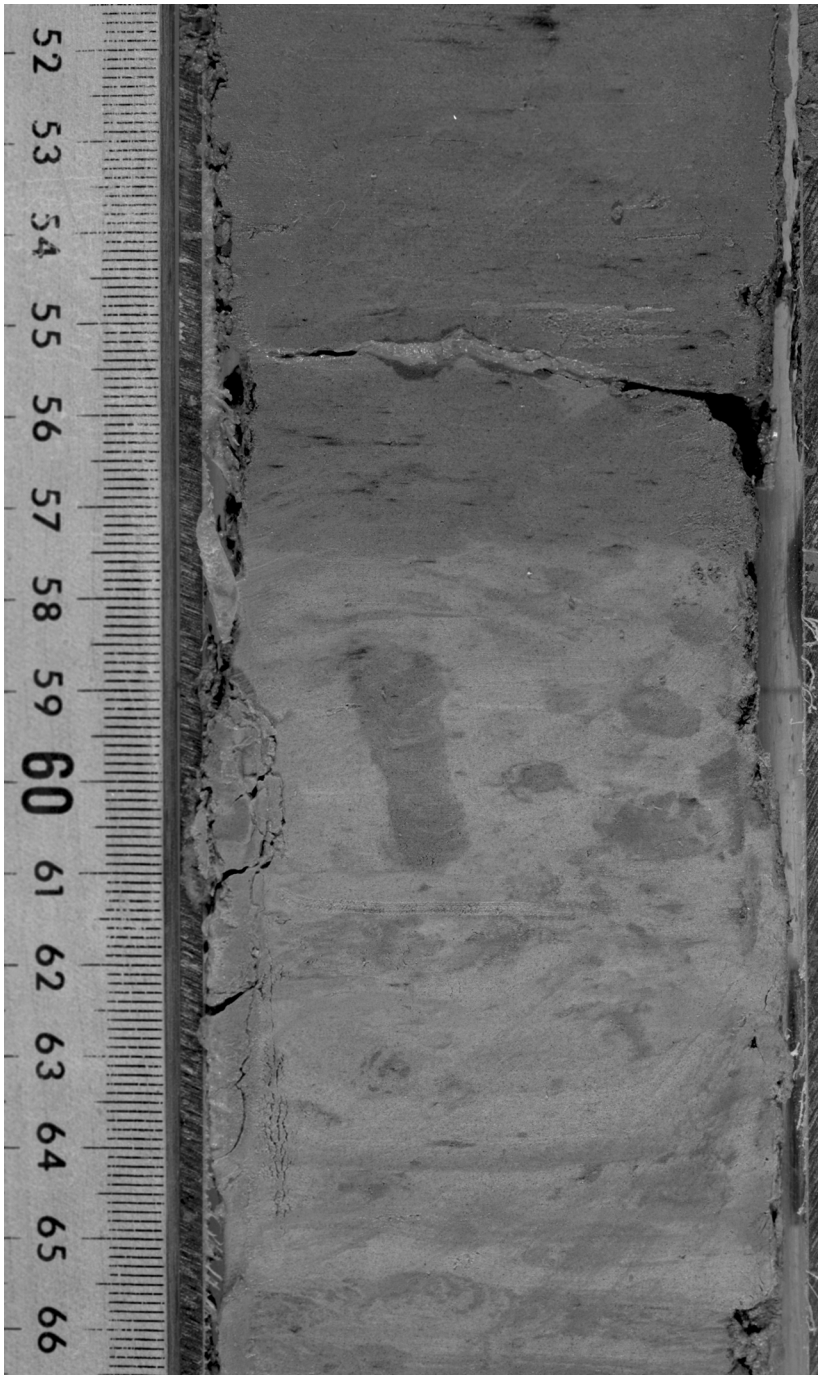

Figure F15. *Chondrites* in Subunit ID (interval 181-1122C-33X-4, 20–35 cm; 285.40–285.55 mbsf).

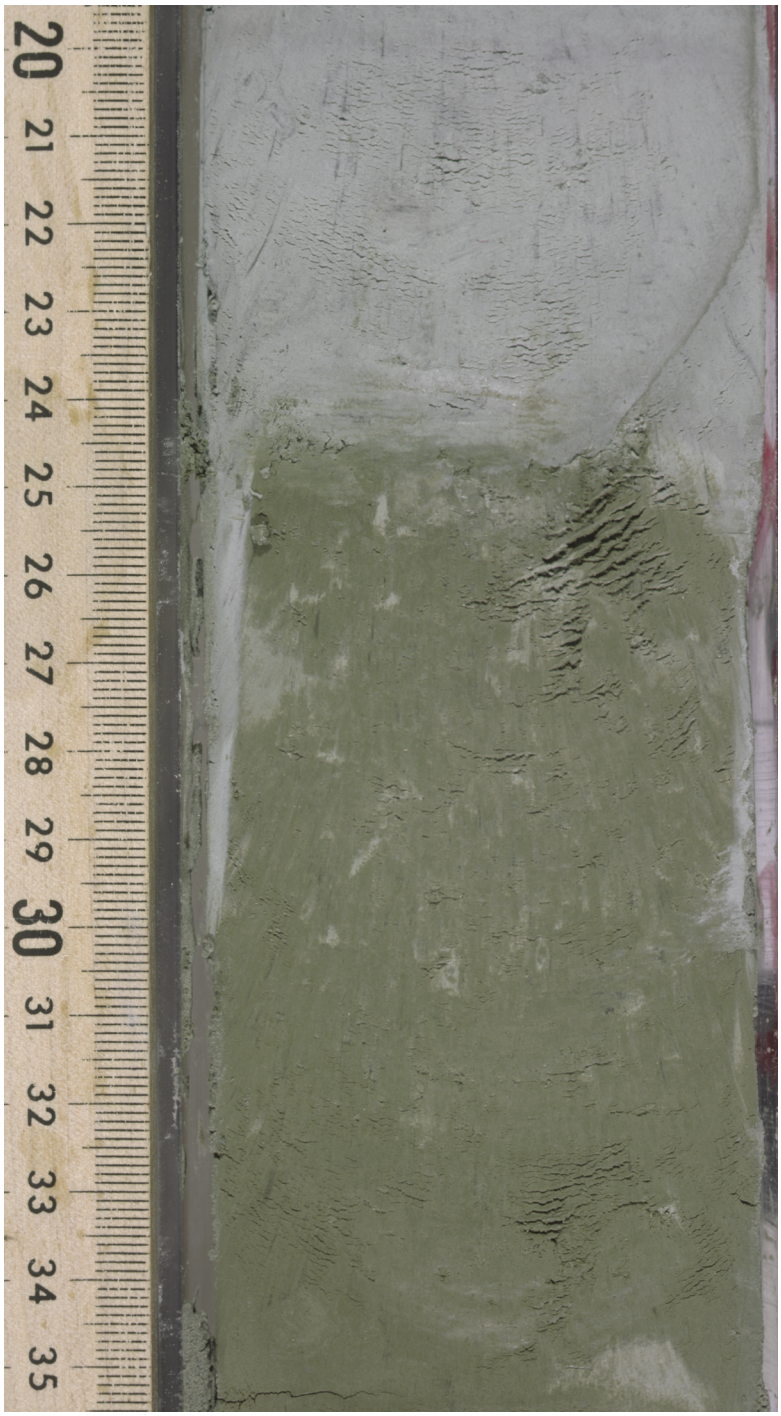

Figure F16. Biostratigraphic summary chart of Site 1122 showing correlation between the four microfossil biohorizons and age assignments. Numbers are ages (Ma).

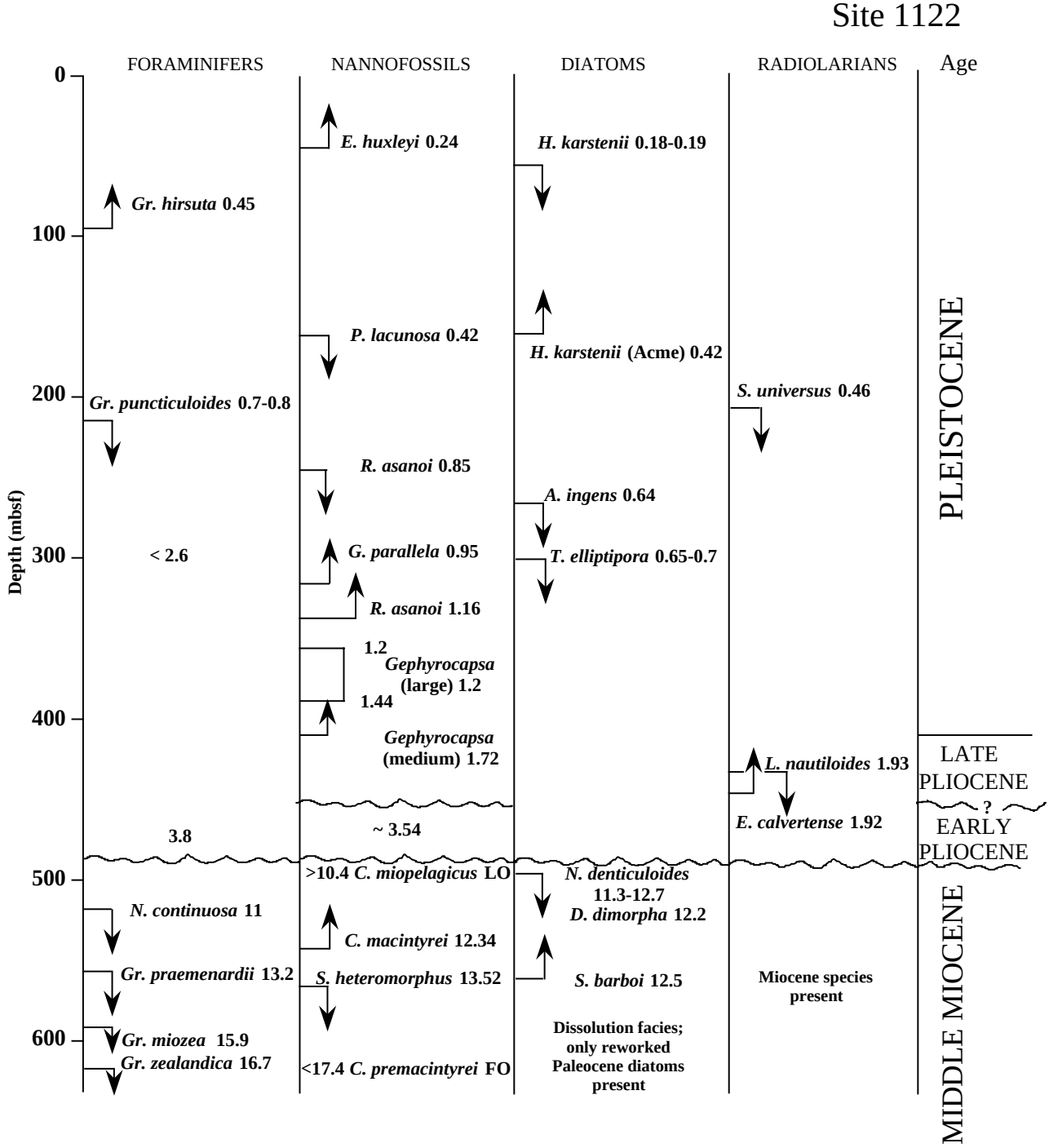

Figure F17. Age-depth curve using multiple microfossil and polarity chron datums for Hole 1122C. The best fit line is drawn according to subjective weighting of the chronostratigraphic and geochronologic precision of the events and approximate average rate of sedimentation. Numbers by datums (e.g., F1) denote events listed in Table T8, p. 127. Wavy line at 490 mbsf represents a stratigraphic disconformity.

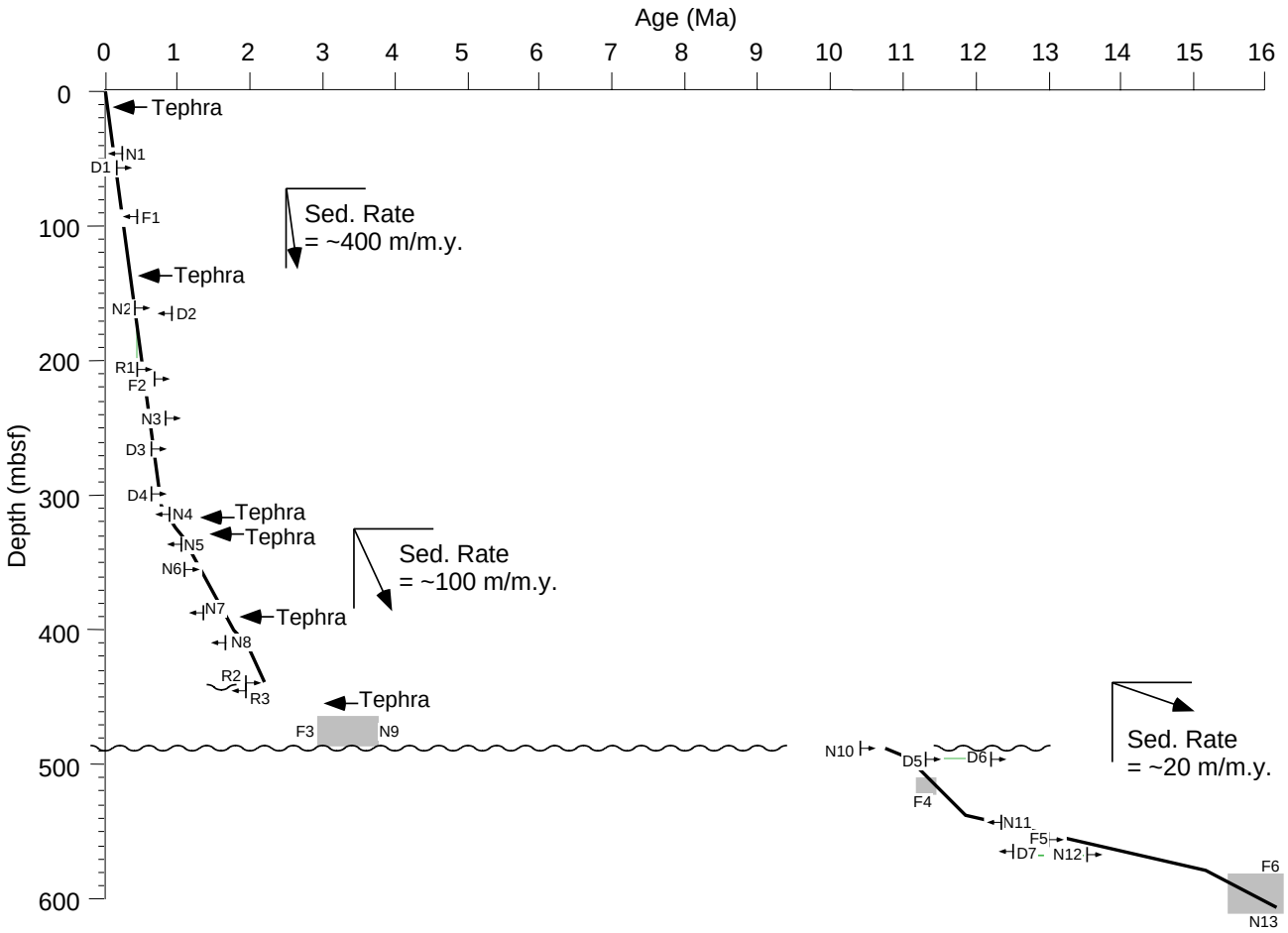

Figure F18. Summary of the changing characteristics of the foraminiferal faunas at Site 1122.

Litho-stratigraphic Unit		Planktonic Fauna	Benthic Fauna		
UNIT I A B C	Turbidite-dominated	Normal, well-preserved, oceanic fauna	Deep-water assemblage with addition of small shelf and bathyal forms		Pliocene-Pleistocene
UNIT I D	Turbidite-dominated	Normal, well-preserved, oceanic fauna	Only deep-water assemblage		Pliocene-Pleistocene
UNIT II A	Contourite-dominated	Large, thick-walled, oceanic fauna, few or no small forms	Only deep-water assemblage	Dissolution	Pliocene-Pleistocene
UNIT II B	Contourite-dominated	Barren or rapidly buried fauna of small forms (winnowings) - minor reworked Oligocene	Barren or only deep-water assemblage	Dissolution	Miocene
UNIT III A	Debris flows and coarse sediments	Variable oceanic fauna	Only deep-water assemblage	Dissolution	Miocene
UNIT III B	Debris flows and coarse sediments	Normal oceanic fauna	Dominantly mid-shelf fauna (large and small) with minor deep-water assemblage		Miocene

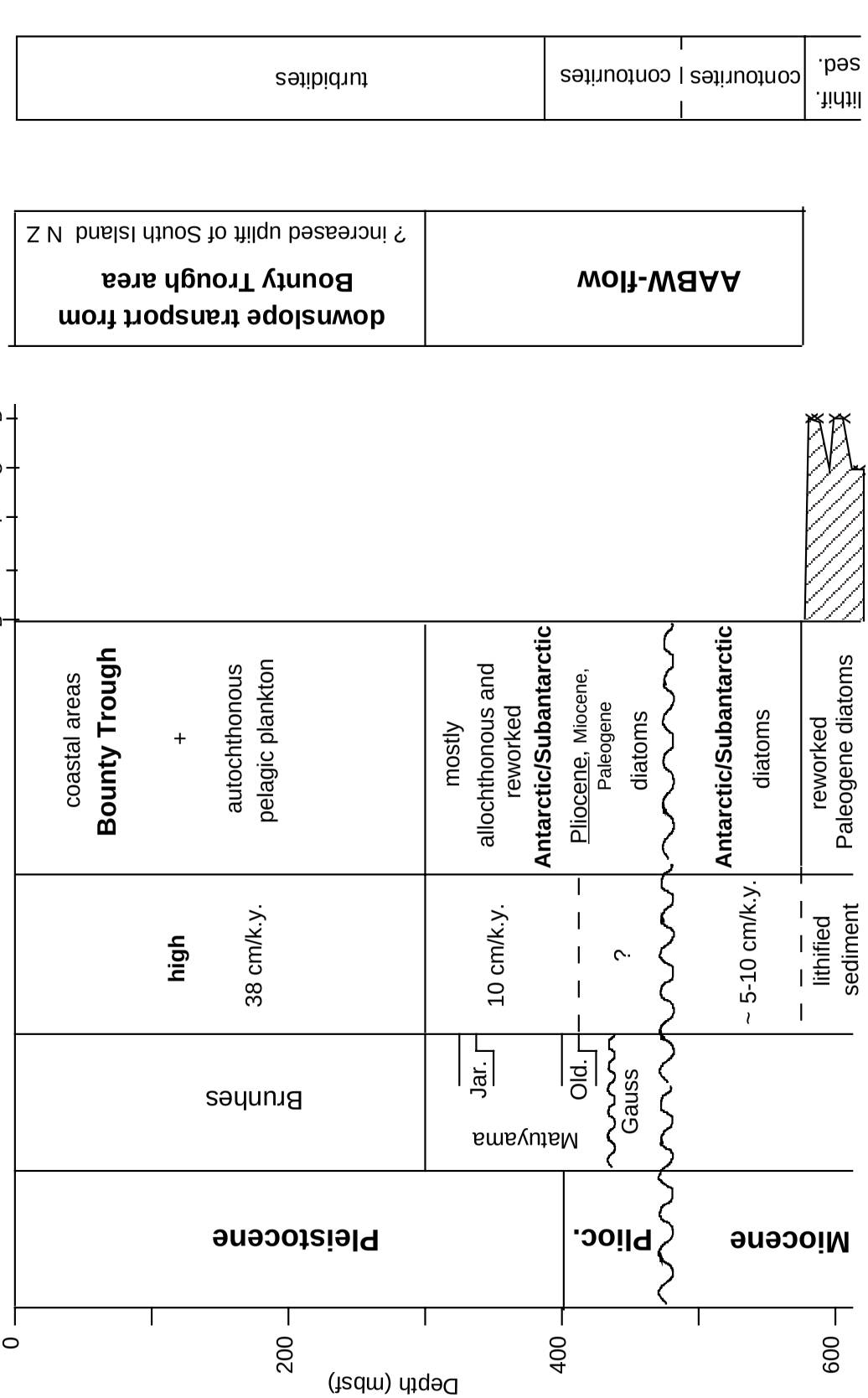

Figure F19. Provenance of diatoms in the Neogene of Hole 1122C and implications for a major change in processes responsible for major sediment input.

Figure F20. Whole-core magnetic susceptibility from Hole 1122C from the Bartington loop of the shipboard automated multisensor track, archive-half continuous measurements of NRM intensity, and intensity of remanence after 20 mT of demagnetization from the pass-though cryogenic magnetometer. Vertical and subvertical lines in the lower 500 mbsf of the hole indicate intervals of nonrecovery of core.

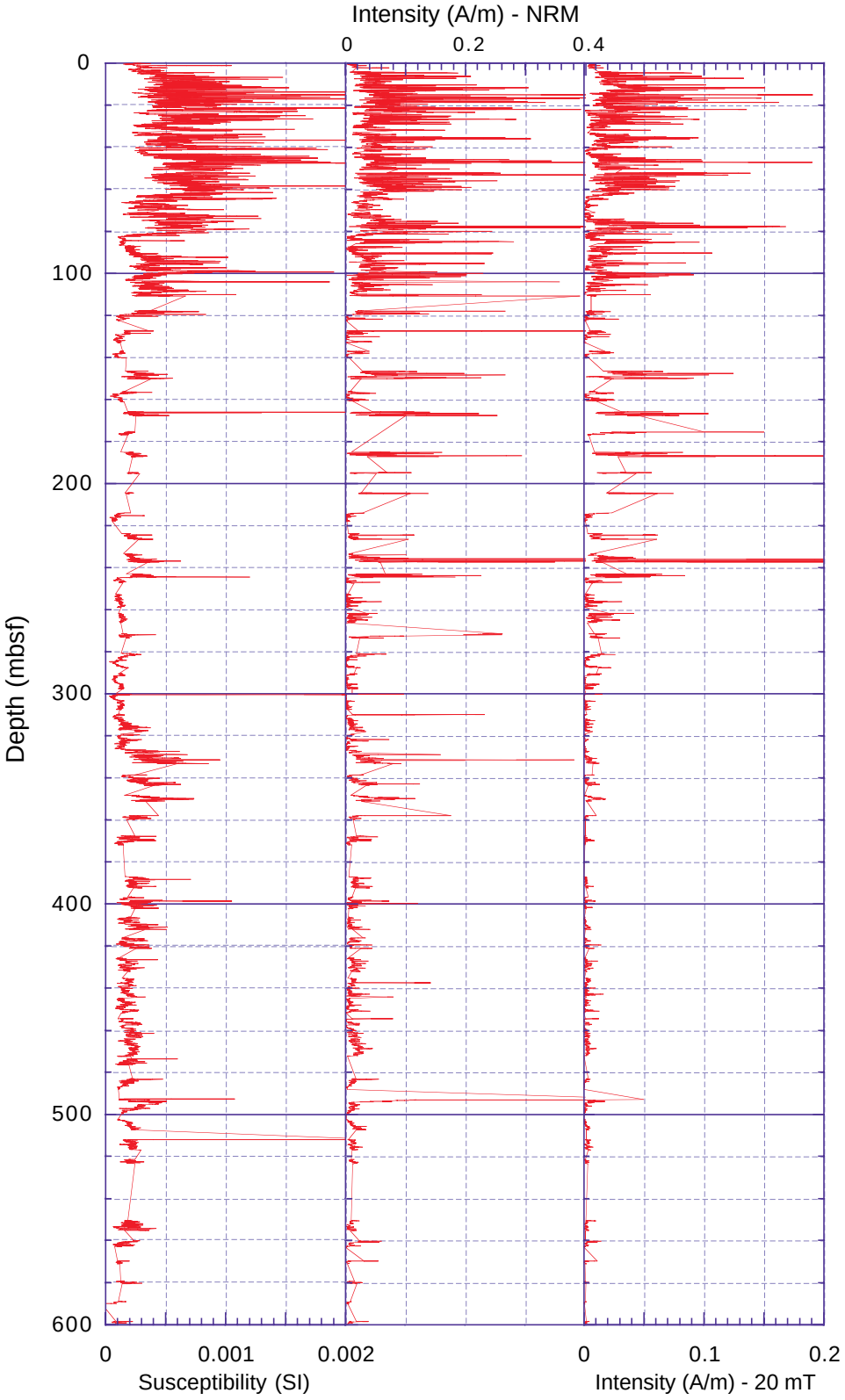

Figure F21. Whole-core inclination of Hole 1122C after alternating-field demagnetization to 20 mT on the pass-though cryogenic magnetometer. Polarity interpretation is given on the right. Black (white) shaded intervals indicate normal (reversed) polarity and hatched shading indicates intervals where polarity could not be determined because of poor recovery. Chrons are identified from correlation with the GPTS (Cande and Kent, 1995; Berggren et al., 1995) constrained by biostratigraphy (see discussion in **"Biostratigraphy,"** p. 13, and Fig. **F25,** p. 66).

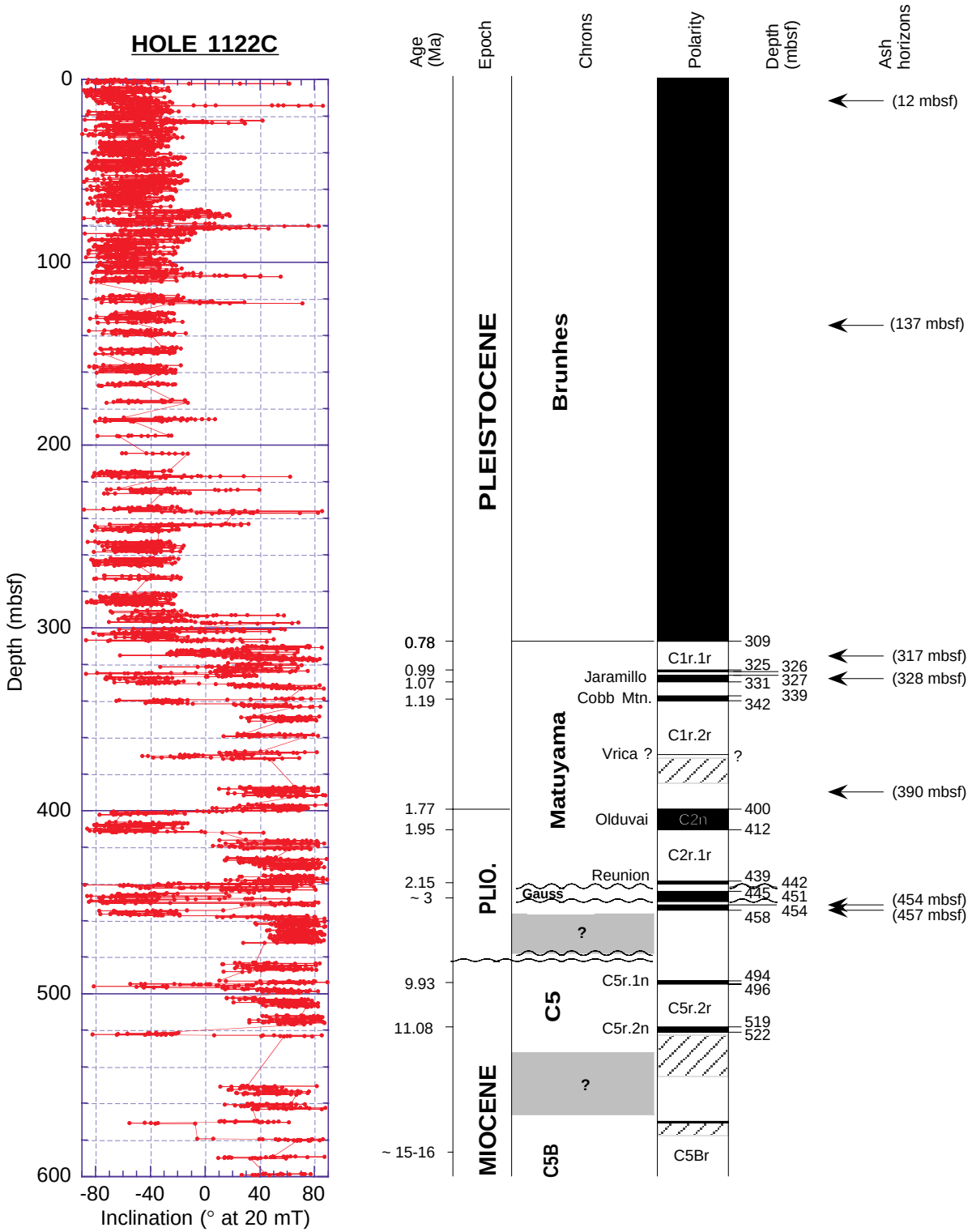

Figure F22. A–I. Vector component diagrams of AF demagnetization behavior of representative discrete samples from Hole 1122C. A, B, G, I show a reversed field drilling-induced overprint on normal polarity samples. B, C show radial remagnetization from attempts to demagnetize samples with AF fields above 50 mT.

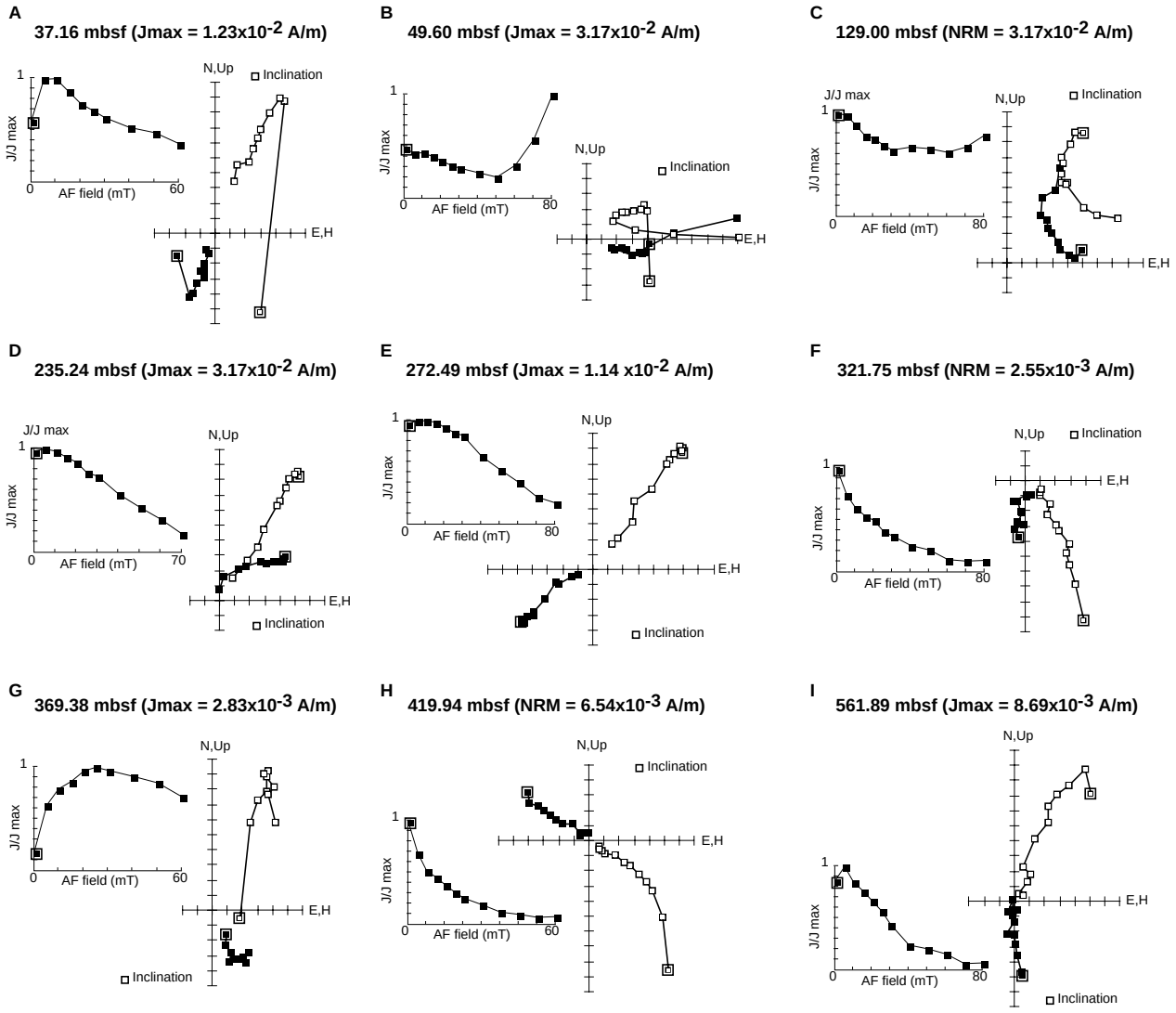

Figure F23. Isothermal remanent magnetization (IRM) and backfield acquisition curves for representative discrete samples from Hole 1122C. **A.** Samples from above 250 mbsf, remanence saturates by 300 mT, and B_{cr} is between 50 and 75 mT. **B.** Samples from 300–400 mbsf, remanence saturates by 300 mT, and B_{cr} is <50 mT. **C.** Samples from beneath 400 mbsf, remanence does not saturate until nearly 1000 mT for samples from 483 and 457 mbsf, B_{cr} values vary between 25 and 75 mT. Remanence does not become saturated until 200–500 mT and B_{cr} is <50 mT for all samples.

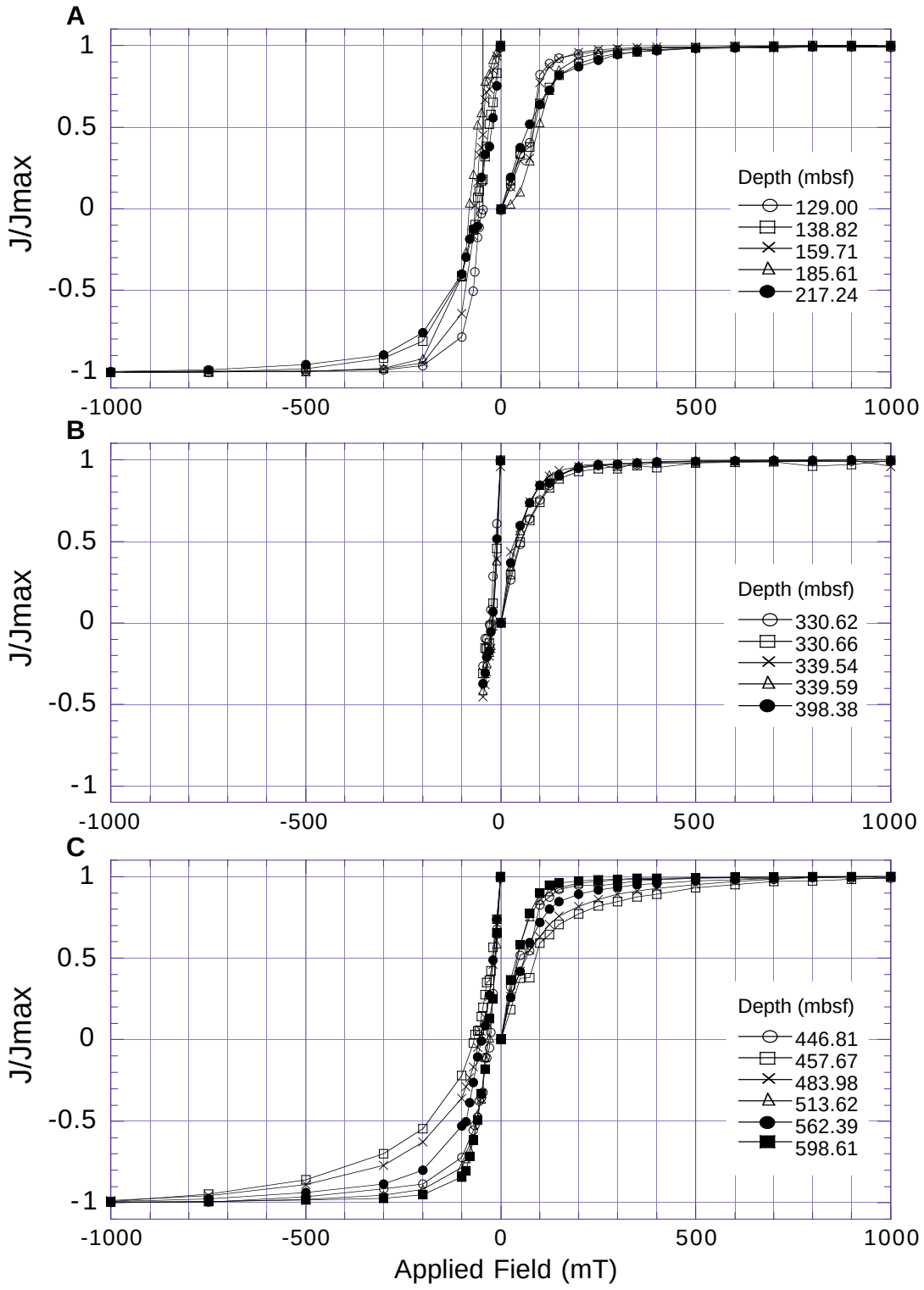

Figure F24. A-F. Plots of normalized intensity of magnetization with progressive AF and thermal demagnetization of saturation isothermal remanent magnetization (SIRM) for selected samples from Hole 1122C.

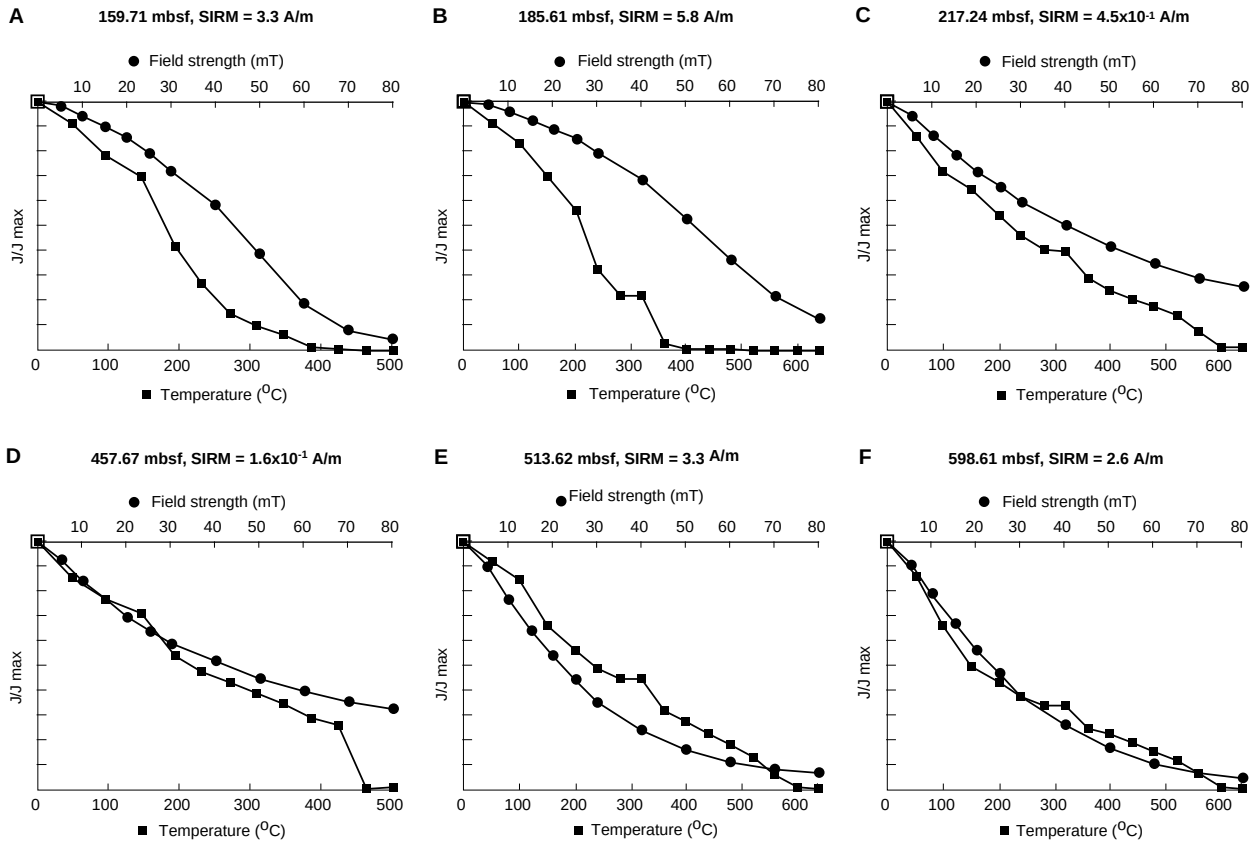

Figure F25. Age model and correlation of Hole 1122C magnetic polarity zonation with the Geomagnetic Polarity Time Scale of Berggren et al. (1995) and Cande and Kent (1995). Where correlation is unambiguous, it is shown by a solid black line. Black (white) shaded intervals indicate normal (reversed) polarity and hatched shading indicates intervals where polarity could not be determined because of nonrecovery. Stippled lines show constraining biostratigraphic datums and shaded lines show magnetic polarity correlations. Undulating lines indicate stratigraphic disconformities and shaded areas indicate levels of uncertainty in datums. Correlation is constrained by the following foraminifer, nannofossil, diatom, and radiolarian datums (see discussion in **"Biostratigraphy,"** p. 13; see also **"Biostratigraphy,"** p. 10, in the "Explanatory Notes" chapter). Foraminifers: F1 (FO of *Gr. hirsuta,* 0.45 Ma), F2 (LO of *Gr. puncticuloides,* 0.7–0.8 Ma), F3 (several forms younger than ~3.4 Ma, see **"Biostratigraphy,"** p. 13), F4 (occurrence of *N. continuosa* and *N. pachyderma,* ~11.3 Ma), F5 (LO of *Gr. praemenardii,* ~13.0 Ma), F6 (co-occurrence of *Gr. zealandica* and *Gr. miozea,* 16.3–16.7 Ma). Nannofossils: N1 (FO of *Emiliania huxleyi,* 0.24 Ma), N2 (LO of *Pseudoemiliania lacunosa,* 0.42 Ma), N3 (LO of *R. asanoi,* 0.83 Ma), N4 (FO of *G. parallela,* 0.9 Ma), N5 (FO of *R. asanoi,* 1.06 Ma), N6 and N7 (range of *Gephyrocapsa* [large], 1.1–1.36 m.y.), N8 (FO of *Gephyrocapsa* [medium], 1.66 Ma), N9 (several forms co-occurring, ~3.45 Ma, see **"Biostratigraphy,"** p. 13), N10 (LO of *C. miopelagicus,* > 10.4 Ma), N11 (FO of *C. macintyrei,* 12.34 Ma), N12 (LO of *S. heteromorphus,* 13.52 Ma), N13 (absence of *C. premacintyrei* FO, <17.4 Ma). Diatoms: D1 (LO of *Hemidiscus karstenii,* 0.18–0.19 Ma), D2 (*H. karstenii,* acme, 0.92 Ma), D3 (LO of *A ingens,* 0.64 Ma), D4 (LO of *T. elliptipora,* 0.65–0.7 Ma), D5 (LO of *Nitzschia denticuloides,* 11.3–22.7 Ma), D6 (LO of *D. dimorpha,* 12.2 Ma), D7 (FO of *S. barboi,* 12.5 Ma). Radiolarians: R1 (LO of *Stylatractus universus,* 0.46 Ma), R2 (LO of *L. nautiloides,* 1.93 Ma), R3 (FO of *E. calvertense,* 1.92 Ma). (**Figure shown on next page.**)

Figure F25 (continued).

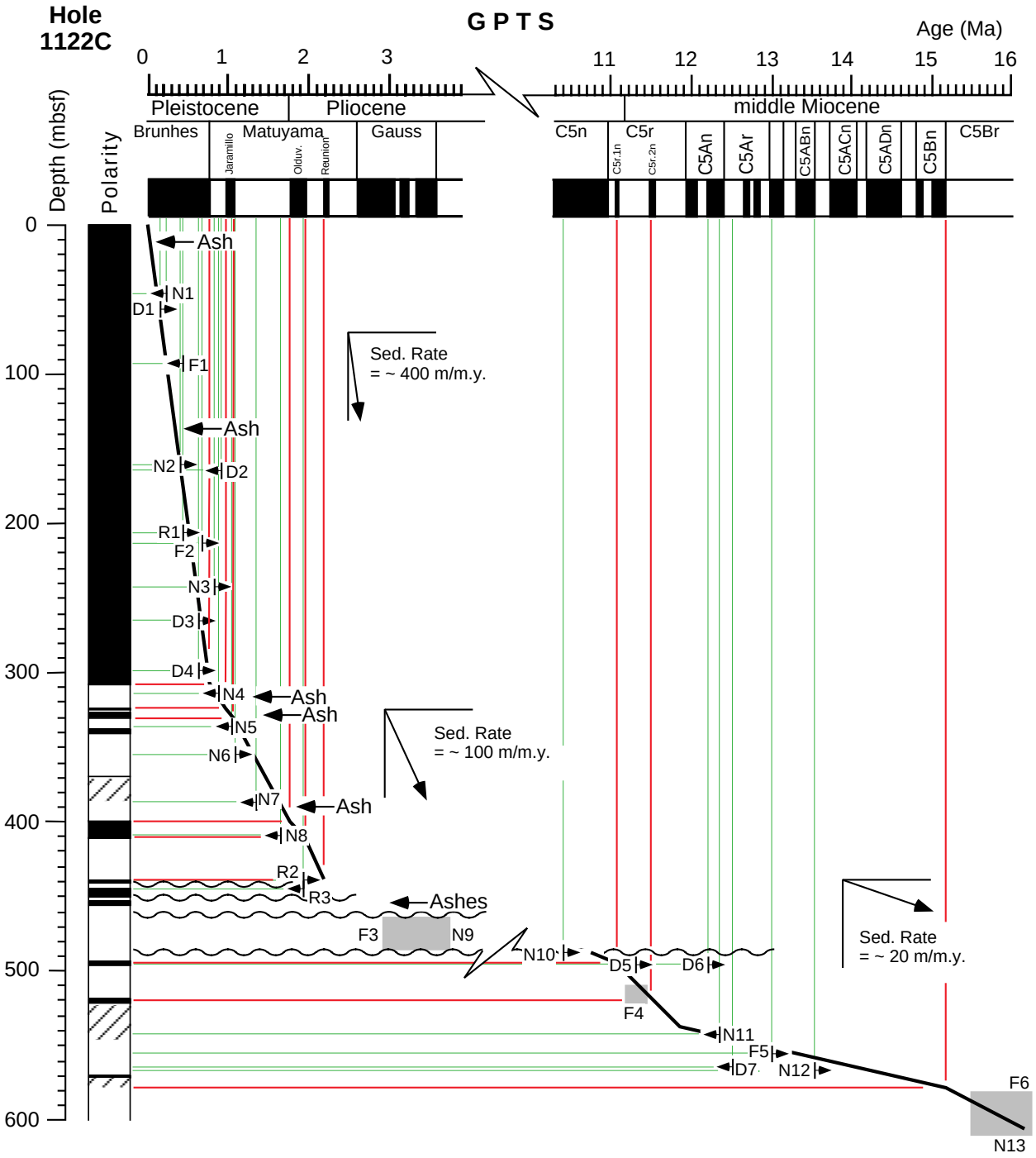

Figure F26. Composite sections for MS, GRAPE, and reflectance percentage at 550 nm. For convenience, MS values from Holes 1122B, 1122C, and Core 181-1122C-3H are offset by 70 × 10^{-5}, 140 × 10^{-5}, and 240 × 10^{-5}, respectively; GRAPE values are offset by 0.4, 0.8, and 1.2 g/cm^3, respectively; and reflectance values are offset by 8%, 16%, and 22%, respectively. Gaps in the composite section are indicated with triangles. Cores are indicated by small numbers. KK indicates the approximate depth of the Kawakawa Tephra (12.62 mcd in Core 181-1122A-1H, 13.14 mcd in Core 2H, and 12.74 mcd in Core 3H). (Continued on next page.)

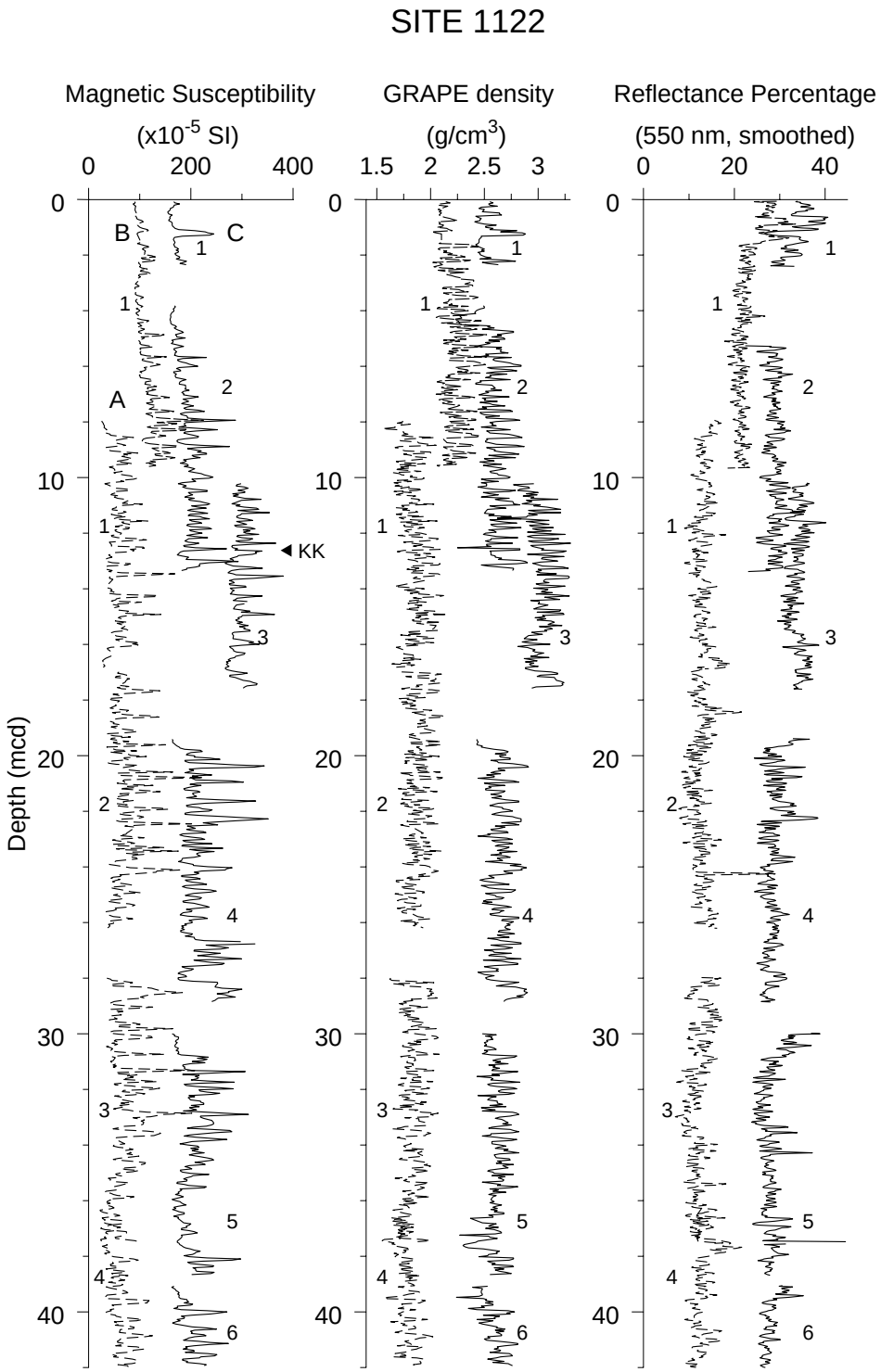

Figure F26 (continued).

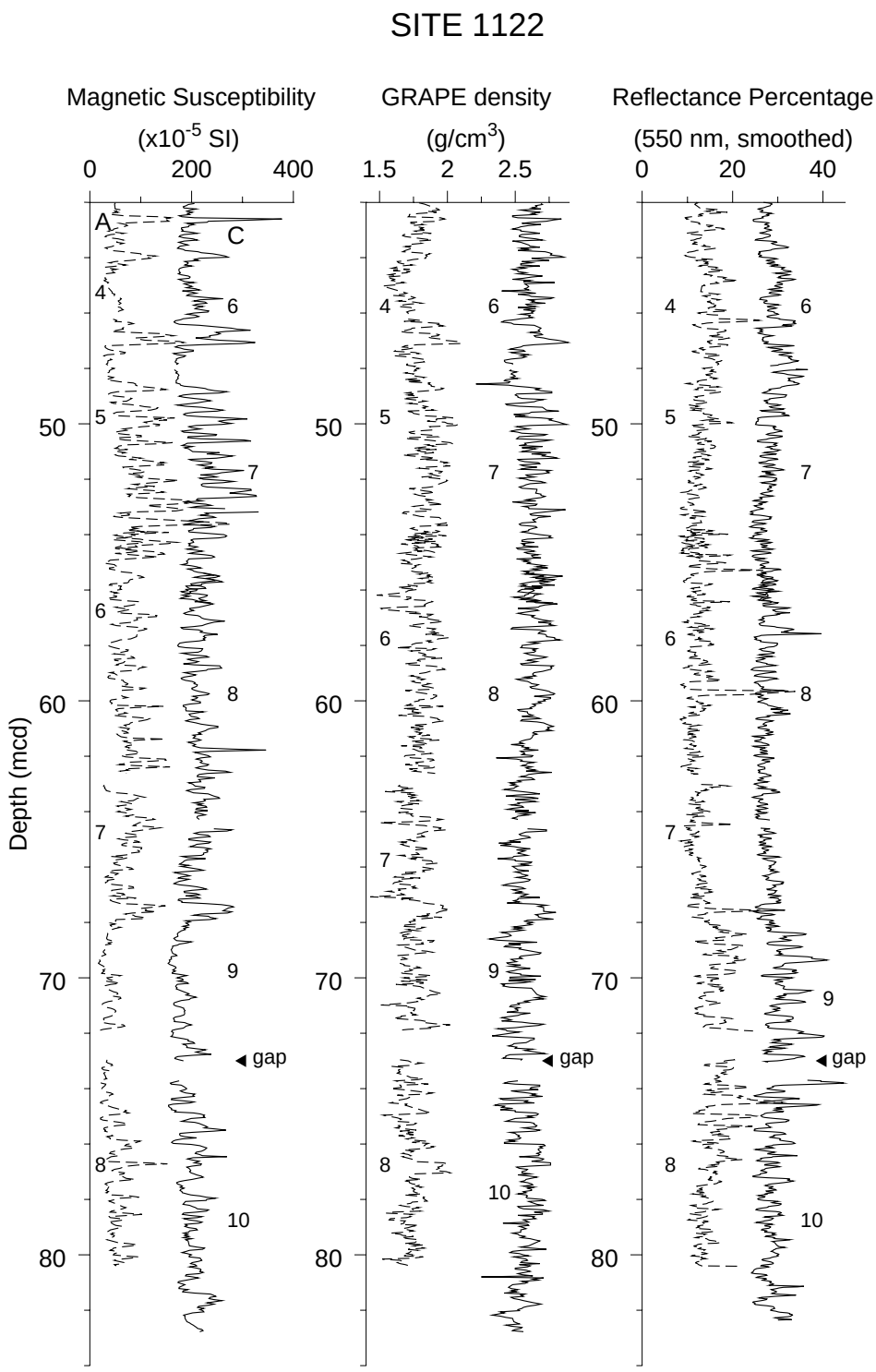

Figure F27. Downhole depth offsets between the mbsf and mcd scales for Site 1122. Solid line indicates the trend for a typical 10% stretch model between mbsf and mcd depths. Composite depth offsets are unusually constant downhole and do not follow a stretch model.

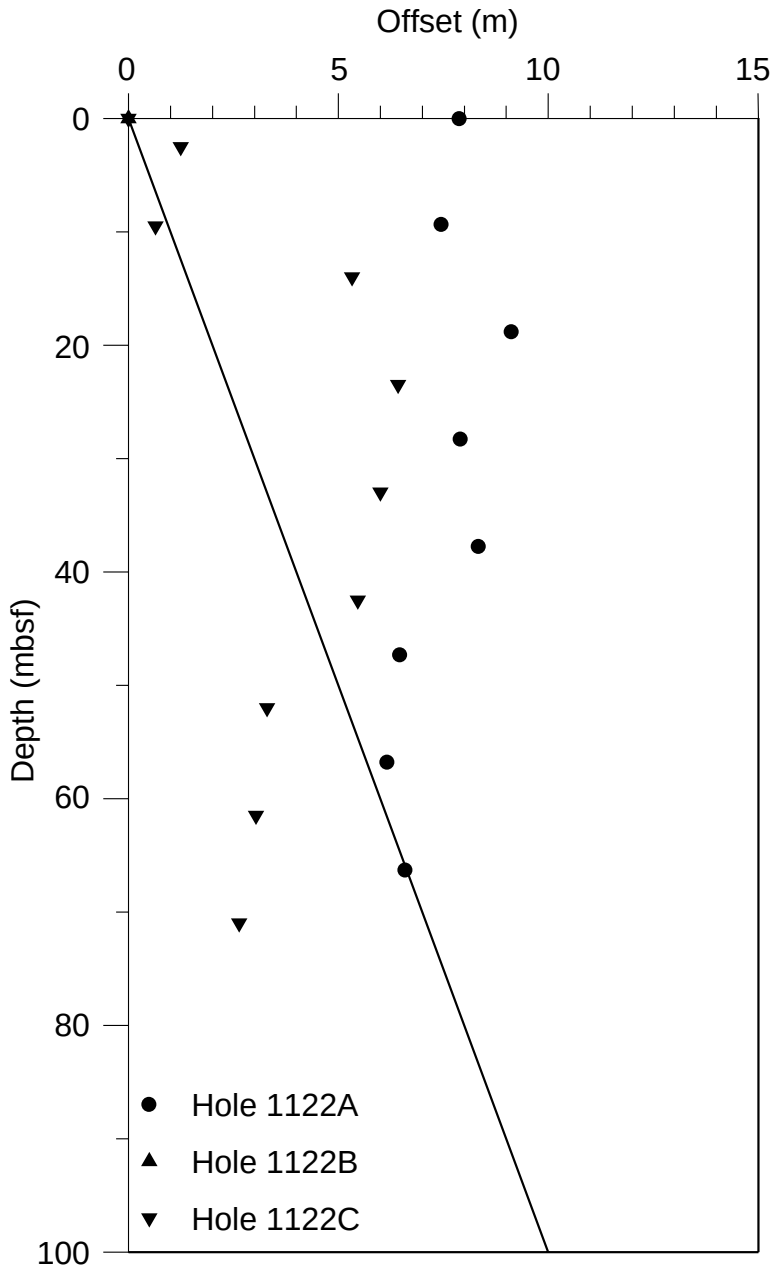

Figure F28. Spliced record for Site 1122. To reduce noise, MS, GRAPE density, and reflectance data illustrated were smoothed with a 5-point Gaussian window.

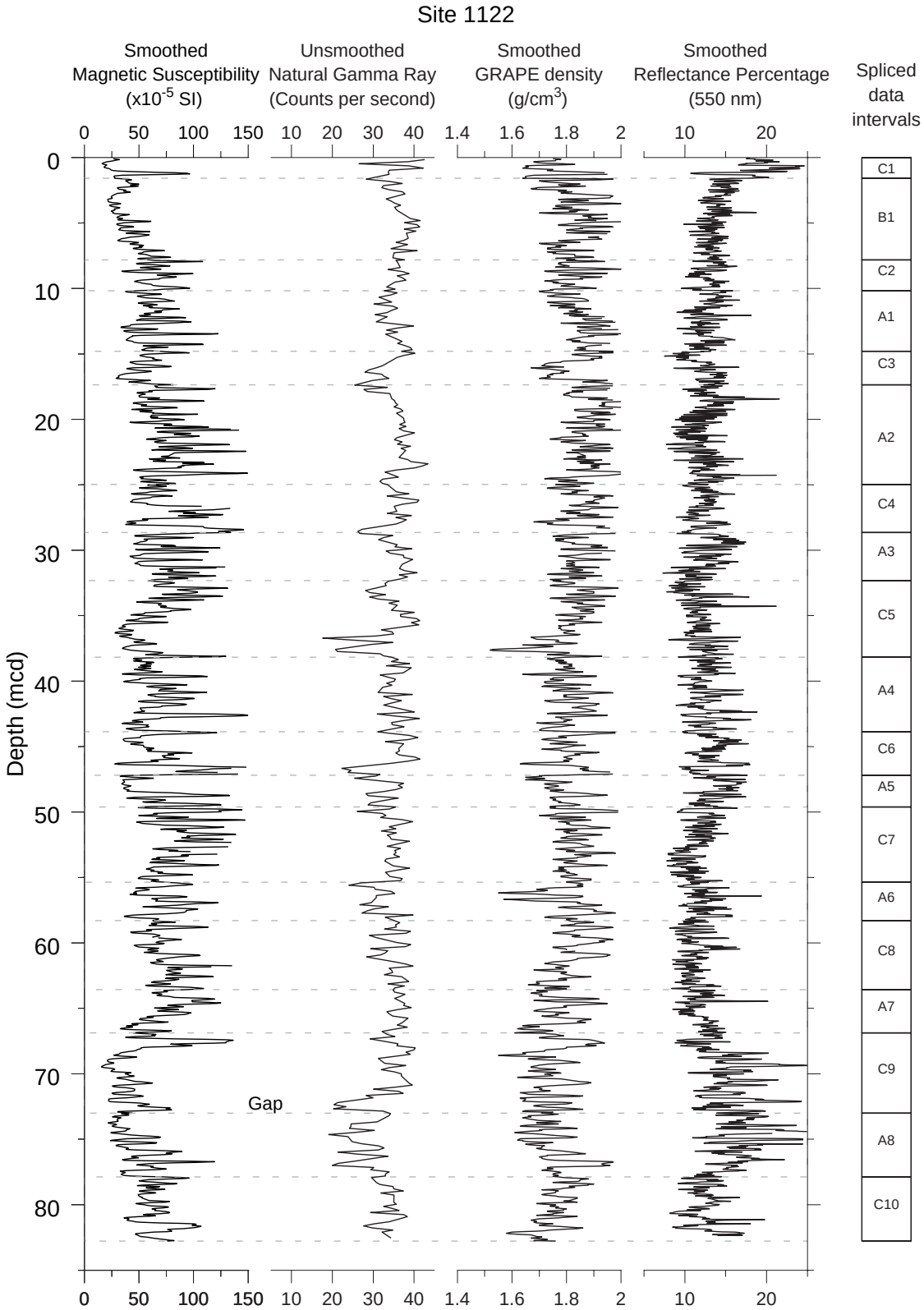

Figure F29. Sketch of oceanic subsidence history of Site 1122, Bounty Fan, in almost 4500-m present-day water depth. The site is slightly to the east of marine magnetic Anomaly 32 (late Campanian, ~72 Ma). Over 600 m of Neogene turbiditic and "drift" type sediment fill was cored at Site 1122. Campanian–Paleocene siliceous clays, overlying ocean basement at the site, are inferred from analog strata cored at Site 1121 and DSDP Site 275 (see **"Lithostratigraphy,"** p. 3, in the "Site 1121" chapter) and from multichannel seismic data at Site 1122. The basal, oceanic sediments are estimated to be ~1 km thick.

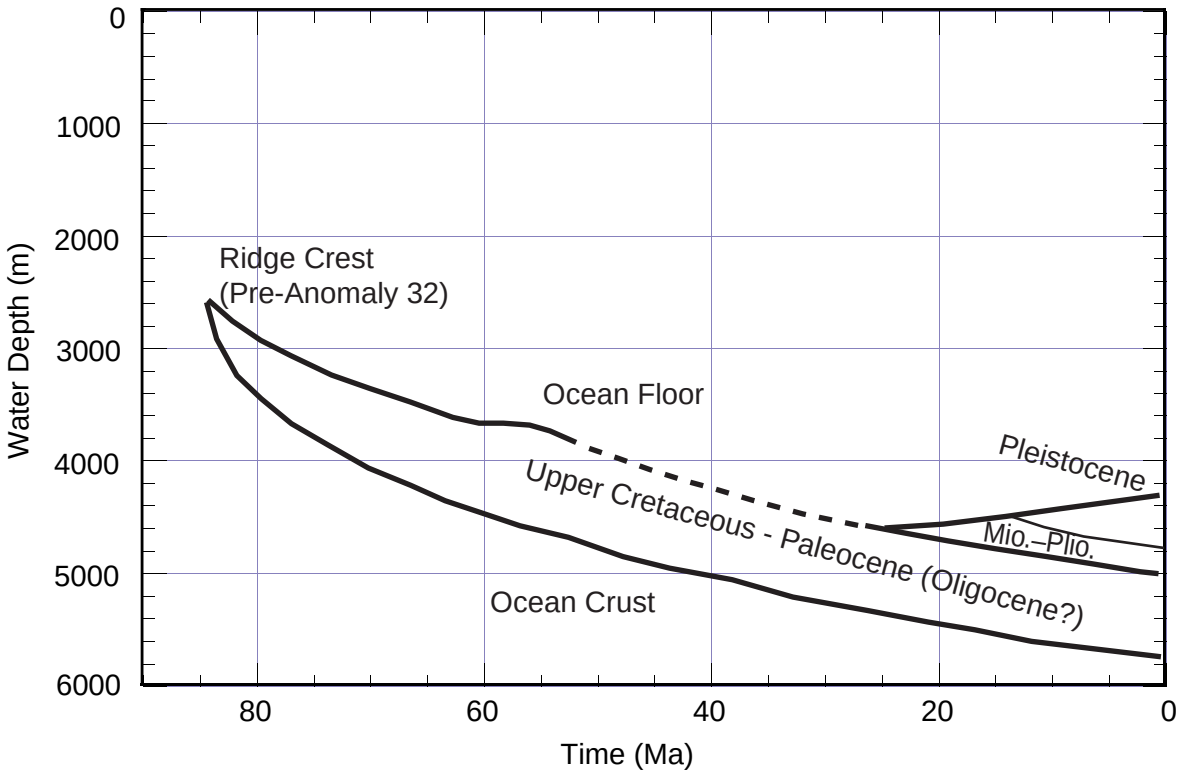

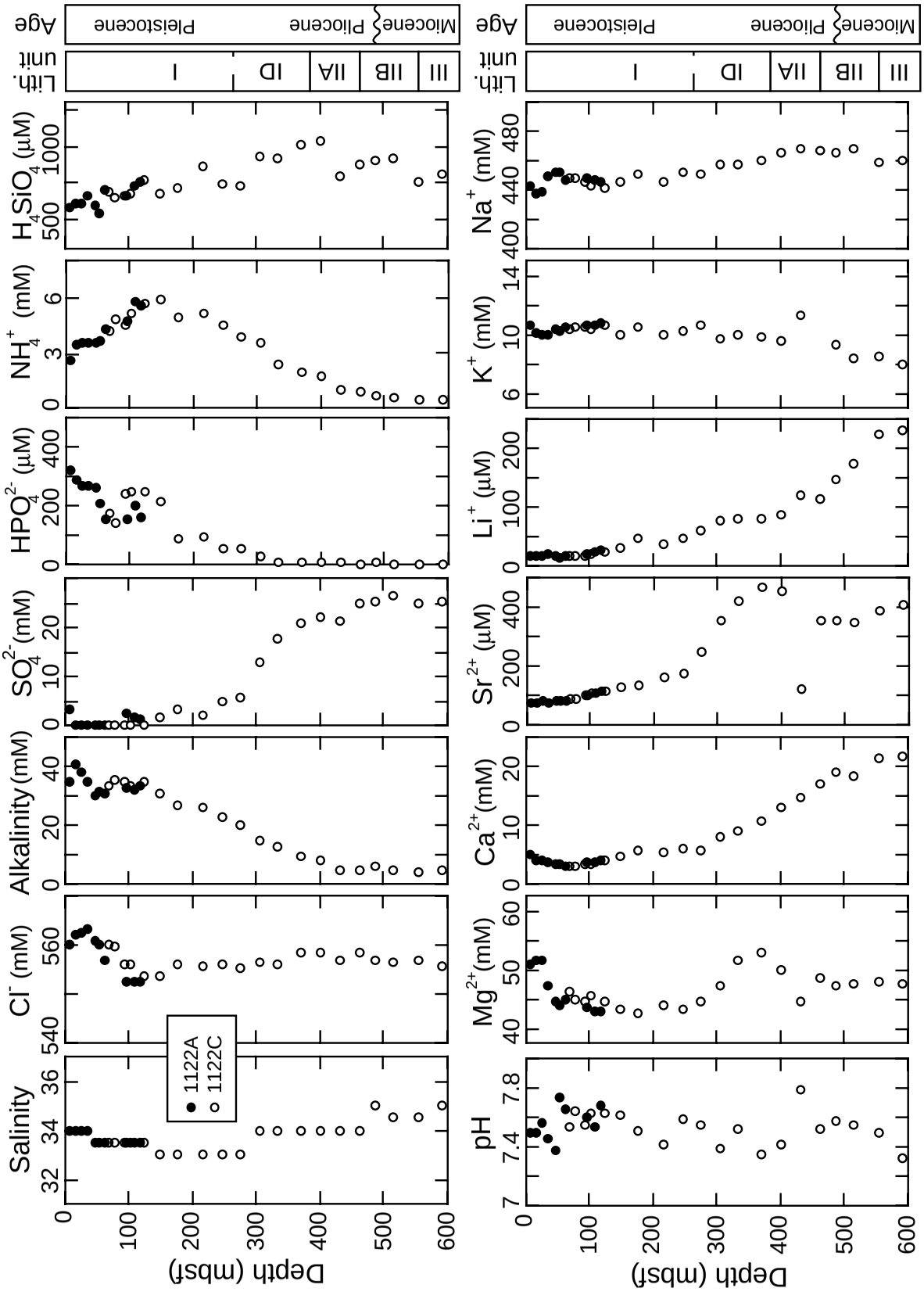

Figure F30. Depth profiles of interstitial-water constituents at Site 1122.

Figure F31. Headspace methane concentrations in sediments from Holes 1122A, 1122C, and, for comparison, Site 1119.

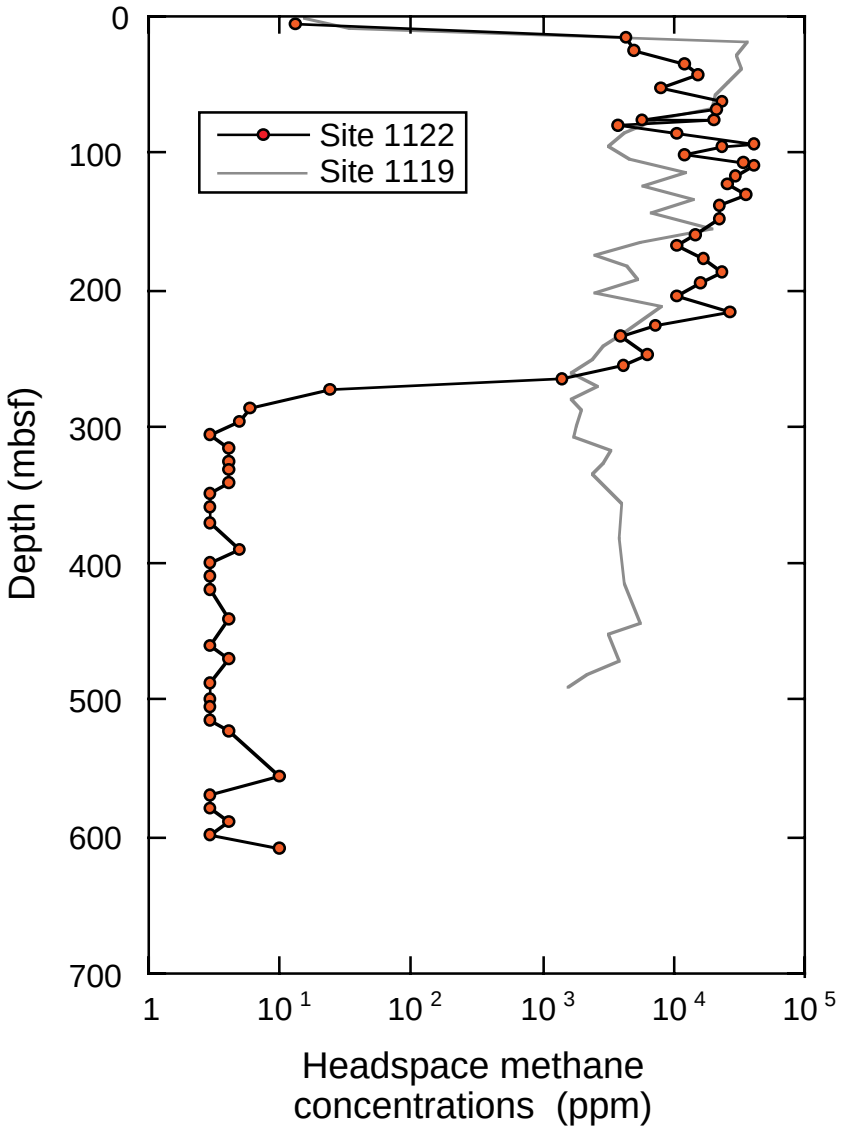

Figure F32. Carbonate contents in sediments from Holes 1122A and 1122C.

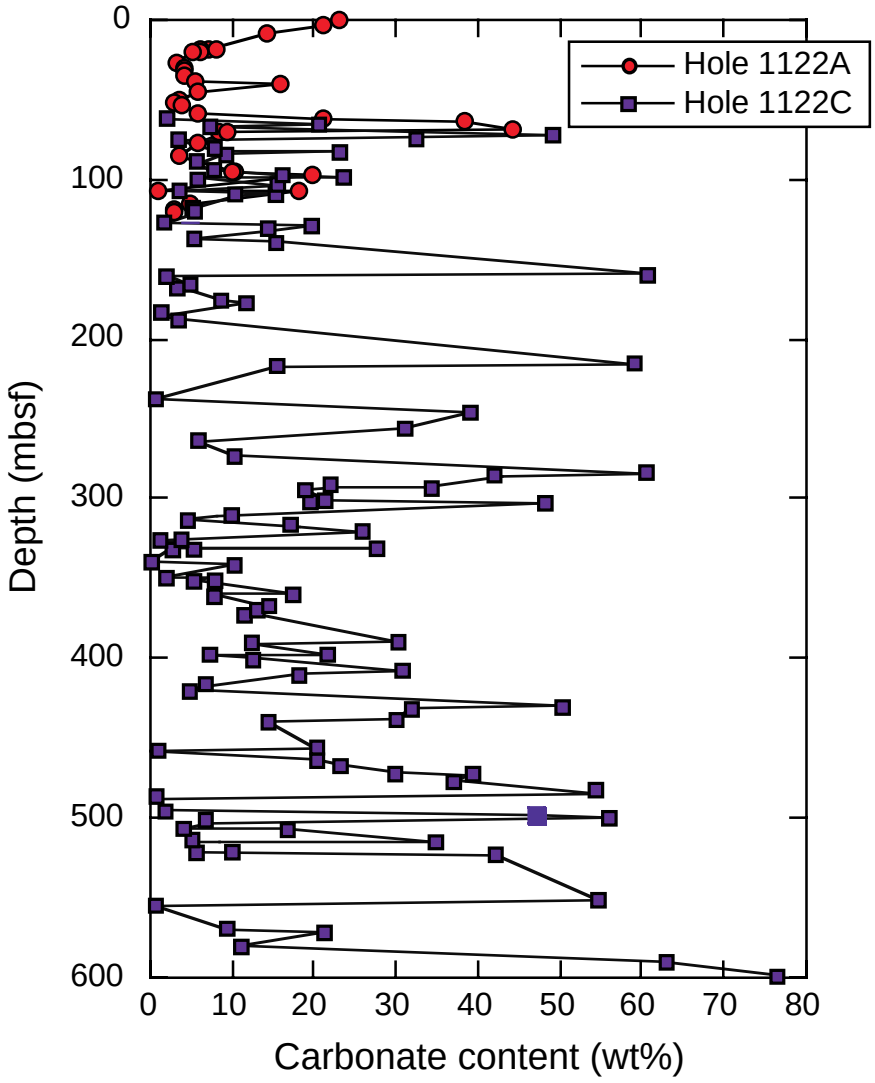

Figure F33. Organic carbon contents in sediments from Holes 1122A and 1122C.

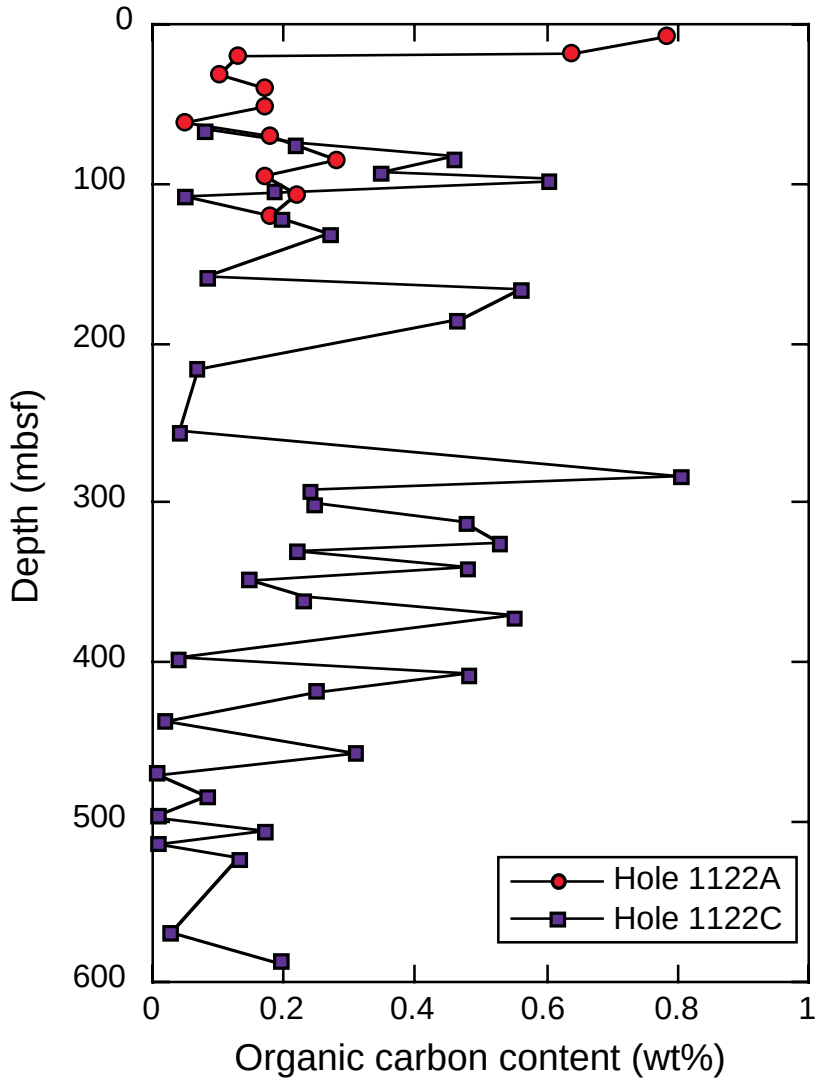

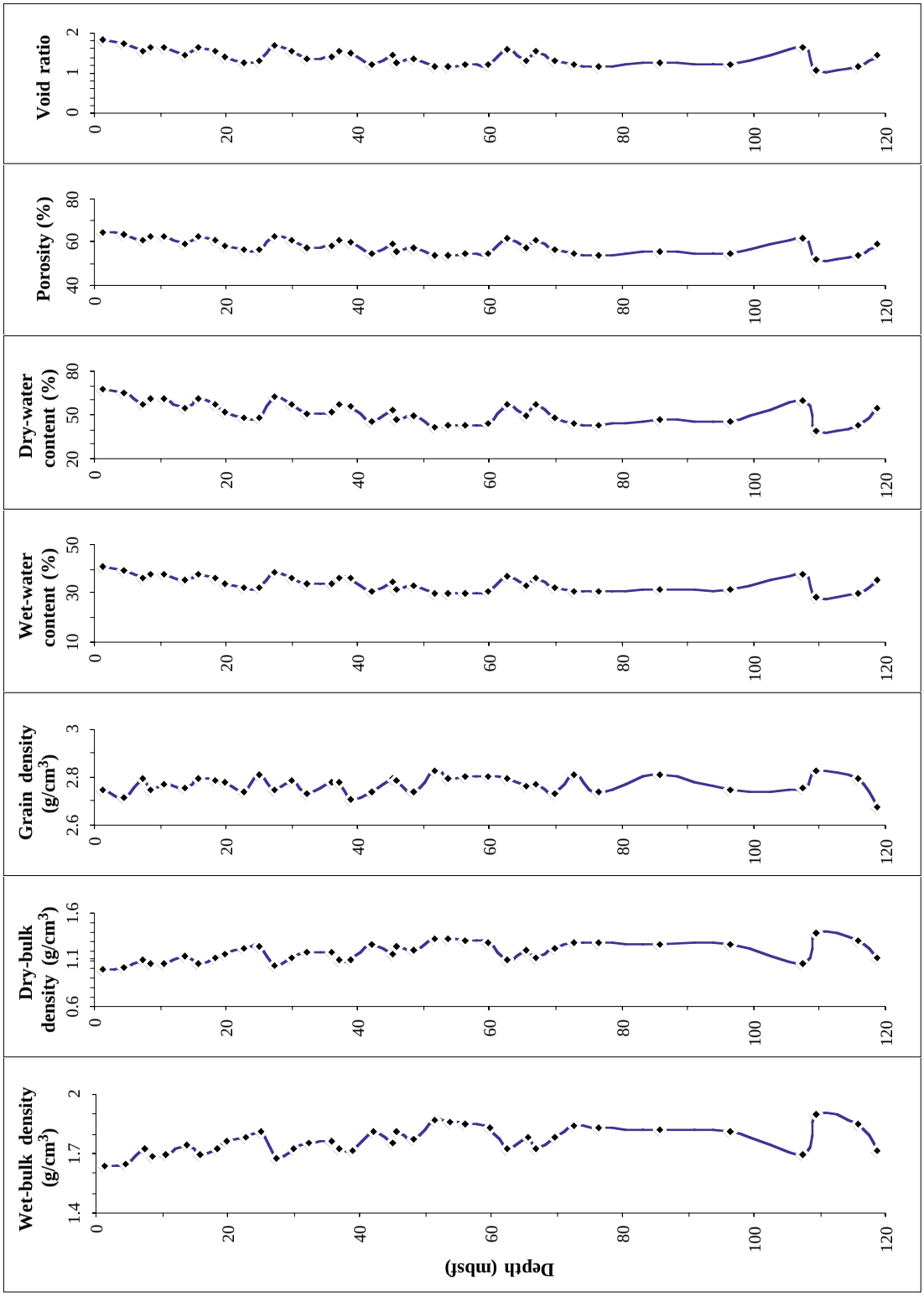

Figure F34. Index properties measurements from cores from Hole 1122A.

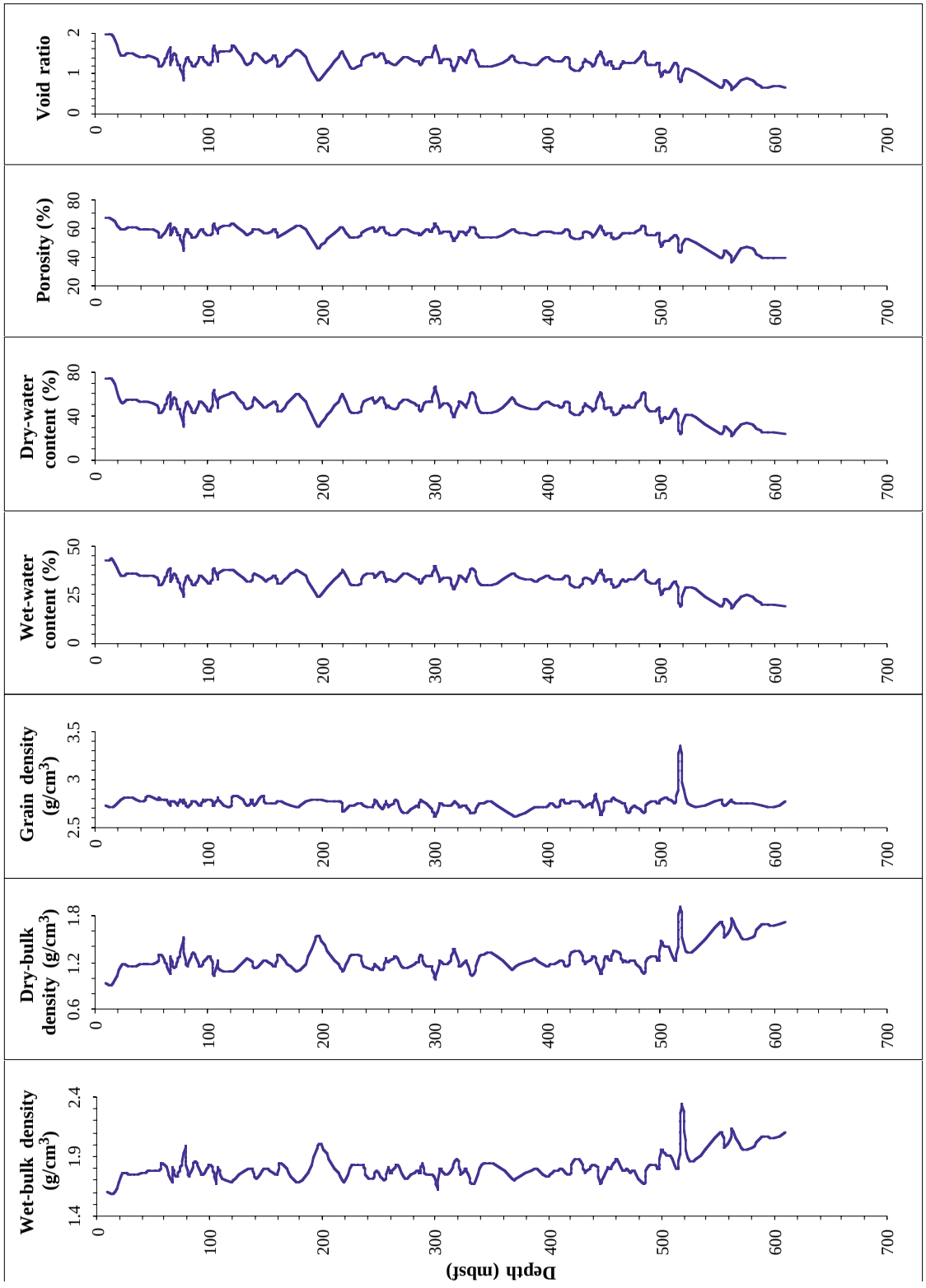

Figure F35. Index properties measured from cores from Hole 1122C.

Figure F36. MST measurements from Hole 1122A including GRAPE density, magnetic susceptibility, natural gamma-ray intensity, and *P*-wave velocity.

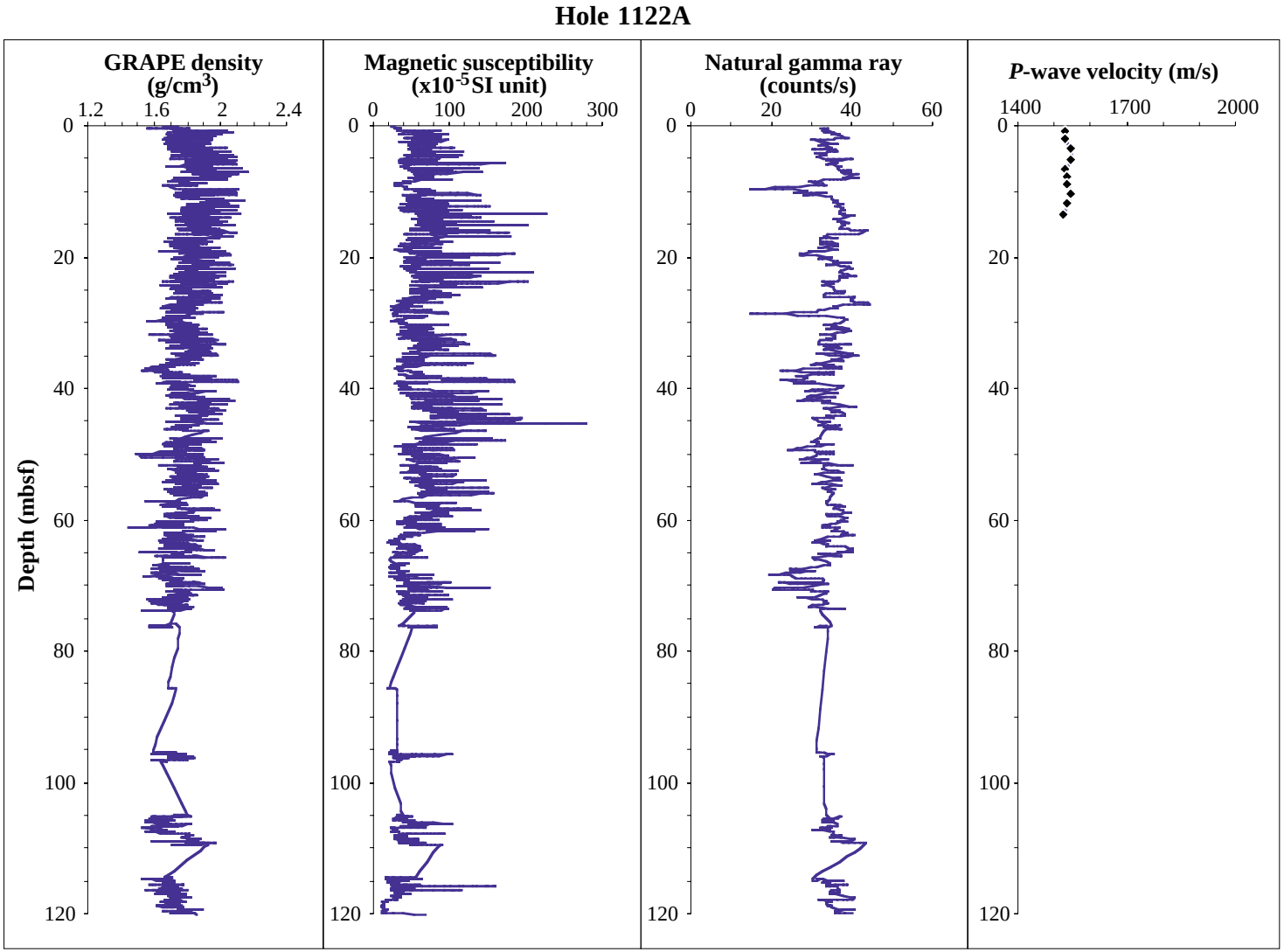

Figure F37. MST measurements from Hole 1122C including GRAPE density, magnetic susceptibility, natural gamma-ray intensity, and *P*-wave velocity.

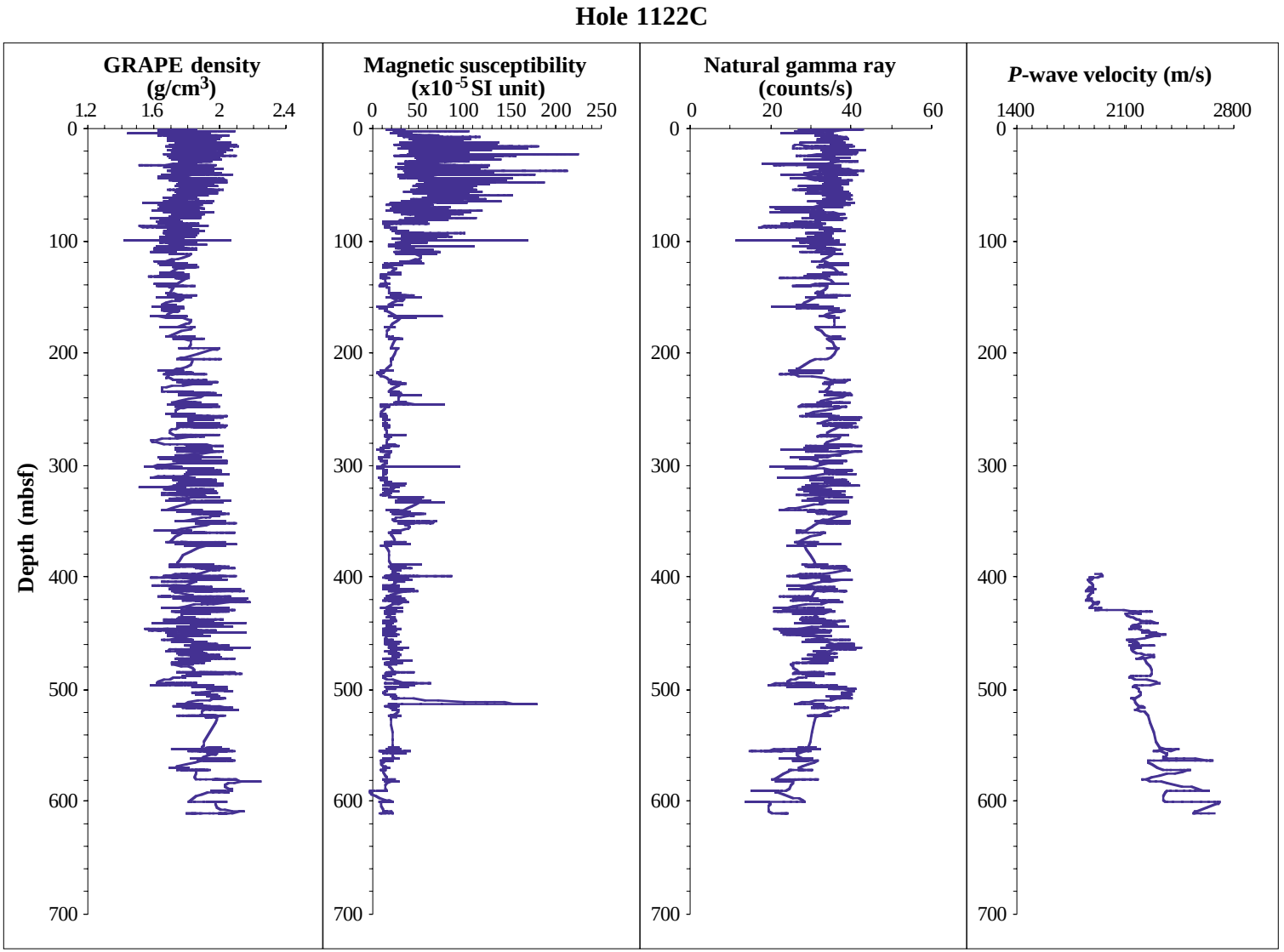

Figure F38. Density measurements in Hole 1122C using the GRAPE instrument on the MST in comparison with index properties. The circle markers indicate the distribution of wet-bulk density based on index property measurement.

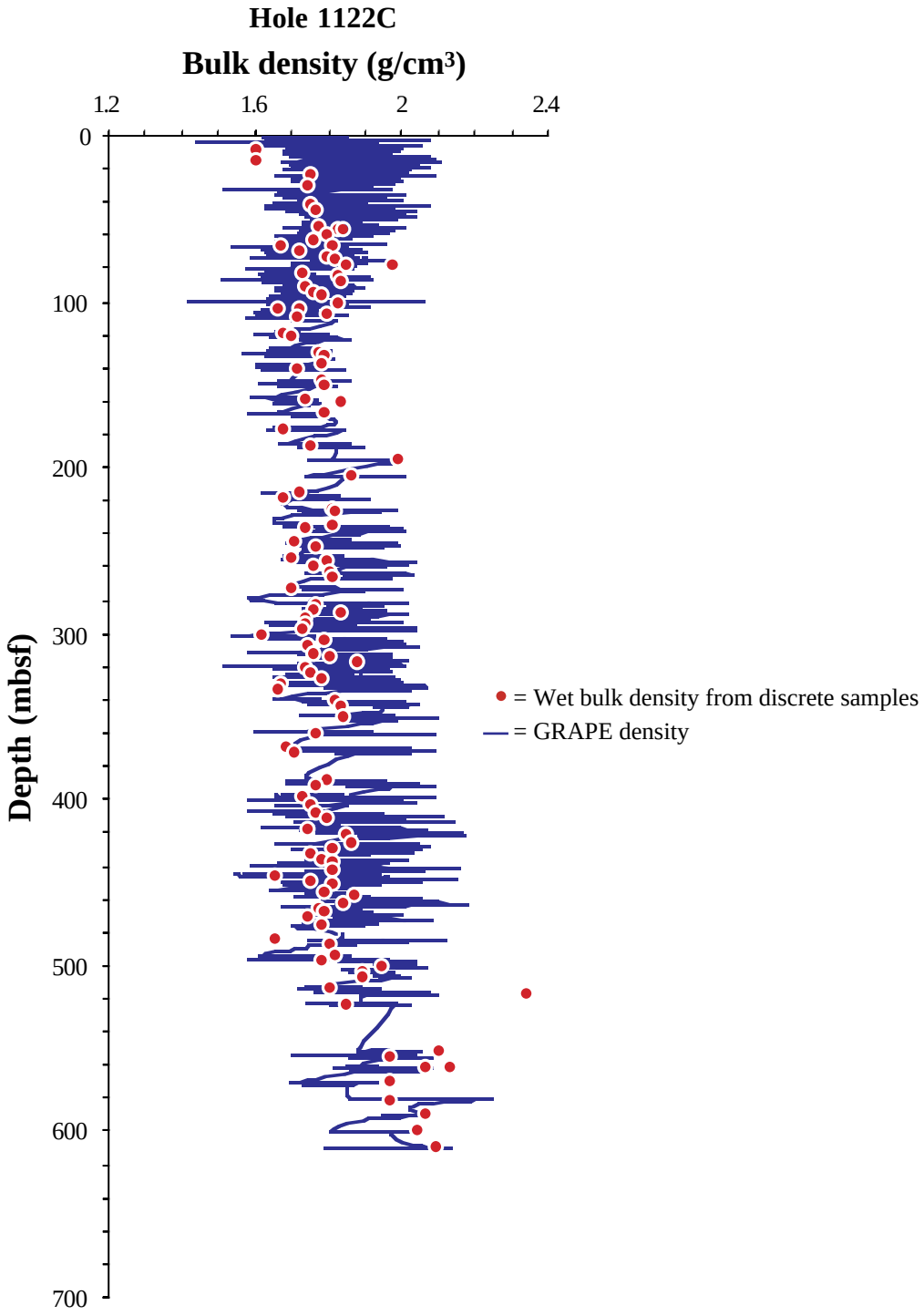

Figure F39. Distribution of shear strength in cores and the ratio of vane shear strength to overburden pressure determined from Holes 1119B, 1122A, and 1122C.

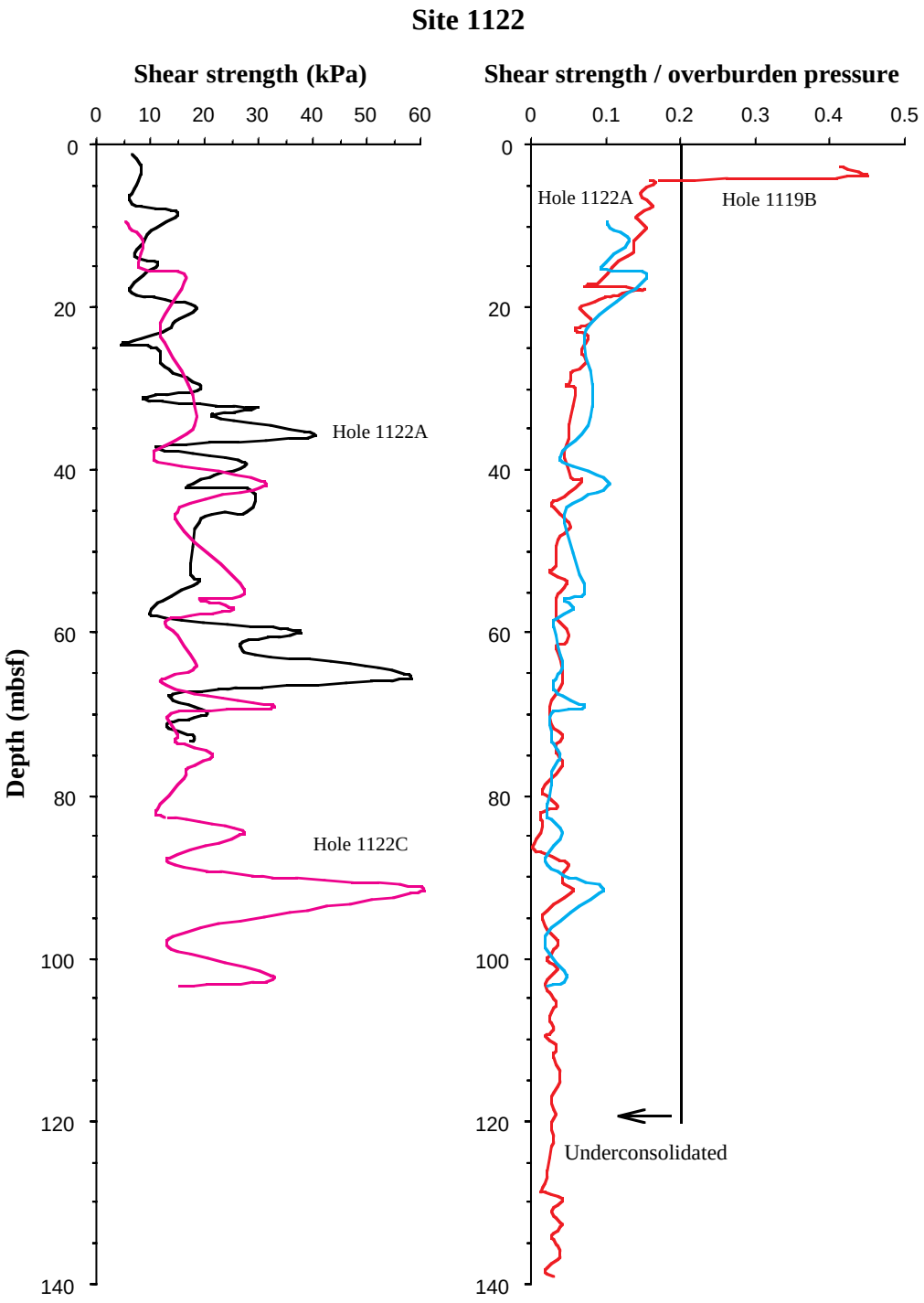

Table T1. Summary of seismic units and depth reflectors.

Plotted using assumed velocity profile							
Reflector	Unit	Time to top (ms TWT)	Assumed velocity (m/s)	Depth to reflector (m)	Thickness (m)	Cumulative thickness (m)	Character of reflections within units
Seabed				0	60		
R-1a		80	1510	60	69		Reflectors separate bundles of grouped waves
R-1b		170	1520	129	100		
R-1c		300	1530	230	68		
R-1d		387	1540	298	66		Faint reflectors; muddier subunit
	A				364	364	South-migrating sediment waves
R-2a		470	1550	364	54		
R-2b		523	1600	418	82		
	B				136	500	N-onlapping S-prograding and downlapping
R-3		580	1725	500			*Paraconformity (onlaps north)*
Depth drilled to 627 m							
	C				139	639	North-onlapping sediment prism
R-4		730	1750	639			*Unconformity Y (Davey, 1977)*
	D				1069	1708	Postrift sedimentary cover
Basement		1485	2300	1708			Oceanic crust
Estimated thickness to basement: 1708 m							

Plotted using velocity profile provided by downhole measurements							
Reflector	Unit	Time to top (ms TWT)	Assumed velocity (m/s)	Depth to reflector (m)	Thickness (m)	Cumulative thickness (m)	Character
Seabed				0	62		
R-1a		80	1548	62	73		Reflectors separate bundles of grouped waves
R-1b		170	1591	135	109		
R-1c		300	1629	244	74		
R-1d		387	1645	318	72		Faint reflectors; muddier subunit
	A				390	390	South-migrating sediment waves
R-2a		470	1660	390	57		
R-2b		523	1710	447	54		
	B				111	501	N-onlapping S-prograding and downlapping
R-3		580	1728	501			*Paraconformity (onlaps north)*
Depth drilled to 627 m							
	C				130	631	North-onlapping sediment prism
R-4		730	1730	631			*Unconformity Y (Davey, 1977)*
	D				1076	1708	Post-rift sedimentary cover
Basement		1485	2300	1708			Oceanic crust
Estimated thickness to basement: 1708 m							

Note: Horizontal lines separate the main seismic units recognized. Italics indicate unconformities.

Table T2. Site 1122 expanded coring summary. (**See table note.** Continued on next 12 pages).

Core	Date (September 1998)	Time (UTC)	Core depth (mbsf) Top	Core depth (mbsf) Bottom	Length (m) Cored	Length (m) Recovered	Recovery (%)	Section	Length (m) Liner	Length (m) Curated	Section depth (mbsf) Top	Section depth (mbsf) Bottom	Catwalk samples	Comment
181-1122A-														
1H	6	0040	0	9.3	9.3	9.32	100.2							
								1	1.5	1.5	0	1.5		
								2	1.5	1.5	1.5	3		
								3	1.5	1.5	3	4.5		
								4	1.5	1.5	4.5	6	IW	
								5	1.5	1.5	6	7.5	HS	
								6	1.5	1.5	7.5	9		
								7	0.14	0.14	9	9.14		
								CC	0.18	0.18	9.14	9.32	PAL	
									9.32	9.32				
2H	6	0155	9.3	18.8	9.5	9.66	101.7							
								1	1.5	1.5	9.3	10.8		
								2	1.5	1.5	10.8	12.3		
								3	1.5	1.5	12.3	13.8		
								4	1.5	1.5	13.8	15.3	IW	
								5	1.5	1.5	15.3	16.8	HS	
								6	1.5	1.5	16.8	18.3		
								7	0.48	0.48	18.3	18.78		
								CC	0.18	0.18	18.78	18.96	PAL	
									9.66	9.66				
3H	6	0300	18.8	28.3	9.5	9.77	102.8							
								1	1.5	1.5	18.8	20.3		
								2	1.5	1.5	20.3	21.8		
								3	1.5	1.5	21.8	23.3		
								4	1.5	1.5	23.3	24.8	IW	
								5	1.5	1.5	24.8	26.3	HS	
								6	1.5	1.5	26.3	27.8		
								7	0.63	0.63	27.8	28.43		
								CC	0.14	0.14	28.43	28.57	PAL	
									9.77	9.77				
4H	6	0425	28.3	37.8	9.5	10.05	105.8							
								1	1.5	1.5	28.3	29.8		
								2	1.5	1.5	29.8	31.3		
								3	1.5	1.5	31.3	32.8		
								4	1.5	1.5	32.8	34.3	IW	
								5	1.5	1.5	34.3	35.8	HS	
								6	1.5	1.5	35.8	37.3		
								7	0.9	0.9	37.3	38.2		
								CC	0.15	0.15	38.2	38.35	PAL	
									10.05	10.05				
5H	6	0530	37.8	47.3	9.5	8.82	92.8							
								1	1.5	1.5	37.8	39.3		
								2	1.5	1.5	39.3	40.8		
								3	1.5	1.5	40.8	42.3		
								4	1.5	1.5	42.3	43.8		

Table T2 (continued).

Core	Date (September 1998)	Time (UTC)	Core depth (mbsf) Top	Core depth (mbsf) Bottom	Length (m) Cored	Length (m) Recovered	Recovery (%)	Section	Length (m) Liner	Length (m) Curated	Section depth (mbsf) Top	Section depth (mbsf) Bottom	Catwalk samples	Comment
								5	1.4	1.4	43.8	45.2	IW, HS	
								6	1.27	1.27	45.2	46.47		
								CC	0.15	0.15	46.47	46.62	PAL	
									8.82	8.82				
6H	6	0630	47.3	56.8	9.5	9.06	95.4							
								1	1.5	1.5	47.3	48.8		
								2	1.5	1.5	48.8	50.3		
								3	1.5	1.5	50.3	51.8		
								4	1.5	1.5	51.8	53.3	IW	
								5	1.5	1.5	53.3	54.8	HS	
								6	1.41	1.41	54.8	56.21		
								CC	0.15	0.15	56.21	56.36	PAL	
									9.06	9.06				
7H	6	0735	56.8	66.3	9.5	9.13	96.1							
								1	1.5	1.5	56.8	58.3		
								2	1.5	1.5	58.3	59.8		
								3	1.5	1.5	59.8	61.3		
								4	1.5	1.5	61.3	62.8	IW	
								5	1.5	1.5	62.8	64.3	HS	
								6	1.48	1.48	64.3	65.78		
								CC	0.15	0.15	65.78	65.93	PAL	All to PAL
									9.13	9.13				
8H	6	0845	66.3	75.8	9.5	7.69	80.9							
								1	0.64	0.64	66.3	66.94		Crushed liner
								2	1.5	1.5	66.94	68.44		
								3	1.5	1.5	68.44	69.94		
								4	1.5	1.5	69.94	71.44		
								5	1.5	1.5	71.44	72.94		
								6	0.9	0.9	72.94	73.84		
								CC	0.15	0.15	73.84	73.99	PAL	All to PAL
									7.69	7.69				
9X	6	1005	75.8	85.4	9.6	0.81	8.4							
								1	0.66	0.66	75.8	76.46	HS	All to PAL
								CC	0.15	0.15	76.46	76.61	PAL	
									0.81	0.81				
10X	6	1105	85.4	95	9.6	0.44	4.6							
								1	0.29	0.29	85.4	85.69	HS	
								CC	0.15	0.15	85.69	85.84	PAL	
									0.44	0.44				
11X	6	1225	95	104.7	9.7	1.92	19.8							
								1	1.5	1.5	95	96.5	IW	
								2	0.27	0.27	96.5	96.77	HS	
								CC	0.15	0.15	96.77	96.92	PAL	All to PAL
									1.92	1.92				

Table T2 (continued).

Core	Date (September 1998)	Time (UTC)	Core depth (mbsf) Top	Core depth (mbsf) Bottom	Length (m) Cored	Length (m) Recovered	Recovery (%)	Section	Length (m) Liner	Length (m) Curated	Section depth (mbsf) Top	Section depth (mbsf) Bottom	Catwalk samples	Comment
12X	6	1335	104.7	114.3	9.6	5.02	52.3							
								1	1.5	1.5	104.7	106.2		
								2	1.5	1.5	106.2	107.7	IW	
								3	1.5	1.5	107.7	109.2	HS	
								4	0.32	0.32	109.2	109.52		
								CC	0.2	0.2	109.52	109.72	PAL	
									5.02	5.02				
13X	6	1440	114.3	123.9	9.6	5.77	60.1							
								1	1.5	1.5	114.3	115.8		
								2	1.5	1.5	115.8	117.3	IW	
								3	1.5	1.5	117.3	118.8	HS	
								4	1.12	1.12	118.8	119.92		
								CC	0.15	0.15	119.92	120.07	PAL	
									5.77	5.77				
				Totals:	123.9	87.46	70.60							
181-1122B-														
1H	6	1845	0	9.5	9.5	9.81	103.3							
								1	1.5	1.5	0	1.5		
								2	1.5	1.5	1.5	3		
								3	1.5	1.5	3	4.5		
								4	1.5	1.5	4.5	6		
								5	1.5	1.5	6	7.5		
								6	1.5	1.5	7.5	9		
								7	0.66	0.66	9	9.66		
								CC	0.15	0.15	9.66	9.81	PAL	All to PAL
									9.81	9.81				
				Totals:	9.5	9.81	103.30							
181-1122C-														
1H	6	2005	0	2.5	2.5	2.51	100.4							
								1	1.5	1.5	0	1.5		
								2	0.91	0.91	1.5	2.41		
								CC	0.1	0.1	2.41	2.51	PAL	All to PAL
									2.51	2.51				
2H	6	2130	2.5	9.5	7	9.75	139.3							
								1	1.5	1.5	2.5	4		
								2	1.5	1.5	4	5.5		
								3	1.5	1.5	5.5	7		
								4	1.5	1.5	7	8.5		
								5	1.5	1.5	8.5	10		
								6	1.5	1.5	10	11.5		
								7	0.65	0.65	11.5	12.15		
								CC	0.1	0.1	12.15	12.25	PAL	All to PAL
									9.75	9.75				

Table T2 (continued).

Core	Date (September 1998)	Time (UTC)	Core depth (mbsf) Top	Core depth (mbsf) Bottom	Length (m) Cored	Length (m) Recovered	Recovery (%)	Section	Length (m) Liner	Length (m) Curated	Section depth (mbsf) Top	Section depth (mbsf) Bottom	Catwalk samples	Comment
3H	6	2235	9.5	14	4.5	7.64	169.8							
								1	1.5	1.5	9.5	11		
								2	1.5	1.5	11	12.5		
								3	1.5	1.5	12.5	14		
								4	1.11	1.11	14	15.1		
								5	1.5	1.5	15.1	16.6		
								6	0.39	0.39	16.6	17		
								CC	0.14	0.14	17	17.14	PAL	
									7.64	7.64				
4H	6	2355	14	23.5	9.5	9.7	102.1							
								1	1.5	1.5	14	15.5		
								2	1.5	1.5	15.5	17		
								3	1.5	1.54	17	18.5		
								4	1.5	1.5	18.54	20.04		
								5	1.5	1.5	20.04	21.54		
								6	1.37	1.37	21.54	22.91		
								7	0.68	0.68	22.91	23.59		
								CC	0.15	0.15	23.59	23.74	PAL	
									9.70	9.74				
5H	7	110	23.5	33	9.5	8.95	94.2							
								1	1.5	1.5	23.5	25		
								2	1.5	1.5	25	26.5		
								3	1.5	1.5	26.5	28		
								4	1.5	1.5	28	29.5		
								5	1.5	1.5	29.5	31		
								6	1.3	1.3	31	32.3		
								CC	0.15	0.15	32.3	32.45	PAL	
									8.95	8.95				
6H	7	155	33	42.5	9.5	9.16	96.4							
								1	1.5	1.5	33	34.5		
								2	1.5	1.5	34.5	36		
								3	1.5	1.5	36	37.5		
								4	1.5	1.5	37.5	39		
								5	1.5	1.5	39	40.5		
								6	1.43	1.43	40.5	41.93		
								CC	0.23	0.23	41.93	42.16	PAL	
									9.16	9.16				
7H	7	300	42.5	52	9.5	8.72	91.8							
								1	1.5	1.5	42.5	44		
								2	1.5	1.5	44	45.5		
								3	1.5	1.5	45.5	47		
								4	1.5	1.5	47	48.5		
								5	1.5	1.5	48.5	50		
								6	1.07	1.07	50	51.1		
								CC	0.15	0.15	51.07	51.22	PAL	All to PAL
									8.72	8.72				

Table T2 (continued).

Core	Date (September 1998)	Time (UTC)	Core depth (mbsf) Top	Core depth (mbsf) Bottom	Length (m) Cored	Length (m) Recovered	Recovery (%)	Section	Length (m) Liner	Length (m) Curated	Section depth (mbsf) Top	Section depth (mbsf) Bottom	Catwalk samples	Comment
8H	7	410	52	61.5	9.5	9.44	99.4							
								1	1.5	1.5	52	53.5		
								2	1.5	1.5	53.5	55		
								3	1.5	1.5	55	56.5		
								4	1.5	1.5	56.5	58		
								5	1.5	1.5	58	59.5		
								6	1.5	1.5	59.5	61		
								7	0.28	0.28	61	61.3		
								CC	0.16	0.16	61.28	61.44		
									9.44	9.44				
9H	7	510	61.5	71	9.5	8.67	91.3							
								1	1.5	1.5	61.5	63		
								2	1.5	1.5	63	64.5		
								3	1.5	1.5	64.5	66		
								4	1.5	1.5	66	67.5	IW	
								5	1.5	1.5	67.5	69	HS	
								6	1	1	69	70		
								CC	0.17	0.17	70	70.2	PAL	
									8.67	8.67				
10H	7	630	71	80.5	9.5	9.43	99.3							
								1	1.5	1.5	71	72.5		
								2	1.5	1.5	72.5	74		
								3	1.5	1.5	74	75.5		
								4	1.5	1.5	75.5	77	IW	
								5	1.5	1.5	77	78.5	HS	
								6	1.24	1.24	78.5	79.74		
								7	0.45	0.45	79.74	80.19		
								CC	0.24	0.24	80.19	80.43	PAL	
									9.43	9.43				
11H	7	800	80.5	86.9	6.4	6.48	101.3							
								1	1.5	1.5	80.5	82	HS	
								2	1.5	1.5	82	83.5		
								3	1.5	1.5	83.5	85		
								4	0.98	0.98	85	86		
								5	0.85	0.85	85.98	86.83		
								CC	0.15	0.15	86.83	86.98	PAL	All to PAL
									6.48	6.48				
12H	7	900	86.9	94.9	8	7.9	98.8							
								1	1.5	1.5	86.9	88.4		
								2	1.5	1.5	88.4	89.9		
								3	1.5	1.5	89.9	91.4		
								4	1.5	1.5	91.4	92.9	IW	
								5	1.5	1.5	92.9	94.4	HS	
								6	0.24	0.24	94.4	94.64		
								CC	0.16	0.16	94.64	94.8	PAL	
									7.90	7.90				

Table T2 (continued).

Core	Date (September 1998)	Time (UTC)	Core depth (mbsf) Top	Core depth (mbsf) Bottom	Length (m) Cored	Length (m) Recovered	Recovery (%)	Section	Length (m) Liner	Length (m) Curated	Section depth (mbsf) Top	Section depth (mbsf) Bottom	Catwalk samples	Comment
13H	7	1010	94.9	103.7	8.8	8.8	100							
								1	1.5	1.5	94.9	96.4		
								2	1.5	1.5	96.4	97.9		
								3	1.5	1.5	97.9	99.4		
								4	1.5	1.5	99.4	100.9	IW	
								5	1.5	1.5	100.9	102.4	HS	
								6	1	1	102.4	103.4		
								CC	0.3	0.3	103.4	103.7	PAL	
									8.80	8.80				
14X	7	1130	103.7	108	4.3	4.32	100.5							
								1	1.5	1.5	103.7	105.2		
								2	1.5	1.5	105.2	106.7		
								3	1.22	1.22	106.7	107.92		
								CC	0.1	0.1	107.92	108.02	PAL	All to PAL
									4.32	4.32				
15X	7	1225	108	117.6	9.6	3.38	35.2							
								1	1.5	1.5	108	109.5		
								2	1.5	1.5	109.5	111	HS	
								CC	0.38	0.38	111	111.38	PAL	
									3.38	3.38				
16X	7	1335	117.6	127.2	9.6	5.38	56							
								1	1.5	1.5	117.6	119.1		
								2	1.5	1.5	119.1	120.6		
								3	1.5	1.5	120.6	122.1	IW	
								4	0.63	0.63	122.1	122.73	HS	
								CC	0.25	0.25	122.73	122.98	PAL	
									5.38	5.38				
17X	7	1440	127.2	136.9	9.7	6.25	64.4							
								1	1.5	1.5	127.2	128.7		
								2	1.5	1.5	128.7	130.2		
								3	1.5	1.5	130.2	131.7	HS	
								4	1.5	1.5	131.7	133.2		
								CC	0.25	0.25	133.2	133.45	PAL	
									6.25	6.25				
18X	7	1545	136.9	146.5	9.6	3.71	38.6							
								1	1.5	1.5	136.9	138.4		
								2	1.5	1.5	138.4	139.9	HS	
								3	0.52	0.52	139.9	140.42		
								CC	0.19	0.19	140.42	140.61	PAL	
									3.71	3.71				
19X	7	1645	146.5	156.1	9.6	4.08	42.5							
								1	1.5	1.5	146.5	148	IW	
								2	1.5	1.5	148	149.5	HS	
								3	0.93	0.93	149.5	150.43		
								CC	0.15	0.15	150.43	150.58	PAL	
									4.08	4.08				

Table T2 (continued).

Core	Date (September 1998)	Time (UTC)	Core depth (mbsf) Top	Core depth (mbsf) Bottom	Length (m) Cored	Length (m) Recovered	Recovery (%)	Section	Length (m) Liner	Length (m) Curated	Section depth (mbsf) Top	Section depth (mbsf) Bottom	Catwalk samples	Comment
20X	7	1745	156.1	165.7	9.6	5.21	54.3							
								1	1.5	1.5	156.1	157.6		
								2	1.5	1.5	157.6	159.1		
								3	1.5	1.5	159.1	160.6	HS	
								4	0.52	0.52	160.6	161.12		
								CC	0.19	0.19	161.12	161.31	PAL	
									5.21	5.21				
21X	7	1845	165.7	175.3	9.6	2.44	25.4							
								1	1.5	1.5	165.7	167.2		
								2	0.79	0.79	167.2	167.99	HS	
								CC	0.15	0.15	167.99	168.14	PAL	All to PAL
									2.44	2.44				
22X	7	1945	175.3	185	9.7	1.73	17.8							
								1	1.4	1.4	175.3	176.7	IW	
								2	0.23	0.23	176.7	176.93	HS	
								CC	0.1	0.1	176.93	177.03	PAL	All to PAL
									1.73	1.73				
23X	7	2050	185	194.7	9.7	2.38	24.5							
								1	1.5	1.5	185	186.5		
								2	0.78	0.78	186.5	187.28	HS	
								CC	0.1	0.1	187.28	187.38	PAL	All to PAL
									2.38	2.38				
24X	7	2150	194.7	204.3	9.6	0.82	8.5							
								1	0.72	0.72	194.7	195.42	HS	
								CC	0.1	0.1	195.42	195.52	PAL	All to PAL
									0.82	0.82				
25X	7	2325	204.3	214	9.7	0.67	6.9							
								1	0.57	0.57	204.3	204.87	HS	
								CC	0.1	0.1	204.87	204.97	PAL	All to PAL
									0.67	0.67				
26X	8	30	214	223.7	9.7	4.09	42.2							
								1	1.5	1.5	214	215.5		
								2	1	1	215.5	216.5	IW	
								3	1.49	1.49	216.5	217.99	HS	
								CC	0.1	0.1	217.99	218.09	PAL	All to PAL
									4.09	4.09				
27X	8	135	223.7	233.3	9.6	3.51	36.6							
								1	1.5	1.5	223.7	225.2		
								2	1.5	1.5	225.2	226.7		
								3	0.23	0.23	226.7	226.93	HS	
								CC	0.28	0.28	226.93	227.21	PAL	
									3.51	3.51				

Table T2 (continued).

Core	Date (September 1998)	Time (UTC)	Core depth (mbsf) Top	Core depth (mbsf) Bottom	Length (m) Cored	Length (m) Recovered	Recovery (%)	Section	Length (m) Liner	Length (m) Curated	Section depth (mbsf) Top	Section depth (mbsf) Bottom	Catwalk samples	Comment
28X	8	230	233.3	242.9	9.6	4.48	46.7							
								1	1.5	1.5	233.3	234.8	HS	
								2	1.5	1.5	234.8	236.3		
								3	1.3	1.3	236.3	237.6		
								CC	0.18	0.18	237.6	237.78	PAL	
									4.48	4.48				
29X	8	330	242.9	252.5	9.6	4.83	50.3							
								1	1.5	1.5	242.9	244.4		
								2	1.5	1.5	244.4	245.9		
								3	1.5	1.5	245.9	247.4	IW	
								4	0.23	0.23	247.4	247.63	HS	
								CC	0.1	0.1	247.63	247.73	PAL	All to PAL
									4.83	4.83				
30X	8	425	252.5	261.7	9.2	6.73	73.2							
								1	1.5	1.5	252.5	254		
								2	1.5	1.5	254	255.5		
								3	1.5	1.5	255.5	257	HS	
								4	1.5	1.5	257	258.5		
								5	0.51	0.51	258.5	259.01		
								CC	0.22	0.22	259.01	259.23	PAL	
									6.73	6.73				
31X	8	525	261.7	271.3	9.6	4.69	48.9							
								1	1.5	1.5	261.7	263.2		
								2	1.5	1.5	263.2	264.7		
								3	1.48	1.48	264.7	266.18	HS	
								CC	0.21	0.21	266.18	266.39	PAL	
									4.69	4.69				
32X	8	630	271.3	280.7	9.4	2.55	27.1							
								1	1.5	1.5	271.3	272.8	IW	
								2	0.79	0.79	272.8	273.59	HS	
								CC	0.26	0.26	273.59	273.85	PAL	
									2.55	2.55				
33X	8	730	280.7	290.4	9.7	7.33	75.6							
								1	1.5	1.5	280.7	282.2		
								2	1.5	1.5	282.2	283.7		
								3	1.5	1.5	283.7	285.2		
								4	1.5	1.5	285.2	286.7		
								5	1.2	1.2	286.7	287.9	HS	
								CC	0.13	0.13	287.9	288.03	PAL	
									7.33	7.33				
34X	8	840	290.4	300	9.6	7.44	77.5							
								1	1.5	1.5	290.4	291.9		
								2	1.5	1.5	291.9	293.4		
								3	1.5	1.5	293.4	294.9		
								4	1.5	1.5	294.9	296.4		

Table T2 (continued).

Core	Date (September 1998)	Time (UTC)	Core depth (mbsf) Top	Core depth (mbsf) Bottom	Length (m) Cored	Length (m) Recovered	Recovery (%)	Section	Length (m) Liner	Length (m) Curated	Section depth (mbsf) Top	Section depth (mbsf) Bottom	Catwalk samples	Comment
								5	1.34	1.34	296.4	297.74	HS,HS	
								CC	0.1	0.1	297.74	297.84	PAL	All to PAL
									7.44	7.44				
35X	8	950	300	309.6	9.6	8.01	83.4							
								1	1.5	1.5	300	301.5		
								2	1.5	1.5	301.5	303		
								3	1.5	1.5	303	304.5		
								4	1.5	1.5	304.5	306	IW	
								5	1.5	1.5	306	307.5	HS	
								6	0.17	0.17	307.5	307.67		
								CC	0.34	0.34	307.67	308.01	PAL	
									8.01	8.01				
36X	8	1055	309.6	319.3	9.7	8.7	89.7							
								1	1.5	1.5	309.6	311.1		
								2	1.5	1.5	311.1	312.6		
								3	1.5	1.5	312.6	314.1		
								4	1.5	1.5	314.1	315.6		
								5	1.5	1.5	315.6	317.1	HS	
								6	0.9	0.9	317.1	318		
								CC	0.3	0.3	318	318.3	PAL	
									8.7	8.7				
37X	8	1210	319.3	328.9	9.6	9.07	94.5							
								1	1.5	1.5	319.3	320.8		
								2	1.5	1.5	320.8	322.3		
								3	1.5	1.5	322.3	323.8		
								4	1.5	1.5	323.8	325.3		
								5	1.5	1.5	325.3	326.8	HS	
								6	1.4	1.4	326.8	328.2		
								CC	0.17	0.17	328.2	328.37	PAL	
									9.07	9.07				
38X	8	1320	328.9	338.5	9.6	4.48	46.7							
								1	1.5	1.5	328.9	330.4		
								2	1.5	1.5	330.4	331.9	IW	
								3	1.38	1.38	331.9	333.28	HS	
								CC	0.1	0.1	333.28	333.38	PAL	All to PAL
									4.48	4.48				
39X	8	1430	338.5	348.2	9.7	5.26	54.2							
								1	1.5	1.5	338.5	340		
								2	1.5	1.5	340	341.5		
								3	1.5	1.5	341.5	343	HS	
								4	0.55	0.55	343	343.6		
								CC	0.21	0.21	343.55	343.76	PAL	
									5.26	5.26				

Table T2 (continued).

Core	Date (September 1998)	Time (UTC)	Core depth (mbsf) Top	Core depth (mbsf) Bottom	Length (m) Cored	Length (m) Recovered	Recovery (%)	Section	Length (m) Liner	Length (m) Curated	Section depth (mbsf) Top	Section depth (mbsf) Bottom	Catwalk samples	Comment
40X	8	1540	348.2	357.9	9.7	3.26	33.6							
								1	1.5	1.5	348.2	349.7		
								2	1.5	1.5	349.7	351.2	HS	
								CC	0.26	0.26	351.2	351.46	PAL	
									3.26	3.26				
41X	8	1645	357.9	367.5	9.6	2.08	21.7							
								1	1.5	1.5	357.9	359.4	HS	Liner patch
								2	0.41	0.41	359.4	359.81		Liner patch
								CC	0.17	0.17	359.81	359.98	PAL	
									2.08	2.08				
42X	8	1750	367.5	377.2	9.7	4.69	48.4							
								1	1.5	1.5	367.5	369		
								2	1.5	1.5	369	370.5	IW	
								3	1.5	1.5	370.5	372	HS	
								CC	0.19	0.19	372	372.2	PAL	
									4.69	4.69				
43X	8	1900	377.2	386.9	9.7	0.43	4.4							
								CC	0.43	0.43	377.2	377.63	PAL	
									0.43	0.43				
44X	8	2005	386.9	396.6	9.7	5.74	59.2							
								1	1.5	1.5	386.9	388.4		
								2	1.5	1.5	388.4	389.9		
								3	1.5	1.5	389.9	391.4	HS	
								4	0.93	0.93	391.4	392.33		
								CC	0.31	0.31	392.33	392.64	PAL	
									5.74	5.74				
45X	8	2125	396.6	406.2	9.6	6.01	62.6							
								1	1.5	1.5	396.6	398.1		
								2	1.5	1.5	398.1	399.6	IW	
								3	1.5	1.5	399.6	401.1	HS	
								4	1.19	1.19	401.1	402.29		
								CC	0.32	0.32	402.29	402.61	PAL	
									6.01	6.01				
46X	8	2235	406.2	415.9	9.7	6.34	65.4							
								1	1.5	1.5	406.2	407.7		
								2	1.5	1.5	407.7	409.2		
								3	1.5	1.5	409.2	410.7	HS	
								4	1.5	1.5	410.7	412.2		
								CC	0.34	0.34	412.2	412.54	PAL	
									6.34	6.34				
47X	8	2340	415.9	425.5	9.6	5.71	59.5							
								1	1.5	1.5	415.9	417.4		
								2	1.5	1.5	417.4	418.9		
								3	1.5	1.5	418.9	420.4	HS	
								4	0.84	0.84	420.4	421.24		
								CC	0.37	0.37	421.24	421.61	PAL	
									5.71	5.71				

Table T2 (continued).

Core	Date (September 1998)	Time (UTC)	Core depth (mbsf) Top	Core depth (mbsf) Bottom	Length (m) Cored	Length (m) Recovered	Recovery (%)	Section	Length (m) Liner	Length (m) Curated	Section depth (mbsf) Top	Section depth (mbsf) Bottom	Catwalk samples	Comment
48X	9	50	425.5	435.2	9.7	7.01	72.3							
								1	1.5	1.5	425.5	427		
								2	1.5	1.5	427	428.5		
								3	1.5	1.5	428.5	430		
								4	1.5	1.5	430	431.5	IW	
								5	0.62	0.62	431.5	432.12	HS	
								CC	0.39	0.39	432.12	432.51	PAL	
									7.01	7.01				
49X	9	200	435.2	444.8	9.6	9.31	97							
								1	1.5	1.5	435.2	436.7		
								2	1.5	1.5	436.7	438.2		
								3	1.5	1.5	438.2	439.7		
								4	1.5	1.5	439.7	441.2		
								5	1.5	1.5	441.2	442.7	HS	
								6	1.5	1.5	442.7	444.2		
								CC	0.31	0.31	444.2	444.51	PAL	
									9.31	9.31				
50X	9	310	444.8	454.4	9.6	7.41	77.2							
								1	1.5	1.5	444.8	446.3		
								2	1.5	1.5	446.3	447.8		
								3	1.5	1.5	447.8	449.3		
								4	1.5	1.5	449.3	450.8		
								5	1.07	1.07	450.8	451.87	HS	
								CC	0.34	0.34	451.87	452.21	PAL	
									7.41	7.41				
51X	9	455	454.4	464.1	9.7	9.26	95.5							
								1	1.5	1.5	454.4	455.9		
								2	1.5	1.5	455.9	457.4		
								3	1.5	1.5	457.4	458.9		
								4	1.5	1.5	458.9	460.4	IW, IW	
								5	1.5	1.5	460.4	461.9	HS, HS	
								6	1.5	1.5	461.9	463.4		
								CC	0.26	0.26	463.4	463.66	PAL	
									9.26	9.26				
52X	9	635	464.1	473.4	9.3	8.73	93.9							
								1	1.5	1.5	464.1	465.6		
								2	1.5	1.5	465.6	467.1		
								3	1.5	1.5	467.1	468.6		
								4	1.5	1.5	468.6	470.1		
								5	1.5	1.5	470.1	471.6	HS	
								6	1	1	471.6	472.6		
								CC	0.23	0.23	472.6	472.83	PAL	
									8.73	8.73				
53X	9	810	473.4	483	9.6	4.96	51.7							
								1	1.5	1.5	473.4	474.9		
								2	1.5	1.5	474.9	476.4		
								3	1.5	1.5	476.4	477.9		

Table T2 (continued).

Core	Date (September 1998)	Time (UTC)	Core depth (mbsf) Top	Core depth (mbsf) Bottom	Length (m) Cored	Length (m) Recovered	Recovery (%)	Section	Length (m) Liner	Length (m) Curated	Section depth (mbsf) Top	Section depth (mbsf) Bottom	Catwalk samples	Comment
								CC	0.46	0.46	477.9	478.36	PAL	
									4.96	4.96				
54X	9	955	483	492.7	9.7	5.25	54.1							
								1	1.5	1.5	483	484.5		
								2	1.5	1.5	484.5	486		
								3	1.5	1.5	486	487.5	IW	
								4	0.65	0.65	487.5	488.15	HS	
								CC	0.1	0.1	488.15	488.25	PAL	
									5.25	5.25				
55X	9	1140	492.7	502.3	9.6	7.27	75.7							
								1	1.5	1.5	492.7	494.2		
								2	1.5	1.5	494.2	495.7		
								3	1.5	1.5	495.7	497.2		
								4	1.5	1.5	497.2	498.7		
								5	1.04	1.04	498.7	499.74	HS	
								CC	0.23	0.23	499.74	499.97	PAL	
									7.27	7.27				
56X	9	1330	502.3	511.9	9.6	5.58	58.1							
								1	1.5	1.5	502.3	503.8		
								2	1.5	1.5	503.8	505.3		
								3	1.5	1.5	505.3	506.8	HS	
								4	0.61	0.61	506.8	507.41		
								CC	0.47	0.47	507.41	507.88	PAL	
									5.58	5.58				
57X	9	1520	511.9	521.5	9.6	5.34	55.6							
								1	1.5	1.5	511.9	513.4		
								2	1.5	1.5	513.4	514.9	IW	
								3	1.5	1.5	514.9	516.4	HS	
								4	0.53	0.53	516.4	516.93		
								CC	0.31	0.31	516.93	517.24	PAL	
									5.34	5.34				
58X	9	1710	521.5	531.2	9.7	2.08	21.4							
								1	1.5	1.5	521.5	523		
								2	0.48	0.48	523	523.5	HS	
								CC	0.1	0.1	523.48	523.58	PAL	All to PAL
									2.08	2.08				
59X	9	1905	531.2	540.7	9.5	0.12	1.3							
								CC	0.12	0.12	531.2	531.32	PAL	
									0.12	0.12				
60X	9	2050	540.7	550.4	9.7	0.46	4.7							
								CC	0.46	0.46	540.7	541.16	PAL	
									0.46	0.46				
61X	9	2230	550.4	560	9.6	5.19	54.1							
								1	1.5	1.5	550.4	551.9		
								2	1.5	1.5	551.9	553.4		

Table T2 (continued).

Core	Date (September 1998)	Time (UTC)	Core depth (mbsf) Top	Core depth (mbsf) Bottom	Length (m) Cored	Length (m) Recovered	Recovery (%)	Section	Length (m) Liner	Length (m) Curated	Section depth (mbsf) Top	Section depth (mbsf) Bottom	Catwalk samples	Comment
								3	1.5	1.5	553.4	554.9	IW	
								4	0.46	0.46	554.9	555.36	HS	
								CC	0.23	0.23	555.36	555.59	PAL	
									5.19	5.19				
62X	10	15	560	569.6	9.6	3.41	35.5							
								1	1.5	1.5	560	561.5		
								2	1.5	1.5	561.5	563		
								3	0.31	0.31	563	563.3		
								CC	0.1	0.1	563.31	563.41	PAL	All to PAL
									3.41	3.41				
63X	10	155	569.6	579.3	9.7	1.72	17.7							
								1	1.5	1.5	569.6	571.1	HS	
								CC	0.22	0.22	571.1	571.32	PAL	
									1.72	1.72				
64X	10	345	579.3	588.9	9.6	1.6	16.7							
								1	1.32	1.32	579.3	580.62	HS	
								CC	0.28	0.28	580.62	580.9	PAL	
									1.60	1.60				
65X	10	535	588.9	598.5	9.6	1.78	18.5							
								1	1.5	1.5	588.9	590.4	HS,HS	
								2	0.1	0.1	590.4	590.5	IW, IW	Other
								CC	0.18	0.18	590.5	590.68	PAL	
									1.78	1.78				
66X	10	720	598.5	608.2	9.7	0.95	9.8							
								1	0.9	0.9	598.5	599.4	HS	
								CC	0.05	0.05	599.4	599.45	PAL	All to PAL
									0.95	0.95				
67X	10	900	608.2	617.8	9.6	1.01	10.5							
								1	0.96	0.96	608.2	609.16	HS	
								CC	0.05	0.05	609.16	609.21	PAL	All to PAL
									1.01	1.01				
68X	10	1045	617.8	627.4	9.6	0.05	0.5							
								CC	0.05	0.05	617.8	617.85	PAL	All to PAL
									0.05	0.05				
				Totals:	627.4	351.44	56.00							

Note: IW = interstitial water, HS = headspace, PAL = paleontology. This table is also available in **ASCII format.**

Table T3. Thickness of sand, fine sand, very fine sand/silt, and mud turbidites. (Continued on next 18 pages.)

Core, section	Depth at base of turbidite (cm)	Depth at base of turbidite (mbsf)	Thickness (cm)	Turbidite types
181-1122A-				
1H-1	70	0.7	5	Sand
1H-1	99	0.99	6	Sand
1H-1	126	1.26	7	Sand
1H-1	147	1.47	9	Sand
1H-2	12	1.62	3	Sand
1H-2	21	1.71	1	Fine sand
1H-2	31	1.81	1.5	Fine sand
1H-2	42	1.92	2	Fine sand
1H-2	69	2.19	9	Sand
1H-2	78	2.28	1	Fine sand
1H-2	110	2.6	6	Sand
1H-2	130	2.8	2	Sand
1H-2	150	3	13	Sand
1H-3	10	3.1	2	Sand
1H-3	26	3.26	0.5	Fine sand
1H-3	40	3.4	6	Sand
1H-3	55.5	3.555	3.5	Sand
1H-3	71	3.71	6.5	Sand
1H-3	85	3.85	6	Sand
1H-3	98	3.98	5	Sand
1H-3	118	4.18	6	Sand
1H-3	141	4.41	12	Sand
1H-4	6	4.56	1.5	Fine sand
1H-4	22.5	4.725	12	Sand
1H-4	37	4.87	4	Sand
1H-4	51	5.01	10	Sand
1H-4	77	5.27	12	Sand
1H-4	89	5.39	1	Fine sand
1H-4	98.5	5.485	3.5	Sand
1H-4	117	5.67	13	Sand
1H-4	132	5.82	4	Sand
1H-5	15	6.15	3.5	Sand
1H-5	25	6.25	1.5	Sand
1H-5	43	6.43	10	Sand
1H-5	54	6.54	4	Sand
1H-5	63	6.63	2	Sand
1H-5	77	6.77	3	Sand
1H-5	83	6.83	1.5	Sand
1H-5	99	6.99	9	Sand
1H-5	107.5	7.075	3	Sand
1H-5	117	7.17	5	Sand
1H-5	122.5	7.225	1.5	Fine sand
1H-5	135	7.35	2.5	Sand
1H-5	147	7.47	5.5	Sand
1H-6	14	7.64	12	Sand
1H-6	26	7.76	2.5	Sand
1H-6	41	7.91	8	Sand
1H-6	59	8.09	9	Sand
1H-6	67	8.17	1	Fine sand
1H-6	102	8.52	1	Fine sand
1H-6	109	8.59	3.5	Sand
1H-6	112	8.62	2.5	Fine sand
1H-6	118	8.68	1	Sand
1H-6	121	8.71	1	Fine sand
1H-6	128	8.78	1.5	Fine sand
1H-6	130	8.8	1	Fine sand
1H-6	139	8.89	2	Mud
1H-6	142	8.92	2	Mud
1H-CC	8	9.22	2	Sand
181-1122A-				
2H-1	69	9.99	69	Sand
2H-1	84	10.14	3	Sand
2H-1	100	10.3	13	Sand
2H-1	118	10.48	7	Sand
2H-1	131	10.61	4	Sand
2H-1	139	10.69	3	Fine sand
2H-1	149	10.79	3	Fine sand
2H-2	19	10.99	11	Sand
2H-2	43	11.23	14	Sand
2H-2	50	11.3	5	Fine sand
2H-2	60	11.4	2	Fine sand
2H-2	72	11.52	8	Sand
2H-2	96	11.76	19	Sand
2H-2	110	11.9	4	Sand
2H-2	129	12.09	10	Sand
2H-2	141	12.21	5	Sand
2H-3	7	12.37	5	Fine sand
2H-3	19	12.49	3	Sand
2H-3	30	12.6	5	Sand
2H-3	42	12.72	5	Sand
2H-3	60	12.9	3	Sand
2H-3	68	12.98	4	Sand
2H-3	85	13.15	5	Sand
2H-3	93	13.23	2	Fine sand
2H-3	110	13.4	13	Sand
2H-3	120	13.5	2	Sand
2H-3	134	13.64	4	Sand
2H-3	143	13.73	6	Sand
2H-4	8	13.88	10	Sand
2H-4	19	13.99	3	Fine sand
2H-4	25	14.05	1	Fine sand
2H-4	31	14.11	4	Fine sand
2H-4	38	14.18	4	Sand
2H-4	44	14.24	3	Sand
2H-4	54	14.34	3	Sand
2H-4	69	14.49	14	Sand
2H-4	101	14.81	12	Sand
2H-4	123	15.03	8	Sand
2H-4	137	15.17	7	Fine sand
2H-5	8	15.38	3	Fine sand
2H-5	23	15.53	10	Fine sand
2H-5	41	15.71	8	Sand
2H-5	55	15.85	4	Sand
2H-5	69.5	15.995	3	Sand
2H-5	82.5	16.125	3	Sand
2H-5	100	16.3	12	Sand
2H-5	150	16.8	44	Sand
2H-6	10	16.9	10	Sand
2H-6	20	17	2	Sand
2H-6	45	17.25	5	Sand
2H-6	71	17.51	17	Sand
2H-6	93	17.73	7	Sand
2H-6	121	18.01	16	Sand
2H-7	15	18.45	15	Sand
2H-7	30	18.6	6	Sand
3H-1	6	18.86	1.5	Sand
3H-1	26	19.06	5.5	Sand
3H-1	82	19.62	44	Sand
3H-1	116	19.96	12	Sand
3H-1	130	20.1	4	Fine sand
3H-1	141.5	20.215	1.5	Fine sand
3H-2	6	20.36	1	Fine sand
3H-2	25	20.55	8.5	Sand
3H-2	44	20.74	7	Sand
3H-2	78	21.08	14	Sand

Table T3 (continued).

Core, section	Depth at base of turbidite (cm)	Depth at base of turbidite (mbsf)	Thickness (cm)	Turbidite types
3H-2	113	21.43	3	Fine sand
3H-2	119	21.49	1	Fine sand
3H-2	136	21.66	11	Sand
3H-3	5	21.85	0.5	Fine sand
3H-3	44	22.24	7.5	Sand
3H-3	68	22.48	6.5	Sand
3H-3	83	22.63	9.5	Sand
3H-3	108.5	22.885	9	Sand
3H-3	128	23.08	7	Sand
3H-3	136	23.16	0.5	Fine sand
3H-3	143	23.23	3	Sand
3H-4	6	23.36	8	Sand
3H-4	14	23.44	4.5	Sand
3H-4	23	23.53	1	Mud
3H-4	59	23.89	28	Sand
3H-4	90	24.2	28	Sand
3H-4	126	24.56	22	Sand
3H-5	2	24.82	12	Sand
3H-5	26	25.06	10	Sand
3H-5	37	25.17	1	Fine sand
3H-5	50	25.3	9	Sand
3H-5	89	25.69	25	Sand
3H-5	105	25.85	9	Sand
3H-5	125	26.05	13	Sand
3H-5	149	26.29	14	Sand
3H-6	6.5	26.365	6	Sand
3H-6	21	26.51	7	Sand
3H-6	48	26.78	9.5	Sand
3H-6	58	26.88	2	Fine sand
3H-6	70	27	6	Fine sand
3H-6	89	27.19	9	Fine sand
3H-6	116	27.46	9	Fine sand
3H-6	129	27.59	2	Mud
3H-7	4	27.84	12	Fine sand
3H-7	36	28.16	15	Sand
3H-7	63	28.43	13	Sand
4H-1	2	28.32	2	Sand
4H-1	56	28.86	5	Sand
4H-1	64	28.94	3.5	Fine sand
4H-1	80	29.1	5.5	Fine sand
4H-1	89	29.19	2	Fine sand
4H-1	95	29.25	1.5	Mud
4H-1	101	29.31	1.5	Mud
4H-1	109	29.39	1	Mud
4H-1	116	29.46	2	Mud
4H-1	140	29.7	1	Fine sand
4H-2	2	29.82	3	Fine sand
4H-2	49	30.29	13	Sand
4H-2	58	30.38	1	Mud
4H-2	73.5	30.535	3.5	Fine sand
4H-2	90	30.7	5.5	Fine sand
4H-2	103.5	30.835	5	Fine sand
4H-2	120	31	4	Fine sand
4H-2	137.5	31.175	3	Fine sand
4H-3	16	31.46	5	Sand
4H-3	26	31.56	1	Mud
4H-3	51	31.81	14	Sand
4H-3	68.5	31.985	1.5	Sand
4H-3	70.5	32.005	1	Mud
4H-3	76	32.06	3	Mud
4H-3	79	32.09	1.5	Mud
4H-3	92.5	32.225	1	Fine sand
4H-3	113.5	32.435	9	Sand
4H-3	125	32.55	2.5	Fine sand
4H-3	142	32.72	8	Sand
4H-4	22	33.02	14	Sand
4H-4	27	33.07	2	Fine sand
4H-4	35	33.15	2	Fine sand
4H-4	48	33.28	4.5	Mud
4H-4	67	33.47	9	Sand
4H-4	91	33.71	1	Mud
4H-4	117	33.97	14	Sand
4H-4	129	34.09	5	Fine sand
4H-4	135	34.15	1	Fine sand
4H-5	1	34.31	6	Fine sand
4H-5	10	34.4	3	Fine sand
4H-5	17	34.47	4.5	Fine sand
4H-5	23	34.53	3	Mud
4H-5	51	34.81	22	Sand
4H-5	54	34.84	3	Fine sand
4H-5	58	34.88	2	Fine sand
4H-5	74	35.04	1	Mud
4H-5	79	35.09	2	Mud
4H-5	82	35.12	2.5	Mud
4H-5	94	35.24	4.5	Fine sand
4H-5	119	35.49	9	Fine sand
4H-5	132	35.62	6	Fine sand
4H-5	139	35.69	2.5	Fine sand
4H-6	0.5	35.805	2	Fine sand
4H-6	42	36.22	37	Sand
4H-6	60	36.4	9	Fine sand
4H-6	73	36.53	2.5	Sand
4H-6	84	36.64	2.5	Fine sand
4H-6	91	36.71	1	Mud
4H-6	109	36.89	1	Mud
4H-6	134	37.14	16	Sand
4H-7	28	37.58	5	Fine sand
4H-7	47	37.77	7	Fine sand
4H-7	66	37.96	5	Fine sand
5H-1	36	38.16	14	Sand
5H-1	100	38.8	44	Sand
5H-1	133	39.13	11	Sand
5H-2	2.5	39.325	3	Fine sand
5H-2	14	39.44	0.5	Mud
5H-2	38	39.68	1.5	Mud
5H-2	46.5	39.765	0.5	Mud
5H-2	60	39.9	0.5	Mud
5H-2	70	40	1	Fine sand
5H-2	83	40.13	1.5	Fine sand
5H-2	119	40.49	33	Sand
5H-3	5	40.85	12.5	Sand
5H-3	40	41.2	20	Sand
5H-3	50	41.3	1	Mud
5H-3	95	41.75	35	Sand
5H-3	111	41.91	3	Fine sand
5H-3	133	42.13	7.5	Sand
5H-3	146	42.26	2	Fine sand
5H-4	10	42.4	8	Sand
5H-4	19	42.49	0.5	Mud
5H-4	22	42.52	0.5	Mud
5H-4	30	42.6	3	Fine sand
5H-4	41	42.71	3	Very fine sand
5H-4	61.5	42.915	7.5	Fine sand
5H-4	91	43.21	15	Sand
5H-4	115	43.45	8	Sand
5H-4	127.5	43.575	4	Fine sand
5H-4	150	43.8	11	Sand
5H-5	15	43.95	6	Fine sand
5H-5	38	44.18	13	Fine sand
5H-5	51	44.31	1	Fine sand

Table T3 (continued).

Core, section	Depth at base of turbidite (cm)	Depth at base of turbidite (mbsf)	Thickness (cm)	Turbidite types
5H-5	77.5	44.575	20	Sand
5H-5	103	44.83	23	Sand
5H-5	116	44.96	2.5	Fine sand
5H-5	135	45.15	8	Fine sand
5H-6	15	45.35	12	Sand
5H-6	20	45.4	0.3	Fine sand
5H-6	22.5	45.425	1	Fine sand
5H-6	26	45.46	2	Fine sand
5H-6	36	45.56	3	Fine sand
5H-6	57	45.77	4	Fine sand
5H-6	80	46	9	Fine sand
5H-6	127	46.47	28	Fine sand
6H-1	33	47.63	22	Sand
6H-1	70	48	30	Sand
6H-1	89	48.19	10.5	Fine sand
6H-1	113	48.43	15	Sand
6H-1	142	48.72	13	Fine sand
6H-2	5	48.85	10	Fine sand
6H-2	49	49.29	40	Sand
6H-2	74	49.54	20	Fine sand
6H-2	87	49.67	9	Fine sand
6H-2	99	49.79	6	Fine sand
6H-2	135	50.15	30	Sand
6H-3	3	50.33	7	Fine sand
6H-3	43	50.73	34	Fine sand
6H-3	99	51.29	47	Fine sand
6H-3	119	51.49	2	Mud
6H-3	148	51.78	21	Fine sand
6H-4	21	52.01	17	Fine sand
6H-4	40	52.2	16	Fine sand
6H-4	66	52.46	21	Fine sand
6H-4	78	52.58	1	Mud
6H-4	82	52.62	1	Mud
6H-4	90	52.7	0.5	Mud
6H-4	95	52.75	1	Mud
6H-4	119	52.99	20	Fine sand
6H-5	2	53.32	32	Fine sand
6H-5	15	53.45	12	Fine sand
6H-5	18	53.48	0.5	Mud
6H-5	23	53.53	2	Mud
6H-5	27	53.57	1	Mud
6H-5	30	53.6	1	Mud
6H-5	38	53.68	2	Fine sand
6H-5	51	53.81	11	Fine sand
6H-5	58	53.88	3	Fine sand
6H-5	72	54.02	9	Fine sand
6H-5	109	54.39	32	Fine sand
6H-5	118	54.48	3	Fine sand
6H-5	127	54.57	6.5	Fine sand
6H-5	128	54.58	0.5	Mud
6H-5	142	54.72	11	Fine sand
6H-5	151		3	Fine sand
6H-6	3	54.83	1	Fine sand
6H-6	16	54.96	9	Fine sand
6H-6	35	55.15	14	Fine sand
6H-6	46	55.26	6	Fine sand
6H-6	66	55.46	16	Fine sand
6H-6	68	55.48	1	Mud
6H-6	92	55.72	15	Fine sand
6H-6	99	55.79	2	Mud
6H-6	118	55.98	14	Fine sand
6H-6	126	56.06	3	Mud
6H-6	134	56.14	4	Mud
6H-CC	1	56.22	7	Fine sand
6H-CC	7	56.28	1	Mud
7H-1	12	56.92	7	Mud
7H-1	17	56.97	2	Mud
7H-1	20	57	0.5	Mud
7H-1	27	57.07	1	Mud
7H-1	44	57.24	5	Fine sand
7H-1	66	57.46	17	Fine sand
7H-1	80	57.6	9	Fine sand
7H-1	100	57.8	11	Fine sand
7H-1	118	57.98	10	Fine sand
7H-1	145	58.25	23	Sand
7H-2	22	58.52	19	Fine sand
7H-2	26	58.56	0.5	Mud
7H-2	31	58.61	1	Mud
7H-2	43	58.73	7	Fine sand
7H-2	48	58.78	5	Mud
7H-2	54	58.84	3	Mud
7H-2	63	58.93	5	Fine sand
7H-2	71	59.01	4	Fine sand
7H-2	90	59.2	13	Fine sand
7H-2	101	59.31	8	Fine sand
7H-2	112	59.42	7	Fine sand
7H-2	122	59.52	6	Fine sand
7H-2	125	59.55	0.5	Mud
7H-2	129	59.59	0.5	Mud
7H-2	132	59.62	0.5	Mud
7H-2	137	59.67	1	Mud
7H-2	141	59.71	1	Mud
7H-2	147	59.77	2	Mud
7H-3	14	59.94	14	Fine sand
7H-3	31	60.11	10	Fine sand
7H-3	48	60.28	7	Fine sand
7H-3	83	60.63	8	Fine sand
7H-3	105	60.85	6	Fine sand
7H-3	116	60.96	3	Fine sand
7H-3	132	61.12	1	Mud
7H-4	17	61.47	33	Fine sand
7H-4	40	61.7	12	Fine sand
7H-4	52	61.82	2	Mud
7H-4	62	61.92	3	Mud
7H-4	74	62.04	3	Mud
7H-4	80	62.1	1.5	Mud
7H-4	87	62.17	2	Mud
7H-4	135	62.65	14	Fine sand
7H-5	5	62.85	5-15	Fine sand
7H-5	23	63.03	6	Fine sand
7H-5	58	63.38	1	Fine sand
7H-5	63	63.43	1	Fine sand
7H-5	66	63.46	1	Fine sand
7H-5	68	63.48	0.5	Fine sand
7H-5	73	63.53	5	Fine sand
7H-5	83	63.63	0.5	Fine sand
7H-5	85	63.65	0.5	Fine sand
7H-5	102.5	63.825	9	Fine sand
7H-5	114	63.94	2	Fine sand
7H-5	126	64.06	6	Fine sand
7H-5	142	64.22	1	Fine sand
7H-6	8	64.38	11	Fine sand
7H-6	16	64.46	4	Fine sand
7H-6	29	64.59	5	Fine sand
7H-6	35	64.65	2	Fine sand
7H-6	93	65.23	31	Fine sand
7H-6	105	65.35	0.5	Fine sand
7H-6	112	65.42	0.5	Fine sand
7H-6	138	65.68	19	Fine sand
8H-1	6	66.36	1	Mud

Table T3 (continued).

Core, section	Depth at base of turbidite (cm)	Depth at base of turbidite (mbsf)	Thickness (cm)	Turbidite types
8H-1	32	66.62	8	Fine sand
8H-1	49	66.79	2	Fine sand
8H-1	54	66.84	1	Mud
8H-2	36	67.3	20	Fine sand
8H-2	72	67.66	20	Fine sand
8H-2	142	68.36	38	Fine sand
8H-3	31	68.75	15	Fine sand
8H-3	58	69.02	2	Fine sand
8H-3	68	69.12	3	Fine sand
8H-3	113	69.57	28	Fine sand
8H-3	139	69.83	0.5	Mud
8H-3	149	69.93	1	Mud
8H-4	54	70.48	40	Sand
8H-4	78	70.72	14	Fine sand
8H-4	103	70.97	3	Fine sand
8H-4	111	71.05	1	Mud
8H-4	121	71.15	3	Mud
8H-4	131	71.25	4	Fine sand
8H-4	143	71.37	5	Fine sand
8H-5	34	71.78	24	Fine sand
8H-5	55	71.99	10	Fine sand
8H-5	75	72.19	10	Fine sand
8H-5	85	72.29	1	Fine sand
8H-5	97	72.41	4	Mud
8H-5	104	72.48	3	Mud
8H-5	122	72.66	4	Mud
8H-5	129	72.73	1	Mud
8H-5	137	72.81	1	Mud
8H-6	20	73.14	10	Fine sand
8H-6	42	73.36	5	Mud
8H-6	66	73.6	12	Fine sand
8H-6	82	73.76	6	Mud
9X-1	5	75.85	1	Mud
9X-1	18	75.98	3	Mud
9X-1	40	76.2	13	Fine sand
9X-1	50	76.3	2	Fine sand
12X-4	6	109.26	0.5	Fine sand
12X-4	13	109.33	1.5	Fine sand
12X-4	19	109.39	0.5	Fine sand
12X-4	22.5	109.425	1	Fine sand
12X-4	24.5	109.445	0.5	Fine sand
12X-4	27	109.47	0.7	Fine sand
13X-1	2	114.32	1.5	Mud
13X-1	16.5	114.465	1.5	Mud
13X-1	29	114.59	2	Fine sand
13X-1	40	114.7	2.5	Fine sand
13X-1	53	114.83	2	Fine sand
13X-1	61	114.91	1	Fine sand
13X-1	72	115.02	3	Fine sand
13X-1	83	115.13	1	Mud
13X-1	91	115.21	1.5	Mud
13X-1	94	115.24	1.5	Mud
13X-1	116	115.46	2	Fine sand
13X-1	136	115.66	3.5	Fine sand
13X-1	150	115.8	2	Fine sand
13X-2	21	116.01	1.5	Fine sand
13X-2	29.5	116.095	3.5	Mud
13X-2	37	116.17	1.5	Fine sand
13X-2	40	116.2	0.5	Fine sand
13X-2	43	116.23	1	Fine sand
13X-2	59.5	116.395	0.6	Fine sand
13X-2	72	116.52	1	Fine sand
13X-2	85	116.65	1.5	Fine sand
13X-2	99.5	116.795	3	Fine sand
13X-2	124	117.04	2	Mud
13X-2	137	117.17	0.7	Fine sand
13X-3	13	117.43	1.5	Fine sand
13X-3	17	117.47	1.5	Fine sand
13X-3	22	117.52	1.5	Fine sand
13X-3	30	117.6	1	Fine sand
13X-3	33	117.63	0.5	Fine sand
13X-3	38	117.68	2	Fine sand
13X-3	43.5	117.735	3	Fine sand
13X-3	58	117.88	3.5	Fine sand
13X-3	72	118.02	3	Fine sand
13X-3	114	118.44	10	Fine sand
13X-4	2	118.82	1.5	Fine sand
13X-4	15	118.95	2	Fine sand
13X-4	17	118.97	1	Fine sand
13X-4	21	119.01	1.5	Mud
13X-4	27	119.07	1.5	Fine sand
13X-4	32	119.12	0.7	Fine sand
13X-4	39	119.19	2	Fine sand
13X-4	49	119.29	2.5	Fine sand
13X-4	50	119.3	0.2	Fine sand
13X-4	54	119.34	1	Fine sand
13X-4	57.5	119.375	2	Fine sand
13X-4	62	119.42	3	Fine sand
13X-4	65	119.45	2	Fine sand
13X-4	73	119.53	1.5	Fine sand
13X-4	108	119.88	1.6	Fine sand
13X-CC	1.5	119.935	2	Fine sand
181-1122B-				
1H-1	21	0.21	3.5	Sand
1H-1	56	0.56	5	Sand
1H-1	72	0.72	6	Sand
1H-1	102	1.02	6	Sand
1H-1	116	1.16	6	Sand
1H-1	146	1.46	6.5	Sand
1H-2	12	1.62	12	Sand
1H-2	32	1.82	10	Sand
1H-2	49	1.99	10	Sand
1H-2	82	2.32	9	Sand
1H-2	99	2.49	6	Sand
1H-2	115	2.65	6	Sand
1H-2	140	2.9	11.5	Sand
1H-4	5	4.55	4.5	Sand
1H-4	20	4.7	7	Sand
1H-4	40	4.9	8	Sand
1H-4	53	5.03	2.5	Sand
1H-4	80	5.3	3.5	Sand
1H-4	94	5.44	4.5	Sand
1H-4	118	5.68	6	Sand
1H-4	148	5.98	16.5	Sand
1H-5	8	6.08	10	Sand
1H-5	16	6.16	5	Sand
1H-5	27	6.27	5	Sand
1H-5	52	6.52	7	Sand
1H-5	74	6.74	1.5	Sand
1H-5	87	6.87	2.5	Sand
1H-5	114	7.14	5.5	Sand
1H-5	145	7.45	4	Sand
1H-6	14	7.64	7	Sand
1H-6	45	7.95	11	Sand
1H-6	60	8.1	5	Sand
1H-6	75	8.25	4.5	Sand
1H-6	102	8.52	10	Sand
1H-6	138	8.88	9.5	Sand
1H-7	13	9.13	6.5	Sand
1H-7	31	9.31	3	Sand

Table T3 (continued).

Core, section	Depth at base of turbidite (cm)	Depth at base of turbidite (mbsf)	Thickness (cm)	Turbidite types
1H-7	55	9.55	1.5	Sand
1H-1	27	0.27	5	Fine sand
1H-1	61	0.61	13	Sand
1H-1	100	1	4	Fine sand
1H-1	132	1.32	17	Sand
1H-2	28	1.78	5	Sand
1H-2	40	1.9	1.5	Fine sand
1H-2	64	2.14	7	Fine sand
1H-2	76	2.26	8.5	Fine sand
1H-2	90	2.4	5	Sand
2H-1	106	3.56	5	Sand
2H-1	138	3.88	4	Sand
2H-2	8	4.08	6.5	Sand
2H-2	44	4.44	5	Sand
2H-2	77	4.77	17	Sand
2H-2	95	4.95	5.5	Sand
2H-2	106	5.06	6	Sand
2H-2	127	5.27	5	Fine sand
2H-3	13	5.63	14.5	Sand
2H-3	34	5.84	1.5	Sand
2H-3	68	6.18	3	Fine sand
2H-3	89	6.39	6.5	Sand
2H-3	106	6.56	1.5	Fine sand
2H-3	123	6.73	8	Sand
2H-4	6	7.06	7	Sand
2H-4	32	7.32	9	Sand
2H-4	64	7.64	9.5	Sand
2H-4	92	7.92	9	Sand
2H-4	104	8.04	1	Fine sand
2H-4	118	8.18	1.5	Fine sand
2H-4	131	8.31	2	Fine sand
2H-4	146	8.46	3	Fine sand
2H-5	13.5	8.635	0.5	Fine sand
2H-5	16	8.66	0.3	Fine sand
2H-5	29	8.79	10	Sand
2H-5	41	8.91	1	Mud
2H-5	76	9.26	9	Sand
2H-5	89	9.39	1.5	Mud
2H-5	92	9.42	0.5	Mud
2H-5	102	9.52	3	Fine sand
2H-5	125	9.75	15	Sand
3H-1	40	9.9	3	Fine sand
2H-6	2	10.02	2	Fine sand
2H-6	8	10.08	1	Fine sand
3H-1	65	10.15	3.5	Fine sand
2H-6	24	10.24	10.5	Sand
3H-1	85	10.35	1	Fine sand
2H-6	40	10.4	2	Sand
3H-1	102	10.52	5	Sand
2H-6	60	10.6	6.5	Sand
3H-1	115	10.65	4	Sand
3H-1	123	10.73	1	Fine sand
2H-6	80	10.8	6.5	Sand
3H-1	140	10.9	7	Sand
2H-6	94	10.94	5.5	Sand
3H-2	4	11.04	2.5	Fine sand
2H-6	115	11.15	5.5	Sand
3H-2	20	11.2	2	Fine sand
3H-2	31	11.31	1.5	Fine sand
2H-6	137	11.37	9.5	Sand
3H-2	42	11.42	3.5	Sand
3H-2	60	11.6	7	Sand
2H-7	15	11.65	7	Sand
3H-2	76	11.76	6	Sand
2H-7	38	11.88	15	Sand
3H-2	93	11.93	3	Fine sand
2H-7	58	12.08	5.5	Sand
3H-2	109	12.09	12	Sand
2H-7	65	12.15	4.5	Fine sand
3H-2	123	12.23	4	Fine sand
3H-2	138	12.38	7	Sand
3H-3	14	12.64	10	Sand
3H-3	33	12.83	2.5	Fine sand
3H-3	49	12.99	12	Sand
3H-3	63	13.13	4	Fine sand
3H-3	80	13.3	5.5	Sand
3H-3	91	13.41	2	Fine sand
3H-3	96	13.46	0.5	Fine sand
3H-3	102	13.52	2	Fine sand
3H-3	115	13.65	9	Sand
3H-3	126	13.76	2.5	Fine sand
3H-3	135	13.85	1.5	Fine sand
3H-3	146	13.96	3	Fine sand
3H-4	16	14.16	4.5	Sand
3H-4	27	14.27	2	Sand
3H-4	36	14.36	2	Fine sand
3H-4	52	14.52	1.5	Fine sand
4H-1	59	14.59	6	Sand
3H-4	65	14.65	6	Sand
4H-1	66.5	14.665	1	Fine sand
4H-1	79	14.79	5	Sand
3H-4	83	14.83	12	Sand
3H-4	98	14.98	3	Sand
4H-1	110	15.1	14	Sand
4H-1	123	15.23	1.5	Fine sand
3H-5	15	15.26	5.5	Sand
3H-5	19	15.3	0.5	Fine sand
4H-1	135	15.35	4	Sand
3H-5	26	15.37	1.5	Sand
4H-1	150	15.5	5	Sand
3H-5	50	15.61	0.3	Fine sand
4H-2	13	15.63	7.5	Sand
3H-5	53	15.64	0.1	Fine sand
3H-5	54	15.65	0.1	Fine sand
3H-5	55	15.66	0.1	Fine sand
3H-5	55.5	15.665	0.1	Fine sand
3H-5	56	15.67	0.1	Fine sand
3H-5	58	15.69	1.5	Fine sand
3H-5	63	15.74	2.5	Sand
3H-5	65	15.76	0.2	Fine sand
4H-2	26	15.76	2	Fine sand
3H-5	67	15.78	2	Fine sand
3H-5	72	15.83	1	Mud
4H-2	34	15.84	1	Fine sand
3H-5	75.5	15.865	1	Mud
4H-2	39	15.89	1	Fine sand
3H-5	84	15.95	0.5	Mud
4H-2	48	15.98	3.5	Fine sand
3H-5	91	16.02	1	Mud
4H-2	53	16.03	1.5	Fine sand
3H-5	94	16.05	1	Mud
4H-2	63	16.13	1.5	Fine sand
3H-5	104	16.15	0.5	Mud
4H-2	84	16.34	17	Sand
3H-5	133	16.44	12.5	Sand
3H-5	138	16.49	2.5	Fine sand
4H-2	117	16.67	14	Sand
4H-2	145	16.95	13	Sand
3H-6	38	16.99	45	Sand
4H-3	5	17.05	3	Fine sand

Table T3 (continued).

Core, section	Depth at base of turbidite (cm)	Depth at base of turbidite (mbsf)	Thickness (cm)	Turbidite types
4H-3	16	17.16	2	Fine sand
4H-3	28	17.28	3	Fine sand
4H-3	45	17.45	7.5	Sand
4H-3	69	17.69	12	Sand
4H-3	83	17.83	5	Sand
4H-3	100	18	2	Fine sand
4H-3	115	18.15	5	Fine sand
4H-3	133	18.33	10	Sand
4H-3	142	18.42	3	Fine sand
4H-3	147	18.47	3	Fine sand
4H-4	28	18.82	20	Sand
4H-4	40	18.94	6	Fine sand
4H-4	55	19.09	5	Fine sand
4H-4	78	19.32	7	Fine sand
4H-4	106	19.6	15	Sand
4H-4	130	19.84	10	Sand
4H-5	10	20.14	15	Sand
4H-5	23	20.27	5	Fine sand
4H-5	51	20.55	12	Sand
4H-5	64	20.68	4.5	Fine sand
4H-5	73	20.77	2	Mud
4H-5	80	20.84	2	Mud
4H-5	90	20.94	3	Mud
4H-5	108	21.12	7.5	Fine sand
4H-5	119	21.23	4	Fine sand
4H-5	142	21.46	13	Sand
4H-6	8	21.62	13	Fine sand
4H-6	28	21.82	8	Fine sand
4H-6	46	22	9	Fine sand
4H-6	69	22.23	13	Fine sand
4H-6	85	22.39	6	Fine sand
4H-6	90	22.44	3	Fine sand
4H-6	108	22.62	2	Fine sand
4H-7	46	23.37	57	Sand
5H-1	104	24.54	9	Sand
5H-1	110	24.6	1	Fine sand
5H-1	120	24.7	2	Fine sand
5H-1	125	24.75	0.5	Fine sand
5H-1	129	24.79	0.5	Fine sand
5H-1	136	24.86	1.5	Fine sand
5H-1	137	24.87	0.5	Fine sand
5H-1	149	24.99	7	Sand
5H-2	9	25.09	1.5	Fine sand
5H-2	18	25.18	4	Fine sand
5H-2	32	25.32	7.5	Fine sand
5H-2	55	25.55	8.5	Sand
5H-2	73.5	25.735	7.5	Fine sand
5H-2	89	25.89	2.5	Fine sand
5H-2	111	26.11	11	Sand
5H-2	123	26.23	5	Fine sand
5H-2	129	26.29	1.5	Fine sand
5H-2	132	26.32	1.5	Fine sand
5H-3	8	26.58	17	Sand
5H-3	40	26.9	23	Sand
5H-3	67	27.17	17	Sand
5H-3	94	27.44	14	Sand
5H-3	117	27.67	6.5	Fine sand
5H-3	126	27.76	3.5	Fine sand
5H-3	139	27.89	8	Sand
5H-4	16	28.16	18	Sand
5H-4	29	28.29	5.5	Fine sand
5H-4	44	28.44	4	Mud
5H-4	67	28.67	5.5	Fine sand
5H-4	76	28.76	3.5	Mud
5H-4	90	28.9	2	Mud
5H-4	113	29.13	6	Fine sand
5H-4	123	29.23	1	Mud
5H-4	133	29.33	2.5	Mud
5H-4	150	29.5	9	Mud
5H-5	26	29.76	10	Sand
5H-5	38	29.88	4	Mud
5H-5	61	30.11	3.5	Fine sand
5H-5	147	30.97	2.5	Mud
5H-6	48	31.48	42	Sand
5H-6	60	31.6	2.5	Mud
5H-6	75	31.75	11	Fine sand
5H-6	99	31.99	9	Fine sand
5H-6	108	32.08	3	Mud
5H-6	122	32.22	7.5	Sand
6H-1	76	33.76	5.5	Fine sand
6H-1	84	33.84	1	Fine sand
6H-1	110	34.1	13	Sand
6H-1	124	34.24	0.5	Fine sand
6H-1	127	34.27	1	Mud
6H-1	133	34.33	4	Mud
6H-1	137	34.37	1.5	Mud
6H-2	15	34.65	5.5	Sand
6H-2	24	34.74	1.5	Fine sand
6H-2	40	34.9	3.5	Fine sand
6H-2	47	34.97	1.5	Fine sand
6H-2	70	35.2	8	Fine sand
6H-2	74	35.24	0.5	Fine sand
6H-2	81	35.31	1	Fine sand
6H-2	112	35.62	9.5	Fine sand
6H-2	117.5	35.675	3	Fine sand
6H-2	150	36	12	Fine sand
6H-3	5	36.05	1.5	Mud
6H-3	11	36.11	0.5	Mud
6H-3	17	36.17	0.5	Mud
6H-3	26	36.26	3	Fine sand
6H-3	36.5	36.365	1.5	Fine sand
6H-3	44	36.44	3.5	Fine sand
6H-3	71.5	36.715	11.5	Sand
6H-3	82	36.82	1.5	Mud
6H-3	86	36.86	1.5	Mud
6H-3	95	36.95	1.5	Mud
6H-3	114	37.14	5	Fine sand
6H-3	139	37.39	8	Fine sand
6H-4	3	37.53	7	Fine sand
6H-4	12	37.62	0.5	Mud
6H-4	50	38	24	Sand
6H-4	63	38.13	5	Fine sand
6H-4	73	38.23	2	Fine sand
6H-4	83	38.33	2	Fine sand
6H-4	106	38.56	0.2	Mud
6H-4	125	38.75	4	Fine sand
6H-4	134	38.84	0.5	Fine sand
6H-4	142	38.92	1.5	Fine sand
6H-5	4	39.04	4	Fine sand
6H-5	17	39.17	4	Fine sand
6H-5	31	39.31	3.5	Fine sand
6H-5	51	39.51	8	Fine sand
6H-5	68	39.68	10	Fine sand
6H-5	80	39.8	6.5	Fine sand
6H-5	95	39.95	8	Fine sand
6H-5	117	40.17	6	Fine sand
6H-5	124	40.24	2	Mud
6H-6	61	41.11	69	Sand
6H-6	66	41.16	1.5	Fine sand
6H-6	91	41.41	8	Fine sand

Table T3 (continued).

Core, section	Depth at base of turbidite (cm)	Depth at base of turbidite (mbsf)	Thickness (cm)	Turbidite types
6H-6	107	41.57	2	Fine sand
6H-6	112	41.62	1	Fine sand
6H-6	119	41.69	1	Mud
6H-CC	4	41.97	4	Sand
7H-1	95	43.45	20	Sand
7H-1	132	43.82	14	Sand
7H-2	10	44.1	16	Sand
7H-2	14.5	44.145	0.5	Mud
7H-2	19	44.19	1	Mud
7H-2	58	44.58	30	Sand
7H-2	76	44.76	8	Fine sand
7H-2	98	44.98	7.5	Fine sand
7H-2	108	45.08	1.5	Fine sand
7H-2	121	45.21	9	Fine sand
7H-2	129	45.29	2	Fine sand
7H-2	148	45.48	2.5	Fine sand
7H-3	2	45.52	2.5	Fine sand
7H-3	11	45.61	5	Fine sand
7H-3	29	45.79	13	Sand
7H-3	49	45.99	10	Fine sand
7H-3	60	46.1	6	Fine sand
7H-3	84	46.34	14	Sand
7H-3	91	46.41	1	Mud
7H-3	95	46.45	1.5	Mud
7H-3	119	46.69	8.5	Fine sand
7H-3	128	46.78	1	Mud
7H-3	131	46.81	0.5	Mud
7H-3	151	47.01	15	Sand
7H-4	20	47.2	13	Sand
7H-4	33	47.33	1	Fine sand
7H-4	51	47.51	7	Fine sand
7H-4	74	47.74	10.5	Sand
7H-4	82	47.82	1	Fine sand
7H-4	94	47.94	7	Fine sand
7H-4	100	48	0.5	Fine sand
7H-4	111	48.11	1.5	Fine sand
7H-4	130	48.3	8	Fine sand
7H-4	134	48.34	1	Mud
7H-5	16	48.66	18	Fine sand
7H-5	27	48.77	1	Fine sand
7H-5	39	48.89	0.5	Mud
7H-5	42	48.92	1	Mud
7H-5	51	49.01	4	Fine sand
7H-5	54	49.04	1	Mud
7H-5	65	49.15	5	Fine sand
7H-5	67	49.17	0.5	Fine sand
7H-5	89	49.39	15	Sand
7H-5	95	49.45	1	Mud
7H-5	106	49.56	1	Mud
7H-5	120	49.7	6	Fine sand
7H-5	127	49.77	7	Fine sand
7H-5	134	49.84	1.5	Mud
7H-6	21	50.21	43	Sand
7H-6	26	50.26	1	Fine sand
7H-6	30	50.3	1	Mud
7H-6	49	50.49	1.3	Fine sand
7H-6	56	50.56	3	Mud
7H-6	62	50.62	1	Mud
7H-6	94	50.94	28	Fine sand
7H-6	106	51.06	8	Fine sand
8H-1	9	52.09	3	Fine sand
8H-1	53	52.53	33	Sand
8H-1	73	52.73	6	Fine sand
8H-1	84	52.84	4.5	Fine sand
8H-1	94	52.94	5.5	Fine sand
8H-1	134	53.34	34	Sand
8H-2	2	53.52	6	Fine sand
8H-2	52	54.02	42	Sand
8H-2	102	54.52	42	Sand
8H-2	112	54.62	0.5	Mud
8H-2	114	54.64	0.5	Mud
8H-2	122	54.72	0.2	Mud
8H-2	145	54.95	17	Fine sand
8H-3	14	55.14	11	Fine sand
8H-3	32	55.32	7	Fine sand
8H-3	63	55.63	17	Sand
8H-3	77	55.77	1	Fine sand
8H-3	82	55.82	1	Fine sand
8H-3	89	55.89	0.5	Mud
8H-3	120	56.2	20	Fine sand
8H-4	13	56.63	43	Sand
8H-4	30	56.8	9	Fine sand
8H-4	43	56.93	1	Mud
8H-4	65	57.15	5	Fine sand
8H-4	75	57.25	2.5	Fine sand
8H-4	88	57.38	8	Fine sand
8H-4	132	57.82	30	Sand
8H-4	141	57.91	2	Fine sand
8H-4	150	58	2	Fine sand
8H-5	15	58.15	10	Fine sand
8H-5	27	58.27	2	Fine sand
8H-5	34	58.34	1	Mud
8H-5	49	58.49	7	Fine sand
8H-5	73	58.73	16	Fine sand
8H-5	77	58.77	7	Fine sand
8H-5	106	59.06	11	Fine sand
8H-5	131	59.31	13	Sand
8H-5	136	59.36	15	Fine sand
8H-5	140	59.4	1	Mud
8H-6	2	59.52	7	Fine sand
8H-6	12	59.62	1.5	Fine sand
8H-6	23	59.73	2	Fine sand
8H-6	36	59.86	8	Fine sand
8H-6	73	60.23	17	Fine sand
8H-6	83	60.33	6	Fine sand
8H-6	93	60.43	3	Fine sand
8H-6	105	60.55	6	Fine sand
8H-6	118	60.68	5	Fine sand
8H-6	134	60.84	7	Fine sand
8H-7	2	61.02	12	Fine sand
8H-7	18	61.18	2.5	Fine sand
8H-7	29	61.28	5	Sand
9H-1	2.5	61.525	2.5	Fine sand
9H-1	17	61.67	10	Fine sand
9H-1	38	61.88	7	Fine sand
9H-1	43	61.93	0.5	Mud
9H-1	48	61.98	3	Mud
9H-1	59	62.09	7	Sand
9H-1	67	62.17	2.5	Sand
9H-1	82	62.32	8.5	Sand
9H-1	94	62.44	8.5	Fine sand
9H-1	106.5	62.565	8.5	Fine sand
9H-1	115	62.65	1.5	Sand
9H-1	122	62.72	1	Mud
9H-1	129	62.79	1	Mud
9H-1	142	62.92	1.5	Sand
9H-2	11	63.11	6	Sand
9H-2	28	63.28	2.5	Sand
9H-2	43.5	63.435	3	Sand
9H-2	78	63.78	12	Sand

Table T3 (continued).

Core, section	Depth at base of turbidite (cm)	Depth at base of turbidite (mbsf)	Thickness (cm)	Turbidite types
9H-2	98	63.98	3.5	Sand
9H-2	106.5	64.065	1.5	Sand
9H-2	122	64.22	1.5	Mud
9H-3	12	64.62	32	Sand
9H-3	35	64.85	8.5	Sand
9H-3	46.5	64.965	3	Mud
9H-3	56	65.06	4	Mud
9H-3	66	65.16	2.5	Fine sand
9H-3	74	65.24	2.5	Mud
9H-3	81	65.31	3.5	Mud
9H-3	129.5	65.795	12.5	Sand
9H-4	18	66.18	20.5	Fine sand
9H-4	29	66.29	4.5	Mud
9H-4	39	66.39	3	Mud
9H-4	50	66.5	1.5	Fine sand
9H-4	54	66.54	1.5	Fine sand
9H-4	64	66.64	8	Fine sand
9H-4	75	66.75	3	Mud
9H-4	86.5	66.865	2	Fine sand
9H-4	93	66.93	4.5	Fine sand
9H-4	106	67.06	3.5	Fine sand
9H-4	118	67.18	3	Fine sand
9H-5	7	67.57	3	Fine sand
9H-5	18.5	67.685	6.5	Fine sand
9H-5	24.5	67.745	1.5	Fine sand
9H-5	48	67.98	0.6	Sand
9H-5	52	68.02	0.5	Sand
9H-5	65.5	68.155	1	Fine sand
9H-5	61	68.11	1.5	Fine sand
9H-5	65	68.15	1	Fine sand
9H-5	68	68.18	0.5	Fine sand
9H-5	70.5	68.205	0.5	Fine sand
9H-5	82	68.32	9	Fine sand
9H-5	131	68.81	23	Sand
9H-5	148	68.98	1.5	Mud
9H-6	21	69.21	9	Sand
9H-6	32	69.32	9	Sand
9H-6	75	69.75	37	Sand
9H-6	95	69.95	2.5	Mud
9H-6	100	70	4	Fine sand
10H-1	42	71.42	22	Sand
10H-1	68	71.68	20	Sand
10H-1	90	71.9	10	Sand
10H-1	116	72.16	1	Sand
10H-1	144	72.44	24	Sand
10H-2	43	72.93	37	Sand
10H-3	15	74.15	81	Sand
10H-3	59	74.59	39	Sand
10H-3	90	74.9	3.5	Fine sand
10H-3	98	74.98	2	Fine sand
10H-3	108.5	75.085	3	Fine sand
10H-3	118	75.18	1.5	Fine sand
10H-3	125.5	75.255	5.5	Sand
10H-3	141.5	75.415	11	Sand
10H-4	29.5	75.795	10	Sand
10H-4	50	76	4.5	Fine sand
10H-4	72.5	76.225	8.5	Fine sand
10H-4	82	76.32	1.5	Fine sand
10H-4	99	76.49	7	Fine sand
10H-4	104.5	76.545	1	Fine sand
10H-4	112	76.62	1	Fine sand
10H-4	121.5	76.715	1.5	Fine sand
10H-4	130	76.8	3.5	Mud
10H-4	138.5	76.885	4	Mud
10H-5	1	77.01	1	Fine sand
10H-5	17	77.17	0.5	Fine sand
10H-5	24.5	77.245	1	Mud
10H-5	39	77.39	3.5	Mud
10H-5	62	77.62	10.5	Fine sand
10H-5	76	77.76	2.5	Fine sand
10H-5	104	78.04	14.5	Fine sand
10H-5	122	78.22	5.5	Fine sand
10H-5	129	78.29	1	Fine sand
10H-5	149	78.49	3	Fine sand
10H-6	13	78.63	1.2	Fine sand
10H-6	69	79.19	44.5	Sand
10H-6	95.5	79.455	5.5	Fine sand
11H-1	6	80.56	2.5	Fine sand
11H-1	25	80.75	5.5	Fine sand
11H-1	38	80.88	4.5	Mud
11H-1	52	81.02	4.5	Fine sand
11H-1	67	81.17	4.5	Fine sand
11H-1	86	81.36	6	Sand
11H-1	108	81.58	6	Fine sand
11H-1	127	81.77	2	Fine sand
11H-1	135	81.85	1.5	Mud
11H-1	137	81.87	0.5	Fine sand
11H-1	139.5	81.895	1.3	Fine sand
11H-2	17	82.17	26	Sand
11H-2	40	82.4	11.5	Sand
11H-2	48	82.48	0.7	Fine sand
11H-2	69	82.69	7	Fine sand
11H-2	95	82.95	13	Fine sand
11H-2	118	83.18	7.5	Fine sand
11H-2	126.5	83.265	2.5	Fine sand
11H-2	140	83.4	11	Fine sand
11H-2	146.5	83.465	0.5	Mud
11H-3	5.5	83.555	6.5	Fine sand
11H-3	16	83.66	4.5	Fine sand
11H-3	38	83.88	12	Sand
11H-3	55	84.05	10.5	Fine sand
11H-3	63	84.13	1	Fine sand
11H-3	68.5	84.185	0.5	Mud
11H-3	75	84.25	3	Mud
11H-3	115.5	84.655	30	Sand
11H-4	12	85.12	44	Sand
11H-4	25.5	85.255	6.5	Fine sand
11H-4	39	85.39	9.5	Fine sand
11H-4	58	85.58	8.5	Fine sand
11H-4	73	85.73	2.5	Fine sand
11H-5	84	86.82	97	Sand
12H-1	6	86.96	1	Mud
12H-1	12	87.02	2	Fine sand
12H-1	32.5	87.225	2	Fine sand
12H-1	42	87.32	7	Fine sand
12H-1	49.5	87.395	3	Fine sand
12H-1	54.5	87.445	3	Mud
12H-1	60	87.5	0.5	Fine sand
12H-1	76	87.66	6	Mud
12H-1	81.5	87.715	1.5	Fine sand
12H-1	99	87.89	9.5	Fine sand
12H-1	101	87.91	0.7	Fine sand
12H-1	115	88.05	1.5	Mud
12H-1	117	88.07	1	Fine sand
12H-1	125.5	88.155	1.5	Mud
12H-1	145.5	88.355	7.5	Fine sand
12H-2	14	88.54	3	Fine sand
12H-2	20	88.6	2.5	Fine sand
12H-2	25.5	88.655	2	Fine sand
12H-2	40	88.8	5.5	Fine sand

Table T3 (continued).

Core, section	Depth at base of turbidite (cm)	Depth at base of turbidite (mbsf)	Thickness (cm)	Turbidite types
12H-2	47	88.87	0.5	Fine sand
12H-2	57	88.97	0.7	Fine sand
12H-2	73.5	89.135	5	Fine sand
12H-2	83	89.23	4	Fine sand
12H-2	97	89.37	6	Fine sand
12H-2	102	89.42	2.5	Fine sand
12H-2	118	89.58	8.5	Fine sand
12H-2	130.5	89.705	1.5	Mud
12H-2	144	89.84	5	Fine sand
12H-2	152	89.92	2	Fine sand
12H-3	16	90.06	8	Fine sand
12H-3	19	90.09	2	Mud
12H-3	31	90.21	3	Fine sand
12H-3	53	90.43	13	Fine sand
12H-3	56	90.46	1.5	Fine sand
12H-3	79.5	90.695	4	Fine sand
12H-3	84	90.74	3	Fine sand
12H-3	97	90.87	2	Fine sand
12H-3	104	90.94	2.5	Fine sand
12H-3	115	91.05	2.5	Fine sand
12H-3	125	91.15	3.5	Fine sand
12H-3	126.5	91.165	0.5	Mud
12H-3	134.5	91.245	2.5	Fine sand
12H-3	136.5	91.265	1	Mud
12H-3	142.5	91.325	1.5	Fine sand
12H-4	4	91.44	1	Fine sand
12H-4	11	91.51	0.7	Fine sand
12H-4	20	91.6	1	Fine sand
12H-4	24.5	91.645	1.5	Mud
12H-4	27	91.67	1.2	Mud
12H-4	53	91.93	23	Fine sand
12H-4	61	92.01	4.5	Mud
12H-4	67	92.07	1.3	Mud
12H-4	96	92.36	24	Sand
12H-4	102	92.42	1	Mud
12H-4	113	92.53	2	Mud
12H-4	120	92.6	1	Mud
12H-4	134	92.74	3.5	Fine sand
12H-5	16.5	93.065	6.5	Fine sand
12H-5	19.5	93.095	1.5	Mud
12H-5	30	93.2	2	Fine sand
12H-5	40	93.3	1.5	Fine sand
12H-5	48.5	93.385	1.5	Fine sand
12H-5	58	93.48	2	Fine sand
12H-5	60	93.5	1	Fine sand
12H-5	70	93.6	2	Fine sand
12H-5	83	93.73	4	Fine sand
12H-5	88	93.78	2	Fine sand
12H-5	102	93.92	3.5	Mud
12H-5	111	94.01	1	Sand
12H-5	124	94.14	8.5	Sand
12H-5	144	94.34	13	Fine sand
12H-6	8	94.48	4	Fine sand
12H-6	11	94.51	1	Mud
12H-6	16	94.56	1	Fine sand
12H-CC	6	94.7	6	Fine sand
13H-1	13	95.03	12	Fine sand
13H-1	25	95.15	2	Fine sand
13H-1	30	95.2	1.5	Fine sand
13H-1	51	95.41	3.5	Fine sand
13H-1	83	95.73	6	Fine sand
13H-1	104	95.94	2.5	Fine sand
13H-1	111	96.01	1	Fine sand
13H-1	119	96.09	1.5	Fine sand
13H-1	128	96.18	2	Fine sand
13H-1	137	96.27	1.5	Fine sand
13H-1	143	96.33	2	Mud
13H-2	9	96.49	9	Fine sand
13H-2	20	96.6	4.5	Mud
13H-2	36	96.76	2	Mud
13H-2	43	96.83	3.5	Mud
13H-2	57	96.97	4	Mud
13H-2	67	97.07	2	Mud
13H-2	76	97.16	3.5	Fine sand
13H-2	86	97.26	3.5	Fine sand
13H-2	99	97.39	5	Sand
13H-2	116	97.56	2	Mud
13H-2	123	97.63	2	Fine sand
13H-2	148	97.88	2	Sand
13H-3	8	97.98	2.5	Fine sand
13H-3	25	98.15	5	Sand
13H-3	36	98.26	3.5	Fine sand
13H-3	143	99.33	67	Sand
13H-4	6	99.46	5.5	Sand
13H-4	27	99.67	2	Fine sand
13H-4	36	99.76	3	Fine sand
13H-4	47	99.87	5	Sand
13H-4	56	99.96	1	Fine sand
13H-4	63	100.03	1.5	Fine sand
13H-4	76	100.16	10.5	Sand
13H-4	89	100.29	4.5	Sand
13H-4	100.5	100.405	1.5	Sand
13H-4	106	100.46	1.5	Fine sand
13H-4	113	100.53	1	Fine sand
13H-4	120	100.6	0.5	Fine sand
13H-4	135	100.75	8	Fine sand
13H-5	13	101.03	4	Fine sand
13H-5	36	101.26	10	Sand
13H-5	45	101.35	1	Fine sand
13H-5	49	101.39	1	Fine sand
13H-5	54	101.44	1	Fine sand
13H-5	62	101.52	4	Sand
13H-5	90	101.8	14	Sand
13H-5	100	101.9	1.5	Fine sand
13H-5	103	101.93	1	Fine sand
13H-5	112	102.02	3	Fine sand
13H-5	121	102.11	5.5	Fine sand
13H-5	131	102.21	1	Fine sand
13H-5	136	102.26	1	Fine sand
13H-5	145	102.35	3	Fine sand
13H-5	148	102.38	2	Fine sand
13H-6	1.5	102.415	2.5	Fine sand
13H-6	11.5	102.515	0.5	Fine sand
13H-6	21	102.61	1	Fine sand
13H-6	32	102.72	0.5	Fine sand
13H-6	38	102.78	2.5	Fine sand
13H-6	51	102.91	1	Fine sand
13H-6	61	103.01	4	Mud
13H-6	72.5	103.125	3.5	Fine sand
13H-6	86.5	103.265	3	Fine sand
13H-6	97	103.37	3	Mud
14X-1	34	104.04	1.5	Fine sand
14X-1	52	104.22	3	Fine sand
14X-1	69	104.39	2.5	Fine sand
14X-1	81	104.51	2	Mud
14X-1	108	104.78	0.5	Fine sand
14X-1	115	104.85	2	Fine sand
14X-1	135	105.05	1.5	Fine sand
14X-1	141	105.11	1	Mud
14X-1	146	105.16	1.5	Fine sand

Table T3 (continued).

Core, section	Depth at base of turbidite (cm)	Depth at base of turbidite (mbsf)	Thickness (cm)	Turbidite types
14X-2	2	105.22	1	Fine sand
14X-2	7	105.27	1	Fine sand
14X-2	9	105.29	1.5	Fine sand
14X-2	22	105.42	3	Fine sand
14X-2	30	105.5	1.5	Fine sand
14X-2	39	105.59	1	Fine sand
14X-2	43	105.63	2	Fine sand
14X-2	52	105.72	4	Fine sand
14X-2	58	105.78	1.5	Mud
14X-2	65	105.85	2.5	Mud
14X-2	69	105.89	3	Mud
14X-2	78	105.98	1.5	Mud
14X-2	87.5	106.075	2	Mud
14X-2	110	106.3	3	Mud
14X-2	116	106.36	1.5	Mud
14X-2	127	106.47	4	Mud
14X-2	132	106.52	2	Fine sand
14X-2	138	106.58	2	Fine sand
14X-2	141	106.61	1	Fine sand
14X-2	146	106.66	2	Fine sand
14X-3	6	106.76	2	Fine sand
14X-3	11.5	106.815	1.5	Fine sand
14X-3	15	106.85	1.5	Mud
14X-3	19	106.89	1.5	Fine sand
14X-3	24	106.94	3	Fine sand
14X-3	31	107.01	1.5	Fine sand
14X-3	53	107.23	2	Fine sand
14X-3	55	107.25	1.5	Fine sand
14X-3	58.5	107.285	1	Fine sand
14X-3	64	107.34	1	Fine sand
14X-3	70	107.4	3	Fine sand
14X-3	74	107.44	3	Mud
14X-3	80.5	107.505	2.5	Fine sand
14X-3	88	107.58	2	Mud
14X-3	106	107.76	2.5	Fine sand
14X-3	112	107.82	2.5	Fine sand
15X-1	4	108.04	1.5	Fine sand
15X-1	12	108.12	2.5	Fine sand
15X-1	20	108.2	4	Fine sand
15X-1	36	108.36	1.5	Fine sand
15X-1	49	108.49	5	Fine sand
15X-1	64	108.64	2	Fine sand
15X-1	70	108.7	2	Fine sand
15X-1	133	109.33	1.5	Mud
15X-2	10	109.6	0.5	Fine sand
15X-2	53	110.03	0.7	Fine sand
15X-2	93	110.43	2	Fine sand
15X-2	98	110.48	2.5	Fine sand
15X-2	106	110.56	2.5	Fine sand
15X-2	117	110.67	1.5	Fine sand
15X-2	125	110.75	2.5	Fine sand
15X-2	137	110.87	2	Fine sand
15X-2	141	110.91	3.5	Fine sand
16X-1	13	117.73	1.5	Fine sand
16X-1	21	117.81	1	Fine sand
16X-1	28	117.88	1.5	Fine sand
16X-1	33	117.93	1.5	Fine sand
16X-1	37	117.97	1.5	Fine sand
16X-1	51	118.11	3.5	Fine sand
16X-1	76	118.36	2	Fine sand
16X-1	81	118.41	1.5	Fine sand
16X-1	90	118.5	1.5	Fine sand
16X-1	99	118.59	1.2	Fine sand
16X-1	108	118.68	0.5	Mud
16X-1	116	118.76	1.5	Fine sand
16X-1	128	118.88	2	Mud
16X-1	135	118.95	2	Mud
16X-1	138	118.98	2	Mud
16X-1	141	119.01	0.5	Fine sand
16X-2	2.5	119.125	0.5	Fine sand
16X-2	18	119.28	0.5	Fine sand
16X-2	24.5	119.345	1	Fine sand
16X-2	34.5	119.445	1	Fine sand
16X-2	46	119.56	1.5	Fine sand
16X-2	56	119.66	2.5	Fine sand
16X-2	61	119.71	1	Fine sand
16X-2	74	119.84	1.5	Fine sand
16X-2	86.5	119.965	1.5	Fine sand
16X-2	94.5	120.045	1.5	Fine sand
16X-2	129	120.39	1	Fine sand
16X-3	10	120.7	1	Fine sand
16X-3	32	120.92	1	Fine sand
16X-3	49	121.09	1	Fine sand
16X-3	63	121.23	1	Fine sand
16X-3	68	121.28	1	Fine sand
16X-3	81	121.41	2	Fine sand
16X-3	92	121.52	2	Fine sand
16X-3	107	121.67	3	Mud
16X-3	108	121.68	1	Fine sand
16X-3	120	121.8	4	Fine sand
16X-3	128	121.88	3	Mud
16X-4	135	123.45	1	Fine sand
16X-4	140	123.5	2.5	Mud
16X-4	1	122.11	1	Fine sand
16X-4	28	122.38	1.5	Fine sand
16X-4	35	122.45	2	Fine sand
16X-4	47	122.57	1	Fine sand
16X-4	61	122.71	3	Fine sand
17X-1	6	127.26	1	Fine sand
17X-1	10	127.3	0.5	Fine sand
17X-1	12	127.32	0.5	Fine sand
17X-1	16	127.36	1	Fine sand
17X-1	19	127.39	1	Fine sand
17X-1	28.5	127.485	0.5	Fine sand
17X-1	32	127.52	0.5	Fine sand
17X-1	42	127.62	0.7	Fine sand
17X-1	46	127.66	0.5	Fine sand
17X-1	49	127.69	1.2	Fine sand
17X-1	68	127.88	3	Fine sand
17X-1	82	128.02	1.5	Fine sand
17X-1	88	128.08	3.5	Fine sand
17X-1	101.5	128.215	2	Fine sand
17X-1	111	128.31	1	Mud
17X-1	120	128.4	1	Fine sand
17X-1	129	128.49	1	Fine sand
17X-1	135	128.55	0.7	Mud
17X-1	138	128.58	1	Mud
17X-2	14.5	128.845	0.7	Mud
17X-2	23	128.93	1	Mud
17X-2	32	129.02	1	Fine sand
17X-2	34	129.04	0.6	Fine sand
17X-2	38	129.08	1.5	Fine sand
17X-2	39	129.09	0.5	Fine sand
17X-2	44.5	129.145	2	Fine sand
17X-2	49	129.19	1	Fine sand
17X-2	78	129.48	1	Fine sand
17X-2	127	129.97	2.5	Fine sand
17X-2	146	130.16	4	Fine sand
17X-3	4	130.24	2	Fine sand
17X-3	9.5	130.295	1.5	Fine sand
17X-3	15.5	130.355	1.5	Fine sand
17X-3	19	130.39	0.5	Fine sand
17X-3	29	130.49	1	Fine sand
17X-3	35	130.55	2	Fine sand
17X-3	44.5	130.645	1.5	Fine sand
17X-3	57.5	130.775	1	Fine sand
17X-3	71	130.91	2	Fine sand
17X-3	118	131.38	0.5	Fine sand
17X-3	121	131.41	0.5	Fine sand
17X-3	148.5	131.685	3.5	Fine sand

Table T3 (continued).

Core, section	Depth at base of turbidite (cm)	Depth at base of turbidite (mbsf)	Thickness (cm)	Turbidite types
17X-4	52	132.22	2	Fine sand
17X-4	64	132.34	1.8	Fine sand
17X-4	78	132.48	1	Fine sand
17X-4	89	132.59	2.5	Fine sand
17X-4	103	132.73	2	Fine sand
17X-4	121.5	132.915	1.5	Fine sand
17X-4	135	133.05	0.5	Fine sand
17X-4	141	133.11	1	Fine sand
17X-4	142.5	133.125	0.5	Fine sand
18X-1	7	136.97	2	Silt
18X-1	14	137.04	1	Silt
18X-1	16	137.06	0.5	Silt
18X-1	32	137.22	1	Silt
18X-1	38	137.28	1	Silt
18X-1	48	137.38	2.5	Silt
18X-1	64	137.54	1.5	Silt
18X-1	73	137.63	1.5	Silt
18X-1	79	137.69	1.5	Mud
18X-1	90	137.8	2.5	Silt
18X-1	98	137.88	1	Silt
18X-1	114	138.04	2.5	Mud
18X-1	123.5	138.135	1.5	Silt
18X-1	126	138.16	2.5	Silt
18X-1	129	138.19	2	Silt
18X-1	134	138.24	2	Silt
18X-1	139	138.29	2	Silt
18X-1	146	138.36	1	Silt
18X-2	1	138.41	1	Silt
18X-2	27	138.67	3	Sand
18X-2	36	138.76	1	Silt
18X-2	53	138.93	2	Mud
18X-2	63	139.03	1	Sand
18X-2	94	139.34	1.5	Sand
18X-2	101	139.41	1	Sand
18X-2	117	139.57	4	Mud
18X-2	128	139.68	1	Silt
18X-2	148.5	139.885	2	Silt
18X-3	18	140.08	5	Silt
18X-3	23	140.13	3	Mud
18X-3	28	140.18	2	Silt
18X-3	32	140.22	3	Silt
18X-3	35	140.25	2.5	Silt
18X-3	44	140.34	1	Sand
18X-3	47	140.37	2	Mud
18X-3	51	140.41	2.5	Silt
19X-1	7	146.57	3	Fine sand
19X-1	14	146.64	1.5	Fine sand
19X-1	28	146.78	2.5	Fine sand
19X-1	32	146.82	3	Fine sand
19X-1	37	146.87	2.5	Fine sand
19X-1	41	146.91	3	Fine sand
19X-1	46	146.96	2	Fine sand
19X-1	54	147.04	3.5	Mud
19X-1	56.5	147.065	0.5	Mud
19X-1	64	147.14	4	Fine sand
19X-1	73	147.23	2	Very fine sand
19X-1	76	147.26	1	Fine sand
19X-1	88	147.38	5	Fine sand
19X-1	96	147.46	3	Fine sand
19X-1	108	147.58	3.5	Very fine sand
19X-1	115	147.65	3	Mud
19X-1	121	147.71	2.5	Very fine sand
19X-1	129	147.79	2.5	Fine sand
19X-1	138	147.88	2.5	Fine sand
19X-2	3	148.03	1	Fine sand
19X-2	8	148.08	1.5	Fine sand
19X-2	15	148.15	1	Very fine sand
19X-2	25	148.25	2.5	Fine sand
19X-2	35	148.35	3	Very fine sand
19X-2	45	148.45	5.5	Fine sand
19X-2	58	148.58	9	Fine sand
19X-2	64	148.64	2	Very fine sand
19X-2	66	148.66	0.5	Mud
19X-2	69	148.69	1.5	Very fine sand
19X-2	73	148.73	2	Fine sand
19X-2	75	148.75	1.5	Very fine sand
19X-2	79	148.79	1	Very fine sand
19X-2	82	148.82	1.5	Very fine sand
19X-2	83	148.83	0.5	Very fine sand
19X-2	96	148.96	2	Very fine sand
19X-2	127	149.27	1.5	Very fine sand
19X-2	139	149.39	2.5	Fine sand
19X-3	3	149.53	2	Fine sand
19X-3	7	149.57	0.5	Mud
19X-3	11	149.61	1	Mud
19X-3	18	149.68	1.5	Very fine sand
19X-3	28	149.78	2	Very fine sand
19X-3	38	149.88	4	Fine sand
19X-3	47	149.97	3	Very fine sand
19X-3	55	150.05	3	Fine sand
19X-3	60	150.1	2	Fine sand
19X-3	62	150.12	0.2	Very fine sand
19X-3	63	150.13	0.5	Very fine sand
19X-3	68	150.18	1.5	Mud
19X-3	82	150.32	2.5	Fine sand
19X-3	89	150.39	1.5	Very fine sand
19X-3	92	150.42	2	Very fine sand
20X-1	10	156.2	5.5	Silt
20X-1	21	156.31	4.5	Mud
20X-1	52	156.62	1.5	Silt
20X-1	56	156.66	2	Silt
20X-1	63	156.73	3.5	Silt
20X-1	72	156.82	5.5	Mud
20X-1	88	156.98	7	Silt
20X-1	115	157.25	7	Mud
20X-1	123	157.33	2.5	Mud
20X-1	139	157.49	0.5	Silt
20X-2	21	157.81	1	Silt
20X-2	74	158.34	7	Silt
20X-2	101	158.61	3	Silt
20X-2	117	158.77	1	Silt
20X-2	132	158.92	1	Silt
20X-3	9	159.19	5.5	Mud
20X-3	17	159.27	1.5	Silt
20X-3	28	159.38	7	Silt
20X-3	33	159.43	3	Silt
20X-3	46	159.56	5	Silt
20X-3	56	159.66	5	Silt
20X-3	70	159.8	3	Silt
20X-3	81	159.91	4	Silt
20X-3	85	159.95	2	Silt
20X-3	90	160	2.5	Mud
20X-3	104	160.14	11	Silt
20X-3	118	160.28	1	Silt
20X-3	127	160.37	4	Silt
20X-3	136	160.46	2	Silt
20X-3	140	160.5	1	Silt
20X-3	142	160.52	1	Mud
20X-3	149	160.59	4	Silt
20X-4	10	160.7	6	Silt

Table T3 (continued).

Core, section	Depth at base of turbidite (cm)	Depth at base of turbidite (mbsf)	Thickness (cm)	Turbidite types
20X-4	19	160.79	4.5	Silt
20X-4	26	160.86	2.5	Silt
20X-4	40	161	2.5	Silt
20X-4	51	161.11	6.5	Silt
20X-CC	5.5	161.175	5.5	Silt
21X-1	11	165.81	2	Fine sand
21X-1	20	165.9	1	Mud
21X-1	22	165.92	0.5	Fine sand
21X-1	25	165.95	0.5	Mud
21X-1	32.5	166.025	2.5	Very fine sand
21X-1	36	166.06	2	Fine sand
21X-1	45	166.15	1.5	Fine sand
21X-1	50	166.2	1.5	Fine sand
21X-1	67	166.37	4.5	Fine sand
21X-1	79	166.49	1.5	Fine sand
21X-1	89	166.59	2	Very fine sand
21X-1	100	166.7	2	Fine sand
21X-1	103	166.73	1	Fine sand
21X-1	111	166.81	4	Fine sand
21X-1	114	166.84	2	Fine sand
21X-1	126	166.96	4	Fine sand
21X-1	133	167.03	2	Very fine sand
21X-1	140	167.1	0.5	Fine sand
21X-2	6	167.26	3.5	Fine sand
21X-2	8	167.28	0.5	Very fine sand
21X-2	22	167.42	4	Fine sand
21X-2	39	167.59	4.5	Fine sand
21X-2	46.5	167.665	4	Fine sand
21X-2	51	167.71	2	Fine sand
21X-2	65	167.85	2	Very fine sand
21X-2	69	167.89	1	Mud
21X-2	73	167.93	1	Fine sand
22X-1	18	175.48	6.5	Fine sand
22X-1	31	175.61	2	Very fine sand
22X-1	38	175.68	2.5	Mud
22X-1	49	175.79	2	Mud
22X-1	53	175.83	1.5	Very fine sand
22X-1	60	175.9	3.5	Mud
22X-1	69	175.99	1.5	Fine sand
22X-1	86	176.16	8.5	Fine sand
22X-1	102	176.32	5.5	Fine sand
22X-1	130	176.6	15	Fine sand
22X-2	2	176.72	2	Mud
22X-2	10	176.8	0.5	Mud
22X-2	12	176.82	0.5	Fine sand
22X-2	18	176.88	1	Fine sand
23X-1	12	185.12	2.5	Fine sand
23X-1	19	185.19	2	Fine sand
23X-1	24	185.24	1	Fine sand
23X-1	32	185.32	4.5	Fine sand
23X-1	39	185.39	3.5	Fine sand
23X-1	45	185.45	3.5	Fine sand
23X-1	56	185.56	3.5	Fine sand
23X-1	72	185.72	4	Fine sand
23X-1	80	185.8	2.5	Fine sand
23X-1	86	185.86	3	Fine sand
23X-1	88	185.88	0.5	Mud
23X-1	98	185.98	3	Fine sand
23X-1	101	186.01	2	Fine sand
23X-1	104	186.04	2.5	Fine sand
23X-1	107	186.07	0.5	Mud
23X-1	117	186.17	3.5	Fine sand
23X-1	120	186.2	1.5	Mud
23X-1	127	186.27	3	Fine sand
23X-1	130	186.3	1	Mud
23X-1	139	186.39	3.5	Fine sand
23X-1	146	186.46	1.5	Fine sand
23X-2	2.5	186.525	3	Fine sand
23X-2	10	186.6	2.5	Fine sand
23X-2	30	186.8	8.5	Fine sand
23X-2	46	186.96	4.5	Fine sand
23X-2	58	187.08	6	Fine sand
23X-2	62	187.12	2	Fine sand
23X-2	69.5	187.195	2	Very fine sand
23X-2	72	187.22	1	Very fine sand
23X-2	75	187.25	1.5	Mud
24X-1	7	194.77	2.5	Fine sand
24X-1	18	194.88	2.5	Fine sand
24X-1	23	194.93	1	Very fine sand
24X-1	31	195.01	0.5	Very fine sand
24X-1	39	195.09	1.5	Very fine sand
24X-1	42	195.12	0.5	Mud
24X-1	48	195.18	1	Mud
24X-1	61	195.31	7	Fine sand
24X-1	68	195.38	2.5	Fine sand
25X-1	2	204.32	0.5	Fine sand
25X-1	9	204.39	1	Fine sand
25X-1	14	204.44	1	Mud
25X-1	16	204.46	0.5	Mud
25X-1	19	204.49	1	Fine sand
25X-1	32	204.62	9.5	Fine sand
25X-1	46	204.76	6	Fine sand
25X-1	54	204.84	4.5	Fine sand
26X-1	8	214.08	1	Fine sand
26X-1	20	214.2	3.5	Fine sand
26X-1	29	214.29	2	Fine sand
26X-1	39	214.39	2.5	Fine sand
26X-1	46	214.46	0.5	Mud
26X-1	63	214.63	4	Mud
26X-1	70	214.7	4.5	Mud
26X-1	77	214.77	1	Mud
26X-1	85	214.85	2	Mud
26X-1	97	214.97	3	Fine sand
26X-1	117	215.17	3.5	Fine sand
26X-1	133	215.33	1	Mud
26X-1	144	215.44	5	Mud
26X-2	8	215.58	2	Fine sand
26X-2	21	215.71	2.5	Very fine sand
26X-2	30	215.8	3	Mud
26X-2	32	215.82	0.5	Mud
26X-2	35.5	215.855	1.5	Mud
26X-2	44	215.94	3	Very fine sand
26X-2	49	215.99	2	Mud
26X-2	61	216.11	5	Mud
26X-3	2	216.52	2	Fine sand
26X-3	26	216.76	5	Fine sand
26X-3	56	217.06	3.5	Fine sand
26X-3	108	217.58	13	Fine sand
26X-3	148	217.98	7	Fine sand
27X-1	12	223.82	3	Fine sand
27X-1	24	223.94	2.5	Fine sand
27X-1	33.5	224.035	2.5	Mud
27X-1	38	224.08	2	Very fine sand
27X-1	50	224.2	2.5	Very fine sand
27X-1	63	224.33	2	Very fine sand
27X-1	72	224.42	1.5	Mud
27X-1	77	224.47	2.5	Mud
27X-1	84	224.54	0.5	Mud
27X-1	87	224.57	0.3	Mud
27X-1	93	224.63	1.5	Very fine sand

Table T3 (continued).

Core, section	Depth at base of turbidite (cm)	Depth at base of turbidite (mbsf)	Thickness (cm)	Turbidite types
27X-1	96	224.66	1.5	Very fine sand
27X-1	98	224.68	0.5	Very fine sand
27X-1	114	224.84	1.5	Very fine sand
27X-1	138	225.08	9	Fine sand
27X-1	142	225.12	1.5	Very fine sand
27X-1	148	225.18	2	Very fine sand
27X-2	6	225.26	3.5	Fine sand
27X-2	16	225.36	1.5	Very fine sand
27X-2	31	225.51	4	Very fine sand
27X-2	34	225.54	0.5	Mud
27X-2	49	225.69	3.5	Fine sand
27X-2	62	225.82	2	Very fine sand
27X-2	80	226	3	Very fine sand
27X-2	88	226.08	6	Very fine sand
27X-2	102	226.22	1.5	Very fine sand
27X-2	111	226.31	7	Very fine sand
27X-2	136	226.56	5	Very fine sand
27X-2	143	226.63	4	Very fine sand
27X-3	11	226.81	0.5	Very fine sand
27X-3	15	226.85	2.5	Very fine sand
28X-1	24	233.54	4	Very fine sand
28X-1	56	233.86	1	Very fine sand
28X-1	63.5	233.935	1	Very fine sand
28X-1	88	234.18	2	Very fine sand
28X-1	11.5	233.415	1.5	Very fine sand
28X-1	123.5	234.535	1.5	Very fine sand
28X-1	145	234.75	7	Very fine sand
28X-2	9	234.89	1.5	Very fine sand
28X-2	19	234.99	0.5	Very fine sand
28X-2	31	235.11	2	Very fine sand
28X-2	36	235.16	3	Very fine sand
28X-2	49.5	235.295	1	Very fine sand
28X-2	62.5	235.425	2	Very fine sand
28X-2	78	235.58	7	Very fine sand
28X-2	86.5	235.665	3.5	Mud
28X-2	96	235.76	4	Very fine sand
28X-2	129	236.09	26	Very fine sand
28X-2	142	236.22	2	Very fine sand
28X-3	8	236.38	8	Very fine sand
28X-3	19	236.49	3	Mud
28X-3	33	236.63	10	Mud
28X-3	51	236.81	7	Very fine sand
28X-3	64.5	236.945	4	Very fine sand
28X-3	88	237.18	9.5	Very fine sand
28X-3	101	237.31	7	Very fine sand
28X-3	108	237.38	4	Very fine sand
28X-3	115	237.45	5	Very fine sand
28X-3	125.5	237.555	2	Very fine sand
29X-1	125	244.15	1.5	Mud
29X-1	140	244.3	6.5	Fine sand
29X-2	9	244.49	10	Fine sand
29X-2	12	244.52	1.5	Very fine sand
29X-2	26	244.66	5	Very fine sand
29X-2	32	244.72	4	Very fine sand
29X-2	36	244.76	2.5	Very fine sand
29X-2	39	244.79	1.5	Very fine sand
29X-2	42	244.82	1.5	Very fine sand
29X-2	79	245.19	4.5	Fine sand
29X-2	90	245.3	4	Fine sand
29X-2	93	245.33	1.5	Mud
29X-2	98	245.38	1.5	Mud
29X-2	101	245.41	1	Mud
29X-2	114	245.54	3	Very fine sand
29X-2	129	245.69	3	Very fine sand
29X-2	144	245.84	2.5	Very fine sand
29X-3	19	246.09	7.5	Fine sand
29X-3	22	246.12	1.5	Fine sand
29X-3	28.5	246.185	2.5	Very fine sand
29X-3	30	246.2	0.3	Very fine sand
29X-3	34	246.24	2	Very fine sand
29X-3	40	246.3	1.5	Very fine sand
29X-3	44.5	246.345	2	Very fine sand
29X-3	47	246.37	1	Very fine sand
29X-3	57	246.47	4.5	Very fine sand
29X-3	70.5	246.605	4	Very fine sand
29X-3	78	246.68	1	Mud
29X-3	95	246.85	2.5	Very fine sand
29X-3	106	246.96	1	Mud
29X-3	117	247.07	2	Very fine sand
29X-3	122	247.12	3.5	Very fine sand
29X-3	133	247.23	3	Mud
29X-3	141	247.31	3.5	Mud
29X-4	6	247.46	0.5	Mud
29X-4	11	247.51	2	Mud
29X-4	18	247.58	2.5	Mud
30X-1	15	252.65	1.5	Fine sand
30X-1	37	252.87	1.5	Very fine sand
30X-1	39	252.89	0.7	Very fine sand
30X-1	44	252.94	1	Very fine sand
30X-1	48	252.98	2	Very fine sand
30X-1	49.5	252.995	0.5	Very fine sand
30X-1	60	253.1	0.5	Mud
30X-1	69	253.19	0.5	Mud
30X-1	82	253.32	3	Mud
30X-1	87	253.37	1	Mud
30X-1	92	253.42	1	Mud
30X-1	106	253.56	2	Very fine sand
30X-1	122	253.72	2.5	Very fine sand
30X-2	2	254.02	5.5	Fine sand
30X-2	10	254.1	2	Mud
30X-2	14	254.14	1	Mud
30X-2	24	254.24	2	Mud
30X-2	40	254.4	1.5	Very fine sand
30X-2	55	254.55	3	Fine sand
30X-2	62	254.62	1.5	Very fine sand
30X-2	100	255	4	Very fine sand
30X-2	113	255.13	2	Very fine sand
30X-2	119	255.19	4.5	Very fine sand
30X-2	125	255.25	1	Very fine sand
30X-2	146	255.46	7	Fine sand
30X-3	8	255.58	1	Very fine sand
30X-3	24	255.74	0.5	Very fine sand
30X-3	29	255.79	3	Fine sand
30X-3	42	255.92	0.5	Very fine sand
30X-3	50	256	1	Very fine sand
30X-3	57	256.07	0.5	Very fine sand
30X-3	58.5	256.085	1	Very fine sand
30X-3	66	256.16	2	Very fine sand
30X-3	82	256.32	3	Fine sand
30X-3	124.5	256.745	3.5	Fine sand
30X-3	137	256.87	2.5	Very fine sand
30X-3	142	256.92	2.5	Very fine sand
30X-3	149	256.99	1.5	Very fine sand
30X-4	5	257.05	0.5	Very fine sand
30X-4	11	257.11	1	Very fine sand
30X-4	23	257.23	2.5	Fine sand
30X-4	32	257.32	1.5	Very fine sand
30X-4	40	257.4	2	Fine sand
30X-4	50	257.5	2	Mud
30X-4	67	257.67	2.5	Fine sand

Table T3 (continued).

Core, section	Depth at base of turbidite (cm)	Depth at base of turbidite (mbsf)	Thickness (cm)	Turbidite types
30X-4	88	257.88	2	Fine sand
30X-4	107	258.07	5	Fine sand
30X-4	124	258.24	3	Fine sand
30X-4	141	258.41	2	Fine sand
30X-4	146	258.46	1	Fine sand
30X-5	10	258.6	2.5	Fine sand
30X-5	27	258.77	2.5	Fine sand
30X-5	46	258.96	1.5	Very fine sand
30X-CC	6	259.07	2.5	Very fine sand
31X-1	8	261.78	3.5	Fine sand
31X-1	10	261.8	1	Fine sand
31X-1	16	261.86	2	Very fine sand
31X-1	27	261.97	3	Fine sand
31X-1	34	262.04	2	Very fine sand
31X-1	42	262.12	3	Very fine sand
31X-1	44.5	262.145	0.5	Very fine sand
31X-1	48	262.18	2	Very fine sand
31X-1	57	262.27	1	Very fine sand
31X-1	72	262.42	2	Very fine sand
31X-1	75	262.45	1.5	Very fine sand
31X-1	82	262.52	2.5	Very fine sand
31X-1	85	262.55	1.5	Very fine sand
31X-1	93	262.63	4	Very fine sand
31X-1	97	262.67	2	Very fine sand
31X-1	106	262.76	2	Very fine sand
31X-1	113	262.83	0.5	Very fine sand
31X-1	124	262.94	1.5	Mud
31X-1	131	263.01	1	Mud
31X-1	140	263.1	2	Very fine sand
31X-2	1	263.21	1.5	Very fine sand
31X-2	6	263.26	1.5	Very fine sand
31X-2	10	263.3	1	Very fine sand
31X-2	18	263.38	1	Very fine sand
31X-2	26	263.46	3	Very fine sand
31X-2	39	263.59	2.5	Very fine sand
31X-2	41	263.61	1.5	Very fine sand
31X-2	44	263.64	1.5	Very fine sand
31X-2	45	263.65	0.3	Very fine sand
31X-2	46	263.66	0.3	Very fine sand
31X-2	46.5	263.665	0.3	Very fine sand
31X-2	51	263.71	1.5	Very fine sand
31X-2	65.5	263.855	1	Very fine sand
31X-2	68.5	263.885	1.5	Very fine sand
31X-2	78	263.98	1	Very fine sand
31X-2	86	264.06	2	Mud
31X-2	89	264.09	1	Mud
31X-2	100	264.2	2	Very fine sand
31X-2	106	264.26	2	Mud
31X-2	112	264.32	3	Very fine sand
31X-2	117.5	264.375	0.5	Very fine sand
31X-2	120	264.4	0.5	Very fine sand
31X-2	124	264.44	1	Very fine sand
31X-2	128	264.48	2	Very fine sand
31X-2	130.5	264.505	0.2	Mud
31X-2	132	264.52	0.5	Mud
31X-2	139.5	264.595	2.5	Mud
31X-2	146	264.66	1.5	Very fine sand
31X-3	2	264.72	1.5	Very fine sand
31X-3	7	264.77	0.5	Very fine sand
31X-3	9	264.79	0.5	Very fine sand
31X-3	10.5	264.805	0.5	Very fine sand
31X-3	17	264.87	3	Very fine sand
31X-3	20	264.9	1.5	Very fine sand
31X-3	22	264.92	0.5	Very fine sand
31X-3	27	264.97	1	Mud
31X-3	30	265	1	Very fine sand
31X-3	34	265.04	1.5	Very fine sand
31X-3	42	265.12	2.5	Fine sand
31X-3	49	265.19	1	Very fine sand
31X-3	51	265.21	0.5	Very fine sand
31X-3	60	265.3	1	Mud
31X-3	72	265.42	1.5	Very fine sand
31X-3	82	265.52	1	Very fine sand
31X-3	102	265.72	1	Very fine sand
31X-3	107	265.77	0.5	Very fine sand
31X-3	117	265.87	1	Mud
31X-3	128	265.98	0.5	Very fine sand
31X-3	139	266.09	1	Mud
31X-CC	12	266.3	1.5	Very fine sand
32X-1	4	271.34	1	Very fine sand
32X-1	15	271.45	1	Very fine sand
32X-1	30	271.6	1	Very fine sand
32X-1	35	271.65	1	Very fine sand
32X-1	96	272.26	1	Fine sand
32X-1	115	272.45	1	Very fine sand
32X-1	122	272.52	0.3	Very fine sand
32X-1	123	272.53	0.5	Very fine sand
32X-1	127	272.57	0.5	Mud
32X-1	130	272.6	0.5	Very fine sand
32X-2	2	272.82	0.3	Very fine sand
32X-2	10	272.9	1.5	Very fine sand
32X-2	15	272.95	0.5	Very fine sand
32X-2	17	272.97	0.2	Very fine sand
32X-2	27	273.07	0.5	Very fine sand
32X-2	32	273.12	0.5	Very fine sand
32X-2	50	273.3	0.3	Very fine sand
32X-2	53	273.33	1	Very fine sand
32X-2	58	273.38	1.5	Very fine sand
32X-2	76	273.56	3	Very fine sand
32X-CC	5	273.64	0.3	Very fine sand
33X-1	17.5	280.875	0.7	Fine sand
33X-1	35	281.05	0.5	Fine sand
33X-1	53	281.23	3	Sand
33X-1	58	281.28	2.5	Fine sand
33X-1	65	281.35	1	Fine sand
33X-1	73	281.43	1.5	Fine sand
33X-1	75	281.45	1.6	Sand
33X-1	79	281.49	1.1	Fine sand
33X-1	91.5	281.615	1.9	Sand
33X-1	94.5	281.645	1.3	Sand
33X-1	98.5	281.685	1	Sand
33X-1	101	281.71	1.4	Sand
33X-1	111.5	281.815	1.7	Fine sand
33X-1	116	281.86	1.3	Fine sand
33X-1	119.5	281.895	0.4	Fine sand
33X-1	135	282.05	1.5	Sand
33X-1	140	282.1	1.5	Fine sand
33X-1	149.5	282.195	1	Fine sand
33X-2	15	282.35	2	Fine sand
33X-2	20.5	282.405	0.5	Fine sand
33X-2	27.5	282.475	1.4	Mud
33X-2	35	282.55	1.5	Sand
33X-2	50	282.7	3.5	Sand
33X-2	58	282.78	1.1	Sand
33X-2	78	282.98	2.0	Fine sand
33X-2	95	283.15	2.4	Fine sand
33X-2	110	283.3	0.5	Fine sand
33X-2	123.5	283.435	0.8	Mud
33X-2	127.5	283.475	0.2	Mud
33X-2	147	283.67	2	Fine sand

Table T3 (continued).

Core, section	Depth at base of turbidite (cm)	Depth at base of turbidite (mbsf)	Thickness (cm)	Turbidite types
33X-3	3.5	283.735	2.5	Fine sand
33X-3	24	283.94	1	Fine sand
33X-3	25	283.95	0.3	Fine sand
33X-3	34	284.04	1	Fine sand
33X-3	78	284.48	1	Fine sand
33X-3	118	284.88	1	Fine sand
33X-3	132.5	285.025	1.5	Fine sand
33X-3	148.5	285.185	1.7	Mud
33X-4	50	285.7	1.2	Fine sand
33X-4	88	286.08	1	Fine sand
33X-4	109.5	286.295	2.5	Sand
33X-4	131.5	286.515	1	Fine sand
33X-4	132.5	286.525	0.5	Fine sand
33X-4	136	286.56	2	Fine sand
33X-4	149	286.69	1.5	Fine sand
33X-4	150	286.7	0.5	Fine sand
33X-5	4.5	286.745	1.5	Fine sand
33X-5	11.5	286.815	3	Fine sand
33X-5	21.5	286.915	1.5	Fine sand
33X-5	37	287.07	1.4	Fine sand
33X-5	49	287.19	1	Fine sand
33X-5	58	287.28	2	Fine sand
33X-5	69	287.39	2.5	Fine sand
33X-5	79	287.49	1	Fine sand
33X-5	88	287.58	1	Fine sand
33X-5	91	287.61	1	Fine sand
33X-5	97	287.67	1.5	Fine sand
33X-5	107.5	287.775	3	Sand
33X-5	113.5	287.835	2	Sand
33X-5	119.5	287.895	1	Sand
34X-1	10	290.5	0.3	Fine sand
34X-1	13.5	290.535	1	Fine sand
34X-1	28.5	290.685	0.5	Fine sand
34X-1	34	290.74	0.7	Fine sand
34X-1	38.5	290.785	0.5	Mud
34X-1	52.5	290.925	1.5	Fine sand
34X-1	62	291.02	1	Very fine sand
34X-1	72.5	291.125	1	Very fine sand
34X-1	76	291.16	1	Very fine sand
34X-1	87.5	291.275	2	Fine sand
34X-1	95.5	291.355	1	Fine sand
34X-1	101.5	291.415	1	Sand
34X-2	44	292.34	4	Sand
34X-2	59.5	292.495	1	Sand
34X-2	95	292.85	3	Sand
34X-2	113.5	293.035	0.5	Fine sand
34X-2	120.5	293.105	1	Fine sand
34X-2	138.5	293.285	2	Mud
34X-2	142.5	293.325	0.5	Mud
34X-3	23	293.63	1.5	Sand
34X-3	29.5	293.695	1	Mud
34X-3	39	293.79	1.5	Fine sand
34X-3	46.5	293.865	2	Fine sand
34X-3	94	294.34	5	Very fine sand
34X-3	110	294.5	0.8	Fine sand
34X-3	121	294.61	1.5	Fine sand
34X-3	145	294.85	0.5	Mud
34X-4	13.5	295.035	0.5	Fine sand
34X-4	27.5	295.175	1	Fine sand
34X-4	35	295.25	1.5	Very fine sand
34X-4	46	295.36	4	Fine sand
34X-4	49	295.39	2	Very fine sand
34X-4	51.5	295.415	1.5	Very fine sand
34X-4	54.5	295.445	2.5	Sand
34X-4	56	295.46	0.5	Fine sand
34X-4	60	295.5	2.5	Fine sand
34X-4	62.5	295.525	1	Fine sand
34X-4	67	295.57	3	Fine sand
34X-4	72	295.62	3	Fine sand
34X-4	74	295.64	1.5	Very fine sand
34X-4	79.5	295.695	1.5	Fine sand
34X-4	82.5	295.725	1	Fine sand
34X-4	89	295.79	0.5	Fine sand
34X-4	90	295.8	0.5	Fine sand
34X-4	103.5	295.935	3.5	Fine sand
34X-4	107.5	295.975	2.5	Fine sand
34X-4	120	296.1	3	Fine sand
34X-4	126	296.16	2. 5	Fine sand
34X-4	131	296.21	0.3	Fine sand
34X-4	132	296.22	0.4	Fine sand
34X-4	135	296.25	2	Fine sand
34X-4	141.5	296.315	0.3	Fine sand
34X-4	143	296.33	1.5	Fine sand
34X-5	1.5	296.415	2	Fine sand
34X-5	6.5	296.465	0.5	Fine sand
34X-5	12	296.52	0.5	Mud
34X-5	16.5	296.565	3	Fine sand
34X-5	22.5	296.625	0.8	Fine sand
34X-5	24	296.64	0.5	Fine sand
34X-5	25.5	296.655	0.3	Mud
34X-5	31	296.71	1	Mud
34X-5	43	296.83	1.5	Fine sand
34X-5	54.5	296.945	1.5	Fine sand
34X-5	62.5	297.025	2.5	Fine sand
34X-5	65	297.05	0.8	Fine sand
34X-5	72	297.12	0.5	Fine sand
34X-5	74	297.14	1	Fine sand
34X-5	75	297.15	0.5	Very fine sand
34X-5	76.5	297.165	1	Fine sand
34X-5	78	297.18	0.3	Mud
34X-5	79. 5	297.195	0.3	Very fine sand
34X-5	83	297.23	0.8	Fine sand
34X-5	87	297.27	3	Fine sand
34X-5	89.5	297.295	1	Fine sand
34X-5	93	297.33	3	Fine sand
34X-5	97	297.37	1.5	Fine sand
34X-5	105.5	297.455	0.5	Fine sand
34X-5	109.5	297.495	1.5	Fine sand
34X-5	112	297.52	0.5	Mud
34X-5	116.5	297.565	1	Fine sand
34X-5	119	297.59	1	Fine sand
34X-5	123	297.63	2	Fine sand
35X-1	4.5	300.045	0.6	Fine sand
35X-1	40.5	300.405	0.5	Fine sand
35X-1	58.5	300.585	0.5	Very fine sand
35X-1	64	300.64	1.2	Fine sand
35X-1	70	300.7	1.4	Fine sand
35X-1	76	300.76	1.4	Mud
35X-1	91.5	300.915	0.9	Fine sand
35X-1	126	301.26	1.5	Very fine sand
35X-2	2	301.52	0.7	Very fine sand
35X-2	14.5	301.645	0.9	Fine sand
35X-2	30.5	301.805	1.6	Mud
35X-2	39	301.89	1	Mud
35X-2	76	302.26	1	Very fine sand
35X-2	82	302.32	1.2	Very fine sand
35X-2	104	302.54	0.5	Fine sand
35X-2	114	302.64	0.8	Very fine sand
35X-2	144	302.94	1.1	Fine sand
35X-3	1	303.01	1	Sand

Table T3 (continued).

Core, section	Depth at base of turbidite (cm)	Depth at base of turbidite (mbsf)	Thickness (cm)	Turbidite types
35X-3	7	303.07	0.6	Fine sand
35X-3	17.5	303.175	0.6	Fine sand
35X-3	24	303.24	2	Fine sand
35X-3	34	303.34	0.6	Fine sand
35X-3	44	303.44	1.2	Fine sand
35X-3	50	303.5	1	Fine sand
35X-3	54	303.54	0.6	Very fine sand
35X-3	55.5	303.555	1	Fine sand
35X-3	58	303.58	1	Fine sand
35X-3	60	303.6	1	Fine sand
35X-3	63	303.63	1	Fine sand
35X-3	68.5	303.685	1	Fine sand
35X-3	70	303.7	0.6	Fine sand
35X-3	86	303.86	1.5	Very fine sand
35X-3	101.5	304.015	1	Very fine sand
35X-3	114.5	304.145	1.5	Fine sand
35X-3	137	304.37	1	Very fine sand
35X-4	21.5	304.715	1	Very fine sand
35X-4	27.5	304.775	1	Very fine sand
35X-4	46	304.96	1.2	Very fine sand
35X-4	54	305.04	1.3	Very fine sand
35X-4	64.5	305.145	1	Very fine sand
35X-4	76	305.26	2	Very fine sand
35X-4	81	305.31	1	Very fine sand
35X-4	87.5	305.375	0.2	Very fine sand
35X-4	88.5	305.385	0.7	Very fine sand
35X-4	95	305.45	1.2	Very fine sand
35X-4	99.5	305.495	0.3	Very fine sand
35X-4	100.5	305.505	0.4	Very fine sand
35X-4	106	305.56	1	Very fine sand
35X-4	117	305.67	1. 1	Very fine sand
35X-4	121	305.71	1.7	Very fine sand
35X-4	127	305.77	1	Very fine sand
35X-4	135	305.85	0.8	Very fine sand
35X-5	5	306.05	4.5	Fine sand
35X-5	18.5	306.185	1.5	Fine sand
35X-5	42	306.42	1	Fine sand
35X-5	43	306.43	0.5	Very fine sand
35X-5	46	306.46	0.6	Very fine sand
35X-5	56	306.56	1	Fine sand
35X-5	61	306.61	0.8	Fine sand
35X-5	64.5	306.645	1.5	Fine sand
35X-5	69.5	306.695	1.3	Very fine sand
35X-5	70.5	306.705	0.5	Very fine sand
35X-5	74	306.74	0.6	Mud
35X-5	80	306.8	1.5	Mud
35X-5	88	306.88	1	Fine sand
35X-5	92	306.92	1	Very fine sand
35X-5	101	307.01	0.7	Very fine sand
35X-5	103	307.03	1.6	Fine sand
35X-5	109	307.09	1.3	Fine sand
35X-5	116	307.16	1	Sand
35X-5	120	307.2	1.5	Sand
35X-5	127.5	307.275	0.5	Sand
35X-5	128.5	307.285	0.3	Sand
35X-5	134.5	307.345	1	Sand
35X-5	143	307.43	0.6	Sand
35X-5	148	307.48	1	Sand
35X-6	7	307.57	1.4	Very fine sand
35X-6	13	307.63	1.3	Very fine sand
35X-6	15	307.65	1.5	Fine sand
36X-1	37.5	309.975	1	Fine sand
36X-1	49	310.09	1.5	Fine sand
36X-1	60	310.2	1	Fine sand
36X-1	68.5	310.285	1.5	Fine sand
36X-1	74	310.34	2	Fine sand
36X-2	18	311.28	2	Fine sand
36X-2	96	312.06	1.5	Fine sand
36X-2	114	312.24	2	Fine sand
36X-2	126	312.36	2	Fine sand
36X-2	130	312.4	1.5	Fine sand
36X-2	136.5	312.465	1	Fine sand
36X-3	3	312.63	1	Fine sand
36X-3	8	312.68	2	Fine sand
36X-3	17	312.77	2	Fine sand
36X-3	23	312.83	1	Fine sand
36X-3	28	312.88	0.3	Fine sand
36X-3	45	313.05	1.5	Fine sand
36X-3	55	313.15	1.5	Fine sand
36X-3	73	313.33	0.5	Fine sand
36X-3	78	313.38	1	Fine sand
36X-3	93.5	313.535	0.5	Fine sand
36X-3	115	313.75	1	Fine sand
36X-3	119	313.79	1.5	Fine sand
36X-3	130.5	313.905	0.3	Very fine sand
36X-3	140	314	1	Very fine sand
36X-3	145	314.05	1	Fine sand
36X-4	9	314.19	1	Very fine sand
36X-4	27	314.37	1	Fine sand
36X-4	29	314.39	1.5	Fine sand
36X-4	42.5	314.525	1	Fine sand
36X-4	49.5	314.595	0.5	Very fine sand
36X-4	56	314.66	2	Very fine sand
36X-4	60	314.7	1.5	Mud
36X-4	65.5	314.755	0.8	Very fine sand
36X-4	68	314.78	2	Fine sand
36X-4	69	314.79	0.5	Fine sand
36X-4	75.5	314.855	1.5	Very fine sand
36X-4	83.5	314.935	1	Fine sand
36X-4	101.5	315.115	0.5	Fine sand
36X-4	104.5	315.145	0.5	Fine sand
36X-4	107	315.17	1.5	Fine sand
36X-4	121.5	315.315	1.5	Fine sand
36X-4	126	315.36	1	Fine sand
36X-4	127	315.37	0.8	Fine sand
36X-4	134.5	315.445	0.5	Very fine sand
36X-4	136.5	315.465	0.5	Very fine sand
36X-4	138	315.48	0.5	Very fine sand
36X-4	141	315.51	1	Very fine sand
36X-4	145	315.55	0.8	Very fine sand
36X-4	148.5	315.585	0.8	Very fine sand
36X-4	150.5	315.605	0.8	Very fine sand
36X-5	5	315.65	0.3	Very fine sand
36X-5	13	315.73	1.5	Very fine sand
36X-5	29	315.89	4.5	Fine sand
36X-5	34	315.94	1	Fine sand
36X-5	36	315.96	0.3	Fine sand
36X-5	41.5	316.015	1	Fine sand
36X-5	51	316.11	0.3	Very fine sand
36X-5	58.5	316.185	0.3	Very fine sand
36X-5	106	316.66	1.5	Very fine sand
36X-5	126	316.86	0.5	Mud
36X-5	128	316.88	0.5	Very fine sand
36X-6	31	317.41	1.5	Fine sand
36X-6	40	317.5	3.5	Fine sand
36X-6	50	317.6	0.5	Fine sand
36X-6	54	317.64	0.5	Fine sand
36X-6	63	317.73	2.5	Fine sand
36X-6	69	317.79	1	Very fine sand
36X-6	75	317.85	1	Fine sand

Table T3 (continued).

Core, section	Depth at base of turbidite (cm)	Depth at base of turbidite (mbsf)	Thickness (cm)	Turbidite types
36X-6	81	317.91	1.5	Fine sand
36X-6	89.5	317.995	3	Fine sand
37X-1	5.5	319.355	1	Very fine sand
37X-1	9.5	319.395	0.5	Fine sand
37X-1	19.5	319.495	1	Very fine sand
37X-1	32	319.62	1	Very fine sand
37X-1	35	319.65	1	Fine sand
37X-1	48	319.78	0.7	Fine sand
37X-1	66	319.96	0.5	Fine sand
37X-1	113	320.43	0.5	Fine sand
37X-1	123.5	320.535	0.7	Very fine sand
37X-1	137.5	320.675	0.5	Very fine sand
37X-2	18	320.98	0.5	Fine sand
37X-2	19	320.99	0.7	Fine sand
37X-2	22	321.02	0.7	Fine sand
37X-2	67.5	321.475	0.6	Very fine sand
37X-2	73	321.53	1	Very fine sand
37X-2	77.5	321.575	0.4	Very fine sand
37X-2	89	321.69	1.5	Fine sand
37X-2	101.5	321.815	0.8	Very fine sand
37X-2	107.5	321.875	1.5	Fine sand
37X-2	115	321.95	1	Very fine sand
37X-2	130	322.1	2	Very fine sand
37X-2	142.5	322.225	0.7	Very fine sand
37X-2	143.5	322.235	0.6	Very fine sand
37X-2	149	322.29	2	Very fine sand
37X-3	12	322.42	0.5	Fine sand
37X-3	17.5	322.475	0.6	Very fine sand
37X-3	20.5	322.505	1	Fine sand
37X-3	35.5	322.655	0.7	Very fine sand
37X-3	45.5	322.755	0.7	Very fine sand
37X-3	47.5	322.775	0.6	Very fine sand
37X-3	60	322.9	1.5	Very fine sand
37X-3	69	322.99	0.7	Very fine sand
37X-3	83.5	323.135	1.7	Very fine sand
37X-3	112	323.42	1	Very fine sand
37X-4	2.5	323.825	0.5	Very fine sand
37X-4	54	324.34	1.2	Very fine sand
37X-4	67	324.47	1	Very fine sand
37X-4	79.5	324.595	76	Very fine sand
37X-4	83.5	324.635	1.6	Very fine sand
37X-4	90	324.7	1	Very fine sand
37X-4	94	324.74	1	Very fine sand
37X-4	135	325.15	1.2	Mud
37X-5	1	325.31	1	Fine sand
37X-5	6	325.36	1	Very fine sand
37X-5	14	325.44	1	Very fine sand
37X-5	22	325.52	0.6	Fine sand
37X-5	45	325.75	0.7	Fine sand
37X-5	71	326.01	0.5	Very fine sand
37X-5	82	326.12	0.2	Very fine sand
37X-5	90.5	326.205	1	Very fine sand
37X-5	100	326.3	0.6	Fine sand
37X-5	129	326.59	1.6	Fine sand
37X-5	131	326.61	1	Fine sand
37X-5	143	326.73	1.2	Very fine sand
37X-6	1	326.81	1	Fine sand
37X-6	9.5	326.895		Mud
37X-6	22	327.02		Mud
37X-6	29.5	327.095		Fine sand
37X-6	43	327.23	0.5	Very fine sand
37X-6	47	327.27	3	Fine sand
37X-6	53	327.33	0.3	Very fine sand
37X-6	54.5	327.345	0.7	Very fine sand
37X-6	57.5	327.375	0.5	Very fine sand
37X-6	59.5	327.395	0.2	Very fine sand
37X-6	61.5	327.415	1	Very fine sand
37X-6	64	327.44	1	Very fine sand
37X-6	68.5	327.485	0.8	Very fine sand
37X-6	72.5	327.525	1.6	Very fine sand
37X-6	76.5	327.565	1.1	Very fine sand
37X-6	81	327.61	0.5	Very fine sand
37X-6	82	327.62	0.5	Very fine sand
37X-6	84	327.64	0.5	Very fine sand
37X-6	89	327.69	0.5	Very fine sand
37X-6	94.5	327.745	1.6	Fine sand
37X-6	97.5	327.775	1.2	Fine sand
37X-6	104	327.84	0.7	Very fine sand
37X-6	122	328.02	1.5	Very fine sand
37X-6	127.5	328.075	2.2	Ash
37X-6	130.5	328.105	1.4	Very fine sand
37X-6	139	328.19	0.8	Very fine sand
38X-1	8.5	328.985	1.5	Fine sand
38X-1	14	329.04	1.5	Fine sand
38X-1	19.5	329.095	1	Very fine sand
38X-1	29.5	329.195	0.5	Very fine sand
38X-1	35	329.25	0.8	Very fine sand
38X-1	50	329.4	1.5	Very fine sand
38X-1	53.5	329.435	1	Very fine sand
38X-1	59.5	329.495	3	Very fine sand
38X-1	71	329.61	1.1	Very fine sand
38X-1	80	329.7	1.5	Very fine sand
38X-1	94.5	329.845	1	Very fine sand
38X-1	97.5	329.875	0.5	Very fine sand
38X-1	109	329.99	1.5	Very fine sand
38X-2	1	330.41	1	Fine sand
38X-2	10	330.5	1.5	Very fine sand
38X-2	16.5	330.565	4	Very fine sand
38X-2	20.5	330.605	1	Very fine sand
38X-2	23	330.63	1	Fine sand
38X-2	24.5	330.645	0.8	Fine sand
38X-2	26.5	330.665	0.7	Very fine sand
38X-2	30	330.7	3	Very fine sand
38X-2	31.5	330.715	1	Very fine sand
38X-2	34	330.74	1.2	Very fine sand
38X-2	34.5	330.745	0.3	Very fine sand
38X-2	36.5	330.765	1	Very fine sand
38X-2	38	330.78	0.5	Very fine sand
38X-2	40.5	330.805	0.5	Very fine sand
38X-2	41.5	330.815	0.7	Very fine sand
38X-2	43	330.83	0.5	Very fine sand
38X-2	48	330.88	1.5	Very fine sand
38X-2	52	330.92	0.3	Very fine sand
38X-2	54	330.94	1	Very fine sand
38X-2	55	330.95	0.5	Very fine sand
38X-2	56	330.96	0.8	Very fine sand
38X-2	57	330.97	0.3	Mud
38X-2	58	330.98	0.5	Very fine sand
38X-2	60.5	331.005	1.5	Very fine sand
38X-2	62	331.02	0.8	Very fine sand
38X-2	64	331.04	0.8	Very fine sand
38X-2	65	331.05	1	Very fine sand
38X-2	71	331.11	3	Fine sand
38X-2	76.5	331.165	2.5	Fine sand
38X-2	81.5	331.215	0.8	Very fine sand
38X-2	83.5	331.235	1	Very fine sand
38X-2	86	331.26	1	Very fine sand
38X-2	89	331.29	1	Very fine sand
38X-2	98	331.38	2.5	Very fine sand
38X-2	101	331.41	1.5	Very fine sand

Table T3 (continued).

Core, section	Depth at base of turbidite (cm)	Depth at base of turbidite (mbsf)	Thickness (cm)	Turbidite types
38X-2	103.5	331.435	0.5	Very fine sand
38X-2	113	331.53	2	Very fine sand
38X-2	120	331.6	1.5	Very fine sand
38X-2	121.5	331.615	0.8	Very fine sand
38X-2	123.5	331.635	1	Very fine sand
38X-2	133	331.73	1.1	Very fine sand
38X-2	134.5	331.745	0.5	Very fine sand
38X-2	136.5	331.765	1	Very fine sand
38X-2	138	331.78	1	Very fine sand
38X-3	2.5	331.925	1.5	Fine sand
38X-3	10.5	332.005	0.3	Very fine sand
38X-3	16.5	332.065	1.5	Very fine sand
38X-3	21	332.11	1	Very fine sand
38X-3	32	332.22	1	Very fine sand
38X-3	37	332.27	1.5	Very fine sand
38X-3	41	332.31	1.5	Very fine sand
38X-3	47.5	332.375	1.5	Very fine sand
38X-3	53	332.43	2	Very fine sand
38X-3	55	332.45	0.8	Very fine sand
38X-3	61	332.51	3	Very fine sand
38X-3	62.5	332.525	0.3	Very fine sand
38X-3	65	332.55	2	Very fine sand
38X-3	72.5	332.625	2	Very fine sand
38X-3	73.5	332.635	0.5	Very fine sand
38X-3	75.5	332.655	1	Very fine sand
38X-3	77.5	332.675	0.8	Very fine sand
38X-3	78.5	332.685	0.8	Very fine sand
38X-3	80.5	332.705	1	Very fine sand
38X-3	81.5	332.715	1.7	Very fine sand
38X-3	93	332.83	1	Fine sand
38X-3	97	332.87	2.5	Fine sand
38X-3	102	332.92	2.5	Fine sand
38X-3	110.5	333.005	1	Very fine sand
38X-3	118	333.08	1.5	Very fine sand
38X-3	120.5	333.105	1	Very fine sand
38X-3	121.5	333.115	1.5	Very fine sand
38X-3	126.5	333.165	1	Very fine sand
38X-3	132	333.22	1	Fine sand
38X-3	136.5	333.265	1	Fine sand
39X-1	10.5	338.605	1.5	Very fine sand
39X-1	32	338.82	1.3	Fine sand
39X-1	68	339.18	1.5	Very fine sand
39X-1	80	339.3	1.5	Fine sand
39X-1	83	339.33	1.5	Fine sand
39X-1	87.5	339.375	1.3	Fine sand
39X-1	97	339.47	1	Very fine sand
39X-1	105.5	339.555	0.3	Very fine sand
39X-1	106.5	339.565	0.5	Fine sand
39X-1	127	339.77	0.6	Very fine sand
39X-1	140	339.9	1.8	Very fine sand
39X-2	1	340.01	2	Fine sand
39X-2	7.5	340.075	0.5	Fine sand
39X-2	23	340.23	0.9	Very fine sand
39X-2	24	340.24	0.5	Very fine sand
39X-2	26	340.26	1.3	Fine sand
39X-2	27.5	340.275	1	Very fine sand
39X-2	31.5	340.315	0.7	Very fine sand
39X-2	36	340.36	1	Very fine sand
39X-2	39.5	340.395	1.1	Very fine sand
39X-2	41.5	340.415	0.2	Mud
39X-2	43.5	340.435	0.4	Mud
39X-2	50	340.5	1.9	Very fine sand
39X-2	54	340.54	1.5	Fine sand
39X-2	58	340.58	1.2	Fine sand
39X-2	63	340.63	1	Very fine sand
39X-2	66	340.66	0.6	Mud
39X-2	70.5	340.705	1	Very fine sand
39X-2	72	340.72	1.1	Mud
39X-2	76	340.76	0.5	Very fine sand
39X-2	79	340.79	1.6	Fine sand
39X-2	87.5	340.875	1.6	Fine sand
39X-2	107.5	341.075	1.5	Very fine sand
39X-2	145	341.45	2	Fine sand
39X-3	4	341.54	1.3	Fine sand
39X-3	5.5	341.555	1	Fine sand
39X-3	16	341.66	1	Very fine sand
39X-3	20	341.7	1.1	Fine sand
39X-3	45.5	341.955	1.2	Very fine sand
39X-3	52.5	342.025	0.5	Fine sand
39X-3	53.5	342.035	0.6	Fine sand
39X-3	62.5	342.125	1	Fine sand
39X-3	73	342.23	1.8	Fine sand
39X-3	80	342.3	4.5	Sand
39X-3	86	342.36	2.1	Fine sand
39X-3	91.5	342.415	2	Fine sand
39X-3	95.5	342.455	1.3	Very fine sand
39X-3	100	342.5	2	Very fine sand
39X-3	102	342.52	0.6	Very fine sand
39X-3	103	342.53	1.4	Very fine sand
39X-3	105	342.55	0.5	Fine sand
39X-3	108.5	342.585	1	Very fine sand
39X-3	110	342.6	1	Very fine sand
39X-3	114	342.64	0.9	Very fine sand
39X-3	118	342.68	1.5	Fine sand
39X-3	124.5	342.745	0.4	Fine sand
39X-3	128	342.78	0.4	Fine sand
39X-3	132	342.82	1	Very fine sand
39X-3	138	342.88	1.6	Fine sand
39X-3	143	342.93	1.8	Fine sand
39X-4	6	343.06	1	Very fine sand
39X-4	15	343.15	3.5	Fine sand
39X-4	18	343.18	1	Very fine sand
39X-4	20	343.2	1.7	Fine sand
39X-4	22	343.22	1.2	Very fine sand
39X-4	26.5	343.265	1.3	Fine sand
39X-4	30	343.3	1.5	Fine sand
39X-4	39.5	343.395	2	Fine sand
39X-4	44.5	343.445	0.5	Fine sand
39X-4	50	343.5	1.6	Fine sand
39X-4	52.5	343.525	1.5	Fine sand
40X-1	28	348.48	0.8	Very fine sand
40X-1	41	348.61	0.5	Very fine sand
40X-1	52	348.72	5	Fine sand
40X-1	57	348.77	1	Very fine sand
40X-1	62.5	348.825	1.5	Very fine sand
40X-1	73.5	348.935	3	Fine sand
40X-1	82	349.02	2.5	Very fine sand
40X-1	85	349.05	1	Very fine sand
40X-1	88	349.08	0.8	Very fine sand
40X-1	91	349.11	1.5	Very fine sand
40X-1	95	349.15	1.2	Very fine sand
40X-1	101	349.21	3	Very fine sand
40X-1	110	349.3	1.5	Very fine sand
40X-1	118	349.38	0.5	Mud
40X-1	127	349.47	1.5	Very fine sand
40X-1	131	349.51	2	Very fine sand
40X-1	135	349.55	1.5	Very fine sand
40X-1	141	349.61	3	Very fine sand
40X-1	142.5	349.625	0.5	Very fine sand
40X-1	144.5	349.645	1	Very fine sand

Table T3 (continued).

Core, section	Depth at base of turbidite (cm)	Depth at base of turbidite (mbsf)	Thickness (cm)	Turbidite types
40X-1	146.5	349.665	1	Very fine sand
40X-1	149	349.69	1	Very fine sand
40X-1	149.5	349.695	0.5	Very fine sand
40X-2	3	349.73	1.6	Very fine sand
40X-2	6.5	349.765	0.5	Very fine sand
40X-2	12	349.82	2.5	Very fine sand
40X-2	18	349.88	2	Fine sand
40X-2	26	349.96	1.5	Very fine sand
40X-2	28	349.98	0.5	Very fine sand
40X-2	30.5	350.005	1	Very fine sand
40X-2	37	350.07	3	Very fine sand
40X-2	39	350.09	1.5	Very fine sand
40X-2	40.5	350.105	0.5	Very fine sand
40X-2	42.5	350.125	1	Very fine sand
40X-2	43.5	350.135	0.7	Very fine sand
40X-2	47.5	350.175	3	Very fine sand
40X-2	48.5	350.185	0.2	Mud
40X-2	50.5	350.205	1.5	Very fine sand
40X-2	52.5	350.225	1.5	Very fine sand
40X-2	56	350.26	1.5	Very fine sand
40X-2	57.5	350.275	0.6	Very fine sand
40X-2	59	350.29	1	Very fine sand
40X-2	61	350.31	1	Very fine sand
40X-2	63	350.33	1.5	Very fine sand
40X-2	64.5	350.345	0.5	Very fine sand
40X-2	69.5	350.395	4	Very fine sand
40X-2	77.5	350.475	2	Very fine sand
40X-2	82	350.52	0.3	Very fine sand
40X-2	84	350.54	0.4	Very fine sand
40X-2	87	350.57	1	Very fine sand
40X-2	91.5	350.615	1	Very fine sand
40X-2	106.5	350.765	1	Very fine sand
40X-2	114	350.84	0.3	Very fine sand
40X-2	121.5	350.915	2.5	Very fine sand
40X-2	131	351.01	4	Very fine sand
40X-2	145	351.15	1.5	Very fine sand
40X-2	143	351.13	1.5	Very fine sand
40X-2	146.5	351.165	1.5	Very fine sand
40X-3	3	351.23	1.5	Very fine sand
40X-3	10.5	351.305	1	Very fine sand
41X-1	65	358.55	1.5	Very fine sand
41X-1	80	358.7	1	Very fine sand
41X-1	106	358.96	6	Fine sand
41X-1	113	359.03	1.5	Fine sand
41X-1	116.5	359.065	1.5	Fine sand
41X-1	121	359.11	1.5	Fine sand
41X-1	137.5	359.275	1.5	Very fine sand
41X-2	29	359.69	1.5	Very fine sand
42X-1	23.5	367.735	0.5	Very fine sand
42X-1	32	367.82	0.7	Fine sand
42X-1	35	367.85	1	Fine sand
42X-1	86	368.36	5.5	Fine sand
42X-1	108	368.58	3	Sand
42X-1	133	368.83	2	Sand
42X-1	145	368.95	0.5	Very fine sand
42X-2	23.5	369.235	2.5	Very fine sand
42X-2	26	369.26	2	Very fine sand
42X-2	29	369.29	1	Very fine sand
42X-2	30	369.3	0.7	Very fine sand
42X-2	35	369.35	0.5	Very fine sand
42X-2	43	369.43	2.3	Very fine sand
42X-2	64	369.64	1	Very fine sand
42X-2	72.5	369.725	2	Very fine sand
42X-2	79	369.79	3	Fine sand
42X-2	88.5	369.885	1.5	Fine sand
42X-2	97.5	369.975	5	Fine sand
42X-2	116	370.16	3	Fine sand
42X-2	134	370.34	1.5	Fine sand
42X-3	8	370.58	1	Very fine sand
42X-3	24	370.74	2	Very fine sand
42X-3	56	371.06	2.5	Fine sand
42X-3	92	371.42	4	Fine sand
42X-3	123.5	371.735	5	Fine sand

Table T4. Identification and abundance of nannofossils observed at Site 1122 (**See table note.** Continued on next three pages.)

Core, section, interval (cm)	Depth (mbsf)	Preservation	Group abundance	*Braarudosphaera bigelowii*	*Calcidiscus leptoporus*	*Calcidiscus macintyrei*	*Calcidiscus premacintyrei*	*Chiasmolithus* spp.	*Coccolithus miopelagicus*	*Coccolithus pelagicus*	*Cribrocentrum reticulatum*	*Cruciplacolithus primus*	*Cyclicargolithus abisectus*	*Cyclicargolithus floridanus*	*Dictyococcites antarcticus*	*Dictyococcites bisectus*	*Dictyococcites productus*	*Discoaster adamanteus*	*Discoaster deflandrei*	*Discoaster dilatus*	*Discoaster druggii*	*Discoaster exilis*	*Discoaster variabilis*	*Emiliania huxleyi*	*Fasciculithus* spp.	*Geminilithella rotula*	*Gephyrocapsa* (large)	*Gephyrocapsa* (medium)	*Gephyrocapsa parallela*	*Gephyrocapsa* (small)	*Helicosphaera carteri*	*Helicosphaera euphratis*	*Helicosphaera intermedia*	*Helicosphaera paleocarteri*	*Helicosphaera perch-nielseniae*	*Helicosphaera sellii*	*Helicosphaera stalis*	*Helicosphaera walbersdorfensis*	*Isthmolithus recurvus*	*Neococcolithes minutus*	*Pontosphaera* spp.	*Pseudoemiliania lacunosa*	*Pyrocyclus* spp.
181-1122A-																																										
1H-CC, 8-18	9.22	M	C		F					C			R	R	F		C							C				C		C	F								R			
2H-CC, 8-18	18.86	M	F		R					C				R	F		C							C				F		C	F											
3H-CC, 9-14	28.52	M	C		F	R		R	F	A	R	R	R	F	F	F	C							C	F	R		C		C	F											
4H-CC, 5-15	38.25	M	A		C				F	C					F	R	C							F				A		A	C										R	
5H-CC, 10-15	46.57	G	C		F			R		C				F	F	F	C							C		R		C		C	R										F	
6H-CC, 10-15	56.31	M	C		F					C				F	C	R								C	C			C		C	F							R	R	F	R	
7H-CC, 0-15	65.78	M	A		F					C					F		F							C				C		A	F					R						
8H-CC, 0-15	73.84	M	C		C					C	R	R	R	R	F	R	C						R				C		C	F									R		
9X-CC, 0-15	76.46	M	F		F					C	R		R		F	R	F									R		C		A	F					R						
10X-CC, 10-15	85.79	M	F		R					F	R			R	R	R	C											F		C	C										R	
11X-CC, 0-15	96.77	G	F		R					C				R	R	R	F											R		F												
12X-CC, 10-20	109.62	G	F		F					C				R	R		C											C		C	F					R						
181-1122C-																																										
15X-CC, 28-38	111.28	G	C		F					C					F		A											C		C												
181-1122A-																																										
13X-CC, 5-15	119.97		B																																							
181-1122C-																																										
16X-CC, 15-25	122.88	G	C		F				R	C				R	R	R	A											C		A	C				R							
17X-CC, 15-25	133.35	G	R							F																																
18X-CC, 9-19	140.51	G	C		C			R		C		R			R		A		R									F	R	C	F										R	
19X-CC, 5-15	150.48	M	C							F							A											A		A												
20X-CC, 9-19	161.21	G	R							F							F											F														
21X-CC, 0-15	167.99	G	F							F				R			C											C		A												
22X-CC, 0-10	176.93	M	F		R					R	R						F											C	C	F											R	
23X-CC, 0-10	187.28	G	C							R							C											C	C	A												
24X-CC, 0-10	195.42	G	C		C					C	R		R	R		R	A											C	C	A						R						
25X-CC, 0-10	204.87	G	A		F			R	R	C					F		A				R							C	F	C												
26X-CC, 0-10	217.99	G	A	R	F					C							A											C	C	A	C										F	
27X-CC, 23-28	227.16	G	A		F					A				C			C											A	C	C	R										R	
28X-CC, 13-18	237.73	M	C		R				R	F							A											C	F	C											R	
29X-CC, 0-10	247.63	G	A		F				R	C				C	R	R	C											A	F	A											F	
30X-CC, 12-22	259.13	G	A		F				R	C			R	F		R	C		R									C	R	A	F		R						R	F	
31X-CC, 16-21	266.34	P	T							R																			R										R	F	
32X-CC, 16-26	273.75	M	A		F	R			R	A	R		R			R	A											F	F	A	C								R	F	
33X-CC, 8-13	287.98	P	R												R				R																							
34X-2, 122	293.12	M	C		R				R	C							C											F	C	C											C	
34X-CC, 0-10	297.74	M	F		F					C					R		A									R		F		D	F										F	
35X-CC, 24-34	307.91	G	A		F	R			F	C				R	F													C	F	D	R										F	
36X-2, 49	311.59	G	VA		C	F											A											R	R	D	C	R									C	
36X-CC, 20-30	318.20	G	F			R											F													F												
37X-CC, 7-17	328.27	G	A		F	R			R	C				R	F													A		A	F										R	
38X-CC, 0-10	333.28	M	F		C									R			C													C	F										C	
39X-CC, 11-21	343.66	M	F		R				R	R																															R	R	R
40X-CC, 16-26	351.36		B																																							
41X-1, 106	358.96	G	C		C					F				R		R											A	D												R	F	
41X-CC, 7-17	359.88		B																																							
42X-CC, 9-19	372.09		B																																							
43X-CC, 24-29	377.44	G	F		R	R		R	R	F						R	C										F	F		F										F	
44X-4, 13	391.53	G	C		R	R	R			A			C	R		R	F											F		C	F					C					F	R
44X-CC, 21-31	392.54		B																																							
45X-CC, 22-32	402.51		B																																							
46X-CC, 24-34	412.44	M	R							F																															R	
47X-2, 24	417.64	M	F		R	R				F			R				F														F					F					F	
47X-CC, 32-37	421.56	M	F		R					R							F																				F					F	
48X-CC, 29-39	432.41	M	A		C		R		R	A				F	F		F									R	R				C					C				R	R	
49X-CC, 21-31	444.41	M	A		R	R		R						R	F		A														R					F					C	R
50X-CC, 29-34	452.16	M	R			R				C						R	A																									
51X-2, 58	456.48	G	VA		F				R	A				R	A	R	A																									

Table T4 (continued).

Core, section, interval (cm)	Depth (mbsf)	Preservation	Group abundance	*Reticulofenestra* sp. Z	*Reticulofenestra asanoi*	*Reticulofenestra gelida*	*Reticulofenestra lockerii*	*Reticulofenestra* (medium)	*Reticulofenestra pseudoumbilicus*	*Reticulofenestra* (small)	*Reticulofenestra umbilicus*	*Rhabdosphaera procera*	*Sphenolithus abies*	*Sphenolithus conicus*	*Sphenolithus heteromorphus*	*Sphenolithus moriformis*	*Sphenolithus neoabies*	*Syracosphaera pulchra*	*Tetralithoides symeonidesii*	*Watznaueria barnesae*	Comments
181-1122A-																					
1H-CC, 8-18	9.22	M	C				R			C											
2H-CC, 8-18	18.86	M	F				R		R	C											
3H-CC, 9-14	28.52	M	C				R		F	C	R					F		R	R		
4H-CC, 5-15	38.25	M	A				F		F	C						F					
5H-CC, 10-15	46.57	G	C				R		R	F											
6H-CC, 10-15	56.31	M	C						F	A						R					
7H-CC, 0-15	65.78	M	A						R	D										R	Sponge spicules; coccosphere (*D. productus*)
8H-CC, 0-15	73.84	M	C				R	F	R	A						R					
9X-CC, 0-15	76.46	M	F					F	R	A											
10X-CC, 10-15	85.79	M	F							A											
11X-CC, 0-15	96.77	G	F					R		F											
12X-CC, 10-20	109.62	G	F							F											
181-1122C-																					
15X-CC, 28-38	111.28	G	C																		
181-1122A-																					
13X-CC, 5-15	119.97		B																		
181-1122C-																					
16X-CC, 15-25	122.88	G	C				R	C	R				R			R					
17X-CC, 15-25	133.35	G	R					C		F											
18X-CC, 9-19	140.51	G	C				R		R	A											
19X-CC, 5-15	150.48	M	C						R	A											
20X-CC, 9-19	161.21	G	R							F											Tunicate spicules
21X-CC, 0-15	167.99	G	F							A											
22X-CC, 0-10	176.93	M	F						R	C											
23X-CC, 0-10	187.28	G	C																		
24X-CC, 0-10	195.42	G	C							C						R					
25X-CC, 0-10	204.87	G	A			R	R	C	R	A											
26X-CC, 0-10	217.99	G	A			R		F	C				R								Beautiful *P. lacunosa* + tunicate spicules
27X-CC, 23-28	227.16	G	A			C		R							R						
28X-CC, 13-18	237.73	M	C						R												
29X-CC, 0-10	247.63	G	A			F												R			
30X-CC, 12-22	259.13	G	A		R				R	C								R			
31X-CC, 16-21	266.34	P	T			R															
32X-CC, 16-26	273.75	M	A		R		R	F		A						R					Tunicate spicules
33X-CC, 8-13	287.98	P	R						R												Enriched with diatom fragments
34X-2, 122	293.12	M	C					F	R		R										
34X-CC, 0-10	297.74	M	F							C						R		R			
35X-CC, 24-34	307.91	G	A			F		F													Tunicate spicules
36X-2, 49	311.59	G	VA		F			C		A	R										
36X-CC, 20-30	318.20	G	F		R					F						R					
37X-CC, 7-17	328.27	G	A		F	R		F													
38X-CC, 0-10	333.28	M	F		F				R	C						R					
39X-CC, 11-21	343.66	M	F			R			R	F											
40X-CC, 16-26	351.36		B																		
41X-1, 106	358.96	G	C					F		C											
41X-CC, 7-17	359.88		B																		
42X-CC, 9-19	372.09		B																		
43X-CC, 24-29	377.44	G	F					F		F						R					
44X-4, 13	391.53	G	C									R				R					
44X-CC, 21-31	392.54		B																		
45X-CC, 22-32	402.51		B																		
46X-CC, 24-34	412.44	M	R							F											
47X-2, 24	417.64	M	F						R												
47X-CC, 32-37	421.56	M	F																		
48X-CC, 29-39	432.41	M	A							R											*C. pelagicus* coccosphere
49X-CC, 21-31	444.41	M	A			R				C	R										
50X-CC, 29-34	452.16	M	R			F				A											
51X-2, 58	456.48	G	VA			R			R	A							R				

Table T4 (continued).

Core, section, interval (cm)	Depth (mbsf)	Preservation	Group abundance	*Braarudosphaera bigelowii*	*Calcidiscus leptoporus*	*Calcidiscus macintyrei*	*Calcidiscus premacintyrei*	*Chiasmolithus* spp.	*Coccolithus miopelagicus*	*Coccolithus pelagicus*	*Cribrocentrum reticulatum*	*Cruciplacolithus primus*	*Cyclicargolithus abisectus*	*Cyclicargolithus floridanus*	*Dictyococcites antarcticus*	*Dictyococcites bisectus*	*Dictyococcites productus*	*Discoaster adamanteus*	*Discoaster deflandrei*	*Discoaster dilatus*	*Discoaster druggii*	*Discoaster exilis*	*Discoaster variabilis*	*Emiliania huxleyi*	*Fasciculithus* spp.	*Geminilithella rotula*	*Gephyrocapsa* (large)	*Gephyrocapsa* (medium)	*Gephyrocapsa parallela*	*Gephyrocapsa* (small)	*Helicosphaera carteri*	*Helicosphaera euphratis*	*Helicosphaera intermedia*	*Helicosphaera paleocarteri*	*Helicosphaera perch-nielseniae*	*Helicosphaera sellii*	*Helicosphaera stalis*	*Helicosphaera walbersdorfensis*	*Isthmolithus recurvus*	*Neococcolithes minutus*	*Pontosphaera* spp.	*Pseudoemiliania lacunosa*	*Pyrocyclus* spp.
51X-CC, 21-26	463.61	M	A		R	F								R	R				R											C									R	R	
52X-1, 90	465.00	G	A		F	F		R	R				R	F		R				R										C						R			F		
52X-4, 47	469.07	M	A		F		R	R	C	C				R																R										?	
52X-6, 80	472.40	G	VA		R		R		C	A			R				A									R				R									R		
52X-CC, 18-23	472.78		B																																						
53X-3, 144	477.84	G	A		C	F	R		R	C			R	R	A		C													F									F		
53X-CC, 36-46	478.26	M	A		R			R						R																C											R
54X-CC, 0-10	488.15		B																																						
55X-5, 103	499.73	M	A				F		C	F				F	A		C																							R
55X-CC, 18-23	499.92	M	F							F					F																										
56X-2, 140	505.20	M	C				F								C																										
56X-CC, 37-47	507.78	G	A												A		A																								
57X-2, 97	514.37	M	A			F		R	C	C			R	R	C					R										F											F
57X-CC, 21-31	517.14		B																																						
58X-CC, 0-10	523.48	G	C			F				C			R	F	A		C									R															
59X-CC, 7-12	531.27	M	C			R				C				F												F															
60X-CC, 41-46	541.11	G	A		F	C		R	R	F				C	F		F						R		R	F				F											
61X-1, 74	551.14	M	A		C		R	R	C	A				C	A		C		R											C											
61X-CC, 13-23	555.49	G	F							C				C			C																								
62X-CC, 0-10	563.31	G	A		F		C	R	R	F				C	C	R			R							R				C	C								R		
63X-CC, 17-22	571.27	M	A		C		C	R							A	R										F				C	F										
64X-CC, 18-28	580.80	M	F					R	R	F			R	F	F							R																			
65X-CC, 13-18	590.63	M	A		F		F	R	C	A		R	R	F	A		C									F				C	R			C					R		R
66X-CC, 0-5	599.40	M	F											F		R	F																								R
67X-CC, 0-5	609.16	M	F					R		C			R	C						R										R			R								
68X-CC, 0-5	617.80	G	A				F	F	R	C			R	C	F	R		R	F		R		R							F				R	R			F		F		

Note: Preservation: G = good, M = moderate, and P = poor; total (group) and relative abundance of calcareous nannofossils: D = dominant, VA = very abundant, A = abundant, C = common, F = few, R = rare, T = trace, and B = barren.

Table T4 (continued).

Core, section, interval (cm)	Depth (mbsf)	Preservation	Group abundance	*Reticulofenestra* sp. Z	*Reticulofenestra asanoi*	*Reticulofenestra gelida*	*Reticulofenestra lockerii*	*Reticulofenestra* (medium)	*Reticulofenestra pseudoumbilicus*	*Reticulofenestra* (small)	*Reticulofenestra umbilicus*	*Rhabdosphaera procera*	*Sphenolithus abies*	*Sphenolithus conicus*	*Sphenolithus heteromorphus*	*Sphenolithus moriformis*	*Sphenolithus neoabies*	*Syracosphaera pulchra*	*Tetralithoides symeonidesii*	*Watznaueria barnesae*	Comments
51X-CC, 21-26	463.61	M	A							C						R					
52X-1, 90	465.00	G	A								R	F				F	C				
52X-4, 47	469.07	M	A	R		F		A		C	R					R	R				
52X-6, 80	472.40	G	VA					C	C	A	R	R									
52X-CC, 18-23	472.78		B																		
53X-3, 144	477.84	G	A			F		F		C							R				
53X-CC, 36-46	478.26	M	A					F			R										Many reworked
54X-CC, 0-10	488.15		B																		
55X-5, 103	499.73	M	A			A				A							C				Almost no reworked fossils
55X-CC, 18-23	499.92	M	F													R					
56X-2, 140	505.20	M	C			C	C														
56X-CC, 37-47	507.78	G	A																		
57X-2, 97	514.37	M	A			A			C				F				F				
57X-CC, 21-31	517.14		B																		
58X-CC, 0-10	523.48	G	C			C			C								C				
59X-CC, 7-12	531.27	M	C			A			C							C	C				
60X-CC, 41-46	541.11	G	A					F	F		R					C					
61X-1, 74	551.14	M	A						A		R					F					
61X-CC, 13-23	555.49	G	F							F											
62X-CC, 0-10	563.31	G	A						F		R				F	F					
63X-CC, 17-22	571.27	M	A						C		R	R			R	C					
64X-CC, 18-28	580.80	M	F				R		R	F											
65X-CC, 13-18	590.63	M	A	A							R					F					
66X-CC, 0-5	599.40	M	F													F					Probably all reworked
67X-CC, 0-5	609.16	M	F				R									F					
68X-CC, 0-5	617.80	G	A				C				R					R					

Table T5. Identification and abundance of planktonic foraminifers observed at Site 1122.

Core, section, interval (cm)	Depth (mbsf)	Group abundance	*Catapsydrax unicavus*	*Globigerina bulloides*	*Globigerina euapertura*	*Globigerina falconensis*	*Globigerina praebulloides*	*Globigerina quinqueloba*	*Globigerina* spp.	*Globigerinita glutinata*	*Globigerinita uvula*	*Globigerinoides bisphericus*	*Globoquadrina dehiscens*	*Globorotalia* cf. *hirsuta*	*Globorotalia* cf. *conica*	*Globorotalia crassula*	*Globorotalia hirsuta*	*Globorotalia inflata*	*Globorotalia miotumida*	*Globorotalia miozea*	*Globorotalia praemenardii*	*Globorotalia puncticulata*	*Globorotalia puncticuloides*	*Globorotalia scitula*	*Globorotalia tosaensis*	*Globorotalia truncatulinoides*	*Globorotalia zealandica*	*Globorotalia* cf. *zealandica*	*Neogloboquadrina continuosa*	*Neogloboquadrina pachyderma*	*Orbulina suturalis*	*Orbulina universa*	*Paragloborotalia opima nana*	*Zeaglobigerina woodi*
181-1122A-																																		
?1H-CC, 8-18	9.22	C		A				R	F									F						P		R				A				
181-1122B-																																		
1H-CC, 0-15	9.66	C		F				R									P	R						P		R				A		P		
2H-CC, 8-18	18.86	C		A				R	R									F								P				A				
3H-CC, 9-14	28.52	C		A				F	F									F						P		P				A				
4H-CC, 5-15	38.25	C		A				F	F									F						P		R				A		P		
5H-CC, 10-15	46.57	F		A				F	F									F						P						A				
7H-CC, 0-15	65.78	A		A				F	F								P	A						P		R				A		P		
9X-CC, 0-15	76.46	F		F		P		F	F	P						P		R						P		R				A		P		
10X-CC, 10-15	85.79	C		F				R	F									R												F				
11X-CC, 0-15	96.77	F		R				R	F								P	R								P				F				
12X-CC, 10-20	109.62	R		R				R	F		P							R						P						A				
181-1122C-																																		
15X-CC, 28-38	111.28	F		R				P	F									R							R					F				
13X-CC, 5-15	119.97	C		R				R	F	P								R					R		R					R				
181-1122C-																																		
16X-CC, 15-25	122.88	F		R				P	F							R		F					R	P	P					A		P		
20X-CC, 9-19	161.21	C		R				P	F							R		R					P											
21X-CC, 0-15	167.99	F		R				P	F							P		R																
22X-CC, 0-10	176.93	F		R				P	F							P		R					P											
24X-CC, 0-10	195.42	F		R				F								P		R												A				
25X-CC, 0-10	204.87	F		R				F	F							P		R												A				
26X-2, 7-8	215.57	F		R				A										P						R		P				A				
26X-CC, 0-10	217.99	F		R				F			P					P		P					P							A		P		
27X-CC, 23-28	227.16	F		P				R								P		R					P							A				
29X-CC, 0-10	247.63	F		R				F								R		R					P							A				
30X-CC, 12-22	259.13	F		R										R		R		R					P							A				
31X-CC, 16-21	266.34	F		R				F						R		F		F					P							A				
34X-CC, 0-10	297.74	F		R				F										P					P							D				
35X-CC, 24-34	307.91	F		R				F										P					R											
38X-CC, 0-10	333.28	T		P																			P							R				
40X-CC, 16-26	351.36	T		P				P										P					P							P				
44X-CC, 21-31	392.54	R		R				P	R									P					R							R				
47X-CC, 32-37	421.56	R		F				F															R							A				
48X-CC, 29-39	432.41	R																F					A											
49X-CC, 21-31	444.41	T																																
50X-CC, 29-34	452.16	R																					A											
51X-CC, 21-26	463.61	R		R																		R	A											
53X-CC, 36-46	478.26	R		P																		A								F				
54X-CC, 0-10	488.15	B																																
56X-CC, 37-47	507.78	B																																
57X-CC, 21-31	517.14	B																																
58X-CC, 0-10	523.48	R																	P										F					F
59X-CC, 7-12	531.27	B																																
60X-CC, 41-46	541.11	B																																
61X-CC, 13-23	555.49	B																																
62X-CC, 0-10	563.31	R													P						R										P			A
63X-CC, 17-22	571.27	T																		P	P													F
64X-CC, 18-28	580.8	R											P							P				P					P				R	F
65X-CC, 13-18	590.63	R											P							P								P						F
66X-CC, 0-5	599.4	R	P		R								P							R														A
67X-CC, 0-5	609.16	F											P							R														A
68X-CC, 0-5	617.8	F	P				R					P	P							R							P								A

Note: Total (group) and relative abundance of planktonic foraminifers: D = dominant, A = abundant, C = common, F = few/frequent, R = rare, P = present, T = trace, and B = barren; relative abundance of species.

Table T6. Identification and abundance of benthic foraminifers observed at Site 1122. (**See table note.** Continued on next page).

Core, section, interval (cm)	Depth (mbsf)	Preservation	Group abundance	*Anomalinoides fasciatus*	*Anomalinoides macraglabra*	*Anomalinoides spherics*	*Anomalinoides* spp.	*Astrononion parki*	*Bolivina barbata*	*Bolivina* spp.	*Bolivinita pliozea*	*Bolivinopsis* sp.	*Bulimina marginata*	*Bulimina miolaevis*	*Cassidulina carinata*	*Cassidulina laevigata*	*Cassidulina minuta*	*Cibicides notocenicus*	*Cibicides temperata*	*Cibicidoides pachyderma*	*Cibicidoides perforatus*	*Cibicidoides* spp.	*Cornuspira foliacea*	*Cornuspira involvens*	*Cribrorotalia ornatissima*	*Discarbinella bertheloti*	*Discarbinella complanata*	*Discorotalia tenuissima*	*Eggerella bradyi*	*Ehrenbergina mestayeri*	*Elphidium advenum*	*Elphidium charlottense*	*Epistominella exigua*	*Fissurina* spp.	*Gavelinopsis praegeri*	*Globobulimina turgida*	*Globocassidulina* spp.	*Globocassidulina subglobosa*	*Gyroidinoides* spp.	*Karreriella bradyi*
181-1122A-																																							
1H-CC, 8-18	9.22	G	F				T		T																		T				R	R	R		T					
3H-CC, 9-14	28.52	VG	R							T					R								T	T			T				R	T	R	R				T		
4H-CC, 5-15	38.25	VG	R																												R									T
5H-CC, 10-15	46.57	VG	R																			R	T											F						
7H-CC, 0-15	65.78	VG	F							T					R					R								T	T	R		F					R		T	
9X-CC, 0-15	76.46	VG	R																																					
10X-CC, 10-15	85.79	G	R												R	T				R		R				T					F	R	R	R	R					
11X-CC, 0-15	96.77	G	R																	T								T												
12X-CC, 10-20	109.62	G	R												R	T	T			R						T	T		T		F	T	R	F	R					
13X-CC, 5-15	119.97	M	C												T					T		T		T																
181-1122C-																																								
16X-CC, 15-25	122.88	VG																		R									R			R					T			T
24X-CC, 0-10	195.42	VG																		R									T		F			R						
25X-CC, 0-10	204.87	VG											T		R					F									T		T	T	F	T			T			
26X-2, 7-8	215.57	VG					T						T		F												R				T	T	T	T	T		T			
26X-CC, 0-10	217.99	VG									T				R					R											F			R		T				
27X-CC, 23-28	227.16	VG																		R									T				F							
29X-CC, 0-10	247.63	VG																T		R									R											
30X-CC, 12-22	259.13	VG																		R									R									T		
31X-CC, 16-21	266.34																			R													F			R			R
35X-CC, 24-34	307.91	VG																		R									R							T			T
47X-CC, 32-37	421.56	VG																		R																			
48X-CC, 29-39	432.41	G	T																														R							
50X-CC, 29-34	452.16	M	R																	F									T					R						
51X-CC, 21-26	463.61	G	T																	R																				
52X-CC, 18-23	472.78																																							
53X-CC, 36-46	478.26	M	T																	R									T					R						
54X-CC, 0-10	488.15																																							
55X-CC, 18-23	499.92	M	R				F					T								T		F							T								F	T	R	
58X-CC, 0-10	523.48	M	T																										T								R			T
62X-CC, 0-10	563.31	M	F									T										T															R		T	
63X-CC, 17-22	571.27	P	T																			T																		
64X-CC, 18-28	580.8	M	R				T								T							T																		
65X-CC, 13-18	590.63	P	T		R																																			
66X-CC, 0-5	599.4	P	R	R			F											T			R								T										F	
67X-CC, 0-5	609.16	M	F	F	R					T				T					T	R	R							T											R	
68X-CC, 0-5	617.8	M	F		R	R		T												T	R																			

Table T6 (continued).

Core, section, interval (cm)	Depth (mbsf)	Preservation	Group abundance	*Karreriella cylindrica*	*Kolesnikovella australis*	*Lagena* spp.	*Laticarinina pauperata*	*Lenticulina* spp.	*Martinottiella communis*	*Melonis barleeanus*	*Melonis maorica*	*Melonis pompilioides*	*Miliolinella subrotundata*	*Neouvigerina* sp.	*Nodosaria longiscata*	*Nonionella novozealandica*	*Nonionella turgida*	*Nonionellina flemingi*	*Notorotalia spinosa*	*Notorotalia* spp.	*Nuttallides umbonifera*	*Oolina* spp.	*Oridorsalis umbonatus*	*Patellina corrugata*	*Pileolina* spp.	*Planulina wuellerstorfi*	*Pleurostomella* spp.	*Pullenia bulloides*	*Pullenia quinqueloba*	*Pyrgo murrhina*	*Quinqueloculina* spp.	*Quinqueloculina venusta*	*Siphonina australis*	*Sphaeroidina bulloides*	*Stilostomella vermeuilli*	*Textularia* spp.	*Trifarina angulosa*	*Uvigerina auberiana*	*Uvigerina dirupta*	*Uvigerina* spp.
181-1122A-																																							
1H-CC, 8-18	9.22	G	F					T	T	R			T										T				T	R		T			T			R		R	
3H-CC, 9-14	28.52	VG	R							R							T	R						T			T	T		T		T		T			T		R	
4H-CC, 5-15	38.25	VG	R																											T		T		R					R	
5H-CC, 10-15	46.57	VG	R			T				F																				T							T	R	
7H-CC, 0-15	65.78	VG	F					T	T	R										T	R		T		T		T	T	T		T		T			R	T	R	
9X-CC, 0-15	76.46	VG	R																																				
10X-CC, 10-15	85.79	G	R					T		T			R					T		T			T							T		T					R		R	
11X-CC, 0-15	96.77	G	R						T																									T				T		
12X-CC, 10-20	109.62	G	R							R			R							T			R					R		T				T			F			
13X-CC, 5-15	119.97	M	C					T	T	T										T			T					T	T								T			
181-1122C-																																								
16X-CC, 15-25	122.88	VG								F										T	T		R					R	R	T		R		T		T		T	
24X-CC, 0-10	195.42	VG																		T								R		T						F			
25X-CC, 0-10	204.87	VG								F			R	T								T	R					R	T	T		T		R		T	F			
26X-2, 7-8	215.57	VG								C			T					T					T		T			T						T			C		T	
26X-CC, 0-10	217.99	VG								R			R					R		T												T		R			F			
27X-CC, 23-28	227.16	VG						T		R													R							T		T		T		T				
29X-CC, 0-10	247.63	VG						R		F										T			F					R		T				T			R			
30X-CC, 12-22	259.13	VG								C											R		R					R		T				R			R			
31X-CC, 16-21	266.34									C													T					F		T					T				
35X-CC, 24-34	307.91	VG						T													R							R				R							
47X-CC, 32-37	421.56	VG																					F					R											
48X-CC, 29-39	432.41	G	T							T																		T											
50X-CC, 29-34	452.16	M	R					T		R											R							R		R									
51X-CC, 21-26	463.61	G	T							R													R					R											
52X-CC, 18-23	472.78																																							
53X-CC, 36-46	478.26	M	T				T														R							R	T		T								
54X-CC, 0-10	488.15																																							
55X-CC, 18-23	499.92	M	R				T				R	R										R	F				T						T							
58X-CC, 0-10	523.48	M	T												F								F				T	T					T							
62X-CC, 0-10	563.31	M	F				T	T														F	F				T	T												
63X-CC, 17-22	571.27	P	T													T												T											T	
64X-CC, 18-28	580.8	M	R													T																								
65X-CC, 13-18	590.63	P	T																																					
66X-CC, 0-5	599.4	P	R					T			C					R				F				T									T						T	
67X-CC, 0-5	609.16	M	F		T			T			F					R				F														T					T	R
68X-CC, 0-5	617.8	M	F								F					F				R													T							

Note: Preservation: VG = very good, G = good, M = moderate, and P = poor; total (group) and relative abundance of species: C = common, F = few, R = rare, and T = trace.

Table T7. Identification and abundance of diatoms observed at Site 1122. (**See table note.** Continued on next three pages).

Core, section, interval (cm)	Depth (mbsf)	Clinoptilolite abundance	Diatom abundance	*Actinocyclus actinochilus*	*Actinocyclus curvatulus*	*Actinocyclus ingens*	*Actinocyclus oculatus*	*Actinoptychus senarius*	*Actinoptychus splendens*	*Arachnoidiscus* sp.	*Aulacoseira granulata*	*Azpeitia africana*	*Azpeitia endoi*	*Azpeitia tabularis*	*Cestodiscus novozaelandicus*	*Cestodiscus reticulatus*	*Chaetoceros* resting spores	*Chaetoceros* sp.	*Cocconeis* sp.	*Coscinodiscus asteromphalus*	*Coscinodiscus marginatus*	*Coscinodiscus radiatus*	*Craspedodiscus* sp.	*Cyclotella striata*	*Cymbella* sp.	*Denticulopsis dimorpha*	*Denticulopsis hustedtii*	*Denticulopsis meridionalis*	*Denticulopsis* sp.	*Diploneis* sp.	*Eucampia antarctica*	*Grammatophora* sp.	*Hemiaulus caracteristicus*	*Hemiaulus* sp.	*Hemiaulus velatus*	*Hemidiscus karstenii*	*Hemidiscus karstenii* f.1	*Hemidiscus ovalis*	*Hyalodiscus* sp.	*Navicula directa*	*Nitzschia angulata*
181-1122A-																																								
1H-2, 90	240	B	C			T	T				T	T		R			F						T		T					F				T				T		
1H-4, 28	478	B	S																																					
1H-6, 90	840	B	R											R			F		R			R		R							R									
1H-CC, 8-18	9.22	B	C								R			R			R							R						F	R				R			R		
2H-1, 124	10.46	B	F			T		R						R			F					R							T	T	T						T		T
2H-3, 124	13.46	B	D								T	R		R			F					R								F									
2H-6, 124	14.96	B	D					T						R							T	T								R	T								T
2H-CC, 8-18	18.86	B	C					R	T					R																R									
3H-CC, 9-14	28.52	B	C					R						R			C		F						T													R		
4H-CC, 5-15	38.12	B	F			T		T						F			R																						
5H-1, 100	39.12	B	C	T		R							R	R								T								R				T						
5H-3, 95	42.07	B	F			T	T							R																									
5H-6, 85	46.47	B	F								T			F			T		T			T		T	T					R									
5H-CC, 10-15	46.57	B	F											R				T							R										T			T		
6H-CC, 10-15	56.34	B	D	T		T	T				R			R					T			T		R					T		F				T			T	T	
7H-CC, 0-15	65.8	B	D	R		R		T						R								T									R			T	R					
8H-3, 10	68.9	B	F														R					T										R			T					
8H-CC, 0-15	73.84	B	R																																			T		
9X-CC, 0-15	76.46	B	F														R	R				T		R	T					T	T							R		
10X-CC, 10-15	85.79	B	C	R		T								R																F					R					
12X-CC, 10-20	109.64	B	F											R															T	R					F					
13X-CC, 5-15	119.97	B	F																					R											F					
181-1122C-																																								
14X-CC, 0-10	107.92	B	D	T										R										R							R				F					
15X-CC, 28-38	111.28	B	T																																					
16X-CC, 15-25	122.88	B	C			F								R							T							T			R				C					
17X-CC, 15-25	133.35	B	R											R			R					T									R				F	T				
18X-CC, 9-19	140.51	B	C				T		T					R			R		T						R				T	R				R			T		
19X-CC, 5-15	150.48	B	F			R								R											R						R						R		
20X-2, 80	152.78	B	C	T	T		T							T																	R				T			R		
20X-CC, 9-19	161.21	B	R			R		T										T	R						T														
21X-CC, 0-15	167.99	B	T																																					
22X-CC, 0-10	176.93	B	B																																					
23X-CC, 0-10	187.28	B	F								T																				T							T		
30X-CC, 12-22	259.13	B	F	T		R											F	T	T						T						T									
31X-CC, 16-21	266.34	B	F	R		F											T												T	T									
32X-CC, 16-26	273.75	B	F	T		T			T					T			T			T		T																		
33X-CC, 8-13	287.98	B	R			R								T								R		R																
34X-CC, 0-10	297.74	B	C	T	R	F	R		T					R							R													T						
35X-CC, 24-34	307.84	B	C		R	C			T								T				T																		
36X-CC, 20-30	318.22	B	C			C								R											T													R		
37X-CC, 7-17	328.21	B	R		R				R							T					R																	T		
38X-2, 45	330.16	B	C			C																				R			T		T	T							
38X-CC, 0-10	333.28	B	R			C								T																										
39X-1, 30	333.58	B	R		R	C								R								T												T						
39X-1, 110	334.68	B	C		R	C																						R			T						R		
39X-CC, 11-21	343.66	B	R			F																																	
40X-2, 65.5	345.81	B	R		T																																		
40X-CC, 16-26	351.36	B	F			C																T																T		
41X-CC, 7-17	359.88	B	T																																			T		
42X-CC, 9-19	372.09	B	B																																					
43X-CC, 24-29	377.44	B	C			C																T									T									
44X-2, 18	379.12	B	B																																					
44X-CC, 21-31	392.54	B	R			R											T																							
46X-CC, 24-34	412.44	B	C		R	C											R														R			T			R		
47X-1, 137	413.81	B	F		R	C																						S							R				
47X-CC, 32-37	421.56	B	R																			R				T													
48X-3, 50	425.06	B	F			R																T																	
49X-CC, 21-31	444.41	B	R			R																																		
50X-CC, 29-34	452.18	B	R																			R																R		

Table T7 (continued).

Core, section, interval (cm)	Depth (mbsf)	Clinoptilolite abundance	Diatom abundance	*Nitzschia barronii*	*Nitzschia interfrigidaria*	*Nitzschia kerguelenis*	*Nitzschia panduriformis*	*Nitzschia praeinterfrigidaria*	*Nitzschia reinholdii*	*Nitzschia ritscherii*	*Nitzschia separanda*	*Nitzschia weaveri*	*Paralia sulcata*	*Pinnularia* sp.	*Pseudeunotia doliolus*	*Pyxilla reticulata*	*Rhaphoneis surirelloides*	*Rhizosolenia hebetata*	*Rhizosolenia styliformis*	*Rocella praenitida*	*Rouxia* sp.	*Simonseniella barboi*	*Stephanopyxis turris turris*	*Tabularia* sp.	*Thalassionema nitzschioides*	*T. nitzschioides* var. *parva*	*Thalassiosira elliptipora*	*Thalassiosira fasciculata*	*Thalassiosira gracilis*	*Thalassiosira insigna*	*Thalassiosira inura*	*Thalassiosira kolbei*	*Thalassiosira lentiginosa*	*Thalassiosira oestrupii*	*Thalassiothrix longissima*	*Triceratium barbadense*	*Xanthiopyxis ovalis*
181-1122A-																																				
1H-2, 90	240	B	C			F	R			R	T		T				R													T		F		F		F
1H-4, 28	478	B	S			T																											T				
1H-6, 90	840	B	R			F							R				F																R		R		F
1H-CC, 8-18	9.22	B	C			C	R			R	R		R			T	R				T		T										C		R		
2H-1, 124	10.46	B	F			F	R							T		T	F																F	T			F
2H-3, 124	13.46	B	D			F	R			T			R				R											R					F		F		R
2H-6, 124	14.96	B	D			F	R			R	S		R		T	T	R														T		F		F		F
2H-CC, 8-18	18.86	B	C			C	R				R		R			T	C							R									F		F		R
3H-CC, 9-14	28.52	B	C			R	F			R			R			R	F							R									T				F
4H-CC, 5-15	38.12	B	F			F							R																				F				F
5H-1, 100	39.12	B	C			F	T				T		R			T							T				R					F		R		R
5H-3, 95	42.07	B	F			F	T						R			T											R					F		R		F
5H-6, 85	46.47	B	F			F	R						R											T	R			R	T			F		R		R
5H-CC, 10-15	46.57	B	F			F	R		T	R	T	T	R										T					R				F		F		F
6H-CC, 10-15	56.34	B	D			C	R			R	T		R		T		R												T			F	R	R		
7H-CC, 0-15	65.8	B	D			F	T				R		R										T					R				F		F		
8H-3, 10	68.9	B	F			F											R															F				R
8H-CC, 0-15	73.84	B	R			F																										F		T		
9X-CC, 0-15	76.46	B	F			F	T			R							F			T												R		R		F
10X-CC, 10-15	85.79	B	C			F	R			R	T																					F	T	F		F
12X-CC, 10-20	109.64	B	F			F	R			T							R	T							T							F		F		
13X-CC, 5-15	119.97	B	F			F	T										T															F		F		
181-1122C-																																				
14X-CC, 0-10	107.92	B	D	T		C	R			R	R						T		T									R				R	R	F		
15X-CC, 28-38	111.28	B	T			T																														
16X-CC, 15-25	122.88	B	C			C				R	R																	R	T			F		F		
17X-CC, 15-25	133.35	B	R			F				R																		R				F		F		
18X-CC, 9-19	140.51	B	C			F	R			F			R				R								R	T		R				F	T	R		R
19X-CC, 5-15	150.48	B	F			F	T			R	R		R				F						T									F	R	R		R
20X-2, 80	152.78	B	C				R			C													R		T							F		R		R
20X-CC, 9-19	161.21	B	R	T		R				R																						R		R		F
21X-CC, 0-15	167.99	B	T			T																														
22X-CC, 0-10	176.93	B	B																																	
23X-CC, 0-10	187.28	B	F			F	T										T															R		T		T
30X-CC, 12-22	259.13	B	F			F	R			F							F												T			R				R
31X-CC, 16-21	266.34	B	F			R							R										R				R									R
32X-CC, 16-26	273.75	B	F				T										F								T	T		T						F		R
33X-CC, 8-13	287.98	B	R			R	R			F													R									R		F		
34X-CC, 0-10	297.74	B	C			R	R			F							F					T	R			T						R		F		R
35X-CC, 24-34	307.84	B	C	R			R			R			R					R							R	T						F		F		R
36X-CC, 20-30	318.22	B	C				R			F			R										R				F					F		F		R
37X-CC, 7-17	328.21	B	R			R	R										T					T						R								T
38X-2, 45	330.16	B	C	F						F													R							T		R				
38X-CC, 0-10	333.28	B	R	R		T	T			R			R															R				R				T
39X-1, 30	333.58	B	R	F																								R				R		R		
39X-1, 110	334.68	B	C	R		R							R										T					R				R		F		T
39X-CC, 11-21	343.66	B	R	R																												R		F		
40X-2, 65.5	345.81	B	R																				T									T		T		
40X-CC, 16-26	351.36	B	F	F									T															R						F		T
41X-CC, 7-17	359.88	B	T																																	
42X-CC, 9-19	372.09	B	B																																	
43X-CC, 24-29	377.44	B	C	F						F			R				R		T													R	T			R
44X-2, 18	379.12	B	B																																	
44X-CC, 21-31	392.54	B	R																																	
46X-CC, 24-34	412.44	B	C	C																		R										R	R	C		
47X-1, 137	413.81	B	F	F																												R	R	F		
47X-CC, 32-37	421.56	B	R	R									T										T											R		
48X-3, 50	425.06	B	F																R			R	R										T	F		
49X-CC, 21-31	444.41	B	R																				R											R		
50X-CC, 29-34	452.18	B	R																																	

Table T7 (continued).

Core, section, interval (cm)	Depth (mbsf)	Clinoptilolite abundance	Diatom abundance	*Actinocyclus actinochilus*	*Actinocyclus curvatulus*	*Actinocyclus ingens*	*Actinocyclus oculatus*	*Actinoptychus senarius*	*Actinoptychus splendens*	*Arachnoidiscus* sp.	*Aulacoseira granulata*	*Azpeitia africana*	*Azpeitia endoi*	*Azpeitia tabularis*	*Cestodiscus novozaelandicus*	*Cestodiscus reticulatus*	*Chaetoceros* resting spores	*Chaetoceros* sp.	*Cocconeis* sp.	*Coscinodiscus asteromphalus*	*Coscinodiscus marginatus*	*Coscinodiscus radiatus*	*Craspedodiscus* sp.	*Cyclotella striata*	*Cymbella* sp.	*Denticulopsis dimorpha*	*Denticulopsis hustedtii*	*Denticulopsis meridionalis*	*Denticulopsis* sp.	*Diploneis* sp.	*Eucampia antarctica*	*Grammatophora* sp.	*Hemiaulus caracteristicus*	*Hemiaulus* sp.	*Hemiaulus velatus*	*Hemidiscus karstenii*	*Hemidiscus karstenii* f.1	*Hemidiscus ovalis*	*Hyalodiscus* sp.	*Navicula directa*	*Nitzschia angulata*
51X-CC, 21-26	463.61	B	C			C											R				T																	R		
52X-6, 31	471.42	B	F											T	F											T														
52X-6, 80	471.91	B	R																															T						
52X-CC, 18-23	472.78	B	R			T								T							R					T		T										T		
53X-CC, 36-46	478.26	B	B																																					
54X-3, 68	481.94	B	F											T							T					R									T			T	R	
54X-CC, 0-10	488.15	B	R			R															R		T				T	T		T							T		
55X-3, 64	491.79	B	F			R											T									F								T	T					
55X-CC, 18-23	499.94	B	T																																					
56X-CC, 37-47	507.78	B	F			F							T								R					T														
57X-CC, 21-31	517.14	B	R																															T						
58X-CC, 0-10	523.48	B	T																																					
59X-CC, 7-12	531.27	B	T																		T																			
60X-CC, 41-46	541.11	B	B																																					
61X-CC, 13-23	555.49	B	B																																					
62X-2, 10	557.09	B	B																																					
62X-CC, 0-10	563.31	B	R					T																										T						
63X-1, 13-14	563.45	B	T			T																																		
63X-1, 90	564.21	C	B																																					
63X-CC, 17-22	571.27	R	F			R																										T	T						
64X-1, 3	571.3	A	T																																					
64X-CC, 18-28	580.8	A	B																																					
65X-1, 145	581.08	F	T																																					
65X-1, 145	582.25	F	R																																					
65X-CC, 13-18	590.63	A	R																																					
66X-1, 82.5	591.46	A	B																																					
66X-CC, 0-5	599.4	C	B																																					
67X-1, 69	600.1	A	B																																					
67X-1, 79	600.2	A	B																																					
67X-CC, 0-5	609.16	C	B																																					
68X-CC, 0-5	617.8	C	B																																					

Note: Clinoptilolite and diatom total (group) abundance and relative abundance: D = dominant, A = abundant, C = common, F = few, R = rare, T = trace, and B = barren.

Table T7 (continued).

Core, section, interval (cm)	Depth (mbsf)	Clinoptilolite abundance	Diatom abundance	*Nitzschia barronii*	*Nitzschia interfrigidaria*	*Nitzschia kerguelenis*	*Nitzschia panduriformis*	*Nitzschia praeinterfrigidaria*	*Nitzschia reinholdii*	*Nitzschia ritscherii*	*Nitzschia separanda*	*Nitzschia weaveri*	*Paralia sulcata*	*Pinnularia* sp.	*Pseudeunotia doliolus*	*Pyxilla reticulata*	*Rhaphoneis surirelloides*	*Rhizosolenia hebetata*	*Rhizosolenia styliformis*	*Rocella praenitida*	*Rouxia* sp.	*Simonseniella barboi*	*Stephanopyxis turris turris*	*Tabularia* sp.	*Thalassionema nitzschioides*	*T. nitzschioides* var. *parva*	*Thalassiosira elliptipora*	*Thalassiosira fasciculata*	*Thalassiosira gracilis*	*Thalassiosira insigna*	*Thalassiosira inura*	*Thalassiosira kolbei*	*Thalassiosira lentiginosa*	*Thalassiosira oestrupii*	*Thalassiothrix longissima*	*Triceratium barbadense*	*Xanthiopyxis ovalis*
51X-CC, 21-26	463.61	B	C	C																	R	T						T				R	R	F		
52X-6, 31	471.42	B	F					T	T			R			R							R												F	T	
52X-6, 80	471.91	B	R																															R	T	
52X-CC, 18-23	472.78	B	R									R										R							T					R		
53X-CC, 36-46	478.26	B	B																																	
54X-3, 68	481.94	B	F									R									T	R												R		
54X-CC, 0-10	488.15	B	R									R			T							R			T									R		
55X-3, 64	491.79	B	F								T	R										R												R		
55X-CC, 18-23	499.94	B	T									T																								
56X-CC, 37-47	507.78	B	F									R										R		T										F		
57X-CC, 21-31	517.14	B	R								T											R														
58X-CC, 0-10	523.48	B	T																																	
59X-CC, 7-12	531.27	B	T									T																								
60X-CC, 41-46	541.11	B	B																																	
61X-CC, 13-23	555.49	B	B																																	
62X-2, 10	557.09	B	B																																	
62X-CC, 0-10	563.31	B	R									R			R							T	R													
63X-1, 13-14	563.45	B	T																				T													
63X-1, 90	564.21	C	B																																	
63X-CC, 17-22	571.27	R	F									R											F													
64X-1, 3	571.3	A	T												T								T													
64X-CC, 18-28	580.8	A	B																																	
65X-1, 145	581.08	F	T																				T													
65X-1, 145	582.25	F	R									T			T								T													
65X-CC, 13-18	590.63	A	R									R			F								R													
66X-1, 82.5	591.46	A	B																																	
66X-CC, 0-5	599.4	C	B																																	
67X-1, 69	600.1	A	B																																	
67X-1, 79	600.2	A	B																																	
67X-CC, 0-5	609.16	C	B																																	
68X-CC, 0-5	617.8	C	B																																	

Table T8. Biostratigraphic events identified at Site 1122.

	Event	Age (Ma)	Sample	Depth (mbsf)
F1	FO *Globorotalia hirsuta*	0.45	181-1122A-11X-CC	96.77
F2	LO *Globorotalia puncticuloides*	0.7–0.8	181-1122C-22X-CC	215.57
F3	Several forms younger than ~3.4 (see "Biostratigraphy," p. 13.)	~3.4	181-1122C-52X-CC	472.78
F4	Occurrence of *Neogloboquadrina continuosa* and *N. pachyderma*	~11.3	181-1122C-58X-CC	523.48
F5	LO *Globorotalia praemenardii*	~13.0	181-1122C-62X-CC	563.31
F6	Co-occurrence of *Globorotalia zealandica* and *Gr. miozea*	16.3–16.7	181-1122C-68X-CC	617.8
N1	FO *Emiliania huxleyi*	0.24	181-1122A-5H-CC	46.57
N2	LO *Pseudoemiliania lacunosa*	0.42	181-1122C-20X-CC	161.21
N3	LO *Reticulofenestra asanoi*	0.83	181-1122C-29X-CC	247.63
N4	FO *Gephyrocapsa parallela*	0.9	181-1122C-36X-CC	318.20
N5	FO *Reticulofenestra asanoi*	1.06	181-1122C-38X-CC	333.28
N6–7	Range *Gephyrocapsa* (large)	1.1–1.36	181-1122C-41X through 44X-4, 13 cm	359.88–391.53
N8	FO *Gephyrocapsa* (medium)	1.66	181-1122C-46X-CC	412.44
N9	Several forms co-occurring (see "Biostratigraphy," p. 13)	~3.45	181-1122C-52X-CC	~475
N10	LO *Cargolithus miopelagicus*	>10.4	181-1122C-54X-CC	~485
N11	FO *Calcidiscus macintyrei*	12.34	181-1122C-60X-CC	541.11
N12	LO *Sphenolithus heteromorphus*	13.52	181-1122C-63X-CC	571.27
N13	Absence of FO *Calcidiscus premacintyrei*	<17.4	181-1122C-68X-CC	617.8
D1	LO *Hemidiscus karstenii*	0.18–0.19	181-1122A-6H-CC	56.34
D2	Acme *Hemidiscus karstenii*	0.92	181-1122C-20X-CC	152.78
D3	LO *Actinocyclus ingens*	0.64	181-1122C-30X-CC	259.13
D4	LO *Thalassiosira elliptipora*	0.65–0.7	181-1122C-34X-CC	297.74
D5	LO *Nitzschia denticuloides*	11.3	181-1122C-54X-CC	488.15
D6	LO *Denticulopsis dimorpha*	12.2	181-1122C-54X-CC	488.15
D7	FO *Simonseniella barboi*	12.5	181-1122C-62X-CC	563.31
R1	LO *Stylatractus universus*	0.46	181-1122C-25X-CC	204.87
R2	LO *Lithelius nautiloides*	1.93	181-1122C-48X-CC	432.41
R3	FO *Eucyrtidium calvertense*	1.92	181-1122C-49X-CC	444.41

Note: F = foraminifer, N = nannofossil, D = diatom, R = radiolarian.

Table T9. Identification and abundance of radiolarians observed at Site 1122. (**See table note.** Continued on next two pages).

Core, section, interval (cm)	Depth (mbsf)	Preservation	Group abundance	*Actinomma leptodermum*	*Actinomma* sp.	*Antarctissa denticulata*	*Antarctissa longa*	*Antarctissa strelkovi*	*Axoprunum angelinum*	*Botryostrobus aquilonaris*	*Botryostrobus auritus/australis* gr.	*Botryostrobus* sp.	*Calocycletta* sp.	*Carpocanistrum* sp.	*Cornutella profunda*	*Cycladophora bicornis bicornis*	*Cycladophora davisiana cornutoides*	*Cycladophora davisiana davisiana*	*Cycladophora pliocenica*	*Cyrtocapsella japonica*	*Cyrtocapsella tetrapera*	*Cyrtopera languncula*	*Dictyophimus hirundo*	*Dictyophimus* sp.	*Druppatractus* sp.	*Euchitonia* sp.	*Eucyrtidium calvertense*	*Eucyrtidium* sp.	*Gondwanaria dogieli*	*Heliodiscus asteriscus*	*Helotholus praevema*	*Hexacontium* sp.
181-1122A-																																
1H-CC, 8-18	9.22	VG	C			R	T	F								R		A		R	T		R				T		T			R
2H-CC, 8-18	18.86	P	VR			T																T	T									T
3H-CC, 9-14	28.52	G	VR					R								R																
4H-CC, 5-15	38.25	G	VR			R	T	R			T							R		T												
5H-CC, 10-15	46.57	VG	C	R		F	R	R									R	F	T		T					T						
6H-CC, 10-15	56.31	VG	A	F		A	R	A			R							A	T				R					T				
7H-CC, 0-15	65.78	G	F			R		C		R								R														R
8H-CC, 0-15	73.84	G	VR			R		R																			T					R
9X-CC, 0-15	76.46	G	VR				R	R																								
10X-CC, 10-15	85.79	G	R			F	R	F																								R
11X-CC, 0-15	96.77		B																													
12X-CC, 10-20	109.62	M	VR			R												R					T			R						
13X-CC, 5-15	119.97	G	R					R										R														
181-1122B-																																
1H-CC, 0-15	9.66	G	R	R		R		R										C														
181-1122C-																																
1H-CC, 0-10	2.41		B																													
2H-CC, 0-10	12.15	G	VR		R													R									T					
3H-CC, 9-14	17.09	G	VR																													
4H-CC, 10-15	23.69	G	VR		R			R												T												
5H-CC, 10-15	32.4	M	VR			R																										
6H-CC, 18-23	42.11	G	F			F		F							R			R														R
7H-CC, 0-15	51.07		B																													
9H-CC, 12-17	70.12	G	R			R		C		R																R						
10H-CC, 19-24	80.38	G	R	R		F		R										F														
11H-CC, 0-15	86.83		B																													
12H-CC, 11-16	94.75	G	F	R		R										R							R									
13H-CC, 25-30	103.65	G	VA			A	R	A		R					R	R	R	F					F	F		R		R	R			R
14X-CC, 0-10	107.92	G	A	R		A		A		R								C								R						R
15X-CC, 28-38	111.28	M	VR																													
16X-CC, 15-25	122.88	G	C	F		C	R	C		R								R								R				T		R
17X-CC, 15-25	133.35	G	R	R				F																		R						
18X-CC, 9-19	140.51	M	C	R		C												R								T						R
19X-CC, 5-15	150.48	P	R			C	T											T								F						R
20X-CC, 9-19	161.21	P	T																													
21X-CC, 0-15	167.99	P	VR	T														T														
22X-CC, 0-10	176.93	P	VR			R																										

Core, section, interval (cm)	*Lamprocyrtis maritalis*	*Lamprocyrtis nigriniae*	*Larcopyle* sp.	*Larcospira* sp.	*Lithelius nautiloides*	*Lychnocanoma* sp.	*Peripyramis* sp.	*Phormostichoartus fistula*	*Phorticium clevei*	*Prunopyle antarctica*	*Pterocanium trilobum*	*Pylospira* sp.	*Saccospyris antarctica*	*Saturnalis circularis*	*Siphocampe* sp.	*Spongodiscus osculosus*	*Spongodiscus* sp.	*Spongoplegma antarcticum*	*Spongotrochus glacialis*	*Stichocorys peregrina*	*Stylacontarium acquilonium*	*Stylacontarium bispiculum*	*Stylatractus* sp.	*Stylatractus universus*	*Stylodictya* sp.	*Thecosphaera* sp.	*Theocorythium* sp.	*Theocorythium trachelium trachelium*	*Triceraspyris antarctica*
181-1122A-																													
1H-CC, 8-18			R	R	T				R				R				F		R						R			T	T
2H-CC, 8-18													T				R												
3H-CC, 9-14																	R												
4H-CC, 5-15													T				F							T					
5H-CC, 10-15									R	T			T			R	A	T							R				R
6H-CC, 10-15					R		T		F	F			R			T	A		R						R				R
7H-CC, 0-15			R						R								C						R		R				R
8H-CC, 0-15			R														F								R				
9X-CC, 0-15			R										R				R		R										
10X-CC, 10-15			R							R							C						R		F				
11X-CC, 0-15																													
12X-CC, 10-20																R	A								R				
13X-CC, 5-15			R														F						R						
181-1122B-																													
1H-CC, 0-15			R						R							R	F						R		R				T
181-1122C-																													
1H-CC, 0-10																													
2H-CC, 0-10									R								F			T					R				
3H-CC, 9-14		T	R														R												
4H-CC, 10-15			R														R								R				
5H-CC, 10-15									R				R				R								R				
6H-CC, 18-23	T		F				R	R					R				F					T	R		F				T
7H-CC, 0-15																													
9H-CC, 12-17			F										R				C								F				
10H-CC, 19-24			F														F						R						
11H-CC, 0-15																													
12H-CC, 11-16					T				R				R				C								F				
13H-CC, 25-30			A				R		F	R			F			R	A	R	R	T			C		F	R			R
14X-CC, 0-10			R		T		R		R	R			R			R	A	F	R				R		R	F			R
15X-CC, 28-38			R														R												
16X-CC, 15-25			C				R		R	F			R			R	A			T			F			F			T
17X-CC, 15-25									R				R				C		T	T			T						
18X-CC, 9-19			F		T				R	R			R			R	A			T				T					
19X-CC, 5-15			F														C												
20X-CC, 9-19																	R												
21X-CC, 0-15																	F						R						
22X-CC, 0-10																													

Table T9 (continued).

Core, section, interval (cm)	Depth (mbsf)	Preservation	Group abundance	*Actinomma leptodermum*	*Actinomma* sp.	*Antarctissa denticulata*	*Antarctissa longa*	*Antarctissa strelkovi*	*Axoprunum angelinum*	*Botryostrobus aquilonaris*	*Botryostrobus auritus/australis* gr.	*Botryostrobus* sp.	*Calocycletta* sp.	*Carpocanistrum* sp.	*Cornutella profunda*	*Cycladophora bicornis bicornis*	*Cycladophora davisiana cornutoides*	*Cycladophora davisiana davisiana*	*Cycladophora pliocenica*	*Cyrtocapsella japonica*	*Cyrtocapsella tetrapera*	*Cyrtopera languncula*	*Dictyophimus hirundo*	*Dictyophimus* sp.	*Druppatractus* sp.	*Euchitonia* sp.	*Eucyrtidium calvertense*	*Eucyrtidium* sp.	*Gondwanaria dogieli*	*Heliodiscus asteriscus*	*Helotholus praevema*	*Hexacontium* sp.	*Lamprocyrtis maritalis*
23X-CC, 0-10	187.28	P	T																														
24X-CC, 0-10	195.42		B																														
25X-CC, 0-10	204.87	M	C	R		A		A		R							T	F					T			R				T			
26X-CC, 0-10	217.99	M	VR																														
27X-CC, 23-28	227.16	M	VA			A		A	R								T	R															
28X-CC, 13-18	237.73	M	VR																														
29X-CC, 0-10	247.63	M	C	T		A	R	A										R								R							
30X-CC, 12-22	259.13	M	VR			R		R																									
31X-CC, 16-21	266.34	G	F	F		F		F	T					R			R	R										T					
32X-CC, 16-26	273.75	G	VR																														
33X-CC, 8-13	287.98	M	VR					T																									
34X-CC, 0-10	297.74	M	C			A		A	R																							F	
35X-CC, 24-34	307.91	M	A			A		A			F							C														F	
36X-CC, 20-30	318.2	M	F																													F	
37X-CC, 7-17	328.27	M	A			A		A	C		F			R				R					T			R							
38X-CC, 0-10	333.28	M	F			F		R	C		R																						
39X-CC, 11-21	343.66	M	R			T				R																							
40X-CC, 16-26	351.36		B																														
41X-CC, 7-17	359.88	M	VR																														
42X-CC, 9-19	372.09	M	VR																														
43X-CC, 24-29	377.44	P	VR			R																											
44X-CC, 21-31	392.54	M	VR																														
45X-CC, 22-32	402.51	G	F			F		R																									
46X-CC, 24-34	412.44	M	VR																														
47X-CC, 32-37	421.56	P	VR																														
48X-CC, 29-39	432.41	M	C					R			R							R									C					R	
49X-CC, 21-31	444.41	M	A					F																		A	C						
50X-CC, 29-34	452.16		B																														
51X-CC, 21-26	463.61		B																														
52X-CC, 18-23	472.78	P	VR																														
53X-CC, 36-46	478.26		B																														
54X-CC, 0-10	488.15	P	VR																														
55X-CC, 18-23	499.92	P	VR																														
56X-CC, 37-47	507.78	P	VR																	R													
57X-CC, 21-31	517.14	P	VR																														
58X-CC, 0-10	523.48		B																														
59X-CC, 7-12	531.27		B																														
60X-CC, 41-46	541.11		B																														
61X-CC, 13-23	555.49		B																														
62X-CC, 0-10	563.31	M	C									R	T															T					

Core, section, interval (cm)	*Lamprocyrtis nigriniae*	*Larcopyle* sp.	*Larcospira* sp.	*Lithelius nautiloides*	*Lychnocanoma* sp.	*Peripyramis* sp.	*Phormostichoartus fistula*	*Phorticium clevei*	*Prunopyle antarctica*	*Pterocanium trilobum*	*Pylospira* sp.	*Saccospyris antarctica*	*Saturnalis circularis*	*Siphocampe* sp.	*Spongodiscus osculosus*	*Spongodiscus* sp.	*Spongoplegma antarcticum*	*Spongotrochus glacialis*	*Stichocorys peregrina*	*Stylacontarium acquilonium*	*Stylacontarium bispiculum*	*Stylatractus* sp.	*Stylatractus universus*	*Stylodictya* sp.	*Thecosphaera* sp.	*Theocorythium* sp.	*Theocorythium trachelium trachelium*	*Triceraspyris antarctica*
23X-CC, 0-10																												
24X-CC, 0-10																												
25X-CC, 0-10		C										F			T	A						F	R	F	C			
26X-CC, 0-10																R								R	R			
27X-CC, 23-28		C				R		R	R			R			R	A							R	C				T
28X-CC, 13-18																R												
29X-CC, 0-10		R							R	T		R			R	A		R					R	R	R			R
30X-CC, 12-22				T												R								C				
31X-CC, 16-21		C										R				A								C				
32X-CC, 16-26		R														R								R				
33X-CC, 8-13																R								R				
34X-CC, 0-10		A		T				R	T	T		R			R	C								A	R	R		R
35X-CC, 24-34		A		R					T			R				A	R	T						A				
36X-CC, 20-30		C		R												C						C						
37X-CC, 7-17		A		R					C	R		R	T		R	A					R			C	A			R
38X-CC, 0-10		C		R		R		R	C			R			R	A					R			F	F			
39X-CC, 11-21		F														C								F	R			
40X-CC, 16-26																												
41X-CC, 7-17																R												
42X-CC, 9-19																R												
43X-CC, 24-29																R												
44X-CC, 21-31																								R				
45X-CC, 22-32		C		C								R				A								C	C			
46X-CC, 24-34		F														R									R			
47X-CC, 32-37																R							T					
48X-CC, 29-39		F		R											R	A		R						A	R			
49X-CC, 21-31		A		R		F										A								C	R			
50X-CC, 29-34																												
51X-CC, 21-26																												
52X-CC, 18-23																R												
53X-CC, 36-46																												
54X-CC, 0-10		R														R						R						
55X-CC, 18-23																R												
56X-CC, 37-47																R						R						
57X-CC, 21-31																R						R						
58X-CC, 0-10																												
59X-CC, 7-12																												
60X-CC, 41-46																												
61X-CC, 13-23																												
62X-CC, 0-10		R			R									T		F						T		R				

Table T9 (continued).

Core, section, interval (cm)	Depth (mbsf)	Preservation	Group abundance	*Actinomma leptodermum*	*Actinomma* sp.	*Antarctissa denticulata*	*Antarctissa longa*	*Antarctissa strelkovi*	*Axoprunum angelinum*	*Botryostrobus aquilonaris*	*Botryostrobus auritus/australis* gr.	*Botryostrobus* sp.	*Calocycletta* sp.	*Carpocanistrum* sp.	*Cornutella profunda*	*Cycladophora bicornis bicornis*	*Cycladophora davisiana cornutoides*	*Cycladophora davisiana davisiana*	*Cycladophora pliocenica*	*Cyrtocapsella japonica*	*Cyrtocapsella tetrapera*	*Cyrtopera languncula*	*Dictyophimus hirundo*
63X-CC, 17-22	571.27	P	T											R							T		
64X-CC, 18-28	580.8		B																				
65X-CC, 13-18	590.63		B																				
66X-CC, 0-5	599.4		B																				
67X-CC, 0-5	609.16		B																				
68X-CC, 0-5	617.8		B																				

Core, section, interval (cm)	*Dictyophimus* sp.	*Druppatractus* sp.	*Euchitonia* sp.	*Eucyrtidium calvertense*	*Eucyrtidium* sp.	*Gondwanaria dogieli*	*Heliodiscus asteriscus*	*Helotholus praevema*	*Hexacontium* sp.	*Lamprocyrtis maritalis*	*Lamprocyrtis nigriniae*	*Larcopyle* sp.	*Larcospira* sp.	*Lithelius nautiloides*	*Lychnocanoma* sp.	*Peripyramis* sp.	*Phormostichoartus fistula*	*Phorticium clevei*	*Prunopyle antarctica*	*Pterocanium trilobum*
63X-CC, 17-22																				
64X-CC, 18-28																				
65X-CC, 13-18																				
66X-CC, 0-5																				
67X-CC, 0-5																				
68X-CC, 0-5																				

Core, section, interval (cm)	*Pylospira* sp.	*Saccospyris antarctica*	*Saturnalis circularis*	*Siphocampe* sp.	*Spongodiscus osculosus*	*Spongodiscus* sp.	*Spongoplegma antarcticum*	*Spongotrochus glacialis*	*Stichocorys peregrina*	*Stylacontarium acquilonium*	*Stylacontarium bispiculum*	*Stylatractus* sp.	*Stylatractus universus*	*Stylodictya* sp.	*Thecosphaera* sp.	*Theocorythium* sp.	*Theocorythium trachelium trachelium*	*Triceraspyris antarctica*
63X-CC, 17-22						R									R			
64X-CC, 18-28																		
65X-CC, 13-18																		
66X-CC, 0-5																		
67X-CC, 0-5																		
68X-CC, 0-5																		

Note: Preservation: VG = very good, G = good, M = moderate, and P = poor; total (group) abundance and relative abundance of radiolarians: A = abundant, C = common, F = few, R = rare, VR = very rare, T = trace, and B = barren.

Table T10. Composite depth section, Site 1122. (See table note. Continued on next six pages.)

Leg	Site	Hole	Core	Type	Section	Section length (m)	Depth (mbsf)	Offset (m)	Composite depth (mcd)
181	1122	A	1	H	1	1.50	0.00	7.88	7.88
181	1122	A	1	H	2	1.50	1.50	7.88	9.38
181	1122	A	1	H	3	1.50	3.00	7.88	10.88
181	1122	A	1	H	4	1.50	4.50	7.88	12.38
181	1122	A	1	H	5	1.50	6.00	7.88	13.88
181	1122	A	1	H	6	1.50	7.50	7.88	15.38
181	1122	A	1	H	7	0.14	9.00	7.88	16.88
181	1122	A	1	H	CC	0.18	9.14	7.88	17.02
181	1122	A	2	H	1	1.50	9.30	7.45	16.75
181	1122	A	2	H	2	1.50	10.80	7.45	18.25
181	1122	A	2	H	3	1.50	12.30	7.45	19.75
181	1122	A	2	H	4	1.50	13.80	7.45	21.25
181	1122	A	2	H	5	1.50	15.30	7.45	22.75
181	1122	A	2	H	6	1.50	16.80	7.45	24.25
181	1122	A	2	H	7	0.48	18.30	7.45	25.75
181	1122	A	2	H	CC	0.18	18.78	7.45	26.23
181	1122	A	3	H	1	1.50	18.80	9.12	27.92
181	1122	A	3	H	2	1.50	20.30	9.12	29.42
181	1122	A	3	H	3	1.50	21.80	9.12	30.92
181	1122	A	3	H	4	1.50	23.30	9.12	32.42
181	1122	A	3	H	5	1.50	24.80	9.12	33.92
181	1122	A	3	H	6	1.50	26.30	9.12	35.42
181	1122	A	3	H	7	0.63	27.80	9.12	36.92
181	1122	A	3	H	CC	0.14	28.43	9.12	37.55
181	1122	A	4	H	1	1.50	28.30	7.90	36.20
181	1122	A	4	H	2	1.50	29.80	7.90	37.70
181	1122	A	4	H	3	1.50	31.30	7.90	39.20
181	1122	A	4	H	4	1.50	32.80	7.90	40.70
181	1122	A	4	H	5	1.50	34.30	7.90	42.20
181	1122	A	4	H	6	1.50	35.80	7.90	43.70
181	1122	A	4	H	7	0.90	37.30	7.90	45.20
181	1122	A	4	H	CC	0.15	38.20	7.90	46.10
181	1122	A	5	H	1	1.50	37.80	8.34	46.14
181	1122	A	5	H	2	1.50	39.30	8.34	47.64
181	1122	A	5	H	3	1.50	40.80	8.34	49.14
181	1122	A	5	H	4	1.50	42.30	8.34	50.64
181	1122	A	5	H	5	1.40	43.80	8.34	52.14
181	1122	A	5	H	6	1.27	45.20	8.34	53.54
181	1122	A	5	H	CC	0.15	46.47	8.34	54.81
181	1122	A	6	H	1	1.50	47.30	6.46	53.76
181	1122	A	6	H	2	1.50	48.80	6.46	55.26
181	1122	A	6	H	3	1.50	50.30	6.46	56.76
181	1122	A	6	H	4	1.50	51.80	6.46	58.26
181	1122	A	6	H	5	1.50	53.30	6.46	59.76
181	1122	A	6	H	6	1.41	54.80	6.46	61.26
181	1122	A	6	H	CC	0.15	56.21	6.46	62.67
181	1122	A	7	H	1	1.50	56.80	6.16	62.96
181	1122	A	7	H	2	1.50	58.30	6.16	64.46
181	1122	A	7	H	3	1.50	59.80	6.16	65.96
181	1122	A	7	H	4	1.50	61.30	6.16	67.46
181	1122	A	7	H	5	1.50	62.80	6.16	68.96
181	1122	A	7	H	6	1.48	64.30	6.16	70.46
181	1122	A	7	H	CC	0.15	65.78	6.16	71.94
181	1122	A	8	H	1	0.64	66.30	6.58	72.88
181	1122	A	8	H	2	1.50	66.94	6.58	73.52
181	1122	A	8	H	3	1.50	68.44	6.58	75.02
181	1122	A	8	H	4	1.50	69.94	6.58	76.52
181	1122	A	8	H	5	1.50	71.44	6.58	78.02
181	1122	A	8	H	6	0.90	72.94	6.58	79.52
181	1122	A	8	H	CC	0.15	73.84	6.58	80.42
181	1122	A	9	X	1	0.66	75.80	6.58	82.38
181	1122	A	9	X	CC	0.15	76.46	6.58	83.04
181	1122	A	10	X	1	0.29	85.40	6.58	91.98
181	1122	A	10	X	CC	0.15	85.69	6.58	92.27
181	1122	A	11	X	1	1.50	95.00	6.58	101.58
181	1122	A	11	X	2	0.27	96.50	6.58	103.08
181	1122	A	11	X	CC	0.15	96.77	6.58	103.35

Table T10 (continued).

Leg	Site	Hole	Core	Type	Section	Section length (m)	Depth (mbsf)	Offset (m)	Composite depth (mcd)
181	1122	A	12	X	1	1.50	104.70	6.58	111.28
181	1122	A	12	X	2	1.50	106.20	6.58	112.78
181	1122	A	12	X	3	1.50	107.70	6.58	114.28
181	1122	A	12	X	4	0.32	109.20	6.58	115.78
181	1122	A	12	X	CC	0.20	109.52	6.58	116.10
181	1122	A	13	X	1	1.50	114.30	6.58	120.88
181	1122	A	13	X	2	1.50	115.80	6.58	122.38
181	1122	A	13	X	3	1.50	117.30	6.58	123.88
181	1122	A	13	X	4	1.12	118.80	6.58	125.38
181	1122	A	13	X	CC	0.15	119.92	6.58	126.50
181	1122	B	1	H	1	1.50	0.00	0.00	0.00
181	1122	B	1	H	2	1.50	1.50	0.00	1.50
181	1122	B	1	H	3	1.50	3.00	0.00	3.00
181	1122	B	1	H	4	1.50	4.50	0.00	4.50
181	1122	B	1	H	5	1.50	6.00	0.00	6.00
181	1122	B	1	H	6	1.50	7.50	0.00	7.50
181	1122	B	1	H	7	0.66	9.00	0.00	9.00
181	1122	B	1	H	CC	0.15	9.66	0.00	9.66
181	1122	C	1	H	1	1.50	0.00	0.00	0.00
181	1122	C	1	H	2	0.91	1.50	0.00	1.50
181	1122	C	1	H	CC	0.10	2.41	0.00	2.41
181	1122	C	2	H	1	1.50	2.50	1.24	3.74
181	1122	C	2	H	2	1.50	4.00	1.24	5.24
181	1122	C	2	H	3	1.50	5.50	1.24	6.74
181	1122	C	2	H	4	1.50	7.00	1.24	8.24
181	1122	C	2	H	5	1.50	8.50	1.24	9.74
181	1122	C	2	H	6	1.50	10.00	1.24	11.24
181	1122	C	2	H	7	0.65	11.50	1.24	12.74
181	1122	C	2	H	CC	0.10	12.15	1.24	13.39
181	1122	C	3	H	1	1.50	9.50	0.64	10.14
181	1122	C	3	H	2	1.50	11.00	0.64	11.64
181	1122	C	3	H	3	1.50	12.50	0.64	13.14
181	1122	C	3	H	4	1.11	14.00	0.64	14.64
181	1122	C	3	H	5	1.50	15.11	0.64	15.75
181	1122	C	3	H	6	0.39	16.61	0.64	17.25
181	1122	C	3	H	CC	0.14	17.00	0.64	17.64
181	1122	C	4	H	1	1.50	14.00	5.33	19.33
181	1122	C	4	H	2	1.50	15.50	5.33	20.83
181	1122	C	4	H	3	1.54	17.00	5.33	22.33
181	1122	C	4	H	4	1.50	18.54	5.33	23.87
181	1122	C	4	H	5	1.50	20.04	5.33	25.37
181	1122	C	4	H	6	1.37	21.54	5.33	26.87
181	1122	C	4	H	7	0.68	22.91	5.33	28.24
181	1122	C	4	H	CC	0.15	23.59	5.33	28.92
181	1122	C	5	H	1	1.50	23.50	6.42	29.92
181	1122	C	5	H	2	1.50	25.00	6.42	31.42
181	1122	C	5	H	3	1.50	26.50	6.42	32.92
181	1122	C	5	H	4	1.50	28.00	6.42	34.42
181	1122	C	5	H	5	1.50	29.50	6.42	35.92
181	1122	C	5	H	6	1.30	31.00	6.42	37.42
181	1122	C	5	H	CC	0.15	32.30	6.42	38.72
181	1122	C	6	H	1	1.50	33.00	6.00	39.00
181	1122	C	6	H	2	1.50	34.50	6.00	40.50
181	1122	C	6	H	3	1.50	36.00	6.00	42.00
181	1122	C	6	H	4	1.50	37.50	6.00	43.50
181	1122	C	6	H	5	1.50	39.00	6.00	45.00
181	1122	C	6	H	6	1.43	40.50	6.00	46.50
181	1122	C	6	H	CC	0.23	41.93	6.00	47.93
181	1122	C	7	H	1	1.50	42.50	5.46	47.96
181	1122	C	7	H	2	1.50	44.00	5.46	49.46
181	1122	C	7	H	3	1.50	45.50	5.46	50.96
181	1122	C	7	H	4	1.50	47.00	5.46	52.46
181	1122	C	7	H	5	1.50	48.50	5.46	53.96
181	1122	C	7	H	6	1.07	50.00	5.46	55.46
181	1122	C	7	H	CC	0.15	51.07	5.46	56.53
181	1122	C	8	H	1	1.50	52.00	3.30	55.30

Table T10 (continued).

Leg	Site	Hole	Core	Type	Section	Section length (m)	Depth (mbsf)	Offset (m)	Composite depth (mcd)
181	1122	C	8	H	2	1.50	53.50	3.30	56.80
181	1122	C	8	H	3	1.50	55.00	3.30	58.30
181	1122	C	8	H	4	1.50	56.50	3.30	59.80
181	1122	C	8	H	5	1.50	58.00	3.30	61.30
181	1122	C	8	H	6	1.50	59.50	3.30	62.80
181	1122	C	8	H	7	0.28	61.00	3.30	64.30
181	1122	C	8	H	CC	0.16	61.28	3.30	64.58
181	1122	C	9	H	1	1.50	61.50	3.04	64.54
181	1122	C	9	H	2	1.50	63.00	3.04	66.04
181	1122	C	9	H	3	1.50	64.50	3.04	67.54
181	1122	C	9	H	4	1.50	66.00	3.04	69.04
181	1122	C	9	H	5	1.50	67.50	3.04	70.54
181	1122	C	9	H	6	1.00	69.00	3.04	72.04
181	1122	C	9	H	CC	0.17	70.00	3.04	73.04
181	1122	C	10	H	1	1.50	71.00	2.64	73.64
181	1122	C	10	H	2	1.50	72.50	2.64	75.14
181	1122	C	10	H	3	1.50	74.00	2.64	76.64
181	1122	C	10	H	4	1.50	75.50	2.64	78.14
181	1122	C	10	H	5	1.50	77.00	2.64	79.64
181	1122	C	10	H	6	1.24	78.50	2.64	81.14
181	1122	C	10	H	7	0.45	79.74	2.64	82.38
181	1122	C	10	H	CC	0.24	80.19	2.64	82.83
181	1122	C	11	H	1	1.50	80.50	2.64	83.14
181	1122	C	11	H	2	1.50	82.00	2.64	84.64
181	1122	C	11	H	3	1.50	83.50	2.64	86.14
181	1122	C	11	H	4	0.98	85.00	2.64	87.64
181	1122	C	11	H	5	0.85	85.98	2.64	88.62
181	1122	C	11	H	CC	0.15	86.83	2.64	89.47
181	1122	C	12	H	1	1.50	86.90	2.64	89.54
181	1122	C	12	H	2	1.50	88.40	2.64	91.04
181	1122	C	12	H	3	1.50	89.90	2.64	92.54
181	1122	C	12	H	4	1.50	91.40	2.64	94.04
181	1122	C	12	H	5	1.50	92.90	2.64	95.54
181	1122	C	12	H	6	0.24	94.40	2.64	97.04
181	1122	C	12	H	CC	0.16	94.64	2.64	97.28
181	1122	C	13	H	1	1.50	94.90	2.64	97.54
181	1122	C	13	H	2	1.50	96.40	2.64	99.04
181	1122	C	13	H	3	1.50	97.90	2.64	100.54
181	1122	C	13	H	4	1.50	99.40	2.64	102.04
181	1122	C	13	H	5	1.50	100.90	2.64	103.54
181	1122	C	13	H	6	1.00	102.40	2.64	105.04
181	1122	C	13	H	CC	0.30	103.40	2.64	106.04
181	1122	C	14	X	1	1.50	103.70	2.64	106.34
181	1122	C	14	X	2	1.50	105.20	2.64	107.84
181	1122	C	14	X	3	1.22	106.70	2.64	109.34
181	1122	C	14	X	CC	0.10	107.92	2.64	110.56
181	1122	C	15	X	1	1.50	108.00	2.64	110.64
181	1122	C	15	X	2	1.50	109.50	2.64	112.14
181	1122	C	15	X	CC	0.38	111.00	2.64	113.64
181	1122	C	16	X	1	1.50	117.60	2.64	120.24
181	1122	C	16	X	2	1.50	119.10	2.64	121.74
181	1122	C	16	X	3	1.50	120.60	2.64	123.24
181	1122	C	16	X	4	0.63	122.10	2.64	124.74
181	1122	C	16	X	CC	0.25	122.73	2.64	125.37
181	1122	C	17	X	1	1.50	127.20	2.64	129.84
181	1122	C	17	X	2	1.50	128.70	2.64	131.34
181	1122	C	17	X	3	1.50	130.20	2.64	132.84
181	1122	C	17	X	4	1.50	131.70	2.64	134.34
181	1122	C	17	X	CC	0.25	133.20	2.64	135.84
181	1122	C	18	X	1	1.50	136.90	2.64	139.54
181	1122	C	18	X	2	1.50	138.40	2.64	141.04
181	1122	C	18	X	3	0.52	139.90	2.64	142.54
181	1122	C	18	X	CC	0.19	140.42	2.64	143.06
181	1122	C	19	X	1	1.50	146.50	2.64	149.14
181	1122	C	19	X	2	1.50	148.00	2.64	150.64
181	1122	C	19	X	3	0.93	149.50	2.64	152.14

Table T10 (continued).

Leg	Site	Hole	Core	Type	Section	Section length (m)	Depth (mbsf)	Offset (m)	Composite depth (mcd)
181	1122	C	19	X	CC	0.15	150.43	2.64	153.07
181	1122	C	20	X	1	1.50	156.10	2.64	158.74
181	1122	C	20	X	2	1.50	157.60	2.64	160.24
181	1122	C	20	X	3	1.50	159.10	2.64	161.74
181	1122	C	20	X	4	0.52	160.60	2.64	163.24
181	1122	C	20	X	CC	0.19	161.12	2.64	163.76
181	1122	C	21	X	1	1.50	165.70	2.64	168.34
181	1122	C	21	X	2	0.79	167.20	2.64	169.84
181	1122	C	21	X	CC	0.15	167.99	2.64	170.63
181	1122	C	22	X	1	1.40	175.30	2.64	177.94
181	1122	C	22	X	2	0.23	176.70	2.64	179.34
181	1122	C	22	X	CC	0.10	176.93	2.64	179.57
181	1122	C	23	X	1	1.50	185.00	2.64	187.64
181	1122	C	23	X	2	0.78	186.50	2.64	189.14
181	1122	C	23	X	CC	0.10	187.28	2.64	189.92
181	1122	C	24	X	1	0.72	194.70	2.64	197.34
181	1122	C	24	X	CC	0.10	195.42	2.64	198.06
181	1122	C	25	X	1	0.57	204.30	2.64	206.94
181	1122	C	25	X	CC	0.10	204.87	2.64	207.51
181	1122	C	26	X	1	1.50	214.00	2.64	216.64
181	1122	C	26	X	2	1.00	215.50	2.64	218.14
181	1122	C	26	X	3	1.49	216.50	2.64	219.14
181	1122	C	26	X	CC	0.10	217.99	2.64	220.63
181	1122	C	27	X	1	1.50	223.70	2.64	226.34
181	1122	C	27	X	2	1.50	225.20	2.64	227.84
181	1122	C	27	X	3	0.23	226.70	2.64	229.34
181	1122	C	27	X	CC	0.28	226.93	2.64	229.57
181	1122	C	28	X	1	1.50	233.30	2.64	235.94
181	1122	C	28	X	2	1.50	234.80	2.64	237.44
181	1122	C	28	X	3	1.30	236.30	2.64	238.94
181	1122	C	28	X	CC	0.18	237.60	2.64	240.24
181	1122	C	29	X	1	1.50	242.90	2.64	245.54
181	1122	C	29	X	2	1.50	244.40	2.64	247.04
181	1122	C	29	X	3	1.50	245.90	2.64	248.54
181	1122	C	29	X	4	0.23	247.40	2.64	250.04
181	1122	C	29	X	CC	0.10	247.63	2.64	250.27
181	1122	C	30	X	1	1.50	252.50	2.64	255.14
181	1122	C	30	X	2	1.50	254.00	2.64	256.64
181	1122	C	30	X	3	1.50	255.50	2.64	258.14
181	1122	C	30	X	4	1.50	257.00	2.64	259.64
181	1122	C	30	X	5	0.51	258.50	2.64	261.14
181	1122	C	30	X	CC	0.22	259.01	2.64	261.65
181	1122	C	31	X	1	1.50	261.70	2.64	264.34
181	1122	C	31	X	2	1.50	263.20	2.64	265.84
181	1122	C	31	X	3	1.48	264.70	2.64	267.34
181	1122	C	31	X	CC	0.21	266.18	2.64	268.82
181	1122	C	32	X	1	1.50	271.30	2.64	273.94
181	1122	C	32	X	2	0.79	272.80	2.64	275.44
181	1122	C	32	X	CC	0.26	273.59	2.64	276.23
181	1122	C	33	X	1	1.50	280.70	2.64	283.34
181	1122	C	33	X	2	1.50	282.20	2.64	284.84
181	1122	C	33	X	3	1.50	283.70	2.64	286.34
181	1122	C	33	X	4	1.50	285.20	2.64	287.84
181	1122	C	33	X	5	1.20	286.70	2.64	289.34
181	1122	C	33	X	CC	0.13	287.90	2.64	290.54
181	1122	C	34	X	1	1.50	290.40	2.64	293.04
181	1122	C	34	X	2	1.50	291.90	2.64	294.54
181	1122	C	34	X	3	1.50	293.40	2.64	296.04
181	1122	C	34	X	4	1.50	294.90	2.64	297.54
181	1122	C	34	X	5	1.34	296.40	2.64	299.04
181	1122	C	34	X	CC	0.10	297.74	2.64	300.38
181	1122	C	35	X	1	1.50	300.00	2.64	302.64
181	1122	C	35	X	2	1.50	301.50	2.64	304.14
181	1122	C	35	X	3	1.50	303.00	2.64	305.64
181	1122	C	35	X	4	1.50	304.50	2.64	307.14
181	1122	C	35	X	5	1.50	306.00	2.64	308.64

Table T10 (continued).

Leg	Site	Hole	Core	Type	Section	Section length (m)	Depth (mbsf)	Offset (m)	Composite depth (mcd)
181	1122	C	35	X	6	0.17	307.50	2.64	310.14
181	1122	C	35	X	CC	0.34	307.67	2.64	310.31
181	1122	C	36	X	1	1.50	309.60	2.64	312.24
181	1122	C	36	X	2	1.50	311.10	2.64	313.74
181	1122	C	36	X	3	1.50	312.60	2.64	315.24
181	1122	C	36	X	4	1.50	314.10	2.64	316.74
181	1122	C	36	X	5	1.50	315.60	2.64	318.24
181	1122	C	36	X	6	0.90	317.10	2.64	319.74
181	1122	C	36	X	CC	0.30	318.00	2.64	320.64
181	1122	C	37	X	1	1.50	319.30	2.64	321.94
181	1122	C	37	X	2	1.50	320.80	2.64	323.44
181	1122	C	37	X	3	1.50	322.30	2.64	324.94
181	1122	C	37	X	4	1.50	323.80	2.64	326.44
181	1122	C	37	X	5	1.50	325.30	2.64	327.94
181	1122	C	37	X	6	1.40	326.80	2.64	329.44
181	1122	C	37	X	CC	0.17	328.20	2.64	330.84
181	1122	C	38	X	1	1.50	328.90	2.64	331.54
181	1122	C	38	X	2	1.50	330.40	2.64	333.04
181	1122	C	38	X	3	1.38	331.90	2.64	334.54
181	1122	C	38	X	CC	0.10	333.28	2.64	335.92
181	1122	C	39	X	1	1.50	338.50	2.64	341.14
181	1122	C	39	X	2	1.50	340.00	2.64	342.64
181	1122	C	39	X	3	1.50	341.50	2.64	344.14
181	1122	C	39	X	4	0.55	343.00	2.64	345.64
181	1122	C	39	X	CC	0.21	343.55	2.64	346.19
181	1122	C	40	X	1	1.50	348.20	2.64	350.84
181	1122	C	40	X	2	1.50	349.70	2.64	352.34
181	1122	C	40	X	CC	0.26	351.20	2.64	353.84
181	1122	C	41	X	1	1.50	357.90	2.64	360.54
181	1122	C	41	X	2	0.41	359.40	2.64	362.04
181	1122	C	41	X	CC	0.17	359.81	2.64	362.45
181	1122	C	42	X	1	1.50	367.50	2.64	370.14
181	1122	C	42	X	2	1.50	369.00	2.64	371.64
181	1122	C	42	X	3	1.50	370.50	2.64	373.14
181	1122	C	42	X	CC	0.19	372.00	2.64	374.64
181	1122	C	44	X	1	1.50	386.90	2.64	389.54
181	1122	C	44	X	2	1.50	388.40	2.64	391.04
181	1122	C	44	X	3	1.50	389.90	2.64	392.54
181	1122	C	44	X	4	0.93	391.40	2.64	394.04
181	1122	C	44	X	CC	0.31	392.33	2.64	394.97
181	1122	C	45	X	1	1.50	396.60	2.64	399.24
181	1122	C	45	X	2	1.50	398.10	2.64	400.74
181	1122	C	45	X	3	1.50	399.60	2.64	402.24
181	1122	C	45	X	4	1.19	401.10	2.64	403.74
181	1122	C	45	X	CC	0.32	402.29	2.64	404.93
181	1122	C	46	X	1	1.50	406.20	2.64	408.84
181	1122	C	46	X	2	1.50	407.70	2.64	410.34
181	1122	C	46	X	3	1.50	409.20	2.64	411.84
181	1122	C	46	X	4	1.50	410.70	2.64	413.34
181	1122	C	46	X	CC	0.34	412.20	2.64	414.84
181	1122	C	47	X	1	1.50	415.90	2.64	418.54
181	1122	C	47	X	2	1.50	417.40	2.64	420.04
181	1122	C	47	X	3	1.50	418.90	2.64	421.54
181	1122	C	47	X	4	0.84	420.40	2.64	423.04
181	1122	C	47	X	CC	0.37	421.24	2.64	423.88
181	1122	C	48	X	1	1.50	425.50	2.64	428.14
181	1122	C	48	X	2	1.50	427.00	2.64	429.64
181	1122	C	48	X	3	1.50	428.50	2.64	431.14
181	1122	C	48	X	4	1.50	430.00	2.64	432.64
181	1122	C	48	X	5	0.62	431.50	2.64	434.14
181	1122	C	48	X	CC	0.39	432.12	2.64	434.76
181	1122	C	49	X	1	1.50	435.20	2.64	437.84
181	1122	C	49	X	2	1.50	436.70	2.64	439.34
181	1122	C	49	X	3	1.50	438.20	2.64	440.84
181	1122	C	49	X	4	1.50	439.70	2.64	442.34
181	1122	C	49	X	5	1.50	441.20	2.64	443.84

Table T10 (continued).

Leg	Site	Hole	Core	Type	Section	Section length (m)	Depth (mbsf)	Offset (m)	Composite depth (mcd)
181	1122	C	49	X	6	1.50	442.70	2.64	445.34
181	1122	C	49	X	CC	0.31	444.20	2.64	446.84
181	1122	C	50	X	1	1.50	444.80	2.64	447.44
181	1122	C	50	X	2	1.50	446.30	2.64	448.94
181	1122	C	50	X	3	1.50	447.80	2.64	450.44
181	1122	C	50	X	4	1.50	449.30	2.64	451.94
181	1122	C	50	X	5	1.07	450.80	2.64	453.44
181	1122	C	50	X	CC	0.34	451.87	2.64	454.51
181	1122	C	51	X	1	1.50	454.40	2.64	457.04
181	1122	C	51	X	2	1.50	455.90	2.64	458.54
181	1122	C	51	X	3	1.50	457.40	2.64	460.04
181	1122	C	51	X	4	1.50	458.90	2.64	461.54
181	1122	C	51	X	5	1.50	460.40	2.64	463.04
181	1122	C	51	X	6	1.50	461.90	2.64	464.54
181	1122	C	51	X	CC	0.26	463.40	2.64	466.04
181	1122	C	52	X	1	1.50	464.10	2.64	466.74
181	1122	C	52	X	2	1.50	465.60	2.64	468.24
181	1122	C	52	X	3	1.50	467.10	2.64	469.74
181	1122	C	52	X	4	1.50	468.60	2.64	471.24
181	1122	C	52	X	5	1.50	470.10	2.64	472.74
181	1122	C	52	X	6	1.00	471.60	2.64	474.24
181	1122	C	52	X	CC	0.23	472.60	2.64	475.24
181	1122	C	53	X	1	1.50	473.40	2.64	476.04
181	1122	C	53	X	2	1.50	474.90	2.64	477.54
181	1122	C	53	X	3	1.50	476.40	2.64	479.04
181	1122	C	53	X	CC	0.46	477.90	2.64	480.54
181	1122	C	54	X	1	1.50	483.00	2.64	485.64
181	1122	C	54	X	2	1.50	484.50	2.64	487.14
181	1122	C	54	X	3	1.50	486.00	2.64	488.64
181	1122	C	54	X	4	0.65	487.50	2.64	490.14
181	1122	C	54	X	CC	0.10	488.15	2.64	490.79
181	1122	C	55	X	1	1.50	492.70	2.64	495.34
181	1122	C	55	X	2	1.50	494.20	2.64	496.84
181	1122	C	55	X	3	1.50	495.70	2.64	498.34
181	1122	C	55	X	4	1.50	497.20	2.64	499.84
181	1122	C	55	X	5	1.04	498.70	2.64	501.34
181	1122	C	55	X	CC	0.23	499.74	2.64	502.38
181	1122	C	56	X	1	1.50	502.30	2.64	504.94
181	1122	C	56	X	2	1.50	503.80	2.64	506.44
181	1122	C	56	X	3	1.50	505.30	2.64	507.94
181	1122	C	56	X	4	0.61	506.80	2.64	509.44
181	1122	C	56	X	CC	0.47	507.41	2.64	510.05
181	1122	C	57	X	1	1.50	511.90	2.64	514.54
181	1122	C	57	X	2	1.50	513.40	2.64	516.04
181	1122	C	57	X	3	1.50	514.90	2.64	517.54
181	1122	C	57	X	4	0.53	516.40	2.64	519.04
181	1122	C	57	X	CC	0.31	516.93	2.64	519.57
181	1122	C	58	X	1	1.50	521.50	2.64	524.14
181	1122	C	58	X	2	0.48	523.00	2.64	525.64
181	1122	C	58	X	CC	0.10	523.48	2.64	526.12
181	1122	C	61	X	1	1.50	550.40	2.64	553.04
181	1122	C	61	X	2	1.50	551.90	2.64	554.54
181	1122	C	61	X	3	1.50	553.40	2.64	556.04
181	1122	C	61	X	4	0.46	554.90	2.64	557.54
181	1122	C	61	X	CC	0.23	555.36	2.64	558.00
181	1122	C	62	X	1	1.50	560.00	2.64	562.64
181	1122	C	62	X	2	1.50	561.50	2.64	564.14
181	1122	C	62	X	3	0.31	563.00	2.64	565.64
181	1122	C	62	X	CC	0.10	563.31	2.64	565.95
181	1122	C	63	X	1	1.50	569.60	2.64	572.24
181	1122	C	63	X	CC	0.22	571.10	2.64	573.74
181	1122	C	64	X	1	1.32	579.30	2.64	581.94
181	1122	C	64	X	CC	0.28	580.62	2.64	583.26
181	1122	C	65	X	1	1.50	588.90	2.64	591.54
181	1122	C	65	X	2	0.10	590.40	2.64	593.04
181	1122	C	65	X	CC	0.18	590.50	2.64	593.14

Table T10 (continued).

Leg	Site	Hole	Core	Type	Section	Section length (m)	Depth (mbsf)	Offset (m)	Composite depth (mcd)
181	1122	C	66	X	1	0.90	598.50	2.64	601.14
181	1122	C	66	X	CC	0.05	599.40	2.64	602.04
181	1122	C	67	X	1	0.96	608.20	2.64	610.84
181	1122	C	67	X	CC	0.05	609.16	2.64	611.80

Note: This table is also available in **ASCII format.**

Table T11. Splice tie points, Site 1122.

Site	Hole	Core	Type	Section	Depth in section (cm)	Depth (mbsf)	Depth (mcd)		Site	Hole	Core	Type	Section	Depth in section (cm)	Depth (mbsf)	Depth (mcd)
1122	C	1	H	2	8	1.58	1.58	Tie to	1122	B	1	H	2	8	1.58	1.58
1122	B	1	H	6	32	7.82	7.82	Tie to	1122	C	2	H	3	108	6.58	7.82
1122	C	2	H	5	44	8.94	10.18	Tie to	1122	A	1	H	2	80	2.30	10.18
1122	A	1	H	5	92	6.92	14.80	Tie to	1122	C	3	H	4	16	14.16	14.80
1122	C	3	H	6	12	16.73	17.37	Tie to	1122	A	2	H	1	61	9.92	17.37
1122	A	2	H	6	72	17.52	24.97	Tie to	1122	C	4	H	4	109	19.64	24.97
1122	C	4	H	7	40	23.31	28.64	Tie to	1122	A	3	H	1	72	19.52	28.64
1122	A	3	H	3	140	23.20	32.32	Tie to	1122	C	5	H	2	89	25.90	32.32
1122	C	5	H	6	76	31.76	38.18	Tie to	1122	A	4	H	2	48	30.28	38.18
1122	A	4	H	6	16	35.96	43.86	Tie to	1122	C	6	H	4	36	37.86	43.86
1122	C	6	H	6	68	41.18	47.18	Tie to	1122	A	5	H	1	104	38.84	47.18
1122	A	5	H	3	48	41.28	49.62	Tie to	1122	C	7	H	2	16	44.16	49.62
1122	C	7	H	5	140	49.90	55.36	Tie to	1122	A	6	H	2	9	48.90	55.36
1122	A	6	H	4	4	51.84	58.30	Tie to	1122	C	8	H	2	150	55.00	58.30
1122	C	8	H	6	76	60.26	63.56	Tie to	1122	A	7	H	1	60	57.40	63.56
1122	A	7	H	3	92	60.72	66.88	Tie to	1122	C	9	H	2	84	63.84	66.88
1122	C	9	H	6	96	69.96	73.00	Tie to	1122	A	8	H	1	12	66.42	73.00
1122	A	8	H	4	136	71.30	77.88	Tie to	1122	C	10	H	3	124	75.24	77.88
1122	C	10	H	7	40	80.14	82.78									

Note: This table is also available in **ASCII format.**

Table T12. Compacted and restored rates of sedimentation at Site 1122.

Time interval (Ma)	Compacted rate of sedimentation (m/m.y.)	Restored rate of sedimentation (m/m.y.)
0.0 - 0.2	208	208
0.2 - 0.4	667	732
0.4 - 0.6	536	555
0.6 - 0.7	200	212
0.7 - 0.8	113	120
0.8 - 1.0	76	81
1.0 - 1.1	75	80
1.1 - 1.2	67	71
1.2 - 1.3	183	196
1.3 - 1.4	211	226
1.4 - 1.8	30	33
1.8 - 1.9	71	77
1.9 - 2.2	142	154
2.2 - 3.0	3	3
3.0 - 5.0	17	19
5.0 - 9.9	2	2
9.9 - 11.1	25	27
11.1 - 11.3	0	0
11.3 - 12.3	17	19
12.3 - 13.0	33	37
13.0 - 13.5	14	25
13.5 - 15.8	2	4
15.8 - 16.3	50	80
16.3 - 17.4	48	78

Notes: Calculated with programs DEPOR and BURSUB (Gradstein et al., 1989). For details see **"Age Models and Sedimentation Rates,"** p. 25.

Table T13. Summary of interstitial water geochemistry results for samples from Holes 1122A and 1122C.

Core, section, interval (cm)	Depth (mbsf)	Depth (mcd)	Salinity	Cl^- (mM)	pH	Alkalinity (mM)	Na^+ (mM)	Mg^{2+} (mM)	Ca^{2+} (mM)	SO_4^{2-} (mM)	HPO_4^{2-} (μM)	NH_4^+ (μM)	H_4SiO_4 (μM)	K^+ (mM)	Li^+ (μM)	Sr^{2+} (μM)
181-1122A-																
1H-4, 140-150	5.90	13.78	34.0	560	7.49	34.77	442	50.8	4.9	3.3	321	2.61	575	10.6	18	75
2H-4, 140-150	15.20	22.65	34.0	562	7.50	40.49	438	51.5	4.1	0.0	285	3.43	604	10.1	17	74
3H-4, 140-150	24.70	33.82	34.0	562	7.56	38.17	438	51.6	4.0	0.0	266	3.48	608	10.0	18	77
4H-4, 140-150	34.22	42.10	34.0	563	7.45	34.64	449	47.2	3.5	0.0	264	3.52	665	9.9	19	77
5H-5, 130-140	45.10	53.44	33.5	561	7.38	30.26	452	44.4	3.5	0.0	263	3.47	597	10.4	16	78
6H-4, 140-150	53.20	59.66	33.5	560	7.74	31.56	452	43.8	3.4	0.0	209	3.65	540	10.2	15	82
7H-4, 140-150	62.70	68.86	33.5	557	7.66	30.82	447	44.8	3.0	0.0	156	4.24	706	10.5	18	83
11X-1, 140-150	96.40	102.98	33.5	553	7.60	32.47	448	43.4	3.8	2.5	162	4.73	661	10.6	21	100
12X-2, 140-150	107.60	114.18	33.5	553	7.53	32.26	446	42.9	3.7	1.6	201	5.75	721	10.6	22	109
13X-2, 140-150	117.20	123.78	33.5	553	7.68	33.40	445	42.7	4.1	1.1	160	5.51	758	10.8	28	116
181-1122C-																
9H-4, 140-150	67.40	70.44	33.5	560	7.53	33.05	447	46.0	3.1	0.0	175	4.16	682	10.3	18	87
10H-4, 140-150	76.90	79.54	33.5	559	7.64	35.27	449	44.9	2.9	0.0	143	4.84	646	10.5	18	89
12H-4, 140-150	92.82	95.44	33.5	556	7.55	34.80	446	44.7	3.2	0.0	242	4.48	667	10.4	18	101
13H-4, 140-150	100.80	103.44	33.5	556	7.63	33.61	443	45.4	3.5	0.0	246	5.15	668	10.4	19	109
16X-3, 140-150	122.00	124.64	33.5	554	7.63	34.41	441	44.4	3.9	0.0	243	5.67	765	10.6	23	117
19X-1, 140-150	147.90	150.54	33.0	554	7.62	30.50	445	43.3	4.8	1.7	214	5.90	677	10.0	29	126
22X-1, 130-140	176.60	179.24	33.0	556	7.51	26.65	450	42.6	5.6	3.1	87	4.93	712	10.4	46	131
26X-2, 90-100	216.40	219.04	33.0	556	7.41	26.23	446	43.9	5.3	1.9	93	5.16	873	10.0	37	157
29X-3, 140-150	247.30	249.94	33.0	556	7.59	22.51	452	43.2	6.1	4.9	51	4.47	744	10.2	47	173
32X-1, 140-150	272.70	275.34	33.0	555	7.55	19.81	451	44.6	5.6	5.4	57	3.89	725	10.6	60	248
35X-4, 140-150	305.83	308.54	34.0	557	7.39	14.81	458	47.1	7.9	12.6	25	3.53	941	9.6	78	355
38X-2, 140-150	331.80	334.44	34.0	556	7.52	12.55	457	51.4	9.1	17.6	10	2.37	933	10.0	80	420
42X-2, 140-150	370.40	373.04	34.0	559	7.35	9.67	460	52.9	10.6	20.8	8	1.91	1021	9.8	81	466
45X-2, 140-150	399.50	402.14	34.0	559	7.42	7.86	465	49.7	12.9	21.9	8	1.74	1057	9.5	87	451
48X-4, 140-150	431.40	434.04	34.0	557	7.79	4.58	468	44.5	14.6	21.0	3	0.98	799	11.3	121	117
51X-4, 140-150	460.30	462.94	34.0	559	7.52	4.95	467	48.6	16.9	25.0	3	0.83	886	9.2	112	354
54X-3, 140-150	487.40	490.04	35.0	557	7.58	5.80	466	47.1	18.9	25.3	3	0.66	910	8.3	146	355
57X-2, 140-150	514.80	517.44	34.5	557	7.55	4.84	468	47.4	18.3	26.5	3	0.57	925	8.5	173	346
61X-3, 140-150	554.80	557.44	34.5	557	7.49	4.04	459	47.8	21.4	25.0	3	0.45	749	7.9	224	385
65X-2, 0-10	591.40	593.04	35.0	556	7.32	4.67	460	47.7	21.6	25.3	3	0.39	803	6.5	231	404

Note: This table is also available in **ASCII format.**

Table T14. Inorganic carbon, carbonate, total carbon, total organic carbon, total nitrogen, total sulfur, and atomic organic carbon/nitrogen values for sediments from Holes 1122A and 1122C. (**See table note.** Continued on next two pages.).

Core, section, interval (cm)	Depth (mbsf)	IC (%)	$CaCO_3$ (%)	TC (%)	TOC (%)	TN (%)	TS (%)	$[C/N]_a$ (%)
181-1122A-								
1H-1, 8-9	0.08	2.77	23	1.2	0.78	0.09	ND	10.4
1H-3, 72-73	3.72	2.55	21.2					
1H-6, 90-91	8.4	1.7	14.1					
2H-6, 94-95	17.74	0.86	7.15	1.5	0.64	0.14	0.28	5.5
2H-6, 98-99	17.78	0.76	6.33					
2H-6, 102-103	17.82	0.97	8.08					
3H-1, 79-80	19.59	0.73	6.1	0.86	0.13	0.08	ND	1.8
3H-1, 142-143	20.22	0.64	5.35					
3H-6, 71-72	27.01	0.39	3.29					
4H-2, 88-89	30.68	0.49	4.11					
4H-3, 13-14	31.43	0.49	4.1	0.59	0.1	0.04	0.1	3
4H-5, 102-103	35.32	0.51	4.23					
5H-1, 97-98	38.77	0.66	5.52					
5H-2, 8-9	39.38	1.92	16	2.09	0.17	0.09	0.03	2.2
5H-6, 20-21	45.4	0.7	5.84					
6H-3, 65-66	50.95	0.44	3.68					
6H-4, 67-68	52.47	0.37	3.1	0.55	0.17	0.08	ND	2.6
6H-5, 26-27	53.56	0.46	3.86					
7H-2, 55-56	58.85	0.68	5.71					
7H-4, 92-93	62.22	2.54	21.1	2.59	0.05	0.08	0.07	0.8
7H-5, 26-27	63.06	4.61	38.4					
8H-2, 101-102	67.95	5.32	44.3					
8H-4, 6-7	70	1.04	8.62	1.22	0.18	0.09	0.03	2.4
8H-4, 50-51	70.44	1.12	9.33					
9X-1, 60-61	76.4	0.69	5.76					
10X-1, 17-18	85.57	0.45	3.74	0.72	0.28	0.09	0.04	3.6
10X-1, 23-24	85.63	0.42	3.51					
11X-1, 63-64	95.63	1.24	10.3					
11X-1, 73-74	95.73	1.2	9.97	1.37	0.17	0.09	ND	2.3
11X-1, 124-125	96.24	2.4	20					
12X-2, 55-56	106.75	0.11	0.89					
12X-2, 122-123	107.42	2.19	18.2	2.41	0.22	0.07	ND	3.6
13X-1, 110-111	115.4	0.6	5					
13X-3, 70-71	118	0.36	2.98					
13X-4, 104-105	119.84	0.36	3.01	0.54	0.18	0.08	0.09	2.6
181-1122C-								
9H-1, 34-35	61.84	0.28	2.34					
9H-3, 103-104	65.53	2.5	20.8					
9H-5, 15-16	67.65	0.9	7.51	0.98	0.08	0.07	0.09	1.3
10H-1, 10-11	71.1	3.91	32.6					
10H-1, 16-17	71.16	5.91	49.2					
10H-4, 55-56	76.05	0.44	3.7	0.67	0.22	0.08	ND	3.3
11H-2, 10-11	82.1	0.99	8.23					
11H-2, 41-42	82.41	2.75	22.9					
11H-2, 147-148	83.47	1.09	9.12	1.56	0.46	0.07	ND	7.7
12H-3, 71-72	90.61	0.7	5.83					
12H-5, 52-53	93.42	0.86	7.17					
12H-5, 141-142	94.31	0.88	7.37	1.23	0.35	0.06	0.09	7.4
13H-2, 92-93	97.32	1.84	15.4					
13H-3, 16-17	98.06	2.77	23.1	3.37	0.6	0.07	ND	10.6
13H-3, 135-136	99.25	0.74	6.17	0.95	0.21	0.05	ND	4.8
14X-1, 14-15	103.84	1.85	15.4					
14X-2, 121-122	106.41	0.47	3.9					
15X-1, 140-141	109.4	1.78	14.8	1.83	0.05	0.06	ND	0.9
15X-2, 66-67	110.16	1.25	10.4					
16X-1, 101-102	118.61	0.6	5.03					
16X-4, 40-41	122.5	0.59	4.93	0.78	0.19	0.09	ND	2.4
17X-1, 30-31	127.5	0.24	1.96					
17X-2, 57-58	129.27	2.37	19.7					
17X-4, 39-40	132.09	1.7	14.2	1.97	0.27	0.07	0.09	4.7
18X-1, 42-43	137.32	0.62	5.17					

Table T14 (continued).

Core, section, interval (cm)	Depth (mbsf)	IC (%)	$CaCO_3$ (%)	TC (%)	TOC (%)	TN (%)	TS (%)	$[C/N]_a$ (%)
18X-2, 79-80	139.19	1.87	15.6					
20X-2, 81-82	158.41	7.27	60.5	7.35	0.08	0.07	ND	1.4
20X-4, 30-31	160.9	0.28	2.37					
21X-1, 6-7	165.76	0.56	4.63					
21X-2, 27-28	167.47	0.44	3.67	1	0.56	0.11	ND	6.1
22X-1, 72-73	176.02	1.07	8.94					
22X-2, 21-22	176.91	1.43	11.9					
23X-1, 20-21	185.2	0.17	1.4	0.64	0.47	0.09	ND	6.4
23X-2, 35-36	186.85	0.42	3.46					
26X-2, 7-8	215.57	7.06	58.8					
26X-3, 126-127	217.76	1.85	15.4	1.92	0.07	0.09	ND	0.9
28X-3, 89-90	237.19	0.1	0.8					
29X-3, 9-10	245.99	4.69	39.1					
30X-2, 125-126	255.25	3.7	30.9	3.75	0.04	0.06	0.31	0.9
31X-2, 71-72	263.91	0.7	5.86					
32X-2, 24-25	273.04	1.22	10.2					
33X-3, 112-113	284.82	7.26	60.5	8.06	0.8	0.14	0.37	6.6
33X-4, 6-7	285.26	5.17	43					
34X-2, 36-37	292.26	4.04	33.7					
34X-2, 70-71	292.6	2.75	22.9	2.99	0.24	0.08	0.11	3.3
34X-3, 55-56	293.95	2.26	18.8					
35X-1, 56-57	300.56	2.59	21.6					
35X-1, 86-87	300.86	2.37	19.8	2.63	0.25	0.09	0.45	3.1
35X-2, 70-71	302.2	5.73	47.7					
36X-1, 69-70	310.29	0.96	7.99					
36X-3, 70-71	313.3	0.53	4.39	0.99	0.47	0.09	0.61	6.1
36X-5, 127-128	316.87	2.2	18.4					
37X-2, 4-5	320.84	3.1	25.8					
37X-5, 32-33	325.62	0.13	1.1	0.67	0.53	0.1	0.5	6.4
37X-6, 122-123	328.02	0.45	3.7					
38X-2, 42-43	330.82	0.53	4.43					
38X-2, 44-45	330.84	3.3	27.5	3.52	0.22	0.05	ND	4.8
38X-2, 67-68	331.07	0.3	2.53					
39X-1, 5-6	338.55	0.01	0.11					
39X-2, 95-96	340.95	1.2	10	1.69	0.48	0.05	0.22	11.2
39X-2, 139-140	341.39	1.24	10.3					
40X-2, 2-3	349.72	0.22	1.8					
40X-2, 23-24	349.93	0.89	7.44	1.04	0.15	0.11	0.27	1.6
40X-2, 111-112	350.81	0.68	5.66					
41X-1, 118-119	359.08	2.05	17.1					
41X-2, 6-7	359.46	0.91	7.61	1.14	0.23	0.08	0.05	3.3
42X-1, 11-12	367.61	1.71	14.2					
42X-2, 13-14	369.13	1.61	13.4					
42X-3, 12-13	370.62	1.4	11.7	1.96	0.55	0.1	0.32	6.7
44X-2, 68-69	389.08	3.61	30.1					
44X-3, 74-75	390.64	1.52	12.7					
45X-1, 142-143	398.02	2.62	21.8	2.66	0.04	0.08	ND	0.6
45X-2, 46-47	398.56	0.9	7.52					
45X-2, 123-124	399.33	1.47	12.3					
46X-1, 105-106	407.25	3.66	30.5	4.15	0.48	0.06	0.3	9.8
46X-2, 126-127	408.96	2.22	18.5					
47X-1, 133-134	417.23	0.74	6.18					
47X-3, 50-51	419.4	0.6	5.02	0.85	0.25	0.04	0.06	7.3
48X-3, 48-49	428.98	5.98	49.8					
48X-4, 95-96	430.95	3.82	31.9					
49X-2, 73-74	437.43	3.57	29.8	3.59	0.02	0.06	0.03	0.3
49X-3, 109-110	439.29	1.73	14.4					
51X-2, 61-62	456.51	2.41	20.1					
51X-3, 60-61	458	0.02	0.17	0.33	0.31	0.06	0.03	5.6
51X-6, 106-107	462.96	2.42	20.2					
52X-2, 15-16	465.75	2.78	23.2					
52X-6, 20-21	471.8	3.6	30	3.61	0.01	ND	0.05	
52X-6, 87-88	472.47	4.64	38.6					
53X-3, 6-7	476.46	4.51	37.6					
54X-2, 48-49	484.98	6.55	54.6	6.64	0.08	0.06	0.06	1.5
54X-4, 57-58	488.07	0.1	0.84					
55X-2, 110-111	495.3	0.2	1.66					

Table T14 (continued).

Core, section, interval (cm)	Depth (mbsf)	IC (%)	$CaCO_3$ (%)	TC (%)	TOC (%)	TN (%)	TS (%)	$[C/N]_a$ (%)
55X-4, 24-25	497.44	5.66	47.2	5.61	ND	0.04	ND	
55X-5, 70-71	499.4	6.7	55.8					
56X-1, 7-8	502.37	0.84	7.03					
56X-3, 92-93	506.22	0.52	4.31	0.69	0.17	0.07	0.18	3.1
56X-4, 36-37	507.16	1.96	16.3					
57X-2, 106-107	514.46	4.12	34.3					
57X-2, 109-110	514.49	1	8.32	1.01	0.01	0.06	0.5	0.2
57X-3, 7-8	514.97	0.62	5.13					
58X-1, 17-18	521.67	0.67	5.59					
58X-2, 26-27	523.26	5.09	42.4	5.22	0.13	0.06	ND	2.6
61X-2, 52-53	552.42	6.58	54.8					
61X-4, 30-31	555.2	0.06	0.54					
63X-1, 56-57	570.16	1.12	9.37	1.15	0.03	0.06	ND	0.6
63X-1, 125-126	570.85	2.55	21.2					
64X-1, 56-57	579.86	1.32	11					
65X-1, 57-58	589.47	7.5	62.49	7.71	0.2	0.05	ND	5.2
66X-1, 47-48	598.97	9.17	76.41					

Notes: Carbonate is calculated assuming that all inorganic carbon is calcite. ND = not detected. This table is also available in **ASCII format.**

Table T15. List of index properties measured from Holes 1122A and 1122C. (See table note. Continued on next two pages.)

Leg	Hole	Core	Section	Interval (cm)	Depth (mbsf)	Wet-water content (%)	Dry-water content (%)	Wet-bulk density (g/cm^3)	Dry density (g/cm^3)	Grain density (g/cm^3)	Porosity (%)	Void ratio
181	1122A	1H	1	107-109	1.07	40.3	67.4	1.637	0.978	2.743	64.3	1.81
181	1122A	1H	3	122-124	4.22	39.3	64.7	1.646	1.000	2.713	63.2	1.71
181	1122A	1H	5	127-129	7.27	36.1	56.6	1.720	1.098	2.794	60.7	1.54
181	1122A	1H	6	83-85	8.33	37.7	60.4	1.681	1.048	2.744	61.8	1.62
181	1122A	2H	1	122-124	10.52	37.5	60.0	1.689	1.055	2.767	61.9	1.62
181	1122A	2H	3	122-124	13.52	34.8	53.4	1.734	1.130	2.756	59.0	1.44
181	1122A	2H	5	25-27	15.55	37.5	60.1	1.694	1.059	2.792	62.1	1.64
181	1122A	2H	6	134-136	18.14	35.9	56.0	1.722	1.104	2.787	60.4	1.52
181	1122A	3H	1	92-94	19.72	33.9	51.3	1.757	1.161	2.776	58.2	1.39
181	1122A	3H	3	86-88	22.66	32.0	47.1	1.782	1.212	2.735	55.7	1.26
181	1122A	3H	5	6-8	24.86	31.9	46.9	1.805	1.229	2.808	56.3	1.29
181	1122A	3H	6	90-92	27.20	38.4	62.3	1.668	1.028	2.743	62.5	1.67
181	1122A	4H	1	143-145	29.73	36.0	56.3	1.720	1.101	2.785	60.5	1.53
181	1122A	4H	3	84-86	32.14	33.5	50.3	1.753	1.167	2.731	57.3	1.34
181	1122A	4H	5	145-147	35.75	33.7	50.9	1.761	1.167	2.779	58.0	1.38
181	1122A	4H	6	107-109	36.87	36.2	56.7	1.715	1.094	2.778	60.6	1.54
181	1122A	5H	1	103-105	38.83	35.7	55.5	1.706	1.097	2.706	59.5	1.47
181	1122A	5H	3	113-115	41.93	30.6	44.2	1.809	1.255	2.737	54.2	1.18
181	1122A	5H	5	119-121	44.99	34.5	52.8	1.749	1.144	2.791	59.0	1.44
181	1122A	5H	6	45-47	45.65	31.4	45.9	1.808	1.240	2.787	55.5	1.25
181	1122A	6H	1	91-93	48.21	32.9	49.1	1.765	1.184	2.739	56.8	1.31
181	1122A	6H	3	114-116	51.44	29.3	41.5	1.863	1.317	2.823	53.4	1.14
181	1122A	6H	5	20-22	53.50	29.4	41.6	1.851	1.308	2.789	53.1	1.13
181	1122A	6H	6	126-128	56.06	29.9	42.6	1.845	1.294	2.804	53.9	1.17
181	1122A	7H	2	129-131	59.59	30.5	44.0	1.830	1.271	2.799	54.6	1.20
181	1122A	7H	4	105-107	62.35	36.3	57.1	1.716	1.093	2.795	60.9	1.56
181	1122A	7H	6	112-114	65.42	32.5	48.3	1.778	1.200	2.760	56.5	1.30
181	1122A	8H	1	38-40	66.68	35.9	55.9	1.720	1.103	2.772	60.2	1.51
181	1122A	8H	3	126-128	69.70	32.3	47.6	1.776	1.203	2.731	56.0	1.27
181	1122A	8H	5	110-112	72.54	30.3	43.4	1.840	1.283	2.812	54.4	1.19
181	1122A	9X	1	47-49	76.27	30.0	42.8	1.824	1.278	2.739	53.4	1.14
181	1122A	10X	1	10-12	85.50	31.3	45.5	1.818	1.250	2.809	55.5	1.25
181	1122A	11X	1	126-128	96.26	30.8	44.5	1.808	1.252	2.741	54.3	1.19
181	1122A	12X	2	106-108	107.26	37.3	59.4	1.689	1.059	2.751	61.5	1.60
181	1122A	12X	4	8-10	109.28	27.9	38.7	1.896	1.366	2.828	51.7	1.07
181	1122A	13X	1	131-133	115.61	29.7	42.2	1.846	1.299	2.793	53.5	1.15
181	1122A	13X	3	119-121	118.49	35.1	54.0	1.708	1.109	2.673	58.5	1.41
181	1122C	2H	4	135-137	8.35	42.3	73.2	1.601	0.924	2.725	66.1	1.948
181	1122C	3H	4	108-110	15.08	41.9	72.1	1.601	0.930	2.698	65.5	1.901
181	1122C	4H	6	114-116	22.68	34.5	52.6	1.749	1.146	2.789	58.9	1.433
181	1122C	5H	4	135-137	29.35	35.1	54.0	1.742	1.131	2.801	59.6	1.477
181	1122C	6H	6	114-116	41.64	34.1	51.7	1.749	1.153	2.759	58.2	1.393
181	1122C	7H	2	132-134	45.32	34.1	51.7	1.764	1.163	2.817	58.7	1.421
181	1122C	8H	2	108-110	54.58	33.1	49.5	1.772	1.185	2.777	57.3	1.343
181	1122C	8H	3	65-67	55.65	30.7	44.2	1.827	1.267	2.797	54.7	1.208
181	1122C	8H	4	37-39	56.87	29.8	42.4	1.840	1.292	2.779	53.5	1.150
181	1122C	8H	6	75-77	60.25	31.9	46.9	1.797	1.224	2.781	56.0	1.273
181	1122C	9H	1	110-112	62.60	33.9	51.2	1.758	1.163	2.778	58.2	1.390
181	1122C	9H	3	133-135	65.83	38.0	61.3	1.671	1.036	2.726	62.0	1.633
181	1122C	9H	4	9-11	66.09	30.9	44.8	1.808	1.249	2.752	54.6	1.204
181	1122C	9H	5	139-141	68.89	35.4	54.8	1.725	1.114	2.759	59.6	1.475
181	1122C	10H	1	148-150	72.48	31.1	45.2	1.795	1.236	2.724	54.6	1.204
181	1122C	10H	3	72-74	74.72	30.8	44.6	1.820	1.259	2.787	54.8	1.214
181	1122C	10H	5	15-17	77.15	23.1	30.1	1.973	1.517	2.738	44.6	0.805
181	1122C	10H	5	76-78	77.76	29.3	41.5	1.851	1.308	2.783	53.0	1.127
181	1122C	11H	1	129-131	81.79	34.4	52.5	1.729	1.134	2.708	58.1	1.388
181	1122C	11H	3	81-83	84.31	30.2	43.3	1.828	1.276	2.768	53.9	1.169
181	1122C	11H	3	94-96	84.44	21.6	27.6	2.000	1.567	2.714	42.2	0.731
181	1122C	12H	1	83-85	87.73	29.8	42.6	1.834	1.286	2.763	53.4	1.148
181	1122C	12H	3	147-149	91.37	34.1	51.7	1.738	1.146	2.717	57.8	1.371
181	1122C	12H	5	125-127	94.15	33.8	51.1	1.761	1.166	2.786	58.1	1.389
181	1122C	13H	1	130-132	96.20	32.5	48.1	1.780	1.201	2.761	56.5	1.298
181	1122C	13H	4	115-117	100.55	30.5	43.9	1.824	1.267	2.776	54.4	1.191
181	1122C	13H	6	87-89	103.27	34.9	53.7	1.721	1.120	2.711	58.7	1.421

Table T15 (continued).

Leg	Hole	Core	Section	Interval (cm)	Depth (mbsf)	Wet-water content (%)	Dry-water content (%)	Wet-bulk density (g/cm^3)	Dry density (g/cm^3)	Grain density (g/cm^3)	Porosity (%)	Void ratio
181	1122C	14X	1	70-72	104.40	38.2	61.9	1.665	1.028	2.719	62.2	1.644
181	1122C	14X	3	58-60	107.28	32.0	47.1	1.797	1.221	2.791	56.2	1.285
181	1122C	15X	2	11-13	109.61	36.0	56.3	1.711	1.095	2.750	60.2	1.511
181	1122C	16X	1	52-54	118.12	37.0	58.7	1.680	1.058	2.692	60.7	1.544
181	1122C	16X	3	65-67	121.25	37.5	60.1	1.700	1.062	2.818	62.3	1.653
181	1122C	17X	2	127-129	129.97	33.2	49.8	1.773	1.184	2.789	57.6	1.36
181	1122C	17X	4	104-106	132.74	31.3	45.5	1.790	1.230	2.715	54.7	1.21
181	1122C	18X	1	80-82	137.70	32.7	48.6	1.781	1.199	2.777	56.8	1.32
181	1122C	18X	3	8-10	139.98	35.4	54.8	1.714	1.107	2.717	59.3	1.45
181	1122C	19X	1	68-70	147.18	33.0	49.3	1.784	1.195	2.813	57.5	1.36
181	1122C	19X	3	57-59	150.07	31.7	46.4	1.792	1.224	2.746	55.4	1.24
181	1122C	20X	2	137-139	158.97	34.5	52.8	1.733	1.135	2.733	58.5	1.41
181	1122C	20X	4	33-35	160.93	30.0	42.9	1.832	1.282	2.769	53.7	1.16
181	1122C	21X	1	95-97	166.65	32.0	47.0	1.786	1.215	2.747	55.8	1.26
181	1122C	22X	1	110-112	176.40	37.2	59.3	1.679	1.054	2.706	61.0	1.57
181	1122C	23X	1	109-111	186.09	34.0	51.5	1.749	1.155	2.751	58.0	1.38
181	1122C	24X	1	62-64	195.32	23.2	30.2	1.989	1.527	2.780	45.1	0.82
181	1122C	25X	1	14-16	204.44	28.3	39.5	1.866	1.338	2.764	51.6	1.07
181	1122C	26X	1	120-122	215.20	35.5	55.0	1.721	1.110	2.751	59.6	1.48
181	1122C	26X	3	122-124	217.72	36.9	58.4	1.675	1.057	2.664	60.3	1.52
181	1122C	27X	1	120-122	224.90	30.3	43.4	1.814	1.265	2.728	53.6	1.16
181	1122C	27X	3	17-19	226.87	29.7	42.2	1.821	1.280	2.711	52.8	1.12
181	1122C	28X	1	130-132	234.60	30.5	44.0	1.812	1.259	2.739	54.0	1.18
181	1122C	28X	3	53-55	236.83	34.2	51.9	1.734	1.142	2.711	57.9	1.38
181	1122C	29X	1	121-123	244.11	35.6	55.4	1.708	1.099	2.710	59.4	1.47
181	1122C	29X	3	109-111	246.99	33.5	50.3	1.764	1.174	2.770	57.6	1.36
181	1122C	30X	1	126-128	253.76	35.9	56.0	1.697	1.087	2.686	59.5	1.47
181	1122C	30X	3	68-70	256.18	31.6	46.2	1.799	1.230	2.765	55.5	1.25
181	1122C	30X	5	36-38	258.86	32.6	48.4	1.759	1.185	2.696	56.0	1.27
181	1122C	31X	1	126-128	262.96	31.1	45.0	1.804	1.244	2.746	54.7	1.21
181	1122C	31X	3	94-96	265.64	30.9	44.8	1.814	1.253	2.770	54.8	1.21
181	1122C	32X	1	110-112	272.40	34.9	53.6	1.703	1.109	2.642	58.0	1.38
181	1122C	33X	2	52-54	282.72	32.6	48.4	1.767	1.191	2.724	56.3	1.29
181	1122C	33X	4	14-16	285.34	32.8	48.8	1.758	1.182	2.702	56.3	1.29
181	1122C	33X	5	73-75	287.43	30.2	43.3	1.832	1.279	2.783	54.0	1.18
181	1122C	34X	1	88-90	291.28	34.3	52.1	1.739	1.143	2.732	58.2	1.39
181	1122C	34X	3	122-124	294.62	34.0	51.6	1.734	1.144	2.701	57.6	1.36
181	1122C	34X	5	124-126	297.64	34.1	51.8	1.729	1.139	2.690	57.7	1.36
181	1122C	35X	1	96-98	300.96	39.5	65.3	1.617	0.979	2.600	62.4	1.66
181	1122C	35X	3	35-37	303.35	31.8	46.7	1.786	1.218	2.738	55.5	1.25
181	1122C	35X	5	123-125	307.23	33.8	51.0	1.743	1.154	2.716	57.5	1.35
181	1122C	36X	2	49-51	311.59	33.1	49.5	1.758	1.176	2.725	56.8	1.32
181	1122C	36X	4	19-21	314.29	30.9	44.7	1.802	1.245	2.727	54.3	1.19
181	1122C	36X	6	65-67	317.75	27.9	38.7	1.875	1.352	2.764	51.1	1.04
181	1122C	37X	1	128-130	320.58	34.2	52.0	1.733	1.140	2.706	57.9	1.37
181	1122C	37X	3	116-118	323.46	33.6	50.6	1.749	1.162	2.727	57.4	1.35
181	1122C	37X	5	132-134	326.62	31.7	46.4	1.785	1.219	2.726	55.3	1.24
181	1122C	38X	1	118-120	330.08	36.9	58.5	1.669	1.053	2.641	60.1	1.51
181	1122C	38X	3	127-129	333.17	37.3	59.4	1.664	1.044	2.646	60.6	1.54
181	1122C	39X	1	121-123	339.71	30.3	43.5	1.816	1.265	2.738	53.8	1.16
181	1122C	39X	3	119-121	342.69	29.5	41.9	1.833	1.292	2.740	52.8	1.12
181	1122C	40X	1	102-104	349.22	29.5	41.9	1.842	1.298	2.768	53.1	1.13
181	1122C	41X	2	30-32	359.70	31.9	46.9	1.767	1.203	2.680	55.1	1.23
181	1122C	42X	1	62-64	368.12	35.5	55.0	1.688	1.089	2.626	58.5	1.41
181	1122C	42X	3	14-16	370.64	33.9	51.3	1.710	1.130	2.608	56.7	1.31
181	1122C	44X	1	111-113	388.01	31.0	45.0	1.793	1.237	2.708	54.3	1.19
181	1122C	44X	3	116-118	391.06	32.3	47.7	1.769	1.198	2.709	55.8	1.26
181	1122C	45X	2	17-19	398.27	34.2	51.9	1.730	1.139	2.693	57.7	1.36
181	1122C	45X	4	100-102	402.10	33.7	50.8	1.750	1.161	2.736	57.6	1.36
181	1122C	46X	1	136-138	407.56	32.5	48.1	1.764	1.191	2.705	55.9	1.27
181	1122C	46X	4	45-47	411.15	32.2	47.5	1.793	1.216	2.785	56.3	1.29
181	1122C	47X	1	126-128	417.16	34.1	51.8	1.741	1.146	2.731	58.0	1.38
181	1122C	47X	3	138-140	420.28	29.2	41.3	1.846	1.307	2.763	52.7	1.11
181	1122C	48X	1	92-94	426.42	28.3	39.5	1.862	1.335	2.751	51.5	1.06
181	1122C	48X	3	140-142	429.90	30.3	43.5	1.813	1.263	2.727	53.7	1.16
181	1122C	48X	5	29-31	431.79	33.2	49.8	1.750	1.169	2.705	56.8	1.31

Table T15 (continued).

Leg	Hole	Core	Section	Interval (cm)	Depth (mbsf)	Wet-water content (%)	Dry-water content (%)	Wet-bulk density (g/cm^3)	Dry density (g/cm^3)	Grain density (g/cm^3)	Porosity (%)	Void ratio
181	1122C	49X	1	120-122	436.40	32.0	47.1	1.783	1.213	2.739	55.7	1.26
181	1122C	49X	3	11-13	438.31	30.0	42.9	1.814	1.270	2.710	53.2	1.14
181	1122C	49X	5	120-122	442.40	32.0	47.1	1.811	1.232	2.838	56.6	1.30
181	1122C	50X	1	17-19	444.97	37.6	60.3	1.652	1.031	2.623	60.7	1.55
181	1122C	50X	3	120-122	449.00	33.1	49.4	1.750	1.171	2.692	56.5	1.30
181	1122C	50X	5	13-15	450.93	31.0	44.8	1.809	1.249	2.757	54.7	1.21
181	1122C	51X	1	117-119	455.57	32.0	47.1	1.789	1.216	2.763	56.0	1.27
181	1122C	51X	3	9-11	457.49	28.7	40.2	1.870	1.334	2.802	52.4	1.10
181	1122C	51X	5	140-142	461.80	29.4	41.6	1.840	1.300	2.752	52.8	1.12
181	1122C	52X	1	126-128	465.36	32.4	47.9	1.773	1.199	2.731	56.1	1.28
181	1122C	52X	3	88-90	467.98	31.8	46.6	1.790	1.221	2.745	55.5	1.25
181	1122C	52X	5	114-116	471.24	32.5	48.1	1.747	1.180	2.648	55.4	1.25
181	1122C	53X	2	72-74	475.62	31.9	46.9	1.779	1.211	2.721	55.5	1.25
181	1122C	54X	1	31-33	483.31	37.5	60.0	1.658	1.036	2.637	60.7	1.55
181	1122C	54X	3	97-99	486.97	30.9	44.8	1.802	1.245	2.731	54.4	1.19
181	1122C	55X	1	132-134	494.02	30.4	43.6	1.821	1.268	2.758	54.0	1.18
181	1122C	55X	3	134-136	497.04	32.0	47.0	1.783	1.213	2.739	55.7	1.26
181	1122C	55X	5	74-76	499.44	24.9	33.1	1.946	1.463	2.773	47.3	0.90
181	1122C	56X	1	98-100	503.28	27.5	38.0	1.892	1.372	2.790	50.8	1.03
181	1122C	56X	3	128-130	506.58	27.2	37.3	1.893	1.378	2.772	50.3	1.01
181	1122C	57X	1	133-135	513.23	31.1	45.2	1.806	1.244	2.759	54.9	1.22
181	1122C	57X	4	36-38	516.76	18.9	23.3	2.338	1.897	3.332	43.1	0.76
181	1122C	58X	2	42-44	523.42	28.9	40.7	1.848	1.313	2.748	52.2	1.09
181	1122C	61X	1	117-119	551.57	18.8	23.2	2.100	1.705	2.777	38.6	0.63
181	1122C	61X	4	11-13	555.01	22.9	29.8	1.968	1.517	2.712	44.1	0.79
181	1122C	62X	1	100-102	561.00	19.9	24.9	2.068	1.656	2.770	40.2	0.67
181	1122C	62X	2	15-17	561.65	17.3	20.9	2.131	1.763	2.752	35.9	0.56
181	1122C	63X	1	65-67	570.25	23.5	30.8	1.964	1.502	2.736	45.1	0.82
181	1122C	64X	1	114-116	580.44	23.5	30.7	1.968	1.506	2.746	45.2	0.82
181	1122C	65X	1	35-37	589.25	19.3	23.8	2.063	1.666	2.722	38.8	0.63
181	1122C	66X	1	40-42	598.90	19.7	24.5	2.043	1.641	2.703	39.3	0.65
181	1122C	67X	1	46-48	608.66	18.8	23.2	2.093	1.699	2.762	38.5	0.63

Note: This table is also available in **ASCII format.**